# The clusterin gene in mouse inner ear development: expression analysis and generation of reporter constructs

Faranak Yadollahi

Submitted in part fulfilment of the requirements for the degree of Doctor of Philosophy,

University of Sussex

December 2012

## Declaration

The contents of this thesis are the original work by the author, except where otherwise stated.

I hereby declare that this thesis has not and will not be submitted in whole or in part to any other university for a degree.

Signature…….Faranak Yadollahi

UNIVERSITY OF SUSSEX

This thesis is submitted for the degree of Doctor of Philosophy
by Faranak Yadollahi

**The clusterin gene in mouse inner ear development: expression analysis and generation of reporter constructs**

## Summary

Clusterin has previously been identified as a gene potentially involved in development of the cochlear sensory epithelium. In order to be able to predict the cellular roles that clusterin may play in the development of this organ, an understanding of the spatiotemporal expression pattern is required. Therefore, clusterin gene expression during mouse inner ear development was studied using riboprobes from the mouse gene. Clusterin mRNA demonstrates a dynamic expression pattern within the developing cochlear sensory epithelium. Clusterin mRNA expression is initiated at 12.5dpc (days post coitum) along the entire length of the cochlear sensory epithelium. Throughout *in utero* development, expression is maintained but becomes progressively restricted in this sensory epithelium. Postnataly expression resolves to specific cellular regions, but clusterin expression ceases at some time point between P2-P17.

The analysis of clusterin protein expression revealed this was not restricted to the developing sensory epithelium alone, but also was detected transiently in the periotic mesenchye, otic capsule, as well as Reissner's membrane, a non-sensory epithelium. The detailed localisation of clusterin was compared to other inner ear markers. Using α and β tectorin mRNA markers, clusterin mRNA was shown to localise to the developing inner and outer sulcus and spiral prominence. Clusterin expression also overlaps with both Myosin VIIA and Prox1, markers for hair cells and supporting cells respectively. Clusterin mRNA and protein was absent from the developing mouse vestibular system.

In order to study the regulatory mechanisms underlying inner ear clusterin expression, a clusterin BAC was modified by insertion of ZsGreen reporter gene into clusterin genomic regions using recombineering technique. The pronuclear injection of this construct has not been successful so far although these studies are ongoing. Finally in order to determine the fate of clusterin expressing cells after the expression is ceased in the inner ear, clusterin BAC was modified by insertion of Cre recombinant gene at the same location as ZsGreen gene for the generation of Cre transgenic mouse. This transgenic mouse will be crossed with a silent reporter mouse for future clusterin fate mapping studies.

## Acknowledgemnets

I would like to express my sincere appreciation to my supervisor Dr. Mark Maconochie for his continuous support and advice throughout this journey. Mark I am indebted to you for dedicating your busy time to help me to develop into an independent scientist. I would also like to thank Dr. Androulla Economou for useful discussion and her expert opinions.

Special thanks to Professor Guy Richardson and his team, especially Dr. Kevin Legan and Dr. Richard Goodyear for their support with the IHC and blotting experiments.

I would like to dedicate this work to those members of my family who needed my attention most and patiently tolerated my absence through the duration of my studies, particularly my little loving son, Nick and my dearest mother, Mohtaram. I love you both and hope that this work makes you proud.

I am grateful to those who believed in me and encouraged me to do a PhD, namely my husband, Ali and my beloved father, Hossein. Dear Dad although you are not among us today but I will never forget how much you wanted me to do this work. May your soul rest in peace and god bless you.

Lastly, I offer my regards to those who supported me in any respect during the completion of this project.

## Table of Contents

## List of figures

## List of tables

## Abbreviations

| | |
|---|---|
| BLAST | Basic local alignment search tool |
| Bp | Base pairs |
| BSA | Bovine serum albumin |
| cDNA | Complementary DNA |
| DNA | Deoxyribonucleic acid |
| dNTP | Deoxynucleotide triphosphate |
| dpc | Day post coitum |
| EDTA | Ethylenediaminetetraacetic acid |
| ISH | *In situ* hybridisation |
| Kb | Kilobase Pairs |
| LB | Luria-Bertini |
| ORF | Open reading frame |
| PBS | Phosphate-buffered saline |
| PCR | Polymerase chain reaction |
| PFA | Paraformaldehyde |
| RNA | Ribonucleic acid |
| SSC | Saline sodium citrate |
| TBST | Tris-Buffered Saline Tween-20 |
| Tween-20 | Polyoxyethelene sorbitan monolaurate |
| Xgal | 5-bromo-4-chloro-3-indolyl-β-D-galactoside |
| Math-1 (Atoh1) | Atonal homolog 1 against decapentaplegic (MAD) gene |

# 1. General Introduction

# 1. Introduction

## 1.1 Structure and function of mammalian inner ear

The ear is composed of three anatomical sections: outer, middle and inner ear. The outer ear, is divided into the auricle or pinna and the ear canal leading to the tympanic membrane or ear drum (Figure 1.1 a). The function of outer ear is to gather sound and aid in its localization via the large surface area of the pinna. Amplification is done by middle and inner ear. The tympanic membrane, which separates the outer and middle ear receives sound vibrations that have passed through the ear canal and transfers them to the auditory ossicles of the middle ear. (2) The middle ear is an air filled space that contains three small bones or ossicles; the malleus, incus and stapes (Figure 1.1 a). The auditory ossicles are responsible for transforming sound waves arrived from the outer ear into mechanical vibrations of the endolymphatic fluid contained in the inner ear.

The fluid-filled inner ear has a highly complex structure and is a labyrinth-like organ. The adult inner ear consists of a memberanous labyrinth that is surrounded by the otic capsule encased in the temporal bone (the bony labyrinth). It contains the auditory and vestibular sensory systems and is responsible for the transduction of mechanical stimuli from fluid motions into neuroelectrical impulses that are then transmitted to the brain.

The vestibular system is located in the dorsal portion of the inner ear and contains the sensory organs responsible for detection of balance, angular and linear acceleration. The vestibular portion consists of different chambers, the utricle, saccule, and three semicircular canals (anterior, lateral and posterior) and their associated ampullae (Figure 1.1 b). Each ampulla contains a sensory organ, the crista ampullaris (Figure 1.1 c). These three sensory organs, together, sense angular acceleration. Two additional sensory organs, the maculae of the utricle and saccule, are responsible for the detection of gravity, and the macula of the saccule responsible for the detection of linear acceleration (Figure 1.1 d). The total number of vestibular sensory organs varies amongst different vertebrate species. Chicken for instance has seven vestibular sensory organs (three cristae, two maculae, the lagena, and macula neglecta) and only five major

sensory organs in the mouse and man (three cristae and two maculae) which is consistent among all species of amniotes (Chang, Cole et al. 2004).

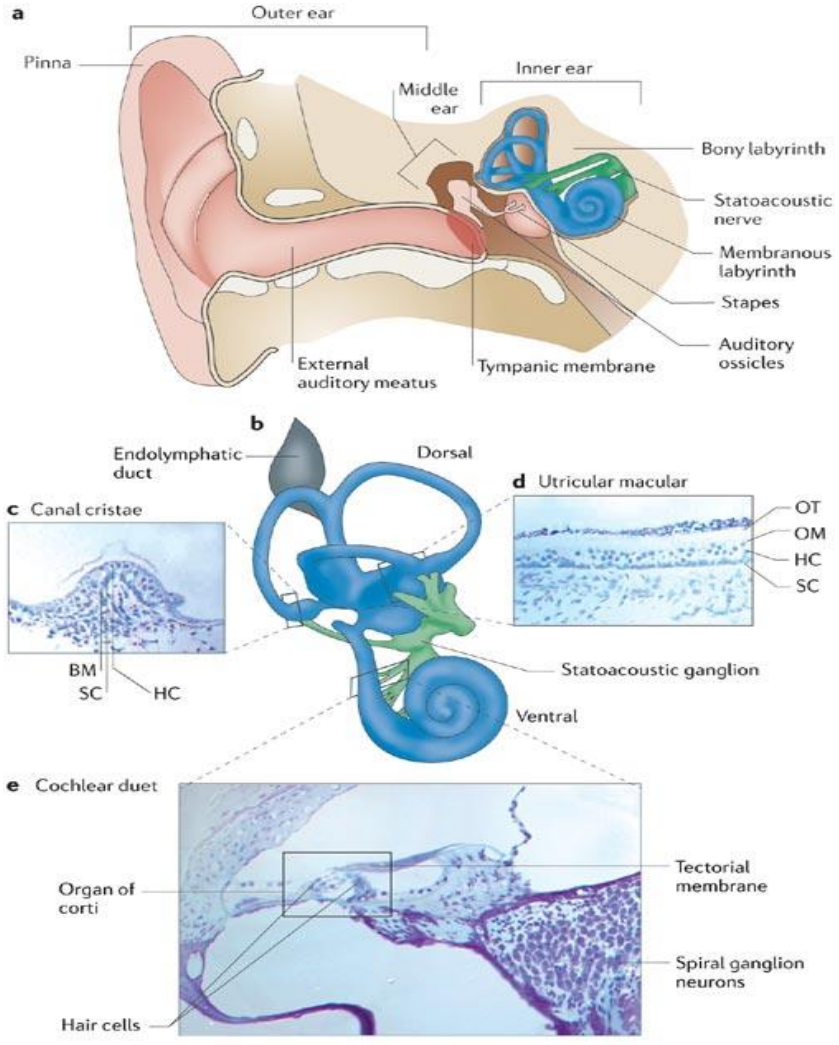


Figure 1.1 a. Schematic representation of adult human ear. This picture demonstrates a cross-section through the human head showing the three (outer, middle and inner) regions of the auditory system. b. The isolated membranous labyrinth, endolymphatic duct and statoacoustic ganglion. Dorsally, the membranous labyrinth includes the vestibular portion that mediates the senses of balance and acceleration, and ventrally includes the auditory region responsible for the sense of hearing. e. A cross-section through the cochlear duct that demonstrates the sensory epithelium (the organ of Corti; boxed region) and the associated spiral ganglion neurons. Adapted from M.W. Kelley (Kelley 2006).

The specialised regions of sensory epithelia, cristae and maculae, consist of two cell types, the mechanosensory hair cells that have a common structure to the organ of Corti's hair cells, and a variety of non-sensory supporting cells arranged together in a mosaic pattern. Hair cells of vestibular organs are covered by gelatinous acellular

membranes that upon head movements stimulate the hair cells upon (Lundberg et al., 2006) (Figure 1.1 c-e).

The auditory portion of the inner ear is the ventrally located cochlea (Figure 1.1 e). The cochlea is a spirally shaped tube and analysis of transverse sections demonstrate the presence of three separate chambers, the scala vestibuli, scala media and scala tympani (Figure 1.2). The endolymph-filled scala media, located in between the perilymphatic fluid filled scala vestibuli and tympani, is separated by Reissner's membrane (vestibular membrane) and the basilar membrane respectively (Figure 1.2).

The perilymph is a sodium-rich fluid and its origin is controversial. Two possibilities have been considered: 1) Perilymph is derived from cerebrospinal fluid (CSF). This is because perilymph has a comparable ionic composition to CSF and also because anatomically it is possible for the CSF to enter the cochlea via the cochlea aqueduct. 2) Perilymph is believed to be formed locally from the blood plasma by ionic or ultrafiltration mechanisms. This is because perilymph like other extracellular fluids has a high sodium ion and a low potassium ion composition and similar to these fluids, it may be formed locally from blood plasma.

A mature cochlea duct contains three walls: the floor which houses the organ of Corti and greater epithelial ridge, the lateral wall or stria vascularis and the medial wall that consists of Reissner's membrane (Figure 1.3). The stria vascularis and spiral limbus are important areas that are thought to play critical roles in setting up and maintaining the high potassium concentration of the endolymph of the scala media. Reissner's membrane has two layers, composed of a simple squamous epithelium at the upper surface and a neuroectodermal squamous epithelium at lower surface and it acts more than just a boundary membrane that separates high $K^+$ and low $Na^+$ endolymph from the perilymph. Reissner's membrane and the outer sulcus are thought to have a role in endolymph homeostasis by absorbing $Na^+$ from endolymph. The outer sulcus also has a role in $K^+$ absorption from endolymph in order to maintain the composition of endolymph that is essential for normal hearing.

The sensory epithelium of cochlea, the organ of Corti, sits on the basilar membrane, extends along the length of the coil of cochlear duct and acts as the primary auditory

organ. This organ has a remarkable structure that consists of two types of machanosensory hair cells, inner and outer hair cells and between five and seven types of non-sensory supporting cells (for instance border, phalangeal, pillar, Deiter's, Claudius', and Hensen's cells) that are arranged into a cellular mosaic. The number of rows of outer hair cells are different in different species with 3-4 in the normal human inner ear (Figure 1.3).

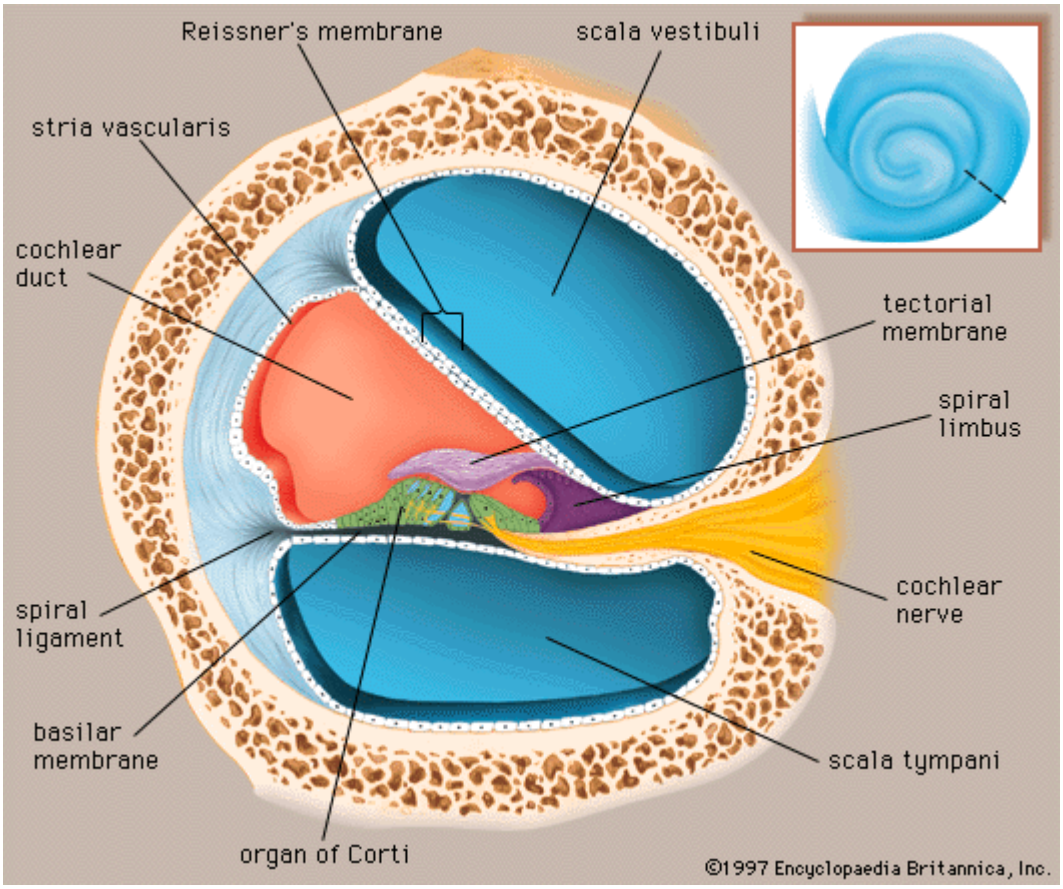


Figure 1.2 Schematic representation of a transverse section of the cochlea demonstrating the three chambers of the cochlea. Adapted from http://austinanatomy.blogspot.co.uk/

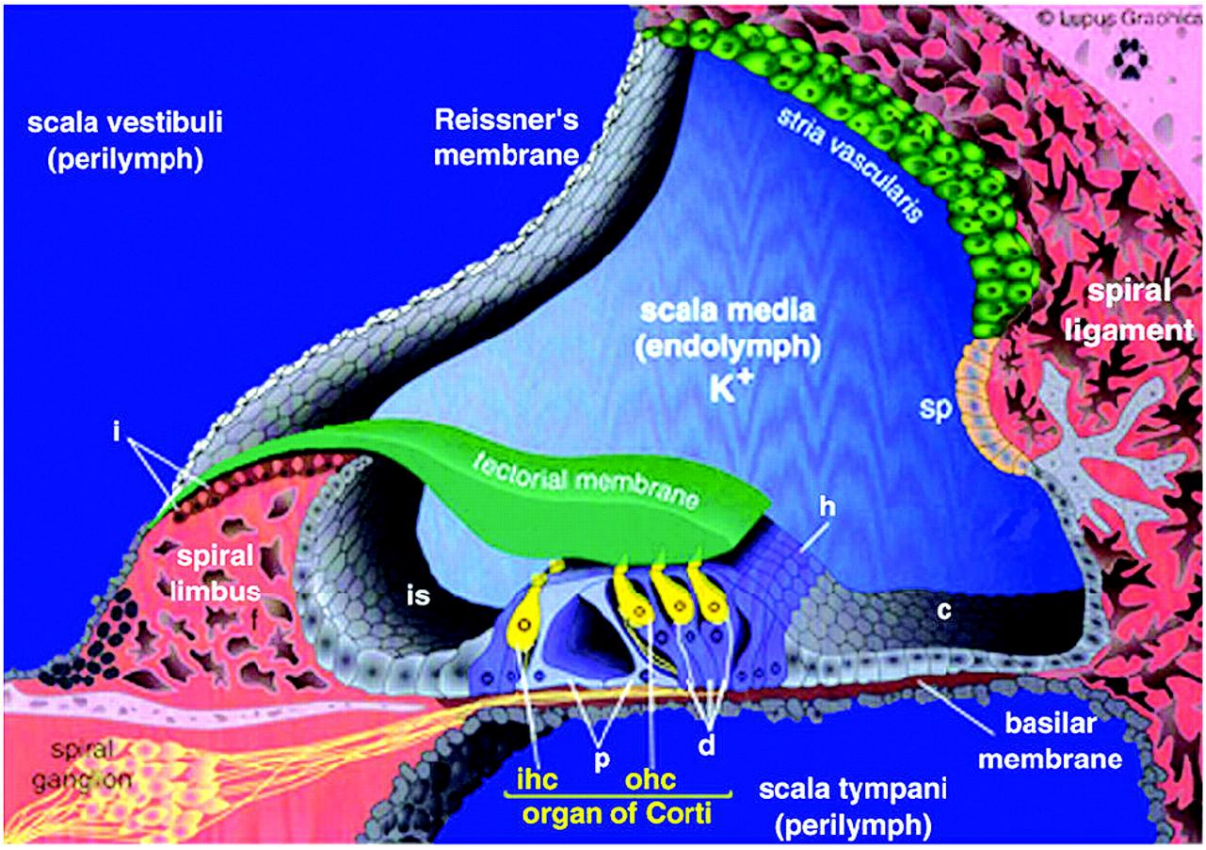


Figure 1.3 Schematic representations of the cochlear duct (scala media) and the organ of Corti. The organ of Corti is positioned on the floor of cochlear duct and consists of sensory hair cells (ihc, ohc) and supporting cells (p, d, h) with the tectorial membrane overlying them. Each sensory hair cell contains a stereociliary bundle on its top surface and will be deflected when the tectorial membrane shears. On the medial and lateral side, the organ of Corti is flanked by the inner sulcus (is) and Claudius' cells (c) respectively. On the lateral wall of the cochlear duct, the stria vascularis (sv) has the responsibility of controlling the unique ionic composition of the endolymph. Perilymph filled scala vestibuli and scala tympani surround the cochlea duct from the top and below respectively. i, interdental cells; ihc, inner hair cells; is, inner sulcus cells; p, pillar cells; ohc, outer hair cells; d, Deiter's cells; h, Hensen's cells; sp, spiral prominence. Adapted from Teubner et al. (Teubner, Michel et al. 2003).

The cochlea shows a tonotopic organisation; where hair cells at different positions along the cochlear duct respond to different sound frequencies. Hair cells at the base of the cochlea are sensitive to high frequencies, whilst those towards the apex are most sensitive to progressively lower frequencies and this continues in a gradient along the cochlear duct. A bundle of actin-filled stereocillia or microvilli is present on the apical surface of each sensory hair cell. These hair bundles are embedded in an overlying tectorial membrane. The tectorial membrane covers the apical surface of the organ of Corti and extends along the entire length of the cochlea.

Hearing is believed to be achieved by the following mechanism. Sound waves vibrate the tympanic membrane and are transferred and amplified by the middle ear ossicles to

the oval window (fenestra vestibule) causing compression of the fenestra vestibuli to the scala vestibule. This leads to the generation of a compression wave in the perilymph and ultimately depression and movement of the basilar membrane relative to the tectorial membrane (Hudspeth 1989; Kaufman 1999). The stiffness of the basilar membrane along the cochlea varies and it vibrates in response to sound-induced movements of the cochlear fluids causing the stereocilia bundles of outer hair cells (OHCs) to shear against the tectorial membrane (Gavara and Chadwick 2009). The OHCs have a role in amplifying the sound whereas it is the inner hair cells that are the primary sensory cells that detect sound and transmit it to the brain via auditory nerve. The stereociliary bundles are asymmetric, directionally sensitive and morphologically polarized in a way that all the bundles within an area of the sensory epithelium are lined up in the same plane (Barald and Kelley 2004). Deflections of stereocilia along its axis in inner and outer hair cells stretches tiplinks that leads to the opening of transduction channels, and therefore induces a receptor potential and modulates neurotransmitter release onto the postsynaptic spiral ganglion neurons (Fettiplace and Hackney 2006).

In addition to the sensory chambers described above, the inner ear consists of the endolymphatic duct (ED), which is positioned dorsally and communicates with the central nervous system (CNS). This communication is believed to be important for the transfer of CSF to the inner ear that following modifications will form the endolymph (Barald and Kelley 2004). The unique ion composition of the endolymph is critical for normal neuronal function. Apart from the CSF, other source of endolymph production has been proposed: (1) Endolymph is produced from perilymph, by ions selectively transporting through the Reissner's membrane. (2) Endolymph is produced by the highly vascularised, secretory cells of stria vascularis and vestibular dark cells (Ciuman 2009).

The developing inner ear epithelium is surrounded by mesenchyme of mesodermal origin (periotic mesenchyme), which in response to induction by otocyst epithelium between 11.0-13.0 days post coitum (dpc) chondrifies and forms the otic capsule between 13.0-14.0dpc.

## 1.2 Embryology of the ear in the mouse

### 1.2.1 Early embryology of the otocyst

The first visible sign of inner ear development is the appearance of bilateral ectodermal thickenings of cephalic surface ectoderm, the otic placode, adjacent to rhombomeres five and six of the developing hindbrain around 8.5dpc in the mouse. The otic placode forms in response to inductive signals from surrounding tissues such as the hindbrain and cranial paraxial mesoderm, which lies under the otic placode. In addition, axial mesoderm and endoderm has also been suggested to play roles in the induction process (Ladher, Wright et al. 2005).

After induction the placodal ectoderm thickens and invaginates to form otic cup by 9.0dpc. The cup then closes and pinches off from the surface ectoderm to form the otocyst or otic vesicle, a simple epithelial-lined sac (Barald and Kelley 2004) . Otic vesicle development until 10.5dpc requires a sequence of inductive signals to and from the hindbrain (Li and McPhee 1979; Water 1983). The epithelium of the otic vesicle gives rise to the primary neurons of vestibuloacoustic ganglion, the sensory epithelia and nonsensory tissues of the mouse inner ear.

*In vitro* explant experiments demonstrated that in mice, the cochlea is derived from the ventral half of the 11- day otic vesicle (Li, Vandewater et al. 1978) and the interaction between the otocyst and the surrounding periotic mesenchyme are necessary for the formation of cochlea, and to a lesser degree, the vestibular part of the inner ear (Water 1983). Furthermore, removal of periotic mesenchyme from the ventral part of the otocyst led to the absence of the coiling of the cochlea (Li and McPhee 1979).

During and after the formation of otocyst, neuroblasts delaminate from the anteroventral part of the otocyst and aggregate to form the developing vestibuloacoustic (VIII) ganglion. The differentiation of these cells gives rise to bipolar neurons that send axons into the presumptive sensory patches and to the brain stem (Knowlton, 1967; Meier, 1978a and b; D'Amico-martel and Noden, 1983). In mouse, after 10.5dpc the otic vesicle elongates along the DV axis (Cantos, Cole et al. 2000).

The otic vesicle then undergoes elaborate morphogenetic changes so that the cochlea, three semicircular canals, the utricle and saccule, and the endolymphatic duct and sac are formed. The morphogenesis of the otic vesicle begins with an evagination of the epithelium at the dorsomedial side to give rise to the primordium of the endolymphatic duct/sac. Cochlea development is initiated by elongation of the ventral portion of the otic vesicle in the ventral direction, and around 11.5dpc the development of semicircular ducts begins by evagination of the dorsal otocyst (Morsli, Choo et al. 1998).

### 1.2.2 Vestibular development

The development of vestibular part of the otic vesicle is similar in higher vertebrates such as mice, chicks and frogs but different from lower vertebrates such as zebrafish. In higher vertebrates, first from the dorsolateral part of the otic epithelium, the vertical canal plate is formed by outpocketing or envagination. The development of a groove in this plate will separate the vertical plate into two regions from which the anterior and posterior semicircular ducts will form. At the same time, from the lateral part of the otic epithelium there is an evagination of the lateral (horizontal) canal plate that will form the lateral semicircular duct (Leon, Sanchez-Galiano et al. 2004; Mansour and Schoenwolf 2005). After the canal plates have been formed, the two epithelial sheets become centrally detached from the mesenchyme that is surrounding them, approach and contact one another at the central region to form a fusion plate (Bissonnette and Fekete 1996). In zebrafish however, semicircular canals form in an entirely different manner. There are no outpouchings of the epithelium from the otic vesicle. Instead the epithelium invaginates from otic vesicle at four sites into the vesicle lumen. These opposing protrusions meet and fuse to form the equivalent of a fusion plate. Central epithelial cells are removed from the fusion plate to generate the canals, leaving a hole where the fusion plate had been (Haddon and Lewis 1996; Leon, Sanchez-Galiano et al. 2004; Mansour and Schoenwolf 2005). The order of the appearance of cell death (or dedifferentiation) in these canals to remove the fusion plate follows the order of semicircular canal development which is first the anterior, then the posterior and finally the lateral. Parallel to the central clearing, an ampulla at the base of each canal is formed which houses its respective crista (Bok, Chang et al. 2007). By 13.5dpc all three semicircular canals are well formed and the superior and posterior semicircular canals

are joined at the crus commune, and by 15.5dpc the ampulla are readily apparent (Morsli, Choo et al. 1998).

### 1.2.3 Molecular biology of cochlear development and sensory epithelia formation

The development of the cochlea begins around 10.75dpc emerging as a ventral bulge of the otocyst (Morsli, Choo et al. 1998). The cochlea anlage then continues to expand ventrally and at 11.5dpc can be seen as an extension of the ventral part of the otocyst (Figure 1.4). At 12.0dpc the cochlea has a more complex shape consisting of proximal and distal parts, with the proximal part extending ventromedially and the distal part extending anteriorly and, adapts a hook-like shape (Morsli, Choo et al. 1998; Bok, Chang et al. 2007) (Figure 1.4). The cochlear duct continues to extend and begins to coil consisting of one and a quarter turns at around 14.0dpc and finally the mature mouse structure consists of one and three quarter turns by 17.5dpc (Figure 1.4).

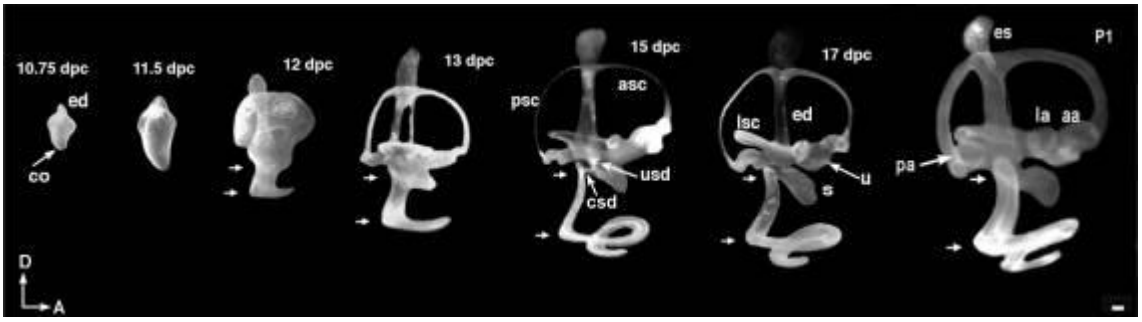


Figure 1.4 Stages of mouse inner ear development. The membranous labyrinth is paintfilled from 10.75dpc to postnatal day (P) 1. Arrows demonstrate the growth of the proximal part of the developing cochlea. aa, anterior ampulla; asc, anterior semicircular canal; co, cochlea; csd, cochleosaccular duct; ed, endolymphatic duct; es, endolymphatic sac; la, lateral ampulla; lsc, lateral semicircular canal; pa, posterior ampulla; psc, posterior semicircular canal; s, saccule; u, utricle; usd, utriculosaccular duct. Orientation: D, dorsal; A, anterior. (Scale bar = 100 μm.) Adapted from Cantos et al. (Cantos, Cole et al. 2000).

All cell types within the membranous labyrinth of the inner ear were originally thought to be derived from multipotent epithelial progenitor cells located in the otocyst together with a contribution from the neural crest derived melanocytes that gives rise to the intermediate cells of the stria vascularis. Recent fate mapping studies, however, demonstrated that the mammalian inner ear is originated not only from the sensory placode ectoderm but also a contribution from the neuroepithelial cells (NECs)

including neural crest cells (Freyer, Aggarwal et al. 2011). The descendants of NECs were shown to be localized to the cochleovestibular ganglion (CVG) and the sensory epithelia of the cochlea, utricle, and saccule.

Cell types in the membranous labyrinth include prosensory cells (that will develop as either hair cells or supporting cells), proneural cells (that will develop as auditory or vestibular neurons), and nonsensory cells (all other otocyst derived cells). The timing of specification of prosensory cells is not yet clear but the expression of *Jagged1, Lfng* and *Bmp4* (markers for prosensory patches) have been detected in the mouse otocyst by E10 (9.5dpc). The deletion of *jagged1* leads to the reduction or absence of most of the prosensory cells within the ear (Kiernan, Ahituv et al. 2001; Tsai, Hardisty et al. 2001; Brooker, Hozumi et al. 2006; Kiernan, Xu et al. 2006) but the deletion of either *Lfng* or *Bmp4* does not result in loss of hair cells or supporting cells (Zhang, Martin et al. 2000; Chang, Lin et al. 2008) but does effect vestibular development. This is suggestive of a role for Notch signalling in the specification of prosensory cells via Jagged1. The *Sox2* transcription factor also plays an important role in prosensory cell specification and is required for its formation (Kiernan, Pelling et al. 2005). The development of the prosensory domain was shown to be severely affected in *Sox2* mice mutants (Kiernan, Pelling et al. 2005). It was demonstrated that when the otocyst-specific promoter of *Sox2* is mutated (*Sox2Lcc* and *Sox2Ysb*) in mice, the formation of the prosensory region is impaired and both mechanosensory hair cells and supporting cells are completely (*Sox2Lcc*) or nearly completely (*Sox2Ysb*) absent (Kiernan, Pelling et al. 2005). These results are consistent with a role for Sox2 in the specification of the prosensory region. *Eyes absent homolog 1 (Eya1),* a transcriptional co-activator, may also be important in prosensory specification. Its expression co-localizes with *Sox2* in the ventral wall of the otocyst, the region that gives rise to the prosensory lineage. As development proceeds, *Eya1* and *Sox2* expression partially overlaps; with *Eya1* expression eventually becoming restricted to hair cells whereas *Sox2* expression becomes restricted to supporting cells (Hume, Bratt et al. 2007; Dabdoub, Puligilla et al. 2008; Zou, Erickson et al. 2008).

By E12, the otocyst has begun to develop morphologically into the cochlea and vestibule. “At 11.5dpc (E12) the progenitors of the hair cells and supporting cells are still dividing” (Ruben 1967) and the organ of Corti is just recognizable as a thickened

epithelial ridge in the cochlear region of the otocyst. By E12.5 (12.0dpc) six different sensory patches in the inner ear can be identified by gene expression. These are three cristae associated with each semicircular canal, the maculae of the utricle and saccule and the organ of Corti.

Precursor cells in the nascent organ of Corti exit the cell cycle between E12 and E16 (11.5dpc and 15.5dpc) (Ruben 1967). More than 80% of these cells exit the cell cycle between E13 and E14, with a higher possibility of the cells located in the apex exiting the cell cycle before those located in the base (Ruben 1967) i.e. an apex-base gradient of cell cycle exit. The factors important for the establishment of this wave of terminal mitosis are not fully known.

Cyclin-dependent kinase inhibitor (CKI) $p27^{Kip1}$ expression is induced in the primordial organ of Corti at the same time as the organ of Corti cells exit the cell cycle. $p27^{Kip1}$ is believed to regulate withdrawal of progenitors of hair cells and supporting cells from the cell cycle and also determines the size of the prosensory precursor cell pool (Chen and Segil 1999; Lee, Liu et al. 2006). When progenitor cells exit the cell cycle, there is very little cell proliferation and apoptosis in this developing sensory epithelium (organ of Corti) (Ruben 1967).

$p27^{Kip1}$, one of the first molecular markers of primordial organ of Corti, begins to be expressed at E12.5 in the apex and by E14 the entire prosensory domain of the cochlear is $p27^{Kip1}$ positive, forming the zone of non-proliferating cells (ZNPC) (Lee, Liu et al. 2006). At around E14, the terminal mitosis in the prosensory domain of the cochlea is complete and it is at postmitotic status. This is when differentiation of hair cells begins in the mid-basal region (in contrast with the apical to basal cell cycle exit pattern) of the cochlear duct and proceeds bidirectionally (Lee, Liu et al. 2006).

A common progenitor in the developing cochlea gives rise to both hair cell and supporting cell lineages (Fekete, Muthukumar et al. 1998). The differentiation of hair cells from this common progenitor requires the function of atonal homolog Math-1 (Atoh1), a basic-helix-loop-helix (bHLH) transcription factor. Atoh1 expression begins between E13.5 and E14.5 in the mid-basal region of the cochlear duct (Chen, Johnson et al. 2002), where the morphological signs of hair cell differentiation first appears (Sher

1971; Lim and Anniko 1985). From E14.5 onwards the wave of expression of Atoh1 in newly postmitotic precursor cells spreads from the cochlear base towards the apex for several days until differentiation is complete at about E17.5 (Lee, Liu et al. 2006) i.e. in the opposite gradient to cell cycle exit. The expression of $p27^{Kip1}$ is downregulated in differentiating hair cells but detectable in the differentiating supporting cells of the mature organ of Corti up to adulthood (Chen and Segil 1999; Lee, Liu et al. 2006). Atoh1 is one of the earliest, and the only factor reported so far whose expression is sufficient for hair cell formation as long as cells are competent to respond to Math1.

The specification of hair cell versus supporting cells following terminal mitosis is mediated in part by Notch signalling "lateral inhibition". Following the expression of Atoh1 which leads to establishment of a prosensory domain, presumptive hair cells within this domain begin to express the Notch ligands, *Jagged2 (Jag2)* and *Delta1 (Dll1)* which results in increased activation of Notch in surrounding cells. This initiates the lateral inhibition process and prevents these surrounding Notch activated cells from adopting the hair cell fate. These neighbouring cells begin to express two Notch target genes *HES1* and *HES5* (Lanford, Shailam et al. 2000; Zheng, Shou et al. 2000) and develop as supporting cells (Kelley 2007). It has been shown that deletion of *Notch1*, *Jag2*, *Dll1*, *HES1* or *HES5* genes leads to an over-production of hair cells (Lanford, Lan et al. 1999; Zheng and Gao 2000; Kiernan, Xu et al. 2006).

At this stage the committed hair cell begins to express further transcription factors that are necessary for its differentiation and survival. These factors include, the Pou-domain transcription factor Pou4f3(Brn3c) (Erkman, McEvilly et al. 1996; Ryan 1997; Xiang, Gao et al. 1998), the zinc-finger transcription factor Gfi 1 (Wallis, Hamblen et al. 2003; Hertzano, Montcouquiol et al. 2004) and the homeodomain protein Barhl1 (Li, Price et al. 2002). In contrast to hair cells, the factors that specify individual supporting cell types are less well understood. Supporting cells are known to be induced by hair cells through unknown signalling molecules (Puligilla and Kelley 2009). However the involvement of FGF signalling in pillar cell formation has been shown since deletion of *Fgfr3 or Fgf8* in the inner ear leads to defects in pillar cell formation (Colvin, Bohne et al. 1996; Hayashi, Cunningham et al. 2007; Jacques, Montcouquiol et al. 2007; Puligilla, Feng et al. 2007).

Sox2, which marks the prosensory damain together with its downstream target Prox1, act as inhibitors of Atoh1 (by antagonism of Atoh1) and its downstream targets such as Gfi 1 and therefore, prevent hair cell formation and assist with supporting cell specification (Dabdoub, Puligilla et al. 2008; Kirjavainen, Sulg et al. 2008).

Development of the organ of Corti continues throughout in utero development and into the early postnatal period, with the onset of hearing function around postnatal day (P) 10 to 14 in mice (Driver and Kelley 2009).

A non-cellular aspect of the ear that is critical for hearing is the correct development of the tectorial membrane to overlay the hair cells. The tectorial membrane consists of collagen fibres together with the α- and β-tectorins, two of the main noncollagenous glycoproteins. α- and β-tectorin have been reported to be transiently expressed in supporting cells during cochlea development in mouse, beginning at E12.5 and not detectable in the cochlea after P22 (Rau, Legan et al. 1999).

### 1.2.4 Programmed cell death during the development of inner ear

Programmed cell death (PCD) is an essential cellular process for accurate morphogenesis during the normal development of the inner ear. The developmental morphogenetic changes depend on cellular division, growth, migration, differentiation and apoptosis. The analysis of apoptosis distribution during the development of human and mouse inner ears by the TUNEL method and computer-assisted three-dimensional reconstruction of serial histological sections demonstrated localized foci of apoptosis are mainly associated with the differentiation of the sensory otic epithelia and also with the innervation of the cochlear and vestibular epithelia from the vestibuloacoustic ganglion (Nishikori, Hatta et al. 1999). The importance of PCD for the accurate development of inner ear in vertebrate is supported by the observation of comparable loci of cell death in fish, frog, birds and mammals (Leon, Sanchez-Galiano et al. 2004).

### 1.2.4.1 Apoptosis at early stages of inner ear development

Cell death occurs from the earliest stages of inner ear development; during initial placodal invagination, otocyst formation and during the vestibuloacoustic ganglion formation. For example in chicken and mammals a high number of apoptotic cells were detected at the edges of the otic cup related to its inward involution. During otocyst formation this spot remains around the otic pore (Figure 1.5). The otic pore closure also comes with cell death. This area is needed to eliminate the otic pore lumen and to separate the otocyst from the surface ectoderm (Alvarez and Navascues 1990; Sanz, Leon et al. 1999; Lang, Bever et al. 2000; Nikolic, Jarlebark et al. 2000).

### 1.2.4.2 Apoptosis during the development of cochlea

A zone of cell death in the ventromedial wall of otic epithelium lasts for some time during the cochlear duct elongation, remaining at the proximal rim of the duct_in the region where it makes contact with the saccule (Figure 1.5) (Marovitz, Shugar et al. 1976; Fekete, Homburger et al. 1997; Nishikori, Hatta et al. 1999; Lang, Bever et al. 2000; Nikolic, Jarlebark et al. 2000). This area is between the dorsal and ventral parts of the developing otic vesicle at a time when the inner ear is going under elaborate morphological changes in both halves, and therefore this region may act as a signalling center for modulating regional differences in the inner ear (Bever and Fekete 1999). The relevance of cell death here is not known but this area of apoptosis region is not present in lower vertebrates (Bever and Fekete 1999). Because the main morphological difference of the lower and higher vertebrate ears is in their ventral part, the lack of this ventromedial apoptotic region might suggest that in higher vertebrates, cell death plays a specialized role in the development of the cochlear duct (Bever and Fekete 1999) however experiments to explore this have not been reported.

As cellular differentiation begins in the auditory organ, other cell death hot spots appear. In the basilar papilla in chicken (Fekete, Homburger et al. 1997; Lang, Bever et al. 2000) and in the precursor of cochlea duct sensory epithelium in rat these hot spots of cell death have been reported between 11.5dpc-15.5dpc (Nikolic, Jarlebark et al. 2000) but not characterised in detail.

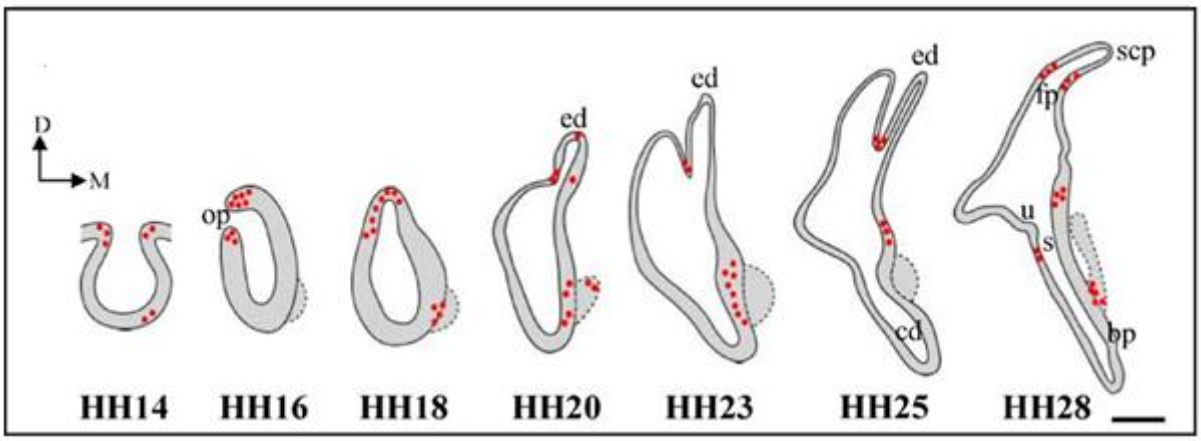


Figure 1.5 Apoptosis during the development of inner ear. Schematic representation of developing chicken inner ear and the apoptotic spots highlighted in red from stage HH14 to the HH28 that represents the apoptotic events taking place in the developing inner ear of mammals. Bar, 100µm. bp: basilar papilla, cd: cochlear duct, ed: endolymphatic duct, fp: fusion plate, op: otic pit, s: saccule, scp: superior canal pouch, u: utricle. Adapted from Leon et al. (Leon, Sanchez-Galiano et al. 2004).

A small but significant amount of apoptotic hot spot is also present during the early stages of hair cell differentiation and in early postnatal stages in the rat and chick (Fekete, Homburger et al. 1997; Zheng and Gao 1997). At stage 29 (about 6.0dpc) in chick these hot spots of cell death are reported in the neck of the cochlear duct, the lateral wall of the duct proximally, the medial wall of the duct distally, where the basilar papilla is forming, and near the lateral ampulla.

### 1.2.4.3 Apoptosis during the development of vestibular organs

Apoptotic hot spots have also been reported around the areas of endolymphatic duct formation, at the base of the evaginating endolymphatic duct, at the fusion site in chicken but not in mouse and human, and at the onset of differentiation in vestibular sensory epithelium (Marovitz, Shugar et al. 1976; Represa, Moro et al. 1990; Martin and Swanson 1993; Fekete, Homburger et al. 1997; Zheng and Gao 1997; Nishizaki, Anniko et al. 1998; Nishikori, Hatta et al. 1999; Sanz, Leon et al. 1999; Lang, Bever et al. 2000; Nikolic, Jarlebark et al. 2000).

### 1.2.4.4 Apoptosis in the vestibuloacoustic ganglion

There is considerable body of evidence that apoptosis is associated with the development of innervation from the vestibuloacoustic ganglion (VIII) in different

species. In mouse (Nishizaki, Anniko et al. 1998; Nishikori, Hatta et al. 1999), human (Represa, Moro et al. 1990; Nishikori, Hatta et al. 1999), chick (Ard and Morest 1984; Sanz, Leon et al. 1999; Lang, Bever et al. 2000), rat (Nikolic, Jarlebark et al. 2000), frog and zebrafish (Bever and Fekete 1999) apoptotic cells have been detected in the developing vestibuloacoustic ganglion throughout the embryonic and early postnatal stages.

In mouse (Nishizaki, Anniko et al. 1998; Nishikori, Hatta et al. 1999) apart from the above mentioned restricted spot of cell death at the ventromedial wall of the otic epithelium (Figure 1.5) that spatiotemporally coincides with the delamination of neuroblasts from the otic vesicle, apoptotic cells have also been detected in both cochlear and vestibular ganglion cells once immature neurons have been formed and cell proliferation has stopped. This apoptotic hot spot is also reported in other higher vertebrates including chick (Ard and Morest 1984; Lang, Bever et al. 2000) and rat (Nikolic, Jarlebark et al. 2000).

In mouse, these two hot spots have been reported at E10.5 and E14, when vestibular and cochlear portions first receive nerve supplies from the vestibuloacoustic ganglion respectively (Nishikori, Hatta et al. 1999).

In addition, the presence of apoptotic cells was also reported in both cochlear and vestibular epithelia at the time of their innervation and sensory epithelium differentiation in both human and mouse. In human at stage 19 and in mouse at 13.5dpc, the cochlea epithelium first receives the nerve supply from the vestibuloacoustic ganglion (Nishikori, Hatta et al. 1999). In the areas that receive nerve supplies, the basement membrane disappears and at the basal side of the epithelium, apoptotic cells were detected (Nishikori, Hatta et al. 1999) that may underlay the encroaching neurons. In rats as well, at late stages of embryonic development when cochlear duct size has increased and its basal, middle and apical turns have formed, apoptotic cells have been detected in the cochlea ganglion in the base and middle turns, which coincides with the areas where the cochlea ganglion is growing (Nikolic, Jarlebark et al. 2000). However the specific identity of cells undergoing apoptosis was not reported.

Finally, the cavitation of perilymphatic spaces that is one of the major steps in later cochlea differentiation, was also shown to be associated with some small spots cell death in rat (Nikolic, Jarlebark et al. 2000).

Overall a picture is emerging of areas of apoptosis that are either (at earlier proliferative stages) involved in the elimination of cells over-produced by mitosis, while more controlled apoptosis at later developmental stage associated with differentiation may remove any unneeded extra cells in both the vestibular and auditory organs (Nishizaki, Anniko et al. 1998). Therefore, the observation of apoptotic cells in the cochlear and vestibular epithelium when innervation and differentiation are simultaneously happening is likely an indication of a programmed elimination of unneeded cells after differentiation of epithelial cells rather than proliferation (Nishikori, Hatta et al. 1999).

### 1.3 Identification of clusterin mRNA from the mouse inner ear

Prior to this project, in an attempt to identify genes that are involved in the normal development of inner ear, suppressive subtractive hybridisation was used to screen normalised 13.5dpc mouse inner ear cDNA against normalised cDNA from the 10.5dpc mouse otic vesicle in a developmental-stage cDNA subtraction (Powles, Babbs et al. 2004). 71 clones were recovered from the subtraction that demonstrated significant induction (more than 5 fold differences in signal intensity) that were subsequently sequenced and following BLAST analysis against the public DNA databases , 33 different genes were identified. Gene specific and control primers were used to confirm the presence of these transcripts in native 13.5dpc mouse inner ear and most importantly to determine relative transcription levels of subtracted genes compared to the 10.5dpc otic vesicle. The mouse clusterin gene was among the subtracted genes that demonstrated a strong upregulation at 13.5dpc when compared to 10.5dpc (Powles, Babbs et al. 2004) (Figure 1.6). *In situ* hybridisation was carried out for a selected few genes isolated in this study at 13.5dpc. Clusterin was the only gene with restricted expression in the developing cochlear sensory epithelium (Ficker, Powles et al. 2004). This result suggests that the clusterin gene may potentially be involved in the development of the auditory sensory organ. Given the highly specific expression in the

cochlear sensory epithelia, this research project was initiated to further explore the expression and regulation of clusterin in the developing inner ear of the mouse. The exact function of clusterin during mouse development has not yet been addressed. However, a number of putative roles have been suggested and are reviewed below.

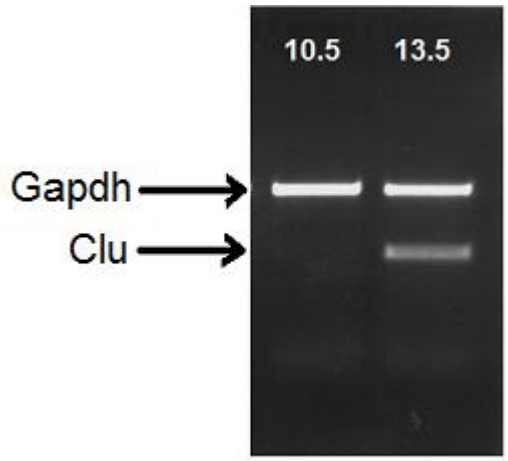


Figure 1.6 Clusterin mRNA upregulaion at 13.5dpc. The relative transcript abundance of clusterin gene in 13.5dpc mouse inner ear was compared with 10.5dpc mouse otic vesicle by RT-PCR using gene-specific primers and Gapdh control primers. Clusterin expression is upregulated at 13.5dpc in comparison to 10.5dpc.

### 1.4 Clusterin gene structure and transcripts in mammals

The clusterin gene is present in all mammalian genomes studied, with very high levels of homology among species. There is 81% nucleotide sequence similarity between mouse and human clusterin gene and 75% similarity at the amino acid level (Jordanstarck, Lund et al. 1994) across the whole gene. Clusterin is encoded by a single gene, located on mouse chromosome 14, and in humans on chromosome 8p21, adjacent to the lipoprotein lipase gene; the gene is present on chromosome 15 in rat (Goldnersauve, Szpirer et al. 1991). Clusterin gene contains nine exons in mouse, human and rat spanning approximately 13Kb in mouse, 18Kb in human and 39Kb in rat. The proximal promoter region is highly conserved between human, mouse, rat and quail clusterin genes which will be discussed in more detail below (1.9).

Several mRNA variants have been reported so far for CLU, although their biological relevance has yet to be demonstrated. The different variants are believed to arise from

the use of “alternative transcriptional initiation start sites” possibly driven by two distinct promoters and “alternative splicing of CLU mRNA”.

In humans, at least two distinct CLU mRNA isoforms that differ in their unique exon I exist as a result of alternative transcriptional initiation start sites, Isoform 1 and Isoform 2 (GenBank accession number NM_001831.2 and NM_203339.1, respectively) (Figure 1.7). Similarlyorganised transcripts have only been detected to date in chimpanzees. Using the ASAP (Alternative Splicing Annotation Project) database (Lee, Atanelov et al. 2003) another probable mRNA transcript seems to be Isoform 11036 (Figure 1.7).

Isoform 1 has a 5’-extended sequence and is predicted to encode a protein of 501 amino acids of molecular weight 57.8 kDa. Computational analysis of isoform 1 predicts subcellular localization using the PSORT programme (Horton, Park et al. 2007), where the protein product should have a cytoplasmic/nuclear localization (Horton, Park et al. 2007) and this has been thought to account for the existence of an intracellular form of CLU that escapes the secretory pathway.

For isoform 2, exon 1 is not translated and a protein with 449 amino acids that is destined for secretion is predicted to be produced from this mRNA. The exon 1 of Isoform 11036, is positioned between the exon 1 of the other two Isoforms (Figure 1.7) with its first functional ATG in exon 1 and is predicted to give rise to a protein of 460 amino acids with prevalent nuclear localization (Horton, Park et al. 2007). Located in exon 3 there is a third ATG, which is again in-frame with the other ATGs (Figure 1.7). A shorter form of the CLU protein would be produced as a result of translation from this ATG, which is again predicted to localize to the nucleus (Scaltriti, Santamaria et al. 2004).

Leskov et al. 2003 reported an alternative CLU mRNA in MCF-7 cells (Leskov, Klokov et al. 2003). In this transcript, exon 2 of isoform 1 is spliced out and therefore exon 1 is

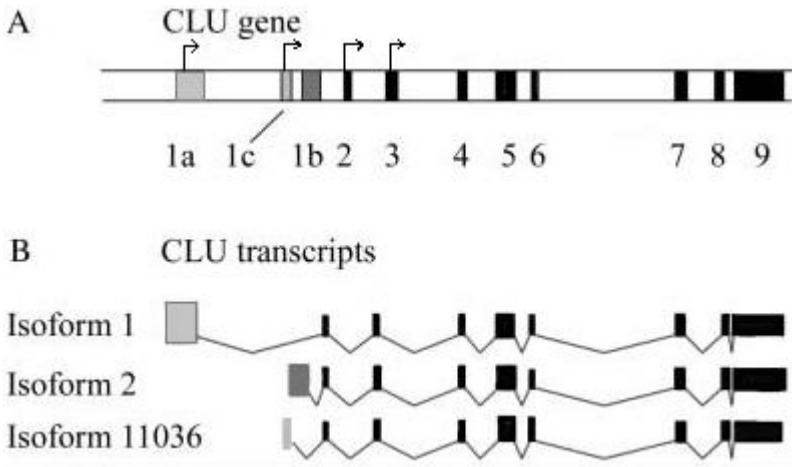


Figure 1.7 Clusterin gene and its transcripts in human. A: Structure of CLU gene on human chromosome 8. Black blocks represent exons 2-9 which are common to all transcripts. Grey blocks represent unique exon 1 of CLU isoforms. B: Schematic representation of CLU mRNA variants. Dark grey exon: exon 1a of isoform 1; medium grey exon: exon 1b of isoform 2; light grey exon: exon 1c of isoform 11036. Black arrows represent the in-frame ATG translational start sites. Isoform 1 contains an ATG in the first exon. Located in exon 2 is a second ATG (the first one for isoform 2 and common to the three transcripts). This second ATG is located right before a functional ER-localization leader sequence. There is also a third ATG common to all transcripts located in exon 3. Adapted from Rizzi et al. (Rizzi and Bettuzzi 2010).

directly spliced onto exon 3. This mRNA variant lacks the ATG in exon 2 and also the ER-localisation sequence. As at the time Isoform 1 was not known, this ATG was considered to be the first functional translational start site. Therefore, the author proposed that using the last ATG present in exon 3 this mRNA codes for a protein precursor called pnCLU (nuclear CLU precursor), a putative nuclear pro-death form. However, the existence of this CLU transcript has never been confirmed in other tissues or cell lines by other researchers so far (Cochrane, Wang et al. 2007; Schepeler, Mansilla et al. 2007).

It is now clear that loss of exon 2 would not result in the use of ATG in exon 3 for translation, but instead the use of an upstream and functional ATG in exon 1 would result in the production of a new protein isoform that is elongated at the N-terminus.

Based on the Leskov's predictions for splicing the 5' end of clusterin, Savokovic et al. (2007) argued that because mouse and rat lack the corresponding human exon 3 ATG start codon, if a splice variant lacking exon 2 exists in rodents it would therefore lack a

start codon (Vuk Savkovic´ a, Ulrich Sack b et al. 2007). This argues against a "Leskov" isoform in mouse/rat.

Whilst human clusterin isoforms have been extensively studied, mouse clusterin mRNA and protein structure has been much less the focus of attention. Ensemble analysis shows the potential for 7-8 isoforms in mouse (Figure 1.8a), whereas the NCBI database (Figure 1.8b) only reports one transcript for mouse clusterin (NM_013492.2), and the translation seems to be from exon 2 (Figure 1.8b). This transcript also contains 9 exons similar to the first ensemble transcript.

There are two in-frame ATG sites in exon 2 and none in exon 1 and 3. The first ATG in exon 2 is used for the translation of sClu. The importance of a second ATG in mouse exon 2 which is a CAG in human is currently unknown.

Although there are reports of detection of the nuclear form of clusterin in the mouse, the molecular mechanisms behind its production is not yet known. Using Western blot and immunohistochemistry analysis, Sun et al. 2007 reported the presence of nClu in normal mammary gland epithelia cells in mouse (Sun, Zhang et al. 2007). The Leskov clusterin alternative splicing theory does not seem to apply for the production of nClu in mouse, as both ATG sites will be lost as a result of exon 2 becoming spliced out. Therefore other mechanisms for nClu production have been proposed. Internal ribosome entry sites (IRES)-dependent translation for instance could be a possible mechanism of nClu production (personal communication with Koch-Brandt, Claudia, Johannes Gutenberg-University of Mainz). The IRES-mediated translation is a cap-independent mechanism that allows translation to take place at internal initiation sites in the mRNA and occurs mostly in the cells undergoing stress, during apoptosis, mitosis or growth arrest (Ovcharenko, Nobrega et al. 2004). Two other proposed ways for clusterin presence in intracellular regions (nuclear and cytosol) include the internalisation of secretory form under stress conditions or even under normal cellular situations that escapes the secretory pathway (Kang, Shin et al. 2005), and retrotranslocation from the Golgi to the cytosol via an ERAD-like pathway (Nizard, Tetley et al. 2007).

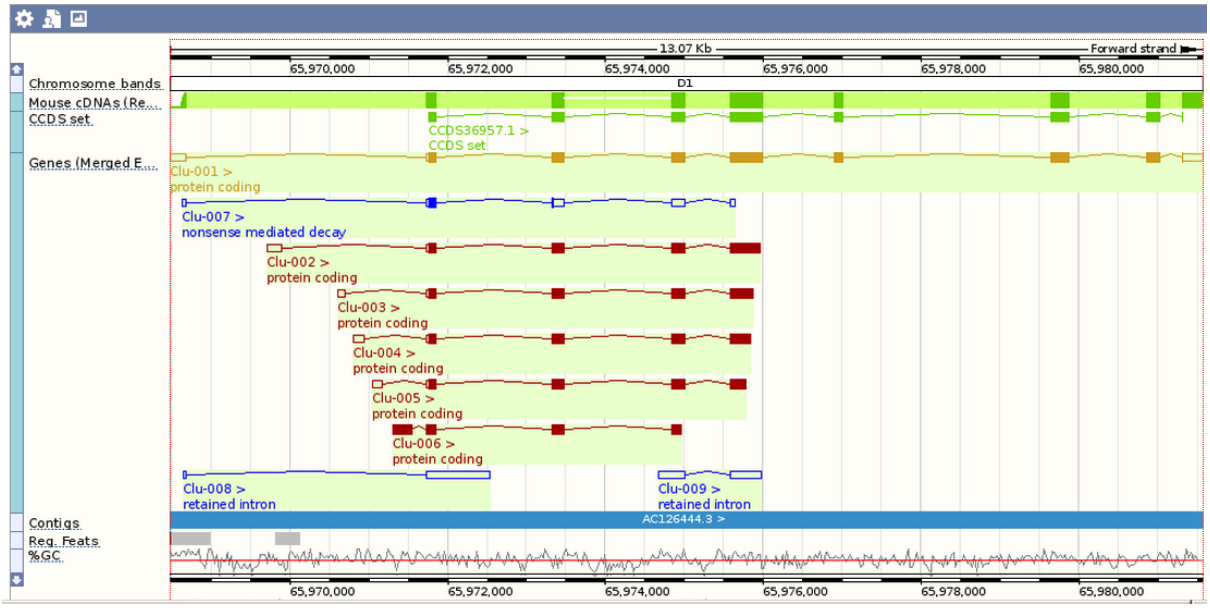


Figure 1.8a Mouse clusterin gene and transcript variants – from ensemble.org (August 2012)

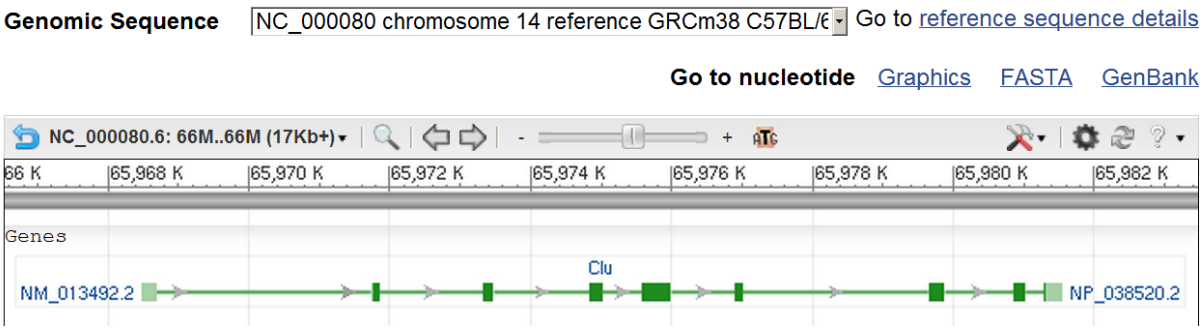


Figure 1.8b Mouse clusterin transcript on NCBI (August 2012)

## 1.5 Clusterin regulation

The expression of clusterin in a wide range of tissues and at very different levels and in response to different stimuli (development, pathology etc) suggests that expression is tightly regulated. A sequence alignment and comparison of the 5'-flanking regions revealed that the region of homology between mammalian (Human, mouse and rat) promoters is confined to a very restricted proximal domain immediately upstream of the transcription start site; regions further than 200bp appear completely diverged (Michel, Chatelain et al. 1997). This sequence comparison revealed that the proximal promoter (up to position -200bp) of clusterin was well conserved between mouse, rat and human

genes, with approximately 85% identity between mouse and rat, and 79% identity between mouse and human (Wong, Taillefer et al. 1994).

It is still unknown whether transcription of alternative mRNAs is initiated from the same or different promoters in mammals. CLU mRNA variants are differentially regulated by diverse signalling pathways (Cochrane, Wang et al. 2007; Schepeler, Mansilla et al. 2007) and also the observation of different CLU responses obtained from the identical growth factors (Trougakos and Gonos 2002) demonstrate the possibility of two alternative promoters in mammals like the avian gene (see below).

Most studies have focused on the defining the activity of the core promoter and closely adjacent 5' flanking sequences. The core promoter contains typical features including TATAA and GCATT boxes as well as several conserved transcription-factor-binding sites, including a heat shock element (HSE) that was mentioned earlier (1.8.1) at position –120bp relative to the transcription start site in the mouse gene that is important for the stress response.

A number of growth factors including transforming growth factor β, nerve growth factor, and epidermal growth factor have been reported to regulate the expression of the clusterin gene (Jin and Howe 1997; Gutacker, Klock et al. 1999; Jin and Howe 1999). These factors require an AP-1 (activator protein-1) motif located at -77bp present in human, mouse and rat promoter regions of the clusterin gene to induce its expression. Unlike the HSE, the AP-1 element is not present in the quail promoter (Michel, Chatelain et al. 1997). c-fos, Fra1, Fra2, JunB, and JunD proteins bind to this regulatory motif *in vitro* (Jin and Howe 1999). Nerve growth factor (NGF) and epidermal growth factor (EGF) induced clusterin mRNA expression in PC12 cells and also the clusterin AP-1 motif conferred reporter gene expression in response to these two growth factors in PC12 cell transfections (Gutacker, Klock et al. 1999).

Other cis-elements in the 5' flanking region of the clusterin gene include motifs for B-myb, nuclear factor (NF1), and CBF transcription factors. B-MYB is thought to have a general role in cellular proliferation, survival and differentiation and is overexpressed or amplified in different kinds of human cancer (Lipsick, Manak et al. 2001). B-MYB binds to the B-myb binding site in the 5' flanking region at position -292bp of the

human CLU promoter and positively regulates its expression in human LAN5 neuroblastoma cell lines (Cervellera, Raschella et al. 2000). It is believed that CLU partly mediates the antiapoptotic effects of B-MYB.

Clusterin mRNA levels increase rapidly and significantly during early involution of the mouse mammary gland after weaning, and in the rat ventral prostate following surgical castration. Using DNase I foot-printing on clusterin 5' sequences apoptosis/involution specific nuclear factor 1 (NF1) binding element present at two position between -317 and -353 in the mouse clusterin proximal promoter region was identified as protected, and western blot analysis showed a 74-kDa NF1 isoform was induced in early involution in the mouse mammary gland; moreover NF1 binds the clusterin element as shown by EMSA and DNase I foot-printing analysis (Furlong, Keon et al. 1996).

The transcription factor CBF (core binding factor) interacts with a region spanning -436 to -302bp in the rat clusterin gene promoter and activates transcription in a Sertoli cell specific manner, as was shown by EMSA combined with hydroxyl radical foot-printing. The Sertoli cell enhancer region (SER) contains a core-enhancer element which in turn has Sp1 binding sites (Lymar, Clark et al. 2000). The Sp1 sites are required for the full activity of the core element as mutation of Sp1 sites resulted in significant decrease in promoter activity (Lymar, Clark et al. 2000).

The first intron of the mammalian clusterin gene may also contain regulatory elements based on a sequence comparison with the quail clusterin gene and also based on the "*in silico*" analysis of the human clusterin gene. There are two different promoters for the quail clusterin gene and both are active in quail QT6 cell lines in transient transfection assays (Michel, Chatelain et al. 1995). The first quail promoter is identical to the mammalian clusterin promoter and the second promoter contains some binding sites that are conserved in the first intron of the mammalian clusterin gene. These include two TGF-β inhibitory elements, an AP-1 and glucocorticoid receptor element. *"In silico"* analysis of human clusterin also revealed a CAAT box, a c-AMP responsive element, three conserved E-box elements which are believed to bind MYCN and several STAT elements (Rizzi, Coletta et al. 2009). The human clusterin gene has also been reported to contain the putative androgen response elements (ARE) in intron 1 (Cochrane, Wang et al. 2007).

## 1.6 Clusterin protein forms and structure

Different closely related forms of the clusterin protein have been reported to arise from the clusterin gene that have distinct sub-cellular and extra-cellular localization as discussed above with different functions attributed to them. The mechanism of production of these protein forms from the previously described clusterin transcripts is controversial amongst researchers.

However, the mouse clusterin protein that is best characterized is a secreted form (sCLU), a 75-80 kDa glycosylated heterodimer consisting of two 40 kDa subunits (α and β). The ATG translation start site for sClu is in exon 2 and produces a precursor protein that is targeted to endoplasmic reticulum (ER) by an initial leader peptide. The protein is then transported to Golgi, where it is heavily glycosylated and proteolytically cleaved at an internal site in the trans-Golgi or post-Golgi. The 21 amino acid long hydrophobic signal peptide is cleaved from the preprotein in the ER. The monomers consist of alpha peptide (residues 1-226) and beta peptide (residues 227-449) and are tightly bound together through five disulfide bonds (Choimiura, Takahashi et al. 1992; Kirszbaum, Bozas et al. 1992). This mature form of clusterin which has 449 amino acids is secreted extracellulary.

Other forms of CLU that has been reported include the intra-cytoplasmic precursor protein that is unglycosylated, and uncleaved sCLU precursors and can be detected at 60-64 kDa.

The nuclear form of clusterin was first reported by Reddy et al. (1996) who demonstrated that the intracellular form of CLU was induced in human liver HepG2 and mink lung CCL64 epithelial cell lines in response to treatment with TGF-β (Reddy, Jin et al. 1996). This shorter uncleaved, unglycosylated form targeting the cell nucleus (nCLU) has been reported by others since (Leskov, Klokov et al. 2003; Caccamo, Scaltriti et al. 2005). The precursor nuclear CLU (pnCLU) is detected in the cytosol that unlike sCLU, does not undergo extensive glycosylation or cleavage (Sun, Zhang et al. 2007). The structure and mechanism of production of nCLU is still unknown but it is known that some stimuli such as TGF-β (Reddy, Jin et al. 1996) and ionizing radiation (Yang, Leskov et al. 2000) prevent sCLU maturation and secretion, and give rise to

CLU translocation to the nucleus and intracellular sites. In response to ionizing radiation, CLU localizes to the nucleus of MCF-7 human breast cancer cells where it interacts with the DNA double-strand break repair protein complex, Ku70/Ku80 (Yang, Leskov et al. 2000). We still do not know about the structural domains characteristic of each different intracellular CLU protein form as well as the domains required for nuclear targeting.

It is very important to note that alternative CLU protein products have never been isolated, purified and crystallized. Therefore, it is unclear if the CLU proteins of different mass are the result of alternative transcription initiation, alternative splicing or represent CLU at different stages of maturation and translational modification (e.g cleaved, uncleaved, at different stages of glycosylation) (Rizzi and Bettuzzi 2010).

The functional clusterin protein is composed of two subunits derived from the clusterin gene. Based on structural and sequence analysis, different functional domains of clusterin protein are predicted. Mouse clusterin contains six potential N-glycosylation sites, a potential $Arginine_{226}$ – $Serine_{227}$ cleavage site to generate $\alpha$ and β subunits, a cluster of five cysteine residues in each subunit, three putative amphipathic α-helices, and four potential heparin binding domains (Jordanstarck, Lund et al. 1994). Furthermore, it contains 2 coiled-coil helices (Wilson and Easterbrook-Smith 2000) and these domains are illustrated in (Figure 1.10). Earlier the interactions of clusterin protein with a variety of molecules was discussed (1.8.1). But how does the clusterin peptide form these interactions? It has been suggested that the human clusterin protein has a highly flexible binding site allowing it to interact with a numerous ligands due to the combination of amphipathic α-helices and a natively disordered region (Bailey, Dunker et al. 2001). The amphipathic α-helices (Figure 1.10) of clusterin are suggested to be important in stabilizing both hydrophobic and hydrophilic interactions of clusterin protein with other molecules and thus are important for its chaperone action that were raised in section 1.8.1.

Apart from these domains, clusterin protein also contains motifs for secretion and differential intracellular localisation including three nuclear localization signals (NLS) in humans. The N-terminal of nCLU contains a NLS, amino acid LEEAKKK (Leskov, Klokov et al. 2003) that is conserved in all clusterin sequences (Jenne and Tschopp

1992) and is present in mouse at residues 73-79 (Appendix V.I). The nuclear localisation signal present in the mature protein is not utilised under normal homeostatic conditions since clusterin is translated in bound ribosomes and the protein is secreted (O'Sullivan, Whyte et al. 2003). Attempts to define the three NLS present in the human sequence showed these sequences were not necessary for nuclear targeting in PC-3 prostate cancer cells (Scaltriti, Santamaria et al. 2004), and in addition the mutation of NLS in MCF-7 cells did not prevent nCLU translocation to the nucleus after treatment with compounds that induce apoptosis (i.e anti-estrogen ICI and TNFα) (O'Sullivan, Whyte et al. 2003).

### 1.7 Clusterin receptors

One of the well-established roles of clusterin protein in the extracelluar context is its extracellular chaperon activity (1.8.1). Clusterin recognises misfolded/stressed proteins via exposed hydrophobicity regions and makes a stable complex with them. Clusterin-stressed protein complexes are then internalised via receptor-mediated-endocytosis in which they bind to the cell surface receptors and the complex is then uptaken into the cells for lysosomal degradation (Wyatt, Yerbury et al. 2009).

Megalin a low density lipoprotein (LDL) receptor, is the first reported clusterin receptor (Kounnas 1995) followed by the identification of ApoE receptor 2 (ApoER2) and very low-density lipoprotein receptor (VLDLR) as clusterin receptors (Bajari 2003).

Megalin is an endocytic receptor for multiple ligands and has been reported to be expressed in the cells of kidney, thyroid, lung, epididymis, breast and eye (Lundgren 1997). Megalin protein expression has also been detected in the cochlea in the rat inner ear in the marginal cells of stria vascularis, epithelial cells of spiral prominence and epithelial cells of Reissner's membrane (Kunihiro Mizuta 1999). Megalin mutant mice (megalin-/-) mice demonstrated progressive hearing loss that maybe due to defective interaction with β-estrogen ligand (Ovidiu Ko¨nig 2008) The function of megalin in inner ear is currently unknown but megalin and its ligands appear to have crucial role/s in hearing .

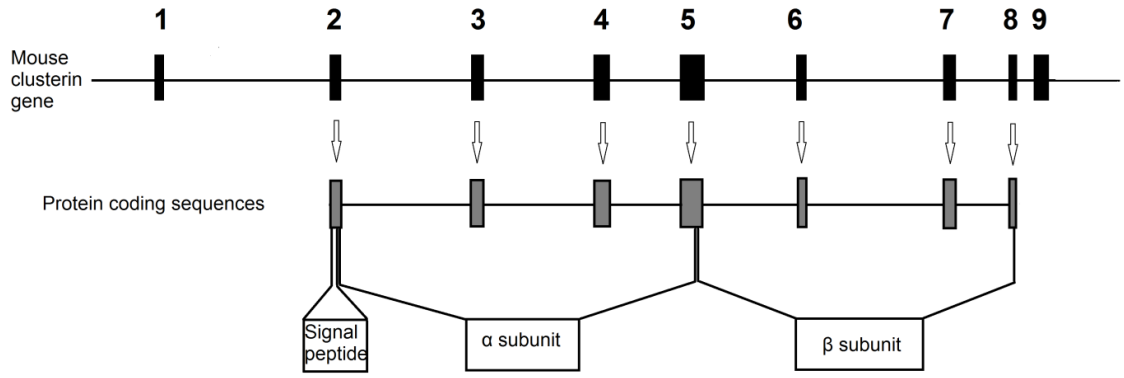


Figure 1.9 The mouse clusterin gene and its protein coding sequences**.** The exonic-intronic mouse clusterin gene structure is shown above and below represents the corresponding protein sequences. Mouse clusterin gene contains 9 exons and 8 introns encompassing about 20Kb. The translation start codons and stop codons are located in exon 2 and at the end of exon 8 respectively. Polyadenylation signal is located in the beginning of exon 9. Exon 2 also contains sequences for encoding the clusterin signal peptide. The α and β subunits of clusterin protein are encoded by the distal exon 2 to 5 and distal exon 5 to 8 respectively. Figure compiled and adapted from Jordanstarck et al. (Jordanstarck, Lund et al. 1994).

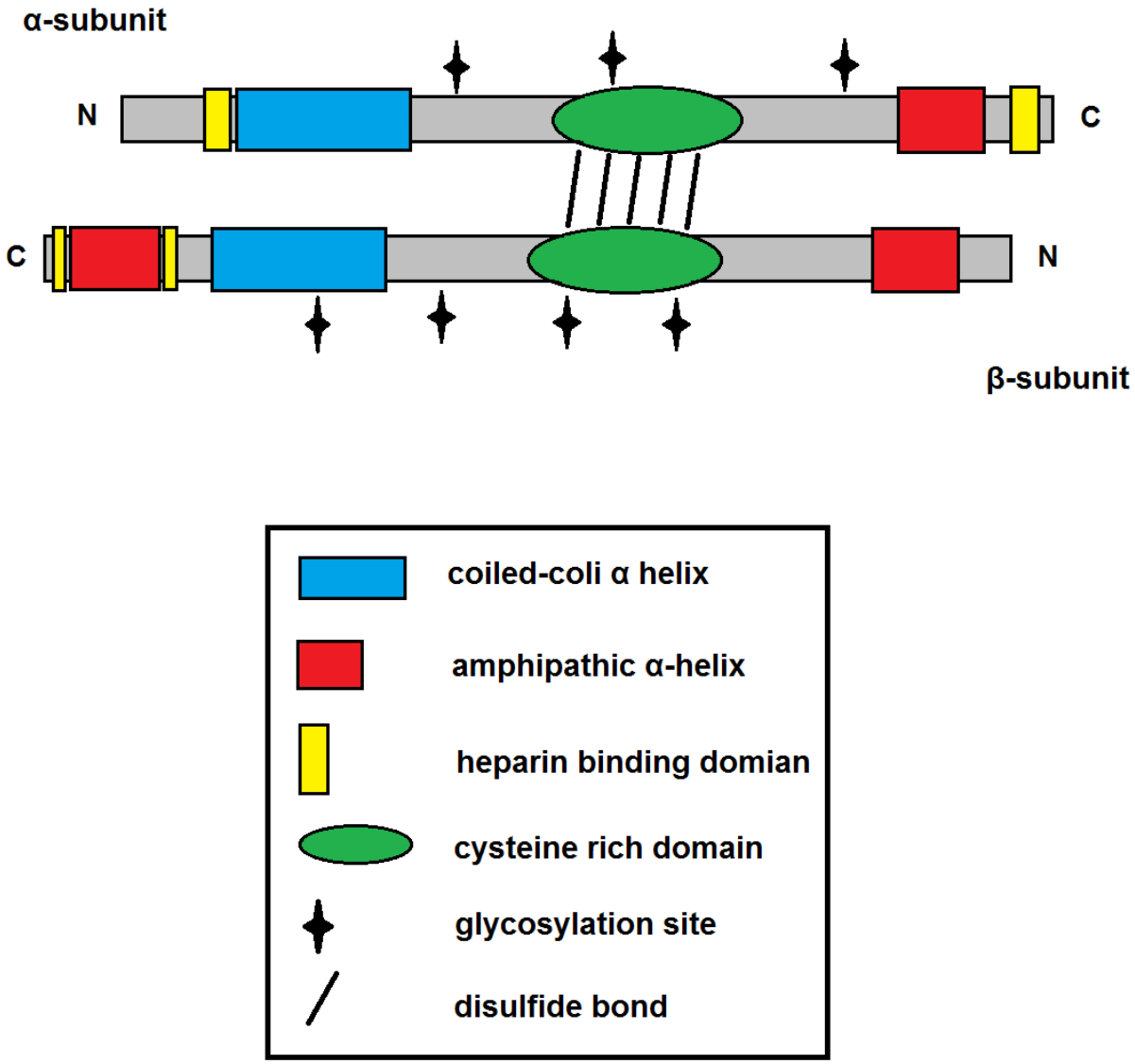


Figure 1.10 Predicted structure of mature mammalian clusterin protein (drawn to approximate scale). Clusterin protein is composed of α and β subunits that are assembled in anti-parallel to form a heterodimeric molecule in which the cysteine-rich centers are connected by disulfide bonds. Based on computer sequence analysis, clusterin is predicted to have multiple protein-protein interaction elements including three amphipathic α-helices, two coiled-coil α-helices, and four potential heparin binding domains. In addition, clusterin protein includes several potential glycosylation sites. Figure compiled and adapted from Jordan-Starck et al. and Wilson et al. (Jordan-Starck 1992; Wilson and Easterbrook-Smith 2000).

## 1.8 The biological functions of clusterin

The clusterin gene encodes a glycoprotein, with a nearly ubiquitous expression pattern and numerous putative biological roles. Clusterin was first purified from ram rete testis fluid in 1983 (Blaschuk, Burdzy et al. 1983) and named clusterin for its ability to cluster sertoli cells (Blaschuk, Burdzy et al. 1983). After this first discovery, other laboratories independently cloned and isolated clusterin and therefore many different names have been given to clusterin often depending on the specific research field (Table 1.1). In accordance with recent consensus among the main researchers in the field regarding terminology, the name clusterin (CLU) was recommended (Trougakos, Djeu et al. 2009) and will be used here.

Table 1.1: Summary of the clusterin protein isolated and/or cloned by different research groups working in widely different areas (adapted from Rizzi and Bettuzzi, 2008).

| **Source** | **Species** | **Name (Gene)** | **Function** | **Reference** |
|---|---|---|---|---|
| Rete testes fluid | Ram | Clusterin (Clu) | Reproduction | (Blaschuk, Burdzy et al. 1983) |
| Adrenal medulla | Bovine | *GPIII* | Chromaffin granules | (Fischercolbrie, Zangerle et al. 1984) |
| Prostate | Rat | *TRMP-2* | Apoptosis | (Leger, Montpetit et al. 1987) |
| Prostate | Rat | *SGP-2* | Reproduction | (Bettuzzi, Hiipakka et al. 1989) |
| Neuroretinal cells | Quail | *T64* | Cell Transformation | (Michel, Gillet et al. 1989) |
| Serum (liver) | Human | *SP-40,40* | Complement modulation | (Kirszbaum, Sharpe et al. 1989) |
| Serum (liver) | Human | *CLI* | Complement modulation | (Jenne and Tschopp 1989) |
| Blood | Human | *ApoJ* | Lipid transport | *(Desilva, Stuart et al. 1990)* |
| Blood | Human | *NA1/NA2* | Lipid transport | (James, Hochstrasser et al. 1991) |
| Retina | Human | *K611* | Retinitis pigmentosa | (Jones, Meerabux et al. 1992) |

Clarification of the biological roles of clusterin has proved challenging due to two main properties of this protein. First its ability to interact with a variety of molecules, including itself, amyloid proteins, lipids, immunoglobulins and components of the

membrane attack complex. Second, is its upregulation during many biological and pathological states. These include developmental remodelling, epithelial cell differentiation, in response to injury and other stresses, as well as in apoptotic disease states such as neurodegeneration.

Proposed clusterin roles include sperm maturation, tissue differentiation, tissue remodelling, membrane recycling, lipid transportation, cell-cell or cell-substratum interactions, cell proliferation, cell death and survival modulation, complement regulation and protein chaperone activity. Apart from these biological processes clusterin is involved or associated with many diverse pathological states, including neurodegeneration, aging and cancer (Shannan, Seifert et al. 2006; Bettuzzi 2009). Recent "large-scale genome-wide association studies have established a link between the human clusterin gene and Alzheimer's disease risk" (Harold, Abraham et al. 2009; Lambert, Heath et al. 2009). It is still unclear whether clusterin is a multifunctional protein or the single primary role of this protein is influenced by the tissue or cellular context taken. Despite all the varied attributed functions to clusterin, inactivation of clusterin gene in mice is "well tolerated and animals develop and live normally" (McLaughlin, Zhu et al. 2000).

Overall clusterin has been implicated in a number of biological and pathological roles and contexts as outline below, and each is explored in turn:

- Chaperone activity
- Regulation of complement activity
- Lipid transport
- Cell interactions
- Membrane recycling

### 1.8.1 Clusterin - protein chaperone activity

The ability of clusterin protein to interact with a broad range of ligands together with its wide distribution in many biological fluids suggests an important role for clusterin as an extracellular chaperone.

The biological distribution of clusterin is striking. Clusterin is present in almost all mammalian tissues and physiological fluids including plasma, urine, milk, cerebrospinal fluid and semen.

Many reports describe "specific" interactions of clusterin with diverse native biological ligands including apoA-I, *β*-amyloid peptide, components of the complement membrane attack complex (MAC), glutathione-*S*-transferase, gp330 or megalin, immunoglobulins, heparin, lipids, paraoxonase, prion peptide, SIC (streptococcal inhibitor of complement), the cell surface of *Staphylococcus aureus* isolates, and the TGF-*β* receptor, misfolded proteins (Wilson and Easterbrook-Smith 2000), and the chemotherapeutic drug Taxol (Park, Yeo et al. 2008). Clusterin binds to hydrophobic regions of misfolded proteins (Poon, Rybchyn et al. 2002). Because clusterin preferentially binds to the hydrophobic ligands, it was suggested that its interaction with these ligands is as a result of its chaperone properties (Wyatt, Yerbury et al. 2009).

Heat shock proteins (HSPs) are well characterised intracellular chaperones that protect cells against heat and other stresses by binding to hydrophobic regions of partially unfolded (stressed proteins), thereby "solubilizing" them and preventing their precipitation that will have otherwise toxic effects on cells. There is now a substantial body of evidence that like all known mammalian HSPs, clusterin has a chaperone action. There is a highly conserved 14-bp element, the heat shock element (HSE), in the clusterin proximal promoter in vertebrates which is capable of binding the transcription factor heat shock factor 1 (HSF1) and that then induces clusterin expression following heat shock in transient expression assays in cell culture. The conserved HSE motif alone was shown to be capable of driving reporter gene expression in response to heat shock (Michel, Chatelain et al. 1997). In addition, clusterin is capable of binding to hydrophobic complexes and denatured proteins to assist their uptake and clearance (Bailey and Griswold 1999). Clusterin potently inhibited the precipitation of stressed proteins by binding to these proteins and forming high-molecular-weight solubilised complexes (Humphreys, Carver et al. 1999). Moreover, clusterin demonstrated a much higher binding affinity for stressed proteins than non-stressed proteins, and also a better ability at inhibiting the precipitation of stress-induced proteins than small heat shock protein (sHSPs, a molecular chaperone) *in vitro* (Humphreys, Carver et al. 1999). Although clusterin can stabilize stressed proteins it did not protect the catalase and

glutathione-S-transferase proteins from heat-induced loss of function (Humphreys, Carver et al. 1999). Therefore when acting alone clusterin cannot refold proteins, a characteristic shared with sHSPs but it may interact with other chaperones to achieve this (Poon, Easterbrook-Smith et al. 2000).

Furthermore, there is evidence that clusterin has some cytoprotective property, suggesting again that it is a functional HSP. Inhibition of clusterin synthesis by treatment of LNCaP cells (an androgen-sensitive human prostatic cancer cell line) with a 21-base oligonucleotide antisense to clusterin increased the cytotoxicity of tumor necrosis factor α (TNFα) (Sensibar, Sutkowski et al. 1995). Also, overexpression of clusterin protected murine L929 cells (from murine fibrosarcoma) and LNCaP cells from the cytotoxicity of TNFα (Sensibar, Sutkowski et al. 1995; Humphreys, Hochgrebe et al. 1997). In line with these reports, A431 cells (from human epidermoid cancer cell line) are more susceptible to heat shock or oxidative stress than controls when transfected with anti-sense clusterin cDNA (Viard, Wehrli et al. 1999).

Finally, clusterin shares some sequence similarity with HSPs. There is 25% similarity between the chaperone active site of αB-crystallin (a type of HSP) and residues 286-343 of clusterin (Wilson and Easterbrook-Smith 2000).

Therefore, at both gene regulation and protein function levels clusterin shares many similarities with HSPs, that are well established as intracellular chaperones (Wilson and Easterbrook-Smith 2000). As clusterin is present in most physiological settings as a secreted protein, it has been suggested that clusterin acts *in vivo* as an extracellular chaperone (Humphreys, Carver et al. 1999; Wilson and Easterbrook-Smith 2000).

In support of this, clusterin was the first described member of a family of abundant extracellular chaperones that assist with extracellular proteostasis by recognizing and, forming stable soluble complexes with misfolded client proteins, and mediating their disposal (1999) (Humphreys, Carver et al. 1999). This extracellular chaperone activity of clusterin prevents the formation of toxic aggregates and facilitates with their bulk uptake and degradation via receptor-mediated endocytosis (Yerbury, Stewart et al. 2005; Wilson, Yerbury et al. 2008; Wyatt, Yerbury et al. 2009; Wyatt and Wilson 2010; Wyatt, Yerbury et al. 2011).

This critical ability of clusterin to modulate protein aggregation via binding, stabilizing and internalizing misfolded extracellular proteins for subsequent degradation is now under extensive investigation with a view to eventually exploit these behaviours in the treatment of "protein conformational disorders" in which inappropriate aggregation and deposition of extracellular proteins cause life-threatening conditions such as Alzheimer's disease, arthritis, type II diabetes, macular degeneration, and atherosclerosis (Wilson, Yerbury et al. 2008; Wyatt, Yerbury et al. 2011).

The extracellular chaperone activity of clusterin *in vivo* was confirmed by accumulation of insoluble protein deposits in the clusterin "knock-out" mouse kidney but not in those of age-matched wild-type mice (Rosenberg, Girton et al. 2002) and also by demonstrating its involvement in the clearance of amyloid β-peptide from the brains of mice (Bell, Sagare et al. 2007).

The imbalance between Aβ anabolism and catabolism gives rise to its accumulation and extracellular plaque formation which is one of the distinctive characteristics of Alzheimer's disease. There are at least two proposed ways that the secreted form of clusterin (sClu) (1.6) modulates Aβ toxicity in the brain. sClu, an 80-kDa glycoprotein, is the most abundant form of clusterin found in virtually all body fluids. sClu promotes Aβ clearance locally by interfering with aggregation of Aβ. This is done by accelerating its transport across the blood brain barrier (BBB) by binding to Aβ and forming a stable complex with it (Calero, Tokuda et al. 1999). Clu-Aβ complex then binds to megalin (LRP-2) a receptor of the LDL receptor family for efficient transportation of sCLU-Aβ complexes from brain into the blood across the BBB and thereby decreases the level of Aβ in the brain. Megalin (LRP-2) is expressed in vascular CNS tissues including the choroid plexus, the BBB endothelium, and the ependyma (Hammad, Ranganathan et al. 1997; Chun, Wang et al. 1999). The use of this transport route for outflow of Aβ from brain into blood via BBB, was demonstrated by the Bell et al. who used an established *in vivo* technique to show that binding of Aβ to sCLU accelerates Aβ clearance at the BBB by 83% (Bell, Sagare et al. 2007). sClu also stimulates removal of soluble Aβ from the interstitial fluid (ISF) locally by receptor-mediated endocytosis of sClu-Aβ into the cell of brain for lysosomal degradation (Wyatt A 2009; Wyatt, Yerbury et al. 2011). Therefore, sClu protects the neighbouring cells (vital cells) of the affected cells from cell death by binding, internalising and finally removing toxic substances

including protein aggregates and potential antigens located in the extracellular environment. Although this cytoprotective property of clusterin probably plays a significant role in normal cellular homeostasis, it is not desirable in tumors, as it can counteract apoptosis that is induced by immune cells or by poor vascularisation.

### 1.8.2 Clusterin – proposed functions in complement regulation

Clusterin has long been speculated to be a complement regulator. Complement system is critical for the integrity of cells and tissue homeostasis. The activation of complement system leads to cell lysis of microorganisms, clearance of apoptotic cells or inflammation. Human clusterin protein was initially identified in glomerular immune complexs in a pattern similar to other terminal complement components (Murphy, Kirszbaum et al. 1988). Several other reports thereafter showed clusterin to be part of the fluid phase membrane attack complex (SC5b-9) and has a complement inhibitory role (Choi, Mazda et al. 1989; Jenne and Tschopp 1989; Kirszbaum, Sharpe et al. 1989). Membrane attack complex (MAC) is composed of the C5b, C6, C7, C8, and C9 complement proteins and causes cell lysis by transmembrane channel formation. It is formed on the surface of pathogens as a result of activation of complement system cascade (C1-C9). Its generation takes place either in fluid phase (SC5b-9) or on a phospholipid membrane (MC5b-9).

*In vitro,* clusterin demonstrates an inhibitory role in complement mediated cytolysis by binding to C5b-6 (the first assembly intermediate formed as a result of C5b binding to C6) and prevents formation of the membrane attack complex inhibitor (Choi, Mazda et al. 1989; Jenne and Tschopp 1989; Kirszbaum, Sharpe et al. 1989). Clusterin also co-localises with the membrane attack complex in a variety of other lesions including myocardial and renal infarcts (Vakeva, Laurila et al. 1993; Vakeva, Meri et al. 1995). Based on clusterin's association with the membrane attack complex in some experiments and human diseases, and its ability to inhibit complement mediated cytolysis *in vitro,* an important role for clusterin as a complement regulator was proposed.

However, one study suggested that under physiological conditions clusterin is unlikely to be an important complement regulator as in cell culture, exogenous clusterin showed no protective effect against serum-derived MAC activity, and also cell-surface localized clusterin did not prevent complement-mediated lysis (Hochgrebe, Humphreys et al. 1999).

### 1.8.3 Clusterin function in lipid transport

sCLU has also been detected associated with high-density lipoprotein (HDL) in serum (Desilva, Harmony et al. 1990) and is often found coupled to HDL and VHDL in most body fluids. HDL is believed to be protective of atherosclerotic disease and is considered as a negative risk factor for vascular disease. This protective role has been explained by an increased HDL concentration that improves reverse transport of cholesterol and stimulates its export from macrophages. In addition HDL has been reported to have other functions such as antithrombotic, anti-inflammatory, and antioxidative functions. The association of sCLU with HDL suggests that it could be protective or help HDL in its protective roles in the presence of proatherogenic conditions. sCLU prevents cell damage by lipid oxidation in blood vessels (Navab, HamaLevy et al. 1997).

The small peptides derived from mature sCLU, are predicted to form amphipathic helices, and in this form are thought to be responsible for the beneficial property of the clusterin protein. *In vivo* studies demonstrated that these peptides significantly enhanced both the export of cholesterol from cells into plasma and HDL anti-inflammatory activities (Navab, Anantharamaiah et al. 2005; Navab, Anantharamaiah et al. 2007). The protective effect of sCLU and its peptides is possibly due to the property of clusterin in removing toxic and harmful substances to prevent an immune reaction and the subsequent atherosclerotic changes of the vessel wall (Klock, Baiersdorfer et al. 2009).

The association of sCLU with lipoprotein particles also suggest a role for clusterin in lipid transport. The upregulation of clusterin during development and injury may demonstrate its function in facilitating lipid recycling at dynamic tissue sites. At physiologically relevant concentrations, clusterin promotes cholesterol and

phospholipid efflux from macrophage-foam cells *in vitro*, and associates with the secreted cholesterol in the culture medium (Gelissen, Hochgrebe et al. 1998). Thus, clusterin may be involved *in vivo* in cellular homoeostasis and may suppress atherosclerosis by promoting lipid export.

### 1.8.4 Clusterin - cell interactions

*In vitro*, clusterin is capable of inducing cell aggregation of a variety of cell types including Sertoli cells, spermatozoa, renal epithelial cells, and erythrocytes (Blaschuk, Burdzy et al. 1983; Fritz, Burdzy et al. 1983; Rosenberg and Silkensen 1995; Silkensen, Skubitz et al. 1995). Clusterin is therefore considered a cell aggregation and adhesion molecule that promotes cell-cell and cell-substratum interactions. Clusterin may promote these contacts during development when critical cell interactions are taking place, and also during tissue damage, for instance in renal tubular injury such cell interactions maintain tissue integrity (Rosenberg and Silkensen 1995).

In renal cell culture, clusterin mRNA expression was induced after disruption of cytoskeleton integrity (that in turn disrupts cell-cell and cell substratum interactions) and after inhibition of cell-matrix interactions (Silkensen, Skubitz et al. 1995).

### 1.8.5 Clusterin function in membrane recycling

It is believed that secretory clusterin binds to hydrophobic membrane fragments produced as a result of cell degradation to maintain the cell membrane and/or promote membrane recycling and tissue remodeling (Sylvester, Morales et al. 1991; Jordan-Starck 1992; Aronow, Lund et al. 1993). This further supports a cytoprotective role for clusterin.

## 1.9 The pathological functions of clusterin

### 1.9.1 Clusterin involvement in tumorigenesis

Clusterin has been reported to be associated with cancer promotion and metastasis (Redondo, Villar et al. 2000; Pucci, Bonanno et al. 2004; Shannan, Seifert et al. 2006) and generally its expression is dysregulated in many cancer types including prostate, breast and lung cancer. There are contradictory reports in the literature about up- or down-regulation of clusterin expression in human cancer and also whether clusterin plays a role in tumor prevention or tumor promotion. There is evidence that clusterin is overexpressed in some cancers supporting an oncogenic role, while its repression in other cancers conversely indicates a tumour suppressor role.

It is now generally agreed that, the role of clusterin in tumor cells may depend on the context of its expression and the microenvironment. The new insight into the dual role of clusterin as a tumor suppressor and a tumor promoter can explain the contradictory findings of clusterin's involvement in cancer. As explained before, sCLU is capable of stabilizing misfolded/stressed proteins upon exposure to oxidants or DNA damaging agents. The accumulation of damaged proteins and the disturbance of cell homeostasis can lead to transformation and in this way, sCLU is envisaged to act as a tumor suppressor.

However, after the treatment of tumor cells with toxic chemotherapeutic agents, sCLU acts as a cell survival factor to protect the tumor cells from DNA damaging agents and maintain the tumor. In addition, the stimulation of sCLU production by growth factors that lead to the proliferation of the tumor cells, and tumor derived factors such as TGF-β1, can mediate tumor or senescent cell survival. In this scenario, sCLU acts as an oncoprotein within the transformed cell. The nuclear form of clusterin (nCLU) (1.6) is generally believed to be pro-apoptotic and it has been suggested that the balance between sCLU and nCLU dictates the fate of cancer cells (Trougakos, Djeu et al. 2009).

In the majority of naive cancers, noticeably during prostate cancer, CLU is downregulated. However, CLU upregulation after cancer treatment has been reported and due to its antiapoptotic properties, it is believed to play a role in promoting a

resistance phenotype to cancer treatments such as androgen ablation therapy in prostate cancer therapy. In prostate cells resistant to chemotherapy or hormontherapy clusterin was reported to be upregulated (Miyake, Chi et al. 2000; Miyake, Nelson et al. 2000).

Many *in vitro* experiments report that silencing of CLU expression can improve the cytotoxicity of androgen ablation therapy (Gleave and Miyake 2005), chemotherapeutic agents (Trougakos and Gonos 2002) and irradiation (Zellweger, Chi et al. 2002) in prostate cancer cell lines. Therefore, CLU is now considered a promising therapeutic target for cancer therapy and CLU antisense oligonucleotide (ASO) therapy has been developed and is currently undergoing clinical trials. CLU ASO is called OXG-011 and is directed against the translational start site in exon 2.

The secreted form of clusterin has been proposed as a biomarker for diagnosis and prognosis of some types of cancer such as prostate and colon cancer.

### 1.9.2 Clusterin involvement in Alzheimer's disease

Clusterin has also been shown to be implicated in Alzheimer's disease (AD). The evidence for this includes an increase in the level of clusterin mRNA and protein in plasma, presence of clusterin in the plaques which are one of the major brain lesions of individuals with Alzheimer's disease, and clusterin has a chaperon role in preventing aggregation and/or clearance of amyloid-beta (Aß) (Ling, Bhongsatiern et al. 2012). "Genome wide association studies have further demonstrated that genetic variation in the clusterin gene sequence is associated with Alzheimer's disease and clusterin single nucleotide polymorphisms (SNP)s are associated with AD risk" (Harold, Abraham et al. 2009; Lambert, Heath et al. 2009).

## 1.10 Possible functions of clusterin during embryonic development

Clusterin expression has been studied during the embryonic development of different organisms such as mouse, rat, zebrafish and human and has been shown to be up-regulated in a variety of tissues during their development.

Clusterin has been proposed to be involved in some of the major events that take place during the normal embryonic development such (1) differentiation and morphogenesis (2) proliferation and (3) apoptosis. These functions will be explored further in turn.

### 1.10.1 Differentiation and morphogenesis

During development of the mouse embryo, clusterin transcripts are detected at 9.0dpc of gestation in the wall of the developing truncus arteriosus of the heart (Witte, Aronow et al. 1994) followed by widespread expression of the gene from 12.5dpc in cells derived from all three germ layers, but most abundant in developing epithelia cells from different organs, and particularly localized within the differentiating rather than proliferative compartments of skin, duodenum and tooth (French, Chonn et al. 1993). Clusterin mRNA expression was also detected in the differentiating epithelial cells of liver, developing inner ear, ventricular cavities of the brain, developing eye, kidney, lung, and vibrissae (French, Chonn et al. 1993). In the developing lung and kidney, clusterin gene expression was associated with differentiating bronchial and tubular epithelial cells respectively. However by 18.5dpc, clusterin expression is completely diminished in the lungs, a time when the process of branching morphogenesis in the developing lung is complete.

The developing mouse hair follicle and mammary gland was also studied separately for clusterin expression (Obryan, Cheema et al. 1993; Seiberg and Marthinuss 1995; Yoko Itahana, Desprez et al. 2007; Charnay Y 2008). Clusterin is reported to be expressed during the growth phase of the hair cycle and not during the apoptotic regression of the hair follicle in mouse. Clusterin expression was found to be localized to the highly differentiated epithelial cells of inner root sheath of the follicle demonstrating a possible

role for clusterin in follicular differentiation and morphogenesis (Seiberg and Marthinuss 1995).

With regards to the developing mammary gland, clusterin was reported to be up-regulated twice during its development. These up-regulation time points coincide with some major phenotypic and functional changes in the developing mammary gland, again suggesting possible involvement of clusterin in morphogenesis and differentiation during development (Yoko Itahana, Desprez et al. 2007).

The rat pancreas has also been reported to express clusterin during embryonic development. Clusterin mRNA was up-regulated at 16.0dpc in the endocrine pancreas and expression increased to reach the highest levels at early postnatal stages (Min, Jeong et al. 1998). During this period pancreatic cells are actively being reorganised to form the pancreatic islet and therefore clusterin was proposed to be involved in tissue remodeling. Clusterin is upregulated in the regenerating pancreas, more specifically in endocrine islet cells undergoing differentiation leading to the proposal that clusterin is a regulatory factor for cytodifferentiation (Min, Kim et al. 2003). This function was further supported by the finding that overexpression of clusterin *in vitro* induced the differentiation of pancreatic duct-lining cells into insulin-secreting cells, and the number of newly differentiated cells increased in a dose-dependent manner (Kim, Kim et al. 2006).

Multiple lines of evidence suggest a key role for clusterin in the regulation of epithelial cell phenotypes. For example the involvement of clusterin in the regulation of tubuloalveolar morphogenesis and alveolar epithelial cell differentiation in the mammary gland of adult rat (French, Soriano et al. 1996) was suggested as it's expression increased in the second part of pregnancy, coinciding with termination of proliferation and initiation of differentiation of mammary epithelial cells into milk expressing cells. Further, the depletion of clusterin by antisense oligonucleotides resulted in an increase in apoptosis in the ovary (Zwain and Amato 2000). Tikhonenko et al. demonstrated that clusterin is capable of suppressing epithelial cell proliferation *in vitro* and *in vivo* (more details in 1.10.2) (Thomas-Tikhonenko, Viard-Leveugle et al. 2004). Treatment of rat mammary epithelial cells with a clusterin small interfering RNA (siRNA) led to a significant decrease in the level of expression of β-casein, a mammary

epithelial cell differentiation marker (Itahana, Piens et al. 2007). Most of these studies however suggest that clusterin is a morphogenic factor and is involved or plays a key role in differentiation rather than in proliferation of cells.

### 1.10.2 Proliferation

Generally the effect of clusterin on cellular proliferation is controversial. Bettuzzi et al. demonstrated that CLU expression is negatively associated with cell proliferation by transiently overexpressing CLU cDNA in human prostate cancer cell lines and retarded cancer growth (Bettuzzi, Scorcioni et al. 2002). The anti-proliferative effect of clusterin was also reported when EGF-mediated proliferation in LNCaP cancer cells was inhibited by purified clusterin protein (Zhou, Janulis et al. 2002). As explained earlier clusterin expression is restricted to differentiating but not proliferating cell layers (1.10.1), this further suggests a possible negative role for clusterin in cell division (Thomas-Tikhonenko, Viard-Leveugle et al. 2004). *In vitro* clusterin knock down via antisense RNA enhances proliferation in neoplastic epidermoid cells (Thomas-Tikhonenko, Viard-Leveugle et al. 2004). The anti-proliferative properties of clusterin was further supported by an *in vivo* study that compared the sensitivity of wild type and clusterin-null mice to topical application of DMBA/TPA, a chemical skin carcinogen that leads to formation of benign papillomas, and this showed clusterin interference with the promotion stage of skin carcinogenesis (Thomas-Tikhonenko, Viard-Leveugle et al. 2004). It has been hypothesised that differentiating cells produced-clusterin blocks cellular proliferation “either directly (as a bona fide autocrine or paracrine growth factor) or indirectly (via sequestration of other growth factors)” (Thomas-Tikhonenko, Viard-Leveugle et al. 2004).

In contrast to the above studies, there are some reports that demonstrate a positive role for clusterin involvement in cell proliferation during development, for instance in pancreatic cells where transfection of cultured duct cells with clusterin cDNA resulted in 2.5-fold increase in cell proliferation (Min, Kim et al. 2003), and transient transfection of MIN6 isulinoma cells (pancreatic beta cell line) with clusterin over-expressing plasmid increased cell proliferation by 31% (Kim, Han et al. 2001; Min, Kim et al. 2003). Furthermore, sCLU is upregulated in reactive astrocytes, which are

formed in response to centrat nervous system injuries or disease (Pasinetti and Finch 1991; Torres-Munoz, Redondo et al. 2001).

### 1.10.3 Apoptosis

Programmed cell death (apoptosis) is an essential part of the development and differentiation that allows tissue remodeling and also preserves tissue homeostasis by counteracting proliferation, and is active in the inner ear (1.2.4). There are many reports for clusterin association with apoptosis based on the detection of clusterin expression at times of apoptosis, although contradictory data exist.

During tissue development and involution clusterin is induced in cells going through apoptosis (Tenniswood, Guenette et al. 1992; Ahuja, Tenniswood et al. 1994; Witte, Aronow et al. 1994; Brown, Moulton et al. 1996; French, Soriano et al. 1996; Min, Jeong et al. 1998). Clusterin was shown to be upregulated during tissue involution in response to a variety of stimuli such as injury, hormonal modulation and developmental stimuli leading to a proposal that clusterin might be a cell death marker (Buttyan, Olsson et al. 1989). For instance, apoptosis of interdigital webbing of developing rat embryonic feet and in chondrocytes in the developing hindlimbs and forelimbs of rat (Buttyan, Olsson et al. 1989). With regards to hormonal modulation, clusterin has been shown to be considerably upregulated in the apoptotic cells of the involuting rat ventral prostate after castration (Buttyan, Olsson et al. 1989; Tenniswood, Guenette et al. 1992). In addition, induction of cell death and atrophy in rat renal tissues by acute ureteral obstruction was also shown be associated with clusterin upregulation in obstructed kidney (Buttyan, Olsson et al. 1989). Strange et al. also reported clustrein upregulation in the apoptotic cells of involuting mammary gland epithelial cells (Strange, Li et al. 1992).

In contrast, some researchers have reported a lack of correlation between clusterin expression and cell death. O'Bryan et al. reported the upregulation of clusterin mRNA and protein during neuronal development in mouse, but found no evidence that clusterin expression is associated with programmed cell death in the developing brain as expression was detected early, at preapoptotic embryonic stages and in the great

majority of neurons in the central nervous system (Obryan, Cheema et al. 1993). Garden et al. also demonstrated clusterin expression in nearly all neurons of developing and mature rat brain, but again found no correlation between clusterin expression with programmed cell death, as clusterin spatio-temporal expression was unrelated to the pattern of programmed cell death (Garden, Bothwell et al. 1991). In hair follicles no correlation between clusterin expression and follicular apoptotic regression was found (Seiberg and Marthinuss 1995). Also, overexpression of clusterin under the regulation of a human photoreceptor specific gene promoter in transgenic mice did not induce apoptosis in photoreceptor cells during the development of retina (Jomary, Chatelain et al. 1999)

### 1.11 Reconciling contradictory reports on clusterin function

Clusterin expression during embryonic development has been suggested to be associated with morphogenesis, remodeling, organisation and differentiation of tissues particularly the epithelial cells although the exact function and mechanisms of action of clusterin during development has not been defined. Secretory clusterin (sCLU), the most abundant isoform, has been shown to be involved in the control of cell fate including differentiation (Kim, Kim et al. 2006), apoptosis (Trougakos, So et al. 2004), and proliferation. sCLU is upregulated in model systems of apoptosis and injury. Clusterin mRNA expression has been shown to be low or undetectable in the dying cells, but specifically upregulated in the surviving neighbour cells of apoptotic tissue (French, Wohlwend et al. 1994) demonstrating that the clusterin gene product, presumably sCLU, is not actively promoting apoptosis but may instead play a role in protecting the vital neighbouring cells. This is in contrast with the intracellular CLU isoform that has been proposed to causally exert apoptotic functions in cells (pro or antiapoptotic) (Yang, Leskov et al. 2000). Clusterin plays its cytoprotective role in surviving cells possibly by assisting in clearing apoptotic debris (Bach, Baiersdorfer et al. 2001) and therefore protects the surviving cells from cell death and restricts inflammation in the areas that undergo apoptosis. Secretory clusterin that preferentially binds to hydrophobic molecules during development, pathologic apoptosis, and in

response to injury, is thought to bind to lipid-based toxic molecules to protect cell membrane at sites of active remodelling (Buttyan, Olsson et al. 1989; French, Chonn et al. 1993).

Indeed clusterin expressing cells do not die by apoptosis (Michel, Moyse et al. 1997) and its overexpression did not induce apoptosis during the development in mouse transgenic retinas (Jomary, Chatelain et al. 1999). Therefore, considering that clusterin is not causally implicated in apoptosis, the detection of clusterin expression in apoptotic as well as differentiating cells in the female reproductive system again suggests a cytoprotective and anti-inflammatory role for clusterin in the cells that undergo specific biochemical and physical changes (Ahuja, Tenniswood et al. 1994).

The reports that demonstrate clusterin dissociation with apoptosis suggest that clusterin is not a necessary molecule for apoptosis initiation. Clusterin, therefore, may have a more general role in cell activities or may simply be produced as a result of apoptosis for instance given that clusterin is capable of promoting cell interactions; it may be induced during apoptosis to prevent the detachment of apoptotic cells.

There are reports of a dual role of clusterin in cell growth as well as during apoptosis, such as in the study of Bursche et al. (1995) who showed the upregulation of clusterin mRNA during both regression and mitosis of rat liver. The author concluded that clusterin protein may be involved in maintaining cell membrane integrity which is needed during both apoptosis and mitosis (Bursch, Gleeson et al. 1995).

Zhou et al. 2002 reported an anti-proliferative role for clusterin in prostate cancer cell line, LNCaP, and argued that clusterin seems to be a rare molecule that has both anti-proliferative and anti-apoptotic properties depending on which force - an anti-apoptotic or the anti-proliferative function, prevails. Zhou et al. also suggested that the cell type and the kind of external stimuli are important determinants as which one of these forces dominates and determines the cell fate (Zhou, Janulis et al. 2002).

Therefore, the contradictory reports of clusterin association with various cell activities (apoptosis, proliferation and differentiation) during development may not necessarily be contradictory, but rather be explained with clusterin having a more general role such as

a “cytoprotective chaperone-like activity” as well as a role in “promoting cell interactions” in various cellular processes.

### 1.12 Aims of this project

Whilst much is known generally about clusterin expression in the embryo and in pathological conditions, clusterin expression and function relevant to inner ear biology and development is largely unknown. In this project, this will be addressed by attempting to address the following aims:

- To define the spatiotemporal pattern of clusterin mRNA expression during mouse inner ear development

- To compare clusterin mRNA expression in the developing inner ear in relation to the markers that delimit the developing organ of Corti

- To determine where clusterin protein is found in the developing inner ear

- To compare clusterin protein expression in the developing inner ear in relation to the hair cell and supporting cell markers

- To generate a bacterial artificial chromosome (BAC) reporter construct that will enable the regulatory mechanisms controlling inner ear clusterin expression to be tested

# 2. Materials and Methods

# 2. Materials and Methods

## 2.1 DNA protocols

### 2.1.1 Enzymatic manipulation of DNA

2µg of linear or plasmid DNA subject to restriction enzyme digestion was incubated with 1-5U/µg of restriction enzyme and the appropriate restriction buffer (based on the company's recommendations) in a total volume of 15-20µl with incubation at 37ºC for 1 hour. The digested DNA samples were visualised and/or purified by agarose gel electrophoresis, the DNA band excised and recovered using the "gene clean" protocol (2.1.2).

For making blunt ends, after digestion, DNA ends were end-filled by using dNTPs and T4 DNA polymerase with incubation at $11^0$C for 30 minutes followed by 10 minutes incubation at $75^0$C.

### 2.1.2 Gene clean method for fragment isolation

This procedure involves excising the required DNA band from the agarose gel, dissolving the agarose gel by heating at 55ºC in three volumes (per agarose weight) of 6M sodium iodide until the gel slice had completely dissolved. Next DNA is bound to glass milk by adding 5µl of a glass milk solution and rolling for 30 minutes at room temperature. The glass milk-DNA conjugate is then pelleted by spinning at 13,000rpm for 30 seconds and washed twice to remove contaminants by resuspending the pellet in a high salt buffer, New Wash solution (50% Ethanol, 2mM Tris-HCl pH 7.5, 1mM EDTA, 100mM NaCl) and spinning at 13,000rpm for 30 seconds. Finally, the pellet was dried at 37ºC and the DNA was eluted from the matrix using a low salt buffer such as TE (10mM Tris/1mM EDTA, pH 7.6) and spinning at full speed for 1.0 minute. Supernatant was recovered to a fresh tube.

### 2.1.3 DNA cloning/subcloning

#### 2.1.3.1 Preparation of insert for cloning

Following restriction enzyme digestion (2.1.1) fragments were resolved in agarose gels of appropriate concentrations and purified for cloning by agarose gel electrophoresis using the "gene clean" method (2.1.2).

DNA fragments obtained from PCR amplification were also purified in the same manner but without resolving in agarose gel electrophoresis. Instead the DNA was bound to glass milk followed by washing and elution.

#### 2.1.3.2 Preparation of vector for cloning

Plasmid DNA subject to cloning experiments was digested with the appropriate restriction endonucleases (2.1.1) followed by dephosphorylation by incubation with 1µl (20U) of calf intestinal alkaline phosphatase (CIP) (New England Biolabs) for 1 hour at 37ºC. Vector was purified by agarose gel electrophoresis, the vector band excised and recovered using the "gene clean" protocol (2.1.2).

#### 2.1.3.3 Estimation of DNA concentration

In order to visually estimate the concentration of DNA, 1µl of the DNA sample was run on an agarose gel along with 2.5µl (125ng) and 5.0µl (250ng) of *HindIII* digested lambda DNA. The DNA sample concentration was estimated by comparing its brightness intensity with the marker bands that have a know concentration.

#### 2.1.3.4 Ligations

Ligation reactions were set up between the purified DNA insert (2.1.3.1) and the purified vector fragments described above (2.1.3.2) using a variety of insert to vector ratios and using 200 units of T4 DNA ligase (New England Biolabs) and 1x ligation buffer (New England Biolabs) at 12ºC overnight.

### 2.1.3.5 Bacterial transformations

An aliquot of bacterial competent cells (2.1.4) was defrosted on ice and mixed, 100µl of cells were transferred into pre-chilled 50ml universal tubes. 2-4µl of ligation mixture or an appropriate quantity (ng quantities) of plasmid DNA was added to the cells and mixed by swirling several times. The mixture was incubated on ice for 30 minutes prior to a heat shock by incubation at 42ºC for 45 seconds followed by incubation on ice for 1-2 minutes.

0.9ml S.O.C medium (Appendix I) was added and the culture was incubated at 37ºC for 45 minutes with shaking at 250rpm. Different quantities of the transformation mixture were plated on LB agar supplemented with appropriate antibiotics with incubation overnight at 37ºC.

### 2.1.4 Preparation of high frequency competent *E. Coli* cells

A single colony of *E. Coli* strain DH5α from a freshly streaked LB agar plate was used to inoculate 5ml of sterile LB medium (Appendix I) and grown for approximately 16 hours at 37ºC with shaking at 250rpm.

0.5 – 1.0ml of fresh overnight culture of DH5α was used to inoculate 50-100ml of SOC medium (Appendix I) and incubated at 37ºC with shaking at 250rpm for approximately two hours until an $OD_{600}$ of 0.375 was reached by the culture. The culture was incubated on ice for 10 minutes prior to centrifugation at 3200rpm for 20 minutes at 4ºC. Supernatant was removed and the cell pellet was resuspended in 20ml Frozen Storage Buffer (FSB, Appendix IV) and incubated on ice for 15 minutes. The suspension was centrifuged at 3200rpm for 15 minutes at 4ºC and the supernatant was removed followed by resuspension of the pellet in 4ml FSB. 140µl DMSO was added and the suspension was incubated on ice for 15 minutes followed by the addition of another 140µl of DMSO and stored on ice while dispending 200µl aliquots of the suspension into chilled 1.5ml eppendorf tubes. The tubes were then snap-frozen by immersing in an IMS dry ice bath.

### 2.1.5 Polymerase Chain Reaction (PCR)

The amplification of linear or circular DNA was carried out using "Taq DNA polymerase (Thermo Scientific)".

| | |
|---|---|
| Water | up to 20µl |
| DMSO | 1.0µl |
| 10XPCR Buffer | 2.0µl |
| $MgCl_2$ (25mM) | 3.5µl |
| dNTPs (5mM each) | 2.0µl |
| Forward primer (1µg/µl) | 1.0µl |
| Reverse primer (1µg/µl) | 1.0µl |
| DNA template | (2ng/µl plasmid or linear DNA, 2-3ng/µl BAC DNA) |
| Taq polymerase (250U/µl) | 0.2µl |

The PCR products were visualized on 1.0% agarose gels

### 2.1.6 High fidelity PCR

In order to maintain a high accuracy and fidelity of amplification of selectable marker and reporter genes for recombineering experiments, PCR using "Phusion Taq DNA polymerase (New England Biolabs)" was used (0.4U/20µl).

PCR reactions included 1.0ng/µl of template, 5mM of each dNTPs, 1XGC phusion buffer (New England Biolabs), 10pmol of each primer and 0.4U of Phusion Taq DNA polymerase (2U/µl, New England Biolabs). A typical PCR reaction profile consisted of: 95°C, 3 minutes, 1 cycle; 95°C, 30 seconds, 57°C, 1 minutes, and 72°C, 2 minutes and 30 seconds, 30 cycles; 72°C, 5 minutes, 1 cycle. The PCR products were visualized on 1.0% agarose gels.

### 2.1.7 Reverse Transcriptase Polymerase Chain Reaction (RT-PCR)

RT-PCR is a PCR reaction that amplifies a cDNA made by reverse transcription of a mRNA. The amplification of cDNA samples was carried out using gene specific primers. The same PCR reactions and conditions as in section 2.1.5 was used, followed by visualization of PCR products on 1.0% agarose gels.

### 2.1.8 Colony PCR

In order to screen colonies for the presence of particular plasmids, colony PCR was used. Single bacterial colonies from transformation plates were resuspended in 40µl water. 30µl of this sample was boiled at 98ºC for 5 minutes and a 2µl aliquot was used as a template for the PCR reaction (2.1.5). 20µl of the remaining suspension was inoculated into 5ml of LB medium conditioned with appropriate antibiotics and incubated at 30ºC or 37ºC overnight for further DNA preparations of positive clones identified through PCR analysis.

### 2.1.9 Southern blot analysis

BAC DNA that was to be analysed by Southern blot analysis was digested with the appropriate restriction enzymes and DNA fragments were separated by agarose gel electrophoresis. DNA was then depurinated in the gel by immersing in 0.25M HCl (Depurination buffer) for 10 minutes, and after 2 washes with water, was denatured using 1.5M NaCl, 0.5M NaOH (Denaturation solution) for 45 minutes. This was followed by 2 washes with water prior to neutralisation with 1.5M NaCl, 0.5M Tris.Cl pH 7.0 (Neutralisation solution) and then set up in a capillary blot.

The DNA was transferred from the agarose gel to Hybond nitrocellulose membranes (Amersham) by means of capillary transfer of DNA following Whatmann 3MM filter paper wick method. After transfer of DNA, membranes were washed in 2XSSC and air dried. The DNA was then fixed to the membrane by baking at 80 $^{o}$C for 2 hours.

### 2.1.10 Colony blot hybridisation

Colony-containing agar plates were overlaid with Hybond-NX nylon membranes circles, and passive transfer of colony materials was allowed to proceed for 1 minute. Membranes were transferred colony-side up to agar plates supplemented with the appropriate antibiotics. After overnight incubation at 37 $^{o}$C, membranes were transferred

colony side up to a series of solution-saturated 3MM paper filters. First a colony lysis step was carried out by using 10% sodium dodecyl sulphate (SDS) and filters incubated for 3 minutes followed by a denaturation step using denaturation buffer containing 1.5M NaCl, 0.5M NaOH for 5 minutes, and subsequently filters were incubated on 3MM soaked in neutralization buffer containing 1.5M NaCl, 0.5M Tris.Cl pH 7.0 for 5 minutes.

Membranes were then vigorously washed in 2XSSC to remove the proteinous debris. Membranes were air dried and the DNA was fixed to the membrane by baking at 80$^{o}$C for 2 hours.

### 2.1.11 Dot blot hybridisation

On some occasions, instead of taking filter lifts directly of colonies from transformations, colonies were picked and gridded out in arrays. Colonies on the plates were dotted onto Hybond-NX nylon membranes and membranes colony uppermost were placed on agar plates conditioned with appropriate antibiotics and were grown at 37$^{o}$C overnight. Replica plates were also prepared by dotting each colony on agar plates conditioned with appropriate antibiotics. Colonies were lysed, denaturated and neutralised and fixed as described above (2.1.9).

### 2.1.12 DNA probe labeling

Radioactive DNA probes were prepared using the "Random primed probe synthesis kit (Mega Prime DNA labelling systems, GE Healthcare)". For each reaction, 20-50ng of purified linearised DNA was labelled with $\alpha^{32}$P-dCTP (3000Ci/mmol). Probe DNA, primer solution (5µl) and water to a total of 10µl were added to a 0.5ml PCR tube. The mixture was heated at 95$^{o}$C for 5 minutes and centrifuged for 30 seconds at 14,500 rpm. Labelling buffer (10µl), 23µl water, 2µl Klenow fragment DNA polymerase and 50 uCi (5µl) $\alpha^{32}$P-dCTP (3000Ci/mmol) were added to the reaction and the tube incubated at 37$^{o}$C for 10 -15 minutes.

Labelled DNA probe was purified using "Illustra Nick columns (GE Healthcare)" to separate unincorporated dNTPs from the $^{32}$P-labelled probe DNA. After uncapping and discarding the storage buffer, columns were equilibrated with 3.0ml of 10mM Tris-HCl pH 8.0. Labelling reactions were applied to the column in a maximum volume of 100µl. Aliquots (400µl) of 10mM Tris-HCl pH 8.0 were added to the columns. The first aliquot was discarded as waste. The second aliquot contains the labelled DNA. Unincorprated $^{32}$P-dCTP was washed off the column with 1.2ml 10mM Tris-HCl pH 8.0 and discarded as radioactive waste. Probe DNA in fraction 2 was denatured by adding 40µl 3M NaOH and incubating at room temperature for 5 minutes followed by neutralisation with 80µl 1M Tris-HCl pH 7.5 and 40µl 3M HCl. The SSC concentration in the probe fraction was then adjusted to 6X by adding 240µl 20xSSC.

### 2.1.13 Hybridisation of filters with $^{32}P$ labelled probes

Membranes from southern blot, colony blot or dot blot were prehybridised at 65$^{o}$C for at least 1 hour in fresh hybridisation buffer (6XSSC, 0.5% SDS, 100µg/ml sonicated salmon sperm, 5X Denhardt's solution) (Appendix II). Hybridizations were performed overnight (approximately 16h) at 65°C, using fresh hybridization buffer containing $^{32}P$ radioactively labelled, denatured DNA probe (2.1.12).

After hybridization, membranes were washed in wash solution 1 (0.1% SDS, 2XSSC) followed by wash solution 2 (0.1% SDS, 0.1X SSC) at the hybridization temperature for 30 minutes each. Membranes were briefly dried on 3MM and then wrapped in Saran wrap, and loaded in a cassette with a phosphoimager screen and then visualized using a Typhoon 9410 variable-mode imager**.**

### 2.1.14 Small scale preparation of plasmid DNA – Miniprep

A single bacterial colony containing plasmid(s) was inoculated in 5ml LB medium supplemented with the appropriate antibiotic and incubated overnight at 37ºC with shaking at 250rpm. 1.5ml of the culture was centrifuged in a 1.5ml microcentrifuge tube

at 13,000rpm for 1 minute at room temperature. The bacterial pellet was resuspended in 100µl of solution I (50mM glucose, 25mM Tris-HCl, 10mM EDTA) with incubation at room temperature for 5 minutes followed by the addition of 200µl of solution II (0.2M NaOH, 1% SDS) to lyse the bacterial cell wall. Solution II contains sodium dodecyl sulphate (SDS) that lyses cell membranes/walls. The solution also contains NaOH to denature chromosomal and plasmid DNA and thus incubations are kept minimal in order to avoid excess plasmid denaturation. In order to neutralise the preparation, 150µl of ice cold solution III (3M potassium acetate, 11.5% glacial acetic acid) was added followed by 5 minutes incubation on ice. The samples were then centrifuged at 13,000rpm for 5 minutes at room temperature to pellet the bacterial protein and chromosomal DNA precipitates. Supernatant was removed and plasmid DNA precipitated using 2 volumes of 100% ethanol with incubation at room temperature for 5 minutes, and DNA was pelleted by centrifugation at 13,000rpm for 5 minutes. Supernatant was removed and the nucleic acid pellet rinsed in 70% ethanol, centrifuged again briefly and allowed to dry at room temperature. DNA was resuspended in 50µl of TE or water and RNAseA was added to a final concentration on 20µg/µl.

### 2.1.15 Large scale preparation of plasmid DNA – Midiprep

BAC or plasmid containing bacterial cells were cultured in 200-600ml LB medium supplemented with appropriate antibiotic(s) for 16 hours. The culture was centrifuged at 3200rpm for 20 minutes at 4ºC. The "Macherey-Nagel NucleoBond Xtra Midi "purification kit was used following manufacturers instruction. Briefly the bacterial pellet was resuspended in 16ml Resuspention buffer followed by the sequential addition of 16ml Lysis buffer and neutralisation by using 16ml Neutralisation buffer. Bacterial chromosomal and protein precipitates were pelleted by centrifugation at 3,000rpm for 30 minutes at room temperature. Supernatant was removed and passed through the filter column provided in the kit. This filter column was equilibrated with 5ml of Equilibration buffer prior to applying the supernatant. The filter was then washed with 5ml of Equilibration buffer and was then removed. The column was washed with 8ml of Wash buffer followed by addition of 5ml of preheated 55ºC Elution buffer. The pass through solution was collected and 2 volumes of isopropanol was used to precipitate the plasmid or BAC DNA by incubation at room temperature for 10 minutes followed by

centrifugation at 20.000 rpm or maximum speed for 30 minutes at 4ºC. The DNA pellet was then rinsed in 70% ethanol, centrifuged briefly again and allowed to dry at room temperature. Plasmid DNA was then resuspended in 100-200µl water, 10mM Tris-HCl pH 8.0 or injection buffer and its concentration was determined using a spectrophotometer.

### 2.1.16 Sample preparation for DNA sequencing

Plasmid or BAC DNA from Midiprep purification (2.1.15) was used as a DNA template for sequencing. For each BAC sequencing reaction, a total of 10 µl of 1µg/µl BAC DNA was sent to Geneservice Company (www.geneservice.co.uk) and for each plasmid sequencing a total of 20µl of 100ng/µl of plasmid DNA was sent to MWG Operon Company (www.eurofinsdna.com).

### 2.1.17 BAC DNA preparation for pronuclear injection into mouse fertilised eggs

400–600µg of the ZsGreen Clu-BAC DNA (4.5.3) was purified using a small spin-X column (Costar) and centrifuged at full speed for 30 seconds, followed by addition of 200µl of injection buffer and incubation at room temperature for 1-2 minutes with centrifugation at full speed for a further 1 minute. The concentration of BAC DNA was visually estimated using a 0.8% agarose gel (2.1.3.3).

### 2.1.18 BAC Recombineering Protocols

BAC DNA was modified using the “Counter-Selection BAC modification Kit” and protocol (GENEBRIDGES technical protocol 2007).

#### 2.1.18.1 Clusterin bacterial artificial chromosome (BAC) clones

Two BAC DNAs, bMQ70i04 and bMQ377e19, from Geneservice (Geneservice.co.uk) were initially used. Both BACs comprise of the approximately 13Kb mouse clusterin

gene but different sizes of flanking sequences cloned into the 11.5Kb pBACe3.6 vector backbone at the *EcoRI* sites (Appendix VI.I). Clu BAC DNAs were transformed and maintained in *E. Coli* DH10B cells.

Clusterin BACs contain the CAT gene (encoding Chloramphenicol acetyltransferase) and also the amp gene resulting in BAC containing cells as Chloramphenicol and Ampicillin resistant. This BAC also bears a sacB gene (encoding levansucrase) for negative selection upon sucrose plates.

In addition these BACs carry two loxP sites in their backbone, one at position 4831-4864bp (loxP) and also a mutated loxP (loxp511) at position 11408-11441bp (Appendix VI.I).

**2.1.18.2 Antibiotic concentrations used in recombineering experiments**

The concentration of antibiotics used in the recombineering experiments are as follows unless otherwise stated. Chloramphenicol 15µg/ml, Tetracycline 3µg/ml, Kanamycin 15µg/ml and Streptomycin 50µg/ml.

**2.1.18.3 Preparation of electrocompetent cells for electroporation of pRed/ET**

Before starting the recombineering experiments, the pRed/ET plasmid was introduced into cells containing the BAC to be manipulated. The glycerol stock of *E. Coli* cells containing the BAC clone was streaked on LB plates conditioned with Chloramphenicol. The day after, one single colony was picked and inoculated in 5ml LB medium with Chloramphenicol to select for cells containing the BAC. The culture was incubated at 37$^{o}$C overnight with shaking at 250rpm. Electrocompetent cells were prepared by inoculation of 30µl of the overnight culture in 1.4ml LB medium conditioned with Chloramphenicol and grown at 37$^{o}$C for 2-3 hours with shaking at 250rpm. The cells were centrifuged at 11,000rpm for 30 seconds at 2$^{o}$C. The pellet of cells was washed twice with 1.0ml of chilled dd$H_2O$ and finally cells were resuspended in 20-30µl of dd$H_2O$.

### 2.1.18.4 Preparation of electrocompetent cells for electroporation of linear DNA cassette

Single colonies of *E. Coli* containing the BAC and pRed/ET plasmids were collected and grown at 30$^{o}$C overnight in 5ml LB supplemented with appropriate antibiotics. 200µl of these cultures were used to inoculate two samples of 20ml LB supplemented with appropriate antibiotics and grown with shaking at 300rpm at 30$^{o}$C until $OD_{600}$ of ~0.3. The expression of the red/ET recombination proteins were induced by addition of 350µl fresh 10% L-arabinose to 10ml of the culture. The remaining 10ml of the cultures were left without induction as negative controls. All the tubes were incubated at 37$^{o}$C, shaking at 250rpm for 1 hour.

Both induced and uninduced cells were prepared for electroporation. Cells were centrifuged twice, once for 15 minutes and once for 10 minutes at 3,200rpm at 2$^{o}$C. Each time supernatant was discarded and the cells were washed with 20ml ice-cold distilled $H_2O$. The cell pellet was then resuspended in 750µl ice-cold distilled $H_2O$. 250µl of the cells were transferred into three pre-chilled microfuge tubes followed by spinning at 11,000rpm for 30 seconds at 2$^{o}$C using a benchtop centrifuge. The supernatant was then removed and the cells were resuspended in 30-50µl of ice-cold distilled $H_2O$.

### 2.1.18.5 Preparation of the linear DNA for electroporation

The linear DNA cassette for electroporation and recombineering was produced by high fidelity PCR (2.1.6). In this PCR, reverse and forward primers that contain the 50bp homology arms to the insertion point (2.4.2, 3, 8 and 10) were used. Samples of the PCR products were visualized on 1.0% agarose gels. Next, the linear PCR products were either digested with Dpn1 at 37$^{o}$C for 1 to 4 hours and extracted from gels or extracted without Dpn1 digestion by the gene clean method (2.1.2) and DNA was resuspended in 5µl 10mM Tris-HCl, pH 8.0. The concentration of the DNA was determined by gel electrophoresis and comparison with 2.5 and 5µl of λ *Hind*III DNA ladder (2.1.3.3).

### 2.1.18.6 Ethanol precipitation of PCR products

In order to concentrate the DNA of PCR products ethanol precipitation was carried out by adding 5µl of 3M sodium acetate (pH 7.0), 150µl of 100% ethanol and mixing. The sample was then incubated at -80$^{o}$C for 5 minutes or at -20$^{o}$C for 30 minutes followed by spinning at maximum speed for 10 minutes. The DNA was washed with 70% ethanol and dried at 37$^{o}$C using a heat block and resuspended in 3-5µl of 10mM Tris-HCl, pH 8.0 (GENEBRIDGES technical protocol 2007).

### 2.1.18.7 Electroporation

A Bio-Rad Gene Pulser II electroporator and a cuvette with a slit size or 1mm or 2mm was used to electroporate plasmid or purified linear DNA into BAC containing cells. 30-50µl of electrocompetent cells (2.1.18.3 and 2.1.18.4) were transferred into a pre-chilled cuvette and 20ng of plasmid DNA or 100-200ng of purified linear DNA cassette was added to the cells and electroporated. The settings used for electroporation was 1350 or 2500 V, 10µF, and 600 Ohms.

The 1350 V was recommended by protocol (GENEBRIDGES technical protocol 2007) for the electroporation of both plasmid and linear DNA cassette. However, the 2.5KV was used in later experiments for the electroporation of linear DNA based on the personal communication with the Gene Bridges company (http://www.genebridges.com) for use of Bio-Rad Gene Pulser II electroporator and also through the finding that at this voltage, the transformation frequencies of supercoiled plasmid DNA was optimal (4.5.2.3).

### 2.1.18.8 Bacterial outgrowth following electroporation

Immediately after electroporation 1.0ml LB medium was added and the culture was incubated at 37$^{o}$C with shaking for at least 70 minutes. 100µl and 200µl of the culture was streaked on LB agar plates containing Chloramphenicol, Kanamycin and Tetracycline. Plates were then incubated at 30$^{o}$C or 37$^{o}$C (the Red/ET recombination

proteins expression plasmid would get lost at 37$^{o}$C, therefore only in the last round of recombineering was incubation carried out at 37$^{o}$C) for 20-40 hours.

### 2.1.18.9 Functional testing of the rpsL-neo selectable marker

In order to test the function of the rpsL-neo cassette in clones obtained from the first recombineering step (insertion of rpsL-neo cassette that should confer resistance to Streptomycin), 12-24 single colonies from the induced plates were inoculated in 1ml LB medium with Chloramphenicol, Kanamycin and Tetracycline followed by shaking at 30ºC for 1-2 hours. These cultures were then used for streaking LB agar plates containing Streptomycin, Chloramphenicol, and Kanamycin for a Streptomycin sensivity test and also for inoculation in LB medium and overnight growth at 37ºC for further analysis (2.1.18.10). The clones with a functional rpsL-neo cassette did not grow on Streptomycin plates.

### 2.1.18.10 Identification and confirmation of the recombined clones

12-24 colonies were inoculated in 5ml LB medium supplemented with the appropriate antibiotics and incubated overnight at 37ºC with shaking at 250rpm. These cultures were then analysed by one, or a combination of the following methods: colony PCR, miniprep followed by PCR, colony blot, dot blot or southern blot hybridisation. In some cases the loss or gain of a selectable marker was checked by streaking the culture on LB agar plates conditioned with the appropriate antibiotics and growth at 30 or 37ºC overnight.

## 2.2 RNA protocols

### 2.2.1 *In situ* hybridisation overview

#### 2.2.1.1 Generation of riboprobe

Plasmid DNA containing the riboprobe to be transcribed was digested to completion with the appropriate restriction enzymes to linearise the plasmid. The digested plasmids were used as templates for *in vitro* transcription of antisense and sense probes. RNA riboprobes were generated using 1µg of linearised plasmid in a transcription reaction containing either T7 or T3 RNA polymerases (Promega) and digoxigenin conjugated UTP ribonucleotides (Roche). Labelling reactions were performed as follows:

1.0µg linearised plasmid
4.0µl 5X transcription buffer
2.0µl 0.1M DTT
2.0µl DIG RNA labelling mix (Roche)
0.5µl RNAsin (Promega)
1.0µl (10 units) RNA polymerase (Promega)
RNAse free water to 20µl

Transcriptions were incubated at 37ºC for 2- 16 hours. 0.5-1.0µl of the reaction was checked on a 1% agarose gel to ensure that the transcription was efficient. Riboprobe was precipitated by the addition of 100µl, TE (pH 7.5), 10µl 4M LiCl and 300µl 100% ethanol at -80ºC overnight. RNA riboprobe was pelleted by centrifugation at full speed for 30 minutes at 4ºC, washed in 70% ethanol dried at room temperature and resuspended in 20µl TE (pH 7.5). Alternatively, micro bio-spin columns (Bio-Rad) were used to purify the riboprobe following manufacturer's instructions.

#### 2.2.1.2 Collection of embryos

Timing of embryo age was by the vaginal plug method, with 12.00 noon on the day the copulation plug was observed referred to as 0.5 day post coitum (dpc). Pregnant females were sacrificed on the appropriate day by cervical dislocation (a Schedule 1 method – in accordance with Animals (Scientific Procedures) Act, 1986), and transferred to

phosphate buffered saline (PBS, Appendix III) chilled on ice, and embryos dissected in PBS using forceps.

#### 2.2.1.3 Section *in situ* hybridisation - tissue preparation

Whole heads or inner ears were dissected from 12.5, 13.5, 15.5, 17.5 and 18.5dpc embryos, and for 11.5dpc stages, the whole embryo was dissected. Ears, heads and embryos were rinsed in PBS (Appendix III) and fixed at 4ºC in 4% paraformaldehyde in PBS (Appendix III) for various periods (depending on the size of tissue; whole heads were fixed overnight and dissected ears for 3-4 hours, both at 4ºC). Inner ear tissues were also harvested after birth at P2 and P17, and the round and oval windows were removed prior to immersion of the inner ear in fixative for 2 hours at room temperature. Fixed samples were rinsed in PBS and P17 ears were decalcified using 0.5 M EDTA pH 8.0 for 4 days at room temperature. Following fixation or fixation and decalcification, all tissues were equilibrated with 30% sucrose in PBS and embedded in a 1:1 mix of 30% sucrose and OCT and were frozen on dry ice. Serial sections of 16-20-µm thickness were taken on a cryostat and lifted onto TESPA (3-aminopropyl-triethoxysilane)-coated glass slides and dried at 37ºC overnight. Sections were then fixed at room temperature in 4% paraformaldehyde in PBS for 5 minutes followed by rinsing in PBT and treated with proteinase K, 10-20µg/ml in PBS at room temperature for 2-5 minutes (depending on the thickness of the sections). Sections were washed with PBT prior to pre-hybridisation.

#### 2.2.1.4 Hybridisation, antibody application and detection

Hybridisation against sections: For sections pre-hybridisation was carried out at 60ºC with hybridisation solution (50% formamide, 5xSSC, 50µg/ml yeast tRNA, 1% SDS, 50µg/ml Heparin, 0.2% Tween 20, 0.5% Chaps, 5mM EDTA) for 2-4 hours followed by hybridisation at 55-63ºC overnight with hybridisation buffer containing digoxigenin-UTP labelled antisense RNA probes to a concentration of 0.1-1.0µg/ml. Following hybridisation, sections were washed 3 times with solution III (50% formamide, 2XSSC pH 5.0, 1% SDS) at room temperature.

Immunohybridisation against sections: Following washing excess riboprobe, sections were equilibrated in TBST by three washes 2-5 minutes each. Blocking of non-specific binding sites was carried out by incubation in TBST with 2% blocking media (Roche) and 10% heat inactivated sheep serum for 1 hour at room temperature. Anti-digoxigenin-AP FAB fragments antibody was added to TBST containing 2% blocking media and 10% heat inactivated sheep serum at 1 in 2000 dilution, and the sections were incubated in this antibody solution overnight at 4ºC.

3-6X 5 minute's washes with TBST were carried out to remove unbound antibody from the sections, followed by 2X 5 minutes washes with NTMT (Appendix III). For detection of hybridised probe, NBT (nitroblue tetrazolium salt, 66.6mg/ml in 70% DMF) and BCIP (5-Bromo-4-chloro-3-indolylphosphate, toluidine salt, 50mg/ml) staining was carried out by incubating sections in the dark in NTMT supplemented with 4.5µl NBT and 3.5µl BCIP per ml staining solution. If there was no signal detected after 20 minutes, PVA/NBT/BCIP (poly vinyl alcohol) staining was carried out by using the above solution supplemented with 10% PVA and with incubation for 2- 16 hours at room temperature until signal was evident. Staining reactions were stopped by washing sections 3 times with PBS. Sections were then fixed using 4% PFA for 5 minutes and 3X washes with BPT (PBS+ 0.1% Tween 20) followed by dehydration through an ethanol series and then sections were cleared by incubation in three 10-20s in histoclear followed by mounting in DPX mountant.

### 2.2.2 Total cellular RNA extraction

Total cellular RNA was isolated using the Trizol RNA extraction method. 50 – 100mg of fresh or frozen tissue was homogenized in 1.0ml TRIZOL reagent (Invitrogen). The homogenized samples were incubated at room temperature for 10 minutes and then 0.2ml of chloroform was added and the mixture put on a shaker for 1 minute, followed by further incubation at room temperature for 2 minutes without agitation. The samples were centrifuged at 11,300 x g for 15 minutes at 8$^{o}$C. Following centrifugation, the mixture separated into a lower red, phenol-chloroform phase, an interphase, and a colourless upper aqueous phase that was transferred carefully without disturbing the

interphase into a fresh tube. The volume of the aqueous phase was measured and RNA precipitated by addition of 0.5ml isopropyl alcohol with incubation of the sample at -20$^{o}$C for 1 hour followed by centrifugation at 12,000 x g for 20 minutes at 4$^{o}$C. The RNA pellet was washed once with 1.5ml of 75% ethanol, mixed by vortexing and centrifuged at 7,000 x g for 5 minutes at 4$^{o}$C. The above washing procedure was repeated, ethanol removed and the pellet air-dried for 10 minutes. The RNA pellet was dissolved in DEPC-treated water and the OD at 260nm and 280nm was checked.

### 2.2.3 cDNA synthesis

The "First-Strand cDNA Synthesis Kit" (Invitrogen) was used to synthesis cDNA from total RNA. First-strand cDNA was synthesised by adding 1.0µg of specific primer resuspended in DEPC water and 10mM dNTPs to 1.6µg of total RNA template. Total RNA was first heat denatured for 5 minutes at 65ºC and then kept on ice for 5 minutes before adding 4µl of 5X first-strand buffer, 1.0µl of 0.1M DTT, 1.0µl of Superscript II RT (Invitrogen) and 1.0µl of RNase inhibitor. The reaction was mixed thoroughly by pipetting and then incubated at 55ºC for 60 minutes followed by heat denaturation at 70ºC for 15 minutes. RT-PCR was carried out as described in section 2.1.7.

## 2.3 Protein protocols

### 2.3.1 Immunohistochemistry

#### 2.3.1.1 Tissue preparation

Mouse embryo heads or whole inner ears were fixed in 4% PFA for 1 hour at room temperature or overnight at 4ºC and washed 3 times with PBS for 5 minutes each.

### 2.3.1.2 Heat mediated antigen retrieval

In order to unmask the antigenic sites from sectioned material, heat-mediated antigen retrieval was performed with steaming either in "Citrate EDTA buffer pH 6.2" or "Citrate buffer pH 6.0 (Appendix IV)". Using a microwave, the buffer was heated in a glass jar until about 90$^{o}$C. The tissue section slide was then transferred to the heated buffer and boiled at medium setting for 5 minutes and subsequently allowed to cool to room temperature.

### 2.3.1.3 Immunohistochemistry on paraffin-embedded tissue sections

Tissues were dehydrated through an ethanol series (70%, 85%, 95% and 2X100%) each for 1 hour in the case of whole embryonic heads or 5 minutes for whole inner ears. Tissues were then cleared using histoclear either overnight or 1 hour for the whole head or inner ear respectively. Tissue was transferred through two changes of paraffin wax at 60$^{o}$C each for 1 hour or 5 minutes each for whole heads or inner ears respectively. Tissues were orientated and set in moulds. Wax sections were taken at 10-µm using a rotary microtome. Sections were floated and lifted onto TESPA treated slides and dried at 37$^{o}$C for about 48 hours. Paraffin was removed with two changes of histoclear, 20 minutes each, and then rehydrated by 2 changes of 100% ethanol, 1X95% ethanol, 1X80% ethanol, 1X60% ethanol and 3 rinses in water 5 minutes each. The "heat mediated antigen retrieval" was carried out as described in section 2.3.1.2.

Following unmasking with Citrate EDTA buffer (pH 6.2), sections were washed 3 times with PBS before being pre-blocked with 10% horse serum in PBS (pre-block buffer) with incubation for 1 hour at room temperature. Sections were incubated overnight at 4ºC with primary antibody, diluted to the desired concentration in pre-block buffer. The following day, sections were washed 4-5 times with PBS. Secondary antibody was diluted in the pre-block buffer and incubated at room temperature for 1 hour. Finally, the sections were washed for three 5 minutes periods with PBS and mounted in vectashield mounting medium (Vector Laboratories Inc.) and visualised using a fluorescence microscope. Images of sections were captured using a "Zeiss Axioplan florescence microscope" with an attached "SPOT RT Slider digital camera".

Unmasking with Citrate buffer (pH 6.0) was carried out as recommended in the Proteintech protocol (www.ptglab.com). For this the same protocol as above was carried out except TBS buffer pH 7.6 (Appendix IV) was used instead of PBS and the pre-block buffer included 3% BSA in TBS (pH 7.6).

#### 2.3.1.4 Immunohistochemistry on cryosections

Fixed tissues were cryoprotected in 30% sucrose overnight at 4ºC, embedded in OCT and frozen on dry ice. Samples were sectioned at 10-µm. Sections were lifted onto TESPA treated slides and dried at 37ºC overnight. The sections were hydrated with PBS for 10 minutes followed by performing a "heat-mediated antigen retrieval" step (2.3.1.2) using Citrate buffer pH 6.0.

Preblocking of sections was carried out in 10% horse serum in PBS, 0.1% Triton X-100 with incubation for 1 hour at room temperature. Sections were then incubated overnight at 4ºC with primary antibody, diluted in 10% horse serum in PBS, 0.1% Triton X-100. The following day, sections were washed 4-5 times with PBS. Secondary antibody was diluted in pre-block buffer and incubated at room temperature for 1 hour followed by 3 washes with PBS. Finally, the sections were washed for three 5 minute periods in PBS, mounted and visualised using a fluorescence microscope. Images of sections were captured using a "Zeiss Axioplan florescence microscope" with an attached "SPOT RT Slider digital camera".

### 2.3.1.5 List of antibodies used in immunohistochemistry

#### 2.3.1.5.1 Clusterin antibodies

##### 2.3.1.5.1.1 Primary anti-CLU antibody (ab69644-Rabbit polyclonal antibody from Abcam)

This antibody is a polyclonal antibody raised in rabbit and reacts with human, mouse and rat. It is a synthetic peptide of EKALQEYRKKHREE by a cysteine residue linker, corresponding to C-terminus amino acids 436-449 of human clusterin. This is from an equivalent mouse peptide of sequence: EKALQEYRRKSRAE.

##### 2.3.1.5.1.2 Primary anti-CLU Ab (ag2889- Rabbit polyclonal antibody from Proteintech)

This antibody is a polyclonal antibody raised in rabbit and is generated against the last 350 amino acids of the human CLU protein (C-terminus). It is a synthetic peptide that reacts with human, mouse and rat.

#### 2.3.1.5.2 Other antibodies

**2.3.1.5.2.1 Primary anti-Myosin VIIA antibody** (gift from Prof Guy Richardson, University of Sussex) used at 1:100 dilution.

**2.3.1.5.2.2 Primary anti-Prox1 antibody** (AB5475-Millipore, Chemicon) gift from Prof Guy Richardson, University of Sussex), is a polyclonal antibody raised in rabbit and reacts with human, mouse, rat and zebrafish. It is synthetic peptide from the C-terminal 15 amino acids of mouse Prox1 protein. It was used against wax and cryosections of mouse at 1:1000 dilution.

**2.3.1.5.2.3 Secondary antibody -** Goat anti-rabbit IgG Alexa fluor 488 secondary antibody (Invitrogen, Gift from Prof Guy Richardson, University of Sussex) was used at 1:500 dilution against all the above mentioned primary antibodies.

## 2.4 PCR primers

### 2.4.1 Primers to analyse the integrity of the E19 BAC

| Primer name | Primer pairs | Sequence **(5' → 3')** | Area of amplification | Size of amplicon |
|---|---|---|---|---|
| F216-Clu ex2<br>R217-Clu int1 | 1 | F:AGACCGGTGAGACAGCTGCAC<br>R:GTATCAAGATGAGCTACAGGGAGCAG | Exon1-Intron1 | 1542 |
| F218-Clu int1<br>R219-Clu int1 | 2 | F:CTGCTCCCTGTAGCTCATCTTGATAC<br>R:TGTCTCCTCATCTGGCATCACTGC | Intron1 | 1390 |
| F220-Clu int1<br>R221-Clu int2 | 3 | F:GTGATGCCAGATGAGGAGACAGATGAG<br>R:CTGGCACTTCTTTGCTACAACGCAC | Intron1–Intron2 | 1314 |
| F222-Clu int2<br>R223-Clu int3 | 4 | F:GTGCGTTGTAGCAAAGAAGTGCCAG<br>R:GGCAGTCCCTTGTTATCAGTTCTTAGCT | Intron2–Intron3 | 1358 |
| F224-Clu int3<br>R225-Clu int4 | 5 | F:GCTAAGAACTGATAACAAGGGACTGCC<br>R:GTGGCCACACGAAACTGACCCAAG | Intron3–Intron4 | 1320 |
| F226-Clu ex5<br>R227-Clu int6 | 6 | F:TCCGAGCTTCCACAACATGTTCCAGC<br>R:GCGTTCACCTAACATGCAGGAGGC | Exon5–Intron6 | 1345 |
| F228-Clu int6<br>R229-Clu int6 | 7 | F:GCCTCCTGCATGTTAGGTGAACGC<br>R:GCAAGACACAGGATTGGAGACCAG | Intron6 | 1401 |
| F230-Clu int6<br>R231-Clu int7 | 8 | F:CTGGTCTCCAATCCTGTGTCTTGC<br>R:TTCAATGCTACAACGTGCATA AGGT | Intron6–Intron7 | 1333 |
| F232-Clu int7<br>R233-Clu ex9 | 9 | F:ACCGTATGCACGTTGTAGCATTG<br>R:TCAGTTCTTCCCGAGAGCAGCAAGT | Intron7–Exon9 | 1496 |

### 2.4.2 rpsL-neo oligos with 50bp homology arms

| Primer | Forward/ Reverse | Sequence **(5' → 3')** |
|---|---|---|
| HRrpsL-for | F | TATGTTCTCTCAGCACACTTCAAGGGTAGAACACATTAT CAACCACGAGCGGCCTGGTGATGATGGCGGGATCG |
| HRneo-rev | R | TCAATGATGTAGCAACACAAGTAAGCCCGAAGGTCAAT GGTCCAAGCAGATCAGAAGAACTCGTCAAGAAGGCG |

Forward and reverse oligos used for the amplification of the rpsL-neo cassette with the 50bp homology arms to the either side of the insertion point at mid intron 2 of the clusterin gene. Clusterin homology arms are highlighted in green and the sequence annealing to the rpsL-neo template is highlighted in yellow.

### 2.4.3 Oligos for replacement of rpsL-neo with "Bglobin-ZsGreen-SV40 pA"

| Primer | Forward/ Reverse | Sequence **(5' → 3')** |
|---|---|---|
| HRZsG-for | F | TATGTTCTCTCAGCACACTTCAAGGGTAGAACACATTA TCAACCACGAGCGGACTAGTCCGGACTAGTCCGGGC |
| HRZsG-rev | R | TCAATGATGTAGCAACACAAGTAAGCCCGAAGGTCAA TGGTCCAAGCAGACGCCTTAAGATACATTGATGAGTT |

Forward and reverse oligos used for the amplification of the "Bglobin-ZsGreen-SV40 pA" reporter cassette with 50bp homology arms to the 5' and 3' flanking regions of insertion point in mid intron 2 of the clusterin gene. Homology arms are highlighted in green and the sequences directed against the Bglobin or SV40 pA are highlighted in yellow.

### 2.4.4 Oligos for PCR analysis of "rpsl-neo" and "Bglobin-ZsGreen-SV40 pA" insertion

| Primer | Forward/ Reverse | Sequence **(5' → 3')** |
|---|---|---|
| F321-Clu int2 | F | CTCTTGCTCATAGCTGACCAGTTC |
| R322-rpsl | R | CGGATCAGGATCACGGAGTGCT |
| F288-Neo1 | F | GTATCCATCATGGCTGATGC |
| R289-Neo2 | R | TGATGCTCTTCGTCCAGATC |
| F220-Clu int1 | F | GTGATGCCAGATGAGGAGACAGATGAG |
| R221-Clu int2 | R | CTGGCACTTCTTTGCTACAACGCAC |
| FClu-begin | F | TCTGGAAGAGCAGCCATCATTC |

### 2.4.4 continued

| Primer | Forward/ Reverse | Sequence **(5' → 3')** |
|---|---|---|
| RClu-begin | R | GACTTCTCCCATCTTCCTGC |
| FClu-end | F | GCATGTATGCTAGCACATCTGC |
| RClu-end | R | CACCATTCTGACCTGGAGTG |
| ZsG3-244 | F | GGAGATGACCATGAAGTACCGCATGG |
| ZsG4-311 | R | GCTTGTGCTGGATGAAGTGCCAGTC |
| ZSG out | R | GGTACTCGGTGAACACGCGGTTGC |

### 2.4.5 Oligos for the analysis of extreme ends of Clu-BAC

| Primer | Forward/ Reverse | Sequence **(5' → 3')** |
|---|---|---|
| FClu-begin | F | TCTGGAAGAGCAGCCATCATTC |
| RClu-begin | R | GACTTCTCCCATCTTCCTGC |
| FClu-end | F | GCATGTATGCTAGCACATCTGC |
| RClu-end | R | CACCATTCTGACCTGGAGTG |

The extreme beginning and end of Clu-BAC (modified and unmodified) was checked by PCR analysis using begin and end oligo pairs.

### 2.4.6 Oligos for introduction of new restriction sites to the Bglobin cassette

| Primer | Forward/ Reverse | Sequence **(5' → 3')** |
|---|---|---|
| Bglobin-BglII | F | GCATCAATAGATCTGGGCTGGGCATAAAAGTCAG GGCA |
| Bglobin-XhoI | R | ATATATCTCGAGCCCATGGCGCCGCGCTCTGCTT |

Forward and reverse oligos used for PCR mutagenesis to introduce BglII and Xho I sites to the beginning and to the end of Bglobin PCR products. BglII and Xho I are highlighted in green. Extra bases added to the oligos are highlighted in yellow.

### 2.4.7 Oligos for the analysis of clones obtained during the generation of the "Bglobin-Cre-SV40 pA" template

| Primer | Forward/ Reverse | Sequence **(5' → 3')** |
|---|---|---|
| Bglobin-BglII | F | GCATCAATAGATCTGGGCTGGGCATAAAAGTCAG GGCA |
| Bglobin-XhoI | R | ATATATCTCGAGCCCATGGCGCCGCGCTCTGCTT |
| 339-CreE | R | GTTGCATCGACCGGTAATGCAG |
| CreORFR1 | R | TAATCGCCATCTTCCAGCAG |

### 2.4.8 Cre oligos with 50bp homology arms

| Primer | Forward/ Reverse | Sequence **(5' → 3')** |
|---|---|---|
| HRCre-for | F | TATGTTCTCTCAGCACACTTCAAGGGTAGAACACATTA TCAACCACGAGCGGGCTGGGCATAAAAGTCAGGGC |
| HRCre-rev | R | TCAATGATGTAGCAACACAAGTAAGCCCGAAGGTCAA TGGTCCAAGCAGAACGCGTTAATGGCTAATCGCCATC |

Forward and reverse oligos used for the amplification of the Bglobin-Cre cassette with 50bp homology arms to the either side of the insertion point at mid intron 2 of the clusterin gene. Homology arms are highlighted in green and the sequences annealing to the Bglobin or Cre template are highlighted in yellow.

### 2.4.9 Oligos for PCR based screening of Cre recombinants

| Primer | Forward/ Reverse | Sequence **(5' → 3')** |
|---|---|---|
| F321-Clu int2 | F | CTCTTGCTCATAGCTGACCAGTTC |
| F220-Clu int1 | F | GTGATGCCAGATGAGGAGACAGATGAG |
| R221-Clu int2 | R | GACCGTGAAGAAACGATGTTGCGTG |
| CreORFR1 | R | TAATCGCCATCTTCCAGCAG |
| CreERT2F1 | F | TGCATTACCGGTCGATGCAACG |
| 339-CreE | R | GTTGCATCGACCGGTAATGCAG |

### 2.4.10 LoxP oligos with 50bp homology arms

| Primer | Forward/ Reverse | Sequence **(5' → 3')** |
|---|---|---|
| HRloxp-for | F | CTTATCGATGATAAGCTGTCAAACATGAGAATTGATCC GGAACCCTTAATTTCAAATATGTATCCGCTCATGAG |
| HRloxP-rev | R | CCGATGCAAGTGTGTCGCTGTCGACGGTGACCCTATAG TCGAGGGACCTATTTATTCTGTCTTTTTATTGCCGTC |

Forward and reverse oligos used for the amplification of rpsL-neo cassette with 50bp homology arms to the either side of the loxP site in the pBACe3.6 vector backbone. Homology arms are highlighted in purple and the sequence annealing to the rpsL or neo template are highlighted in yellow.

### 2.4.11 Oligos for analysis of replacement of loxP by the rpsL-neo cassette

| Primer | Forward/ Reverse | Sequence **(5' → 3')** |
|---|---|---|
| pBACe95 | F | TGATCGCGTAGTCGATAGTG |
| pBACe96 | R | GACCGACAACACGAGTGGGA |
| R322-rpsl | R | CGGATCAGGATCACGGAGTGCT |
| F288-Neo1 | F | GTATCCATCATGGCTGATGC |
| R289-Neo2 | R | TGATGCTCTTCGTCCAGATC |

List of forward and reverse oligos used for the analysis of clones obtained from the step "replacement of loxP site in the pBACe3.6 vector backbone with rpsL-neo cassette".

### 2.4.12 Oligos for the PCR amplification of "lacZ selectable marker" with homology arms

| Primer | Forward/ Reverse | Sequence **(5' → 3')** |
|---|---|---|
| HRloxP511-for | F | CGTAAGCGGGGCACATTTCATTACCTCTTTCTCCGC ACCCGACATAGATACCATTCGCCATTCAGGCTGCG |
| HRloxP511-rev | R | CTAGTAGACTTAATTAAGGATCGATCCGGCGCGCCA ATAGTCATGCCCC GGCGCAACGCAATTAATGTGAGT TAGC |

Forward and reverse oligos used for the amplification of LacZ cassette with 50bp homology arms to the right and left of the loxP511 (11408-11441) site in the pBACe3.6 vector backbone. Homology arms are highlighted in blue and the sequence annealing to the LacZ gene template are highlighted in yellow.

### 2.4.13 Oligos for the PCR amplification of "Bglobin-Cre-SV40 pA" cassette with homology arms

| Primer | Forward/ Reverse | Sequence **(5' → 3')** |
|---|---|---|
| HR-SV40-for | F | TATGTTCTCTCAGCACACTTCAAGGGTAGAACACATTA TCAACCACGAGCGGGCTGGGCATAAAAGTCAGGGC |
| HR-SV40-rev | R | TCAATGATGTAGCAACACAAGTAAGCCCGAAGGTCAA TGGTCCAAGCAGACGCCTTAAGATACATTGATGAGTT |

Forward and reverse oligos used for the amplification of "Bglobin-Cre-SV40 pA" DNA cassette with the 50bp homology arms to the right and to the left of mid intron 2 of clusterin gene. The homology arms are highlighted in green and the sequence annealing to the Bglobin or SV40 pA are highlighted in yellow.

### 2.4.14 Miscellanous oligos

| Primer | Forward/ Reverse | Sequence **(5' → 3')** |
|---|---|---|
| Clu9F | F | GTGTCACTGAGGTGGTGGTGAAGC |
| Clu9R | R | GGTGATGCTTCTATCTCATTCCGC |

Clu9F and Clu9R oligos were used in IHC analysis to check the C-terminus of mouse clusterin gene.

### 2.4.15 Oligos used for sequencing of ZsGreen Clu-BAC

| Primer | Forward/ Reverse | Sequence **(5' → 3')** |
|---|---|---|
| For-seq int2 | F | GCTGTCCATCACCTCAACTTATC |
| Rev-seq int2 | R | CTGGCAACCGCATCAGGTA |

Forward and reverse oligos used from intron 2 and outside the homology region for sequencing of the Clu ZsGreen-BAC.

# 3. Results: Clusterin gene expression during mouse inner ear development

## 3.1 Introduction and aims

Clusterin mRNA had previously been identified from a developmental stage-specific cDNA subtraction during mouse inner ear development at 13.5dpc (1.3). In order to better predict the cellular roles that clusterin may play in the development of this organ, an understanding of the spatiotemporal expression pattern throughout development is required. Therefore, in the first part of this project, a time course of clusterin mRNA expression during mouse inner ear development was investigated. To do this, riboprobes from the clusterin gene were prepared and used against mouse embryos, whole inner ears and inner ear tissue sections for the detection of clusterin mRNA through *in situ* hybridisation. In order to determine how the areas of clusterin mRNA expression relate to clusterin protein products, immunohistochemistry was carried out using two different clusterin antibodies against mouse embryo inner ear tissue sections. Finally to determine more definitively the cell types where clusterin is synthesised, mouse embryo inner ear sections were analysed for expression of supporting cell markers. To do this, alternative sections were analysed for clusterin expression and riboprobes against Tectorin α and Tectorin β riboprobes for detection of supporting cells. In addition at the protein level, Myosin VIIA and Prox1 antibodies were used as markers for hair cells and supporting cells respectively to give a more detailed picture as to the localisation of clusterin expression during inner ear development.

## 3.2 Results

### 3.2.1 Clu-mRNA expression during mouse embryogenesis and postnatal

In order to determine the expression profile of clusterin during inner ear development, a number of key embryonic stages of pre- and postnatal mouse development were examined as outlined below.

#### 3.2.1.1 RNA *in situ* hybridisation at 11.5dpc

RT-PCR demonstrated the upregulation of clusterin at 13.5dpc but not detectable at 10.5dpc (Figure 1.6). So, in order to determine the exact onset of clusterin expression,

*in situ* hybridisation of 11.5dpc mouse head sections using a DIG-labelled mouse clusterin antisense riboprobe was carried out (2.2.1.1). At this developmental stage, no expression could be detected in or near to the developing otic vesicle epithelium (Figure 3.1 and 3.2).

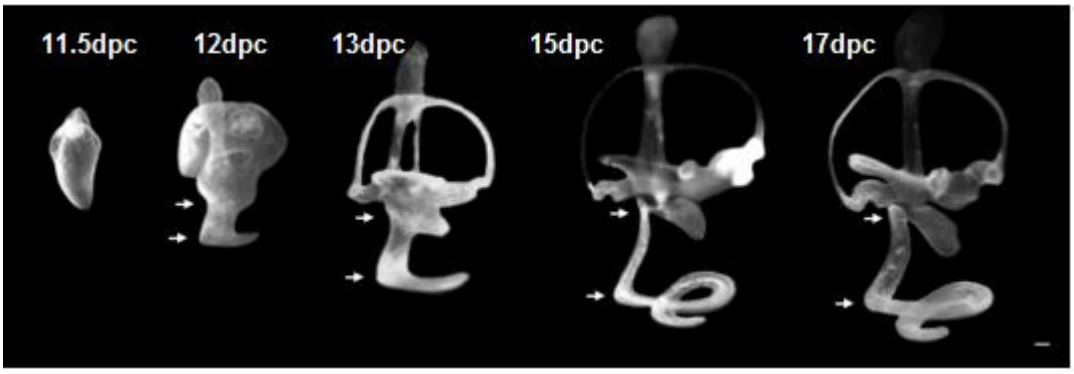


Figure 3.1 Lateral views of pain-filled mouse inner ear membranous labyrinths illustrating the gross morphogenesis of the ear between 11.5-17.0dpc. Scale bar: 100mm. Adapted from Morsli et al. (Morsli, Choo et al. 1998).

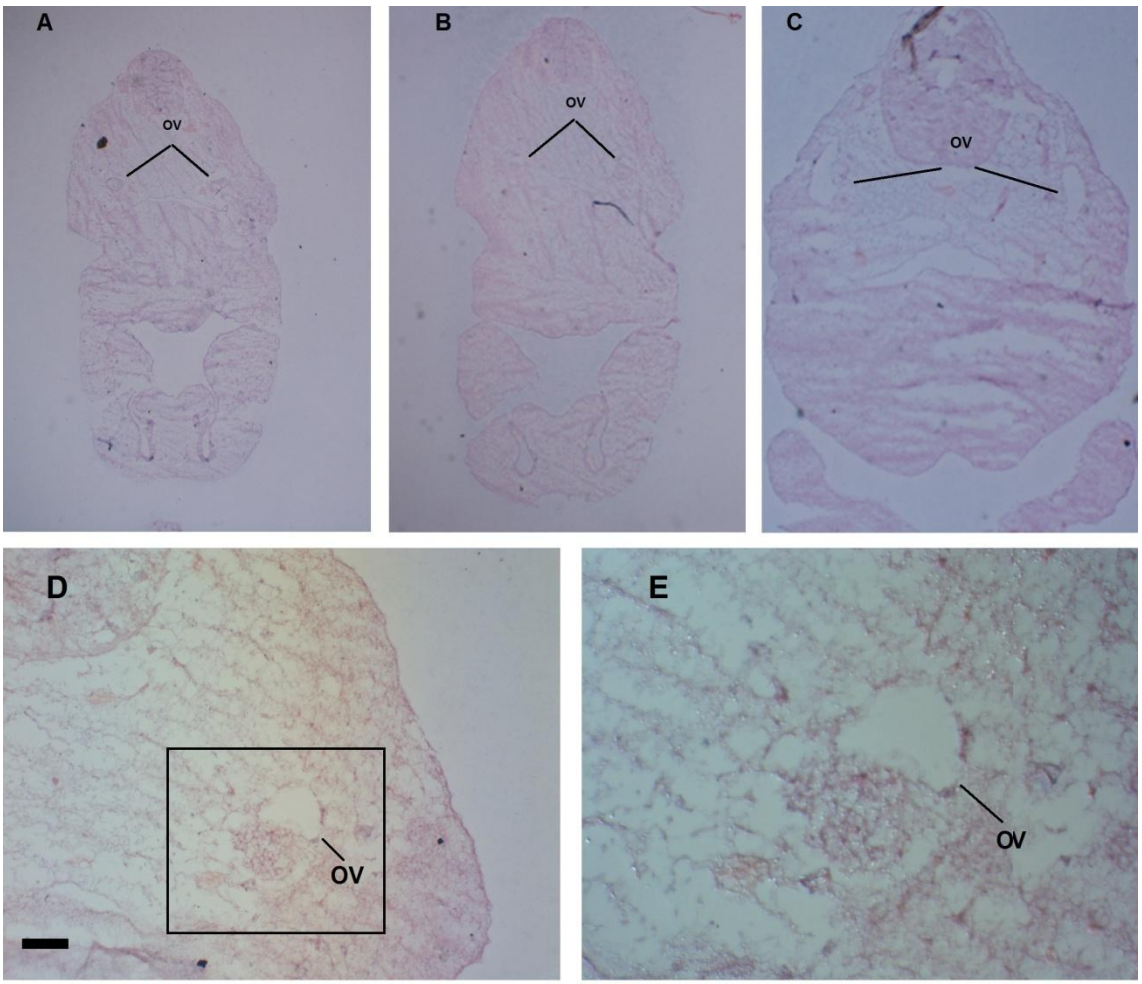

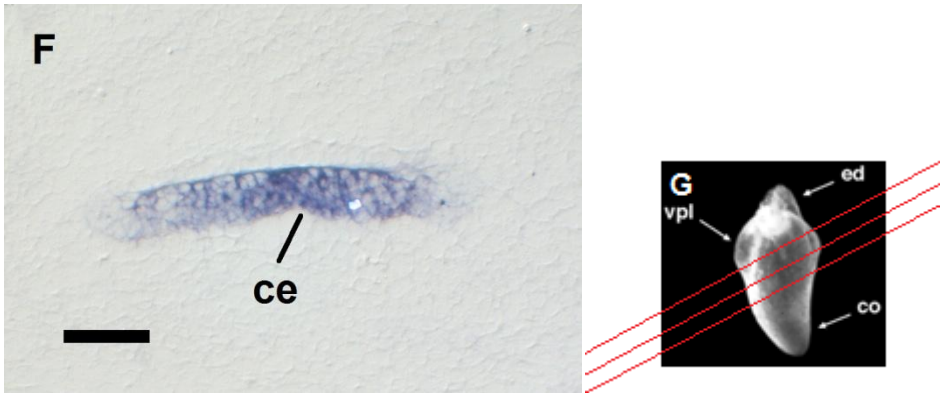


Figure 3.2 Clusterin *in situ* hybridisation against sections at 11.5dpc. A-E: Serial sections through the developing otic vesicle. No staining in the developing otic vesicle sensory epithelium is detected. F: 13.5dpc cochlea section was used as a positive control which demonstrated clusterin mRNA expression in the sensory epithelium. G: Plane of sections through an 11.5dpc mouse inner ear used for *in situ* hybridisation of mouse clusterin. co: cochlea, ed: endolymphatic duct, ce: cochlea epithelium, ov: otic vesicle, vpl: vertical canal plate. Panels A, B, and C taken at the planes shown in F from top to bottom. Panels D and E higher magnification. Scale bar: 100µm.

### 3.2.1.2 RNA *in situ* hybridisation at 12.5dpc

At 12.0dpc cochlea has a more elaborate shape consisting of proximal and a distal part (Morsli, Choo et al. 1998) and at 13.0dpc cochlea has half a turn (Morsli, Choo et al. 1998). At 12.5dpc the proliferating progenitor cells in the organ of Corti begin to exit the cell cycle and the sensory hair cells begin to appear in the vestibular organ (Ruben 1967; Anniko 1983).

In the developing cochlear epithelium at 12.5dpc very low levels of clusterin mRNA could be detected (Figure 3.3). Sections were examined from base to apex along the entire cochlear coil. This low level of clusterin expression was seen in the cochlear epithelium from the base (Figure 3.3 A-E) through mid-cochlear turns (Figure 3.3 F,G) and in apical turns (Figure 3.3 H). Comparison of the sections of the basal and apical turns (e.g. Figure3.3 E with H; Figure 3.3 F with H) suggests that there is gradient of clusterin activation from base to apex (Compare Figure 3.3 E with H). At higher power magnification, clusterin expression appeared to be initiated across the entire width of the presumptive sensory epithelium, but absent from the non-sensory region (Figure 3.3E).

In the vestibular system clusterin expression could not be detected in either sensory or non-sensory epithelium, in the utricle, saccule (Figure 3.3 A-C) or in the early outpocketing semicircular canals (data not shown).

Thus clusterin expression is initiated at 12.5dpc in the cochlear epithelium. It is interesting to note that more than 80% of cells in the primordial organ of Corti exit the cell cycle between E13 and E14 (12.5 – 13.5dpc) (Ruben 1967).

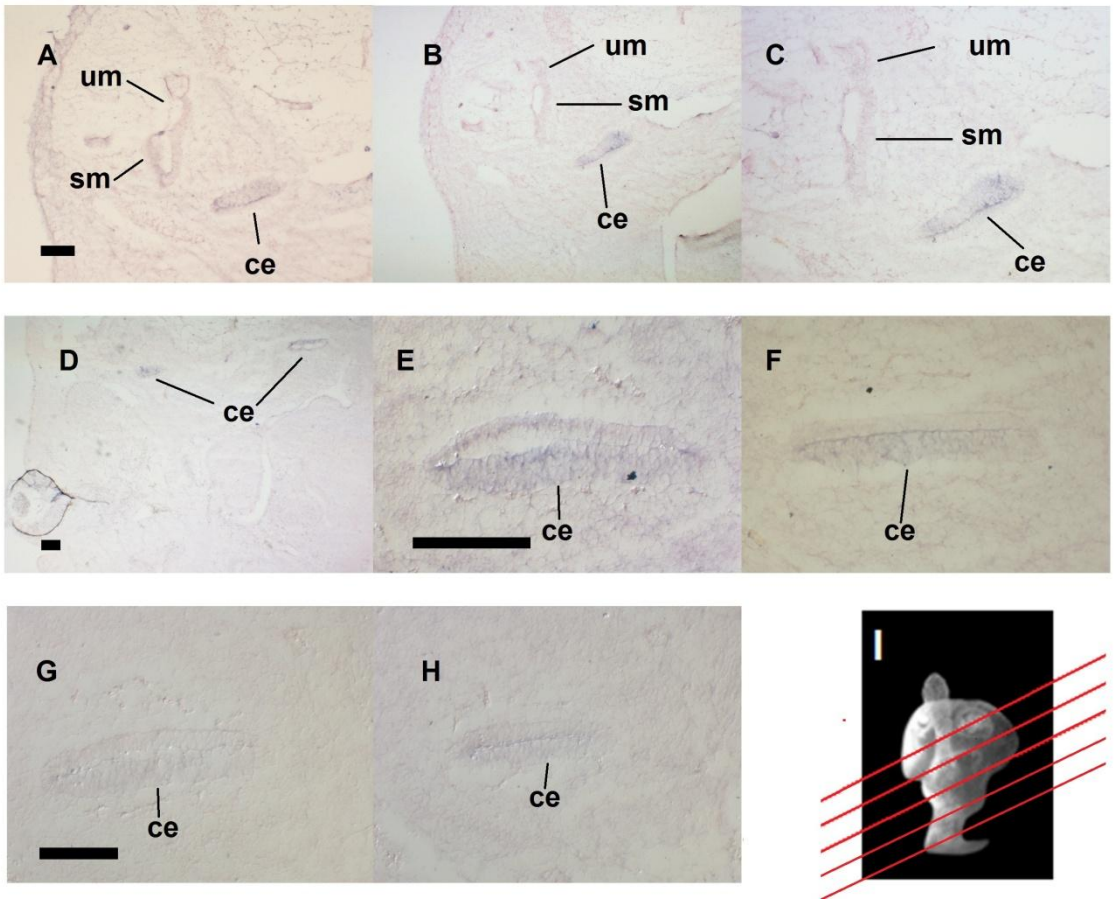


Figure 3.3 Clusterin *in situ* hybridisation against sections at 12.5dpc. A, B and C: Overview of clusterin mRNA expression in developing auditory and vestibular system. D: Expression of clusterin mRNA in both inner ears. E: Low levels of expression of clusterin mRNA at the base of cochlea sensory epithelium. F and G: Low expression levels of clusterin mRNA at the middle of cochlea sensory epithelium. H: Low expression levels of clusterin mRNA at the apex of cochlea sensory epithelium. I: Plane of sections through a 12.5dpc mouse inner ear used for *in situ* hybridisation of mouse clusterin. ce: cochlea epithelium, sm: saccular macula, um: utricluar macula. Scale bars: 100µm.

### 3.2.1.3 RNA *in situ* hybridisation at 13.5dpc

At this stage robust expression of clusterin mRNA was detected that remains restricted to the developing cochlear epithelium (Figure 3.4). Cochlear expression was observed from base to apex (Figure 3.4 D-J). The expression is spread throughout the entire length and thickness of the cochlea sensory epithelium at the base of the cochlea duct (Figure 3.4 D).

From mid-turns towards the more apical regions of the cochlea the expression become progressively restricted to the lateral side of the cochlea sensory epithelium (Figure 3.4 E-J). The expression is not found at the modiolar wall of the cochlea sensory epithelium and as a result the expression becomes confined to the lateral wall (Figure 3.4 arrows in E-F).

Clusterin expression towards more apical regions of the cochlea becomes progressively restricted within the lateral cochlear sensory epithelium, where expression seems to be further confined to a region close to the presumptive prosensory domain and away from Kolliker's organ (Figure 3.4 J). Kolliker's organ will develop as the greater epithelial ridge (GER) while the inner and outer hair cells and their associated supporting cells develop from the prosensory domain. The contrast between clusterin expression in the base and mid-turn of the cochlear epithelium is illustrated in Figure 3.5 A and B respectively.

At 13.5dpc most of the progenitors that will give rise to hair cells and supporting cells have exited the cell cycle and the prosensory domain of the cochlear duct is at postmitotic status. These postmitotic cells will undergo terminal differentiation from this stage onwards.

Clusterin mRNA expression is still absent in the developing vestibular epithelium (cristae of the semicircular canals, utricular and saccular maculae). At low magnification, clusterin expression is clearly absent from vestibular epithelium as no expression was detected in the utricle or saccule (Figure 3.4 B,C). Higher power images (Figure 3.4 K-N) confirm an absence of expression in the sensory patches, the utricular

and saccular maculae and the cristae (Figure 3.4 N) as well as the non-sensory epithelium throughout the vestibule.

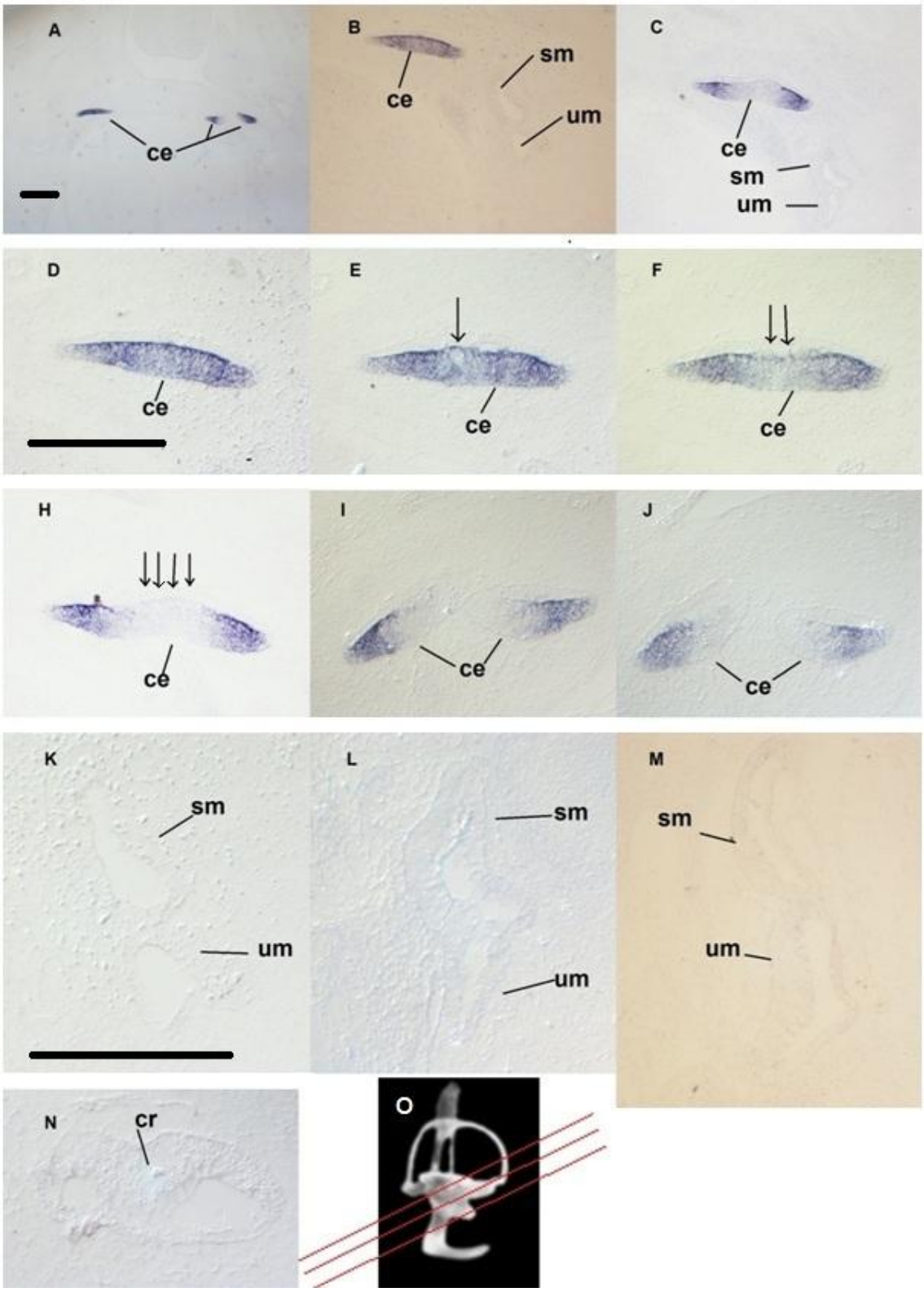


Figure 3.4 Clusterin *in situ* hybridisation against sections at 13.5dpc. A-D: Overview of clusterin mRNA expression in the developing auditory and vestibular system. E-G: Serial sections through the base of the cochlea sensory epithelium, arrows show the area of clusterin mRNA absence. H – J: Serial sections through the middle turns of the cochlea sensory epithelium. K – N: Sections through vestibular structures.

O: Plane of sections through a 13.5dpc mouse inner ear used for *in situ* hybridisation of mouse clusterin. Scale bars: 300µm.

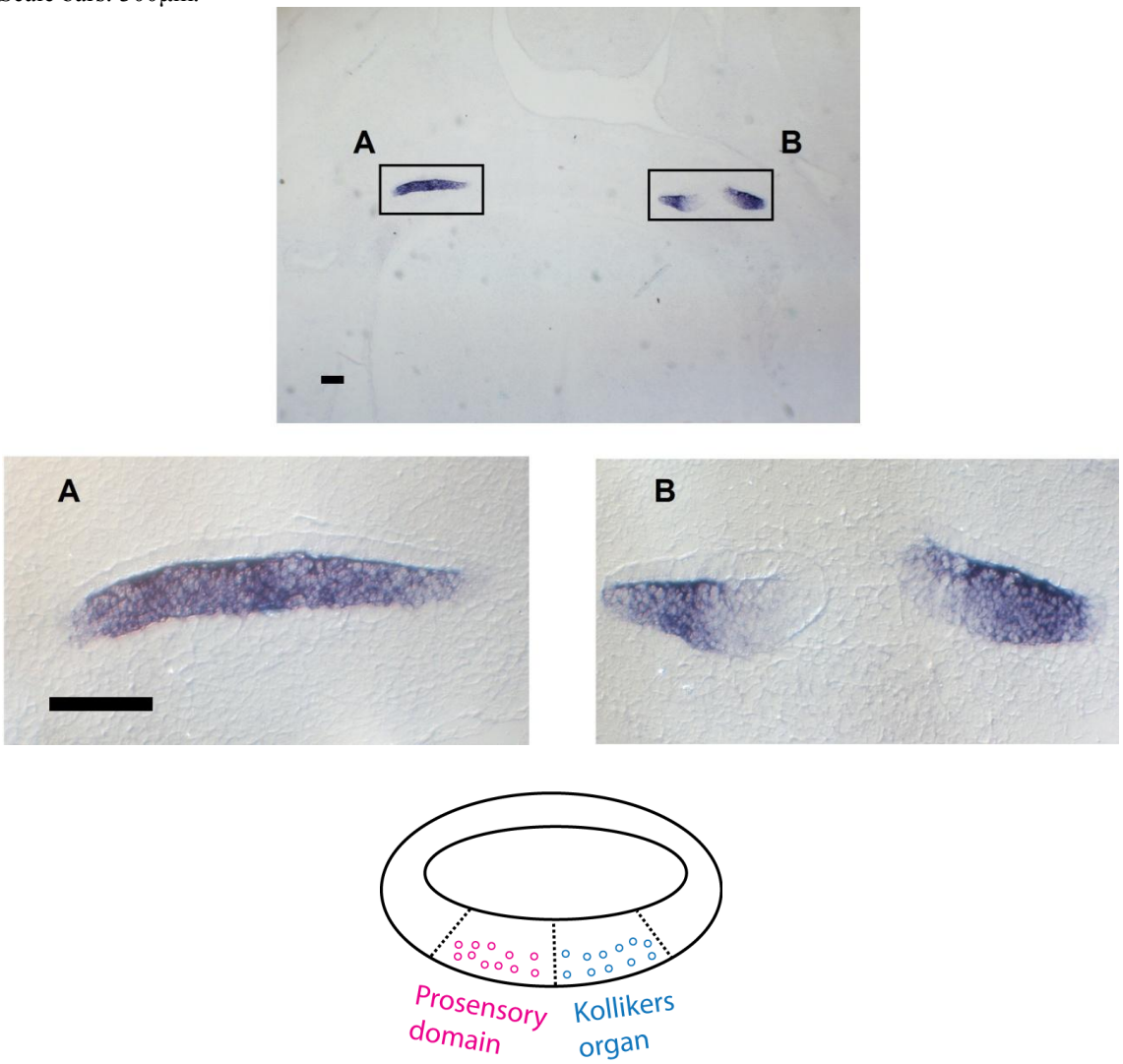


Figure 3.5 Pattern of expression of clusterin mRNA at the base and middle turns of the cochlear sensory epithelium at 13.5dpc. Top figure demonstrates a section through the mouse head at 13.5dpc, where the section has cut through a basal or mid-apical turn of the cochlea on opposite sides of the head. A: Base of the cochlea where clusterin is expressed throughout the sensory epithelium, B: Middle turns of the cochlea where clusterin expression becomes localised to the most of prosensory domain. Bottom figure – schematic of the general organisation of the sensory epithelium at 13.5dpc with modiolar side to the right. Scale bars: 100µm.

### 3.2.1.4 RNA *in situ* hybridisation at stage 15.5dpc

*In situ* hybridisation was also carried out on 15.5dpc mouse head sections using the mouse clusterin riboprobe as before. Clusterin mRNA expression was still restricted in the inner ear to only the developing cochlear epithelium (Figure 3.6 A-C). Expression was detected in all regions (basal, middle, and apical) of the now coiled cochlea (Figure 3.6 G-I).

At this stage the expression of clusterin seems to become more localised/restricted compared to expression at 13.5dpc. From the base through to the mid turns but not in the apex, two distinct regions of expression are detected (Figure 3.6 D-L). This is in contrast with what was observed at 13.5dpc where clusterin expression was detected across the entire width and depth of the cochlea sensory epithelium at the base (Figure 3.5 A), and also in contrast with a single region of expression in the middle turns of cochlea at 13.5dpc (Figure 3.5 B). So, in contrast to the 13.5dpc, expression in basal turns is no longer uniform across the entire cochlear epithelium but rather downregulated in the middle of the epithelium, leaving two areas of expression either side (arrowheads in Figure 3.6 D-F).

In the mid-cochlear regions at 15.5dpc as well, these two regions of expression are also clear either side of the developing cochlea epithelium (arrows in Figure 3.6 J-L). However the ongoing differentiation of the cochlear epithelium parallels some changes in this overall "two-domain" expression of clusterin. The two regions of clusterin expression are unequal, with a broader modiolar domain that seems to cover most of the greater epithelial ridge and a narrower band of expression that covers part of the lesser epithelial ridge (LER) (Figure 3.6 J) and extend towards the future stria vascularis, the lateral wall of the cochlear duct. The cochlear region where clusterin expression is absent appears to approximately coincide where future hair cells will develop (highlighted with arrows heads in Figure 3.6 J-L).

At the base of the cochlea these two regions of expression are also evident (highlighted with arrows and *asterisks* in Figure 3.6 D-F), but with the wider clusterin domain joined from each cochlear turn as a joint patch of expression (asterisks in Figure 3.6 D-F), with the smaller lateral domains also evident as two separate patches of expression (arrows in Figure 3.6 D-F).

Clusterin mRNA expression is still absent from the developing vestibular nonsensory and sensory epithelium (cristae of the semicircular canals, utriclular and saccular maculae) and also absent in the surrounding periotic mesenchyme and the developing otic capsule at 15.5dpc (Figures 3.7 A-F).

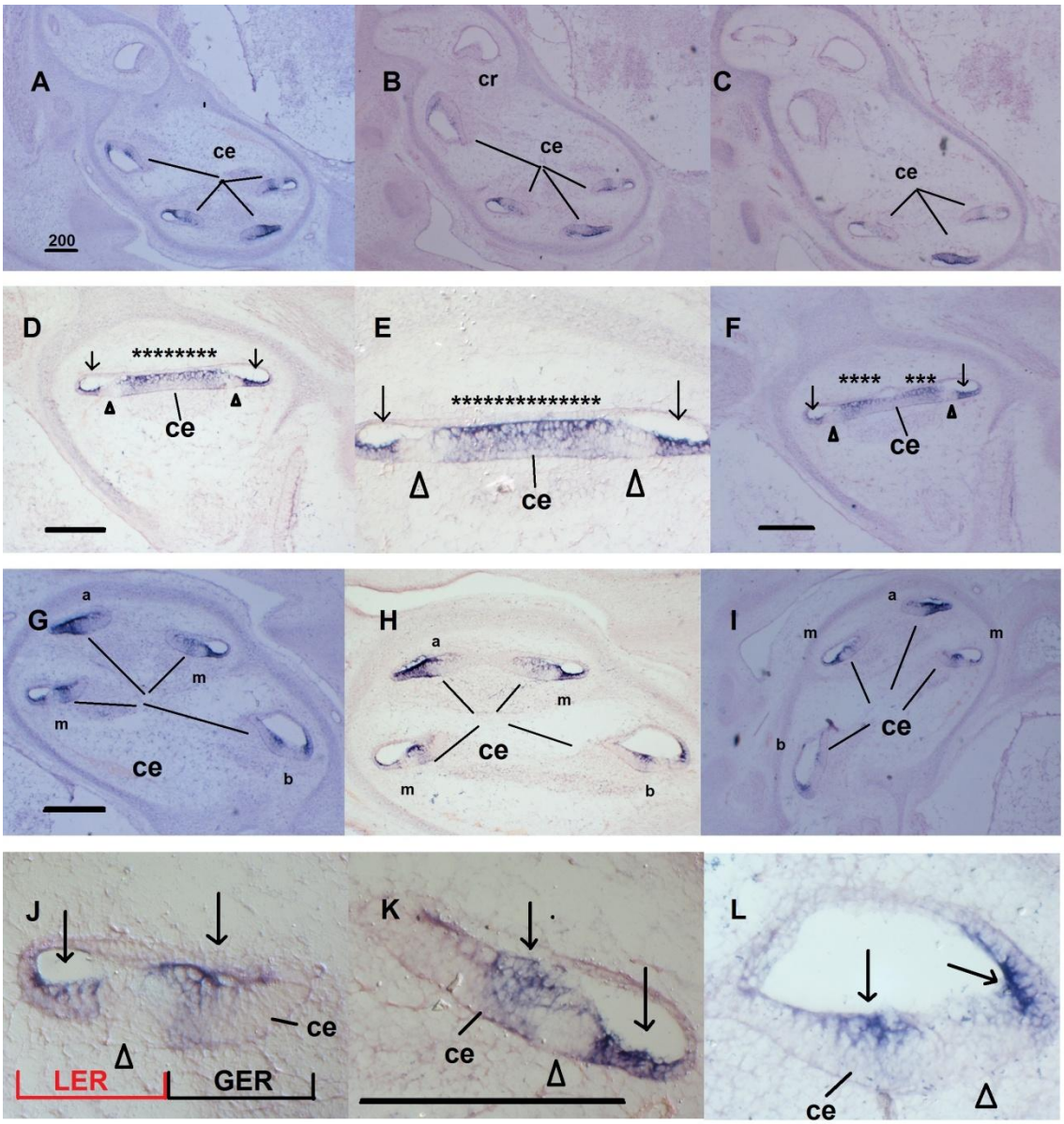


Figure 3.6 Clusterin *in situ* hybridisation against sections at 15.5dpc A-C: Overview of sections through the inner ear and the detection of clusterin mRNA in the developing inner ear. D-F: serial sections through the base of the cochlea. Asterisks point to the wider modiolar domain and arrows point to the narrower lateral region of expression. Arrowheads point to the downregulation areas in D-F G-I: sections through the middle turns of the cochlea demonstrating expression in all profiles of the cochlea duct. J-L: Two distinct regions of clusterin expression in the developing cochlea sensory epithelium pointed to by arrows. Arrowheads point to the location of downregulation of clusterin expression. ce: cochlea epithelium, cr: crista, a: apex turn, b: base turn, m: middle turn, GER: greater epithelial ridge, LER: lesser epithelial ridge. Scale bars: 200µm.

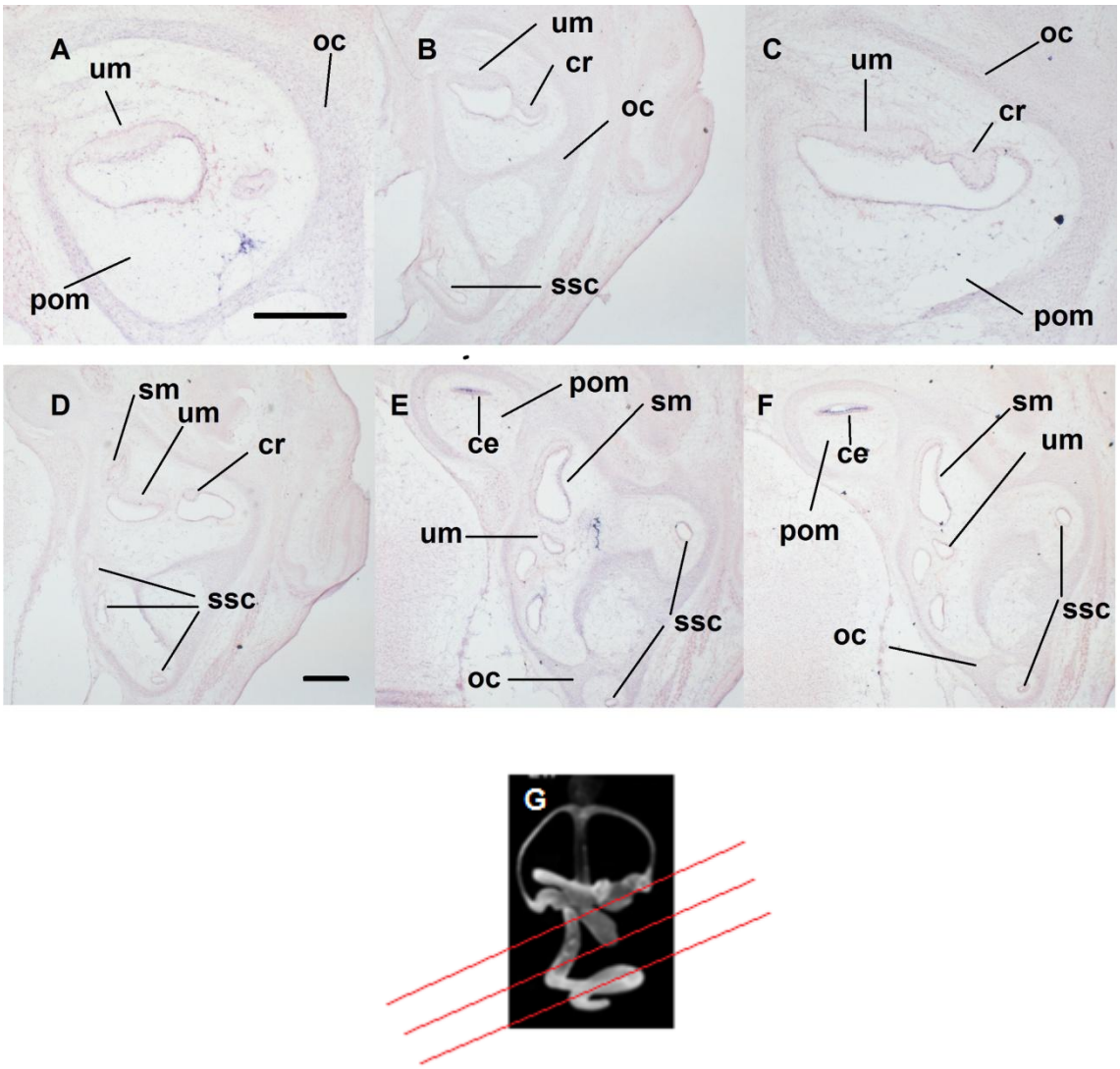


Figure 3.7 Clusterin *in situ* hybridisation against sections at 15.5dpc. A-D: Vestibular sections at 15.5dpc. G: Plane of sections through a 15.5dpc mouse inner ear used for *in situ* hybridisation of mouse clusterin. ce: cochlea epithelium, cr: crista, oc: otic capsule, pom: periotic mesenchyme, sm: saccule macula, ssc: semi circular canals, um: utricle macula. Scale bars: 200µm.

### 3.2.1.5 RNA *in situ* hybridisation at 17.5dpc

At 17.5dpc hair cells have become arranged into the characteristic pattern of three rows of outer and one row of inner hair cells (1.1). At this stage, clusterin expression is still detectable along the full length of the developing cochlear duct. However expression has become yet more localised to a subset of cells within the now fully differentiated cochlear epithelium. At the base of the cochlear duct (Figure 3.8 A,B), a broad medial region of expression in the sensory epithelium (corresponding approximately to the greater epithelia ridge area) is evident with a narrow patch of expression at either side

overlapping to some undefined extent with the lesser epithelial ridge and extending towards the stria vascularis, the lateral wall of the cochlear duct. This pattern of expression is similar to that observed in the 15.5dpc cochlea (3.2.1.4), although perhaps yet more localised (e.g. compare Figure 3.6 D-F with 3.8 A,B).

Clusterin expression extends the entire length of the cochlea (Figure 3.9 L, M and K – base, mid and apical regions shown respectively). The same overall organisation of clusterin expression is seen as a broad medial region and narrow lateral region that extends towards the stria, but more restricted and localised than at 15.5dpc (compare 3.6 J with 3.9 B). The patch of clusterin expression at the strial edge becomes very restricted and sometimes difficult to detect (compare 3.6 K with 3.9 J) and appears to correspond to cells distant from developing outer hair cells.

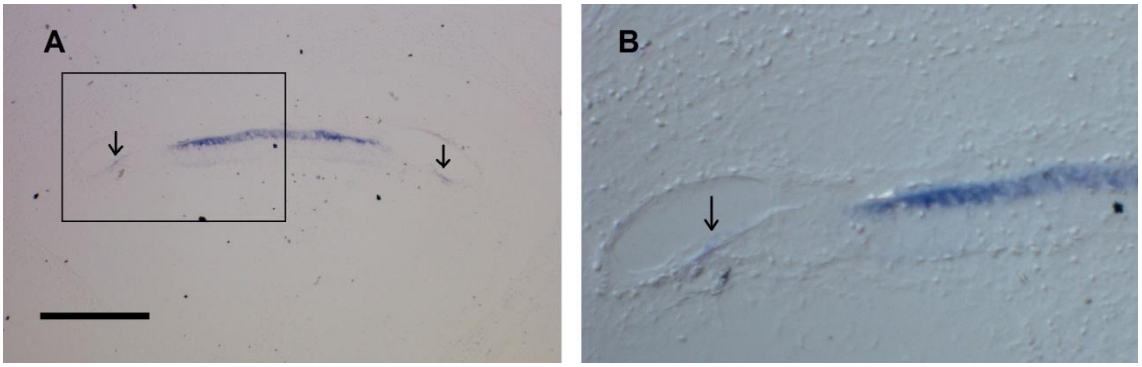


Figure 3.8 Clusterin expression at the base of the cochlea at 17.5dpc. A: Overview of the base of the cochlea at 17.5dpc. B: Higher magnification of the selected area in A. Arrows in A and B point to the narrow clusterin expression towards the strial edge. Scale bar: 200μm.

At the extreme apical end of the cochlea, however, only one wide patch of clusterin expression is detectable. Similar to expression at 15.5dpc it seems that the two regions of expression observed at the base and middle turns of the cochlea epithelium join together at the apex (Figure 3.9 K and N-P). Alternatively, perhaps the lateral narrow domain has been lost, and this analysis is unable to resolve the two possibilities.

As at earlier developmental stages, clusterin mRNA expression is absent throughout the developing vestibular epithelium (including the sensory cristae of the semicircular canals, utricular and saccular maculae), as well in the immediately adjacent tissues, the periotic mesenchyme, otic capsule (Figure 3.10).

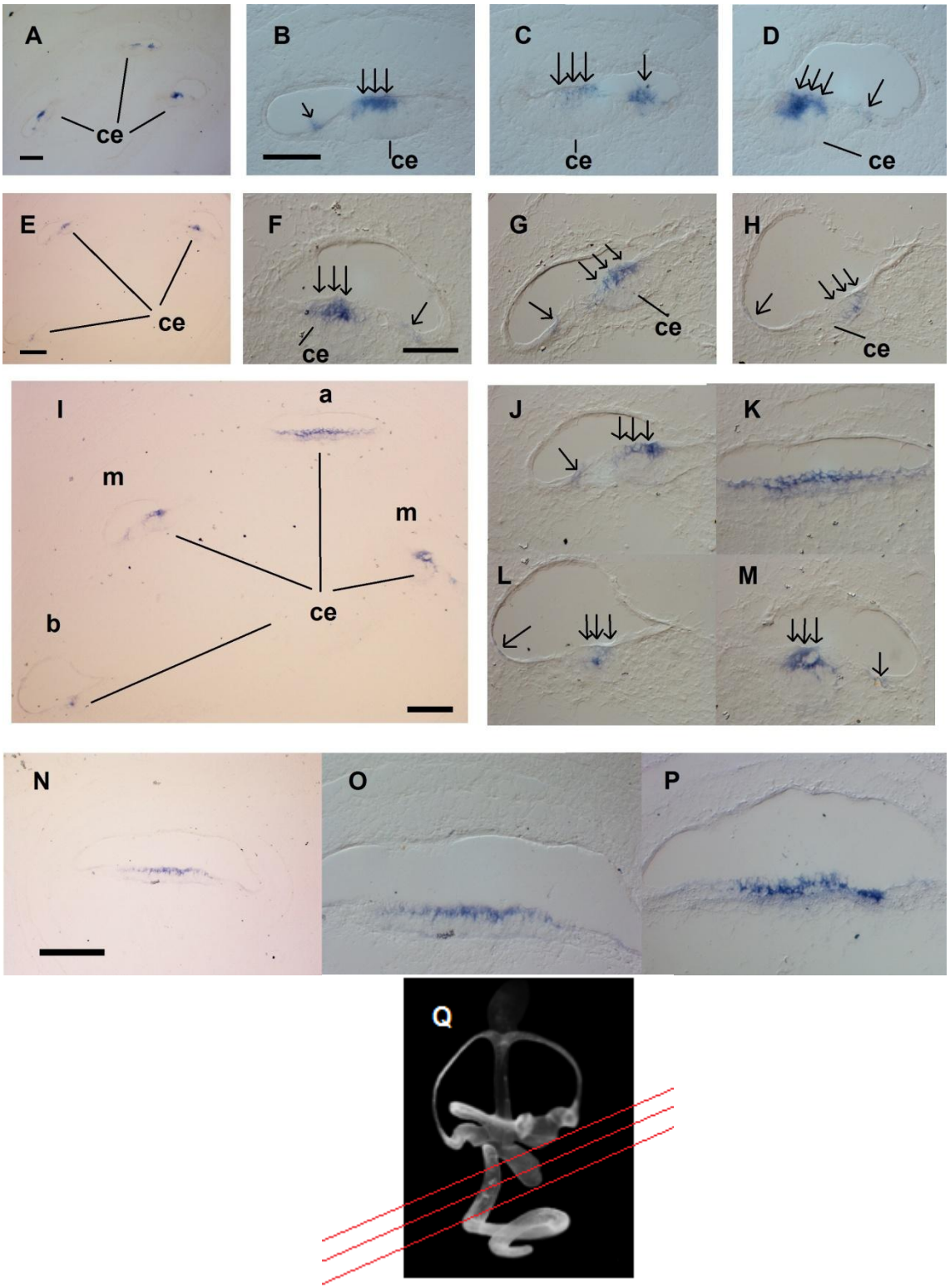


Figure 3.9 Clusterin *in situ* hybridisation against sections at 17.5dpc. Overview of clusterin expression in the cochlea (A, E and I). basal sections (B,D,F,H, and L), middle sections (J and M), apical sections (N-P), and Q: Plane of sections through a 17.5dpc mouse inner ear used for *in situ* hybridisation of mouse clusterin. Triple and single arrows point to the wider (at the GER) and narrower (at the LER) regions of expression respectively. ce: cochlea epithelium, a: apical turn, b: basal turn, m: middle turn. Scale bars: 100µm.

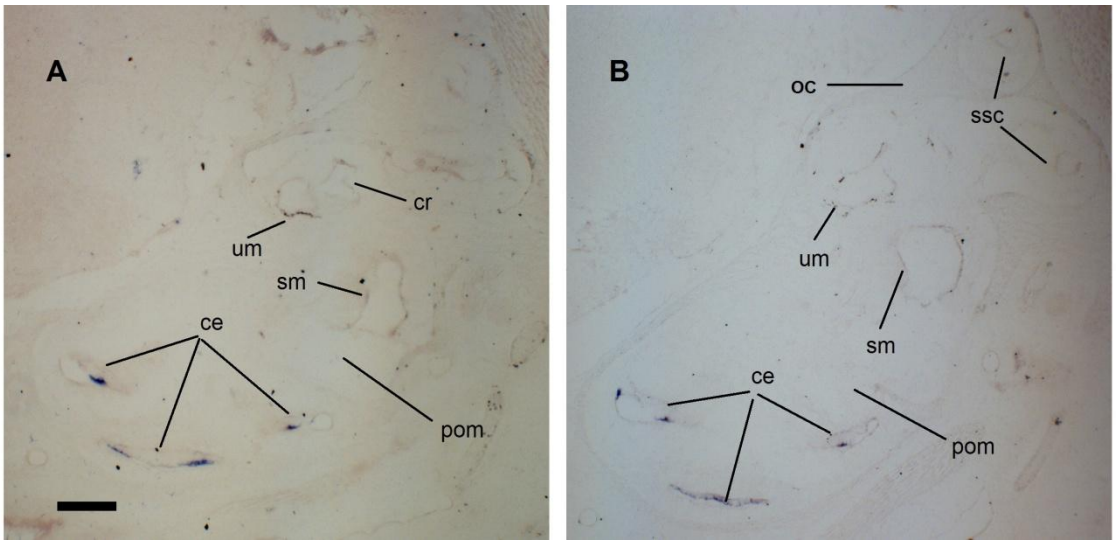


Figure 3.10 Clusterin *in situ* hybridisation against sections at 17.5dpc. In figure A and B clusterin mRNA is expressed in the cochlea sensory epithelium but is absent from the vestibular system, periodic mesenchyme, and otic capsule. ce: cochlea epithelium, cr: crista, oc: otic capsule, pom: periotic mesenchyme, sm: saccule macula, ssc: semi circular canals, um: utricle macula. Scale bar: 200µm.

### 3.2.1.6 RNA *in situ* hybridisation at 18.5dpc

One day later at 18.5dpc, both of the areas of clusterin expression at the greater and lesser epithelial ridge sides of the sensory epithelium (formerly referred to as medial/modiolar and lateral domains) are apically located, restricted to cells in the top layers of the epithelium and are becoming even more restricted, with the narrower lesser epithelial ridge patch becoming extremely localised to a very narrow band of weaker expression but still evident (Figure 3.11 A,B).

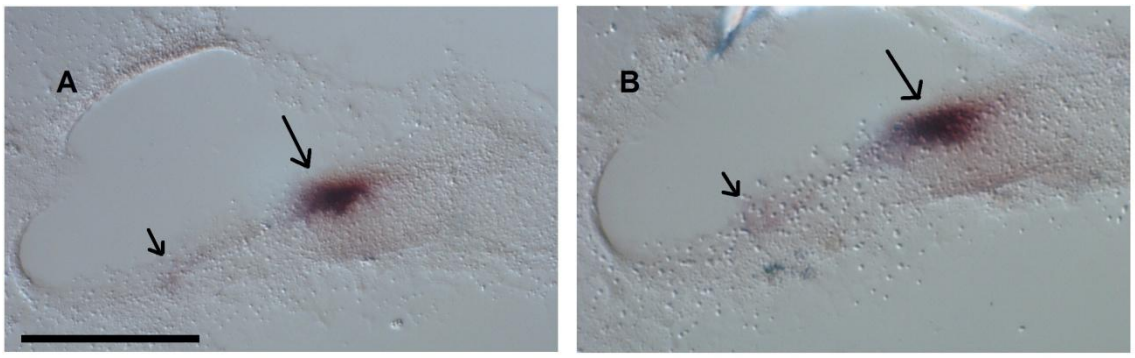


Figure 3.11 Clusterin *in situ* hybridisation against sections at 18.5dpc. Larger and smaller arrows point to the wider (GER) and narrower (LER) regions of clusterin expression respectively. Scale bar: 100µm.

### 3.2.1.7 RNA *in situ* hybridisation at postnatal day 2 (P2)

The dynamic expression of clusterin between 13.5-18.5dpc and the robust expression still evident in the cochlea at 18.5dpc prompted the question as to whether expression persists after birth since expression was still evident at these late developmental stages. At postnatal day 2 (P2), expression of clusterin remained both robust and restricted to the cochlea epithelium, but in common with all prenatal stages examined, is absent from the vestibular system (Figure 3.12 A,B). As had been noted during the ongoing development of the organ of Corti, clusterin expression continued to become yet further localised than the 18.5dpc and does not cover the entire thickness of cochlea epithelium. At the base of the cochlea, a wide region of expression is detected across the cochlear epithelium (Figure 3.12 C). A little further along the basal region of the cochlea however, well before mid-cochlea regions are reached, much of this broad region is downregulated and missing (Figure 3.12 D), while the second narrow region of lateral expression is much narrower at the LER/strial edge but is still apparent (Figure 3.12 D-H) in basal and medial sections. In more apical regions however, the lateral expression appears to be downregulated as was not identified in sections taken from further along the cochlea. Overall however, as at earlier stages of cochlea development, clusterin expression (i.e. the major GER/modiolar domain) was observed throughout the length of the cochlea sensory epithelium in all profiles of cochlea epithelium, base (3.12 C,D), middle (3.12 G,H), and at the apical turns (3.12 F).

Clusterin mRNA expression is still absent from the developing vestibular nonsensory and sensory epithelia (cristae of the semicircular canals, utricle and sacculae maculae) at P2. At this stage the cellular pattern of the organ of Corti is complete but is still before the onset of hearing in mice.

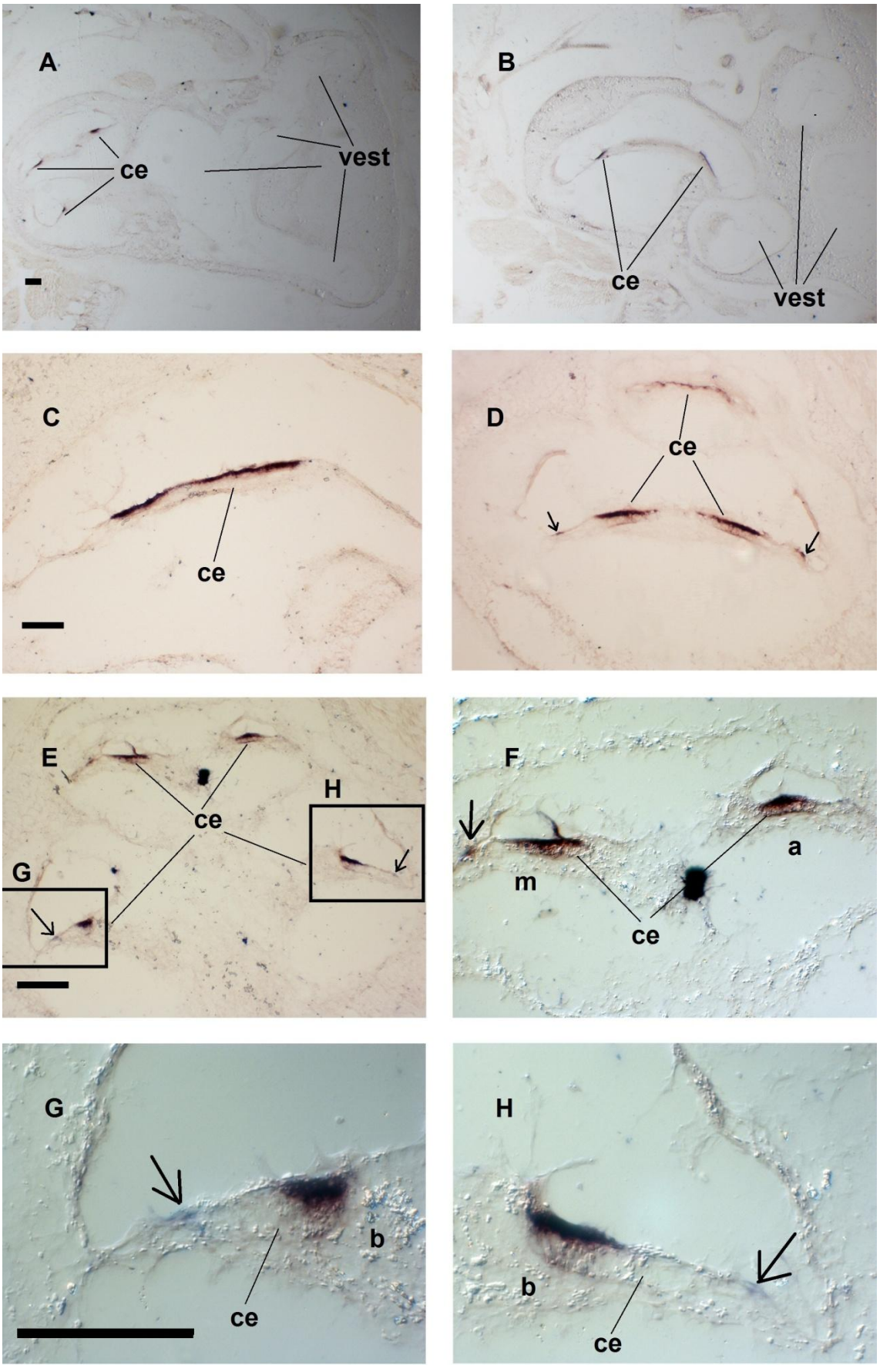
A
ce
vest
B
ce
vest
C
ce
D
ce
E
ce
H
G
F
a
m
ce
G
b
ce
H
b
ce

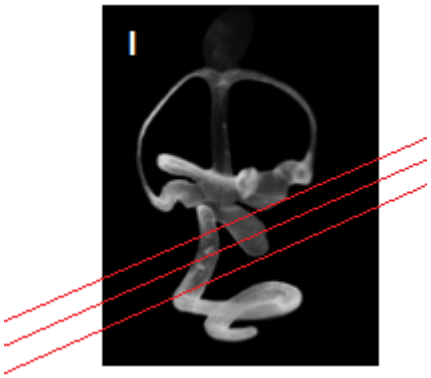


Figure 3.12 Clusterin *in situ* hybridisation against sections at postnatal day 2 (P2). Overview of clusterin expression in the inner ear (A and B), Base of the cochlea (C and D), overview of cochlea section (E), higher magnification of middle and apical turn (F) and basal turn (G and H). I: Plane of sections. ce: cochlea epithelium, vest: vestibular system. a: apical turn, b: basal turn, m: middle turn. Scale bars: 100μm.

### 3.2.1.8 RNA *in situ* hybridisation at postnatal day 17 (P17) and 18 (P18)

In mice the onset of hearing occurs around P10-P14, so it was important to establish whether clusterin expression detected postnatally is maintained from birth through to the onset of hearing and into adulthood. Analysis of sections from P17 however did not reveal any clusterin expression in either cochlear or vestibular sensory and non-sensory epithelia (Figure 3.13) despite repeated attempts, and analysing sections at earlier stages with the same probe identified areas of clusterin expression illustrating absence of expression at P17 is due to complete down regulation in the inner ear epithelium. Figure 3.13 A demonstrates the 3 fully developed chambers of the cochlea duct (Scala tympani (ST), Scala media (SM) and Scala vestibuli (SV)) together with the fully developed organ of Corti (orc) but with a complete absence of clusterin expression. Both regions of clusterin expression are missing from the cochlea sensory epithelium at this stage. The analysis of P18 mouse inner ear was also carried out which was identical to P17 (data not shown).

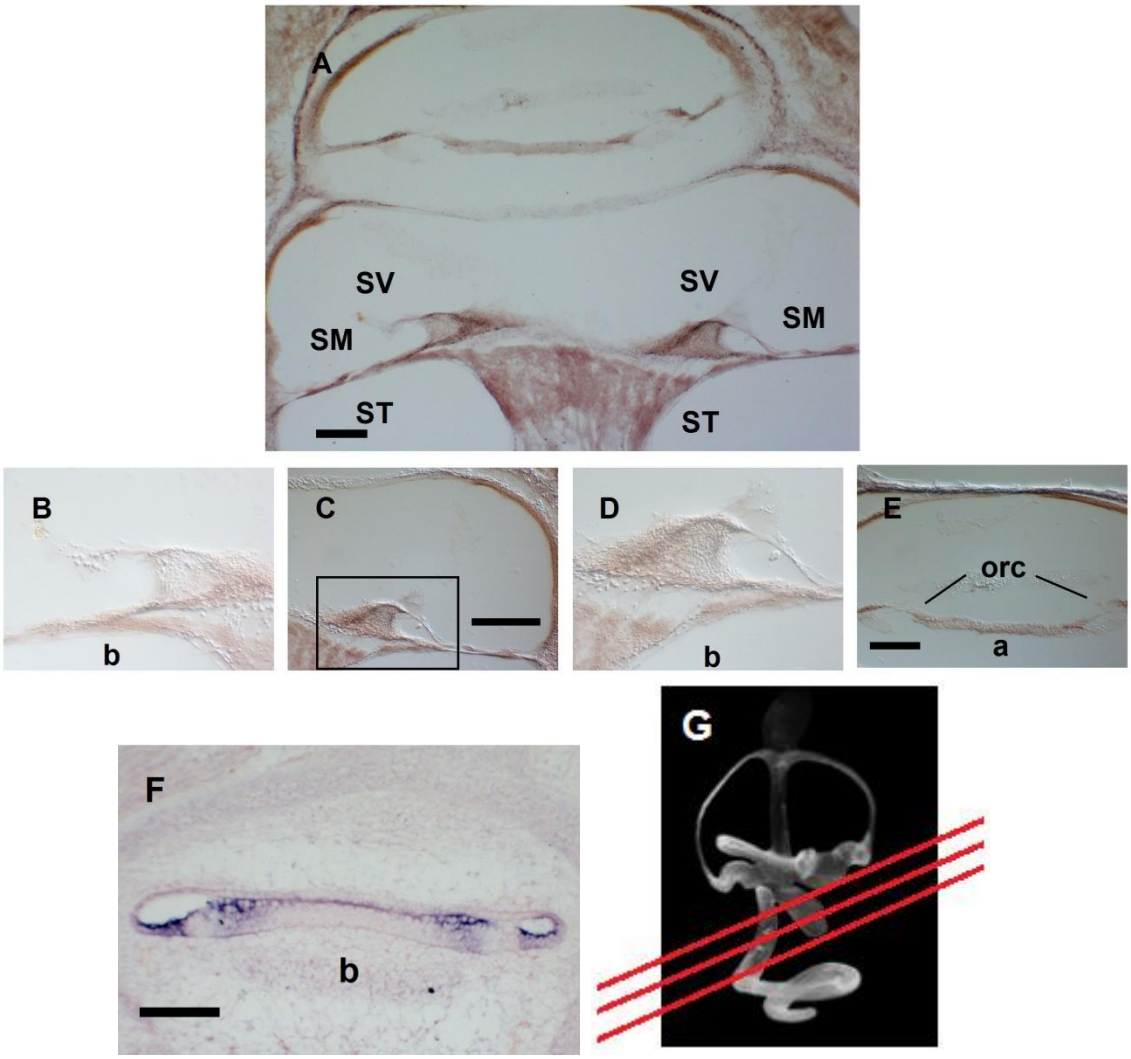


Figure 3.13 Clusterin *in situ* hybridisation against sections at postnatal day 17 (P17). A: Overview of cochlea section (A), higher magnification of basal (B-D) and apical turns (E). F: 15.5dpc mouse cochlea section used in this in situ as a positive control which demonstrated cluserin mRNA expression in the sensory epithelium. G: Plane of sections. orc: organ of Corti, ST: scala tympani, SM: scala media, SV: scala vestibule, b:base, a: apex. Scale bars: 100µm.

### 3.2.2 Expression of the clusterin protein during inner ear development

The mRNA developmental profile of clusterin during development does not necessarily mean that protein is translated in the inner ear. Therefore in order to analyse where the protein product for clusterin is found during inner ear development two different primary antibodies were used (2.3.1.5.1).

3.2.2.1 Immunohistochemistry using clusterin antibody ab69644 (Abcam): The first primary anti-CLU antibody used was from Abcam (ab69644-Rabbit polyclonal antibody). This was raised against C-terminus (β-chain) amino acid 435-449 (Appendix

V.I and Figure 1.10) of human clusterin. A titration of this antibody was carried out on 14.5dpc frozen sections of the head at 1/100, 1/200, 1/400 and 1/800 dilutions, as this is one day after the robust expression of the mRNA had been detected across the entire cochlear epithelium (Figure 3.5). Although, no clear immunoreactivity was detected in the inner ear it seemed that immunoreactivity was present in other regions of the head such as epidermis, brain cavities and eyes for the 1/100 dilution (Figure 3.14, data for brain cavities and eyes are not shown). Therefore, subsequent experiments were carried out using this antibody dilution.

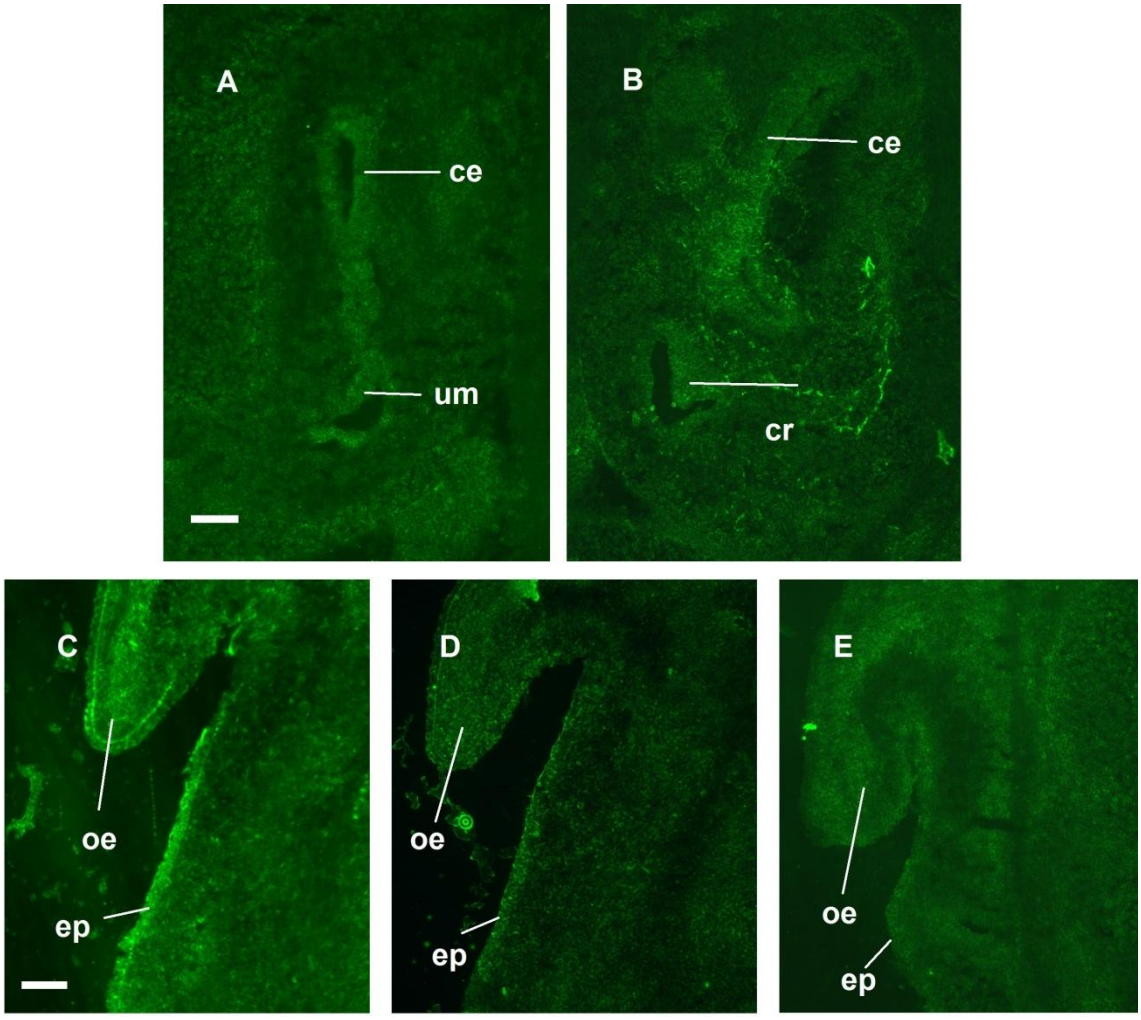


Figure 3.14 Sections through a 14.5dpc mouse head and titration of the Abcam primary antibody against clusterin. A and B: Cochlea sections immunolabeled with 1/800 dilution primary antibody. C, D, and E: Sections of mouse head demonstrating outer ear for 1/100, 1/400 and 1/800 Abcam (ab69644) primary antibody against clusterin respectively. ce: cochlea epithelium, um: utricle macula, cr: cristae, oe: outer ear, and ep: epidermis. Scale bars: 200μm.

Frozen sections of 14.5dpc, 15.5dpc and 16.5dpc mouse heads were incubated in separate experiments with primary clusterin antibody ab69644 and detected using goat

anti-rabbit fluorescent-conjugated secondary antibody (Invitrogen) (2.3.1.5.2.3) at 1/500 dilution. As a control, a slide with sections exposed to secondary antibody alone was used in each experiment. No clusterin immunoreactivity was detected in inner ear epithelia, but the head epidermis and brain cavities revealed some immunoreactivity (Figure 3.15 and 3.16).

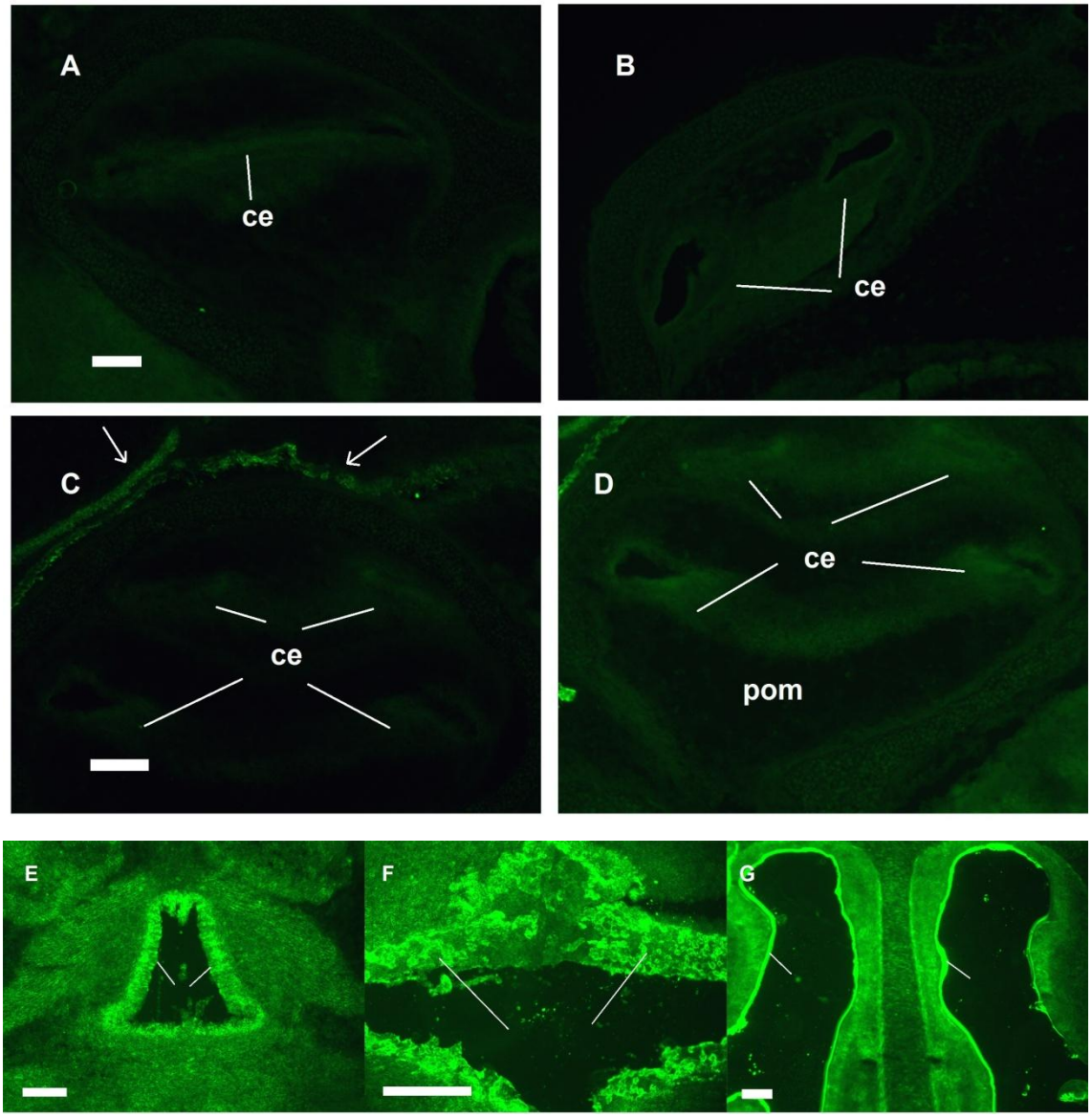


Figure 3.15 Sections through a frozen 16.5dpc mouse inner ear and clusterin protein detection using Abcam (ab69644) primary antibody. Cochlea basal turns (A and B), cochlea middle turns (C and D), brain cavities (E and F), and olfactory system (G). The arrows in E-G point to the detected immunoreactivity in these sections. ce: cochlear sensory epithelium, pom: periodic mesenchyme, oc: otic capsule, cr: crista, and um: utricle macula. Scale bars: 100μm.

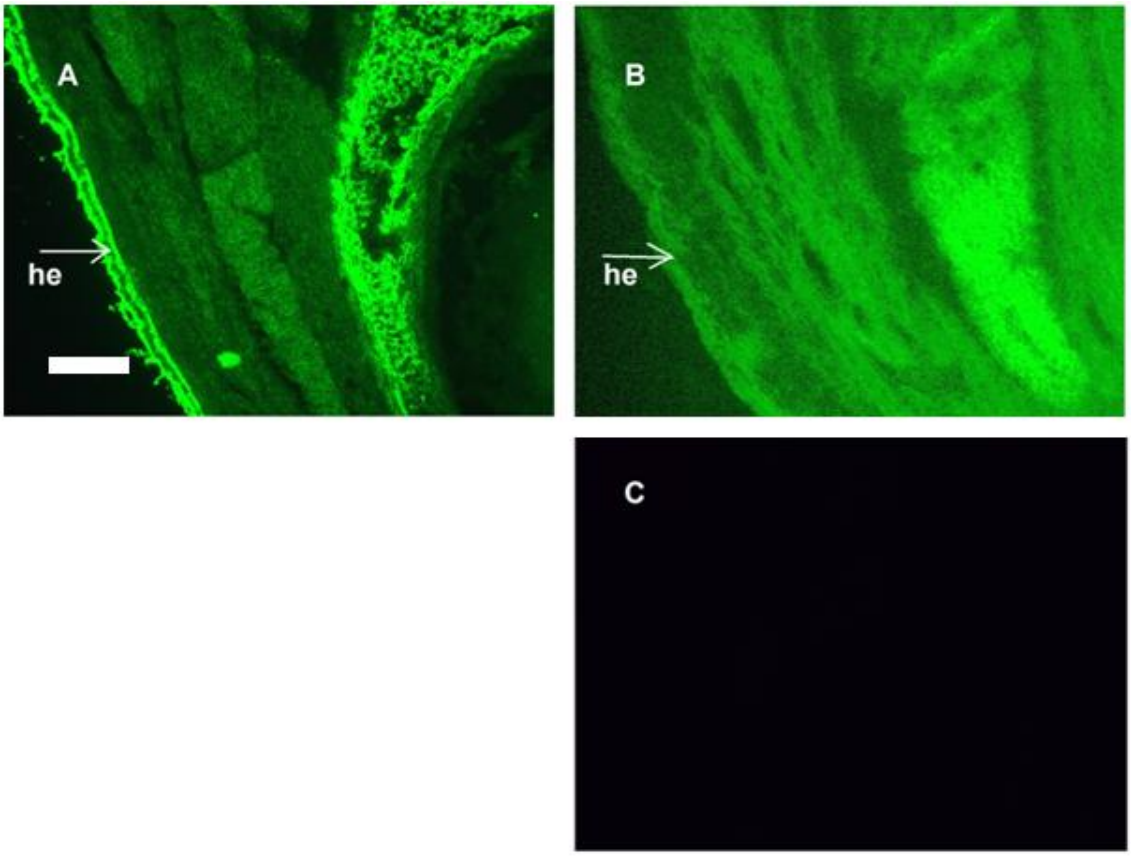


Figure 3.16 Clusterin protein expression in the head epidermis and developing eye at 16.5dpc using frozen sections. Head section incubated with both primary and secondary antibodies (A) and only secondary antibody as a control (B,C). Exposure in (C) is identical to (A) showing specificity of labelling. Extreme overexposure is shown in (B). Scale bar: 100μm.

Whilst some external epithelia appeared to be detected by this antibody, the failure to detect clear clusterin immunoreactivity in inner ear sections lead to consideration of alternate protocols. Frozen sections lead to minimal heating and other processing regimes involved in tissue preparation and thus was first considered to be the technique less likely to lead to destruction of the antigen. However, Abcam recommendations were to use wax-embedded material, and therefore this route was next attempted. Tissues were minimally fixed in 4% PFA only for 1 hour (rather than overnight) and prior to the antibody incubation, the unmasking of the antigenic sites was carried out using heat-mediated antigen retrieval using citrate-EDTA buffer (Appendix IV) (2.3.1.2 and 2.3.1.3). Again a secondary antibody only control was also carried out. Immunoreactivity was identical as previously found using frozen sections. Clusterin immunoreactivity was absent in the developing inner ear at 15.5dpc, with some immunoreactivity in head epidermis, eyes, and brain cavities (Figure 3.17, data not shown for epidermis and brain cavities). In order to establish whether head epidermis

expression is real, the same experiment was repeated on two 15.5dpc slides with the no primary control, and the epidermal immunoreactivity suggests this expression to be genuine (Figure 3.18). However the absence of immunoreactivity in inner ear epithelia was unexpected. There were a few isolated spots of immunoreactivity in the periotic mesenchyme surrounding the coils, inside of the developing capsule, but the epithelium appeared essentially negative.

The ab69644 clusterin antibody (raised in rabbit against human Clu) is a synthesized peptide derived from C-terminus of human clusterin that should recognize the C-terminus of mouse clusterin (clusterin β-chain). This sequence is within the cDNA sequence that clusterin mRNA probe was generated from (Appendix V.I).

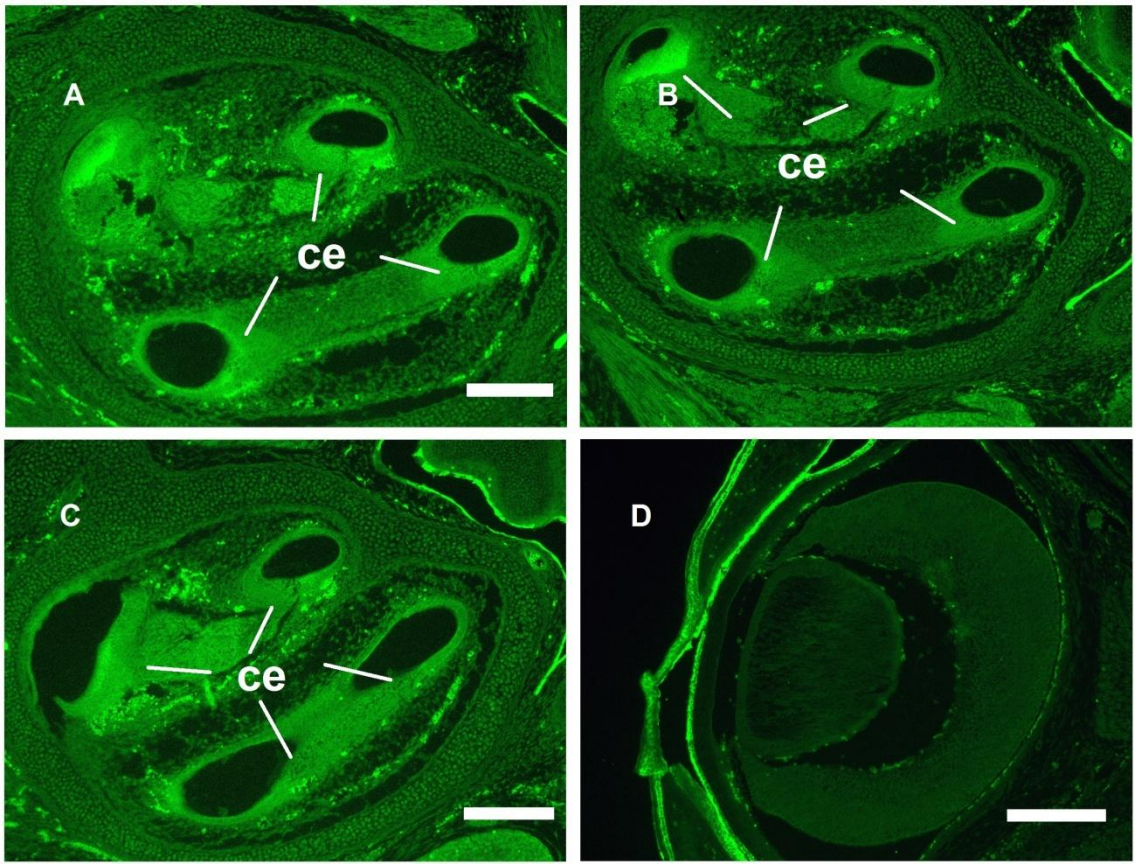

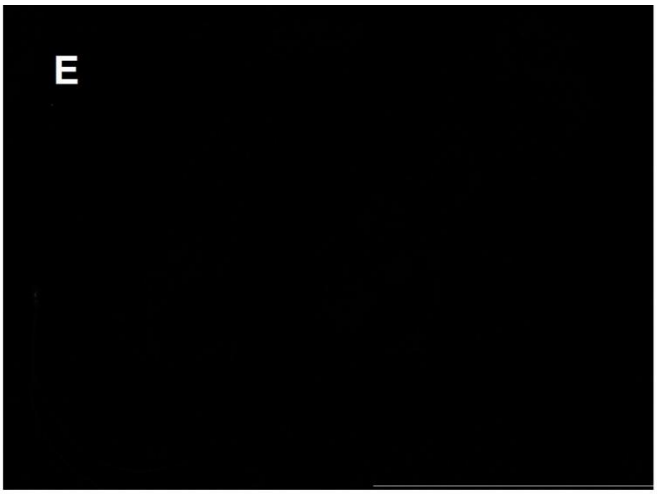


Figure 3.17 15.5dpc wax sections immunolabelled with Abcam (ab69644) primary antibody. Serial sections through developing cochlea (A-C), developing eye (D), and no primary antibody control (E). Scale bars: 200µm.

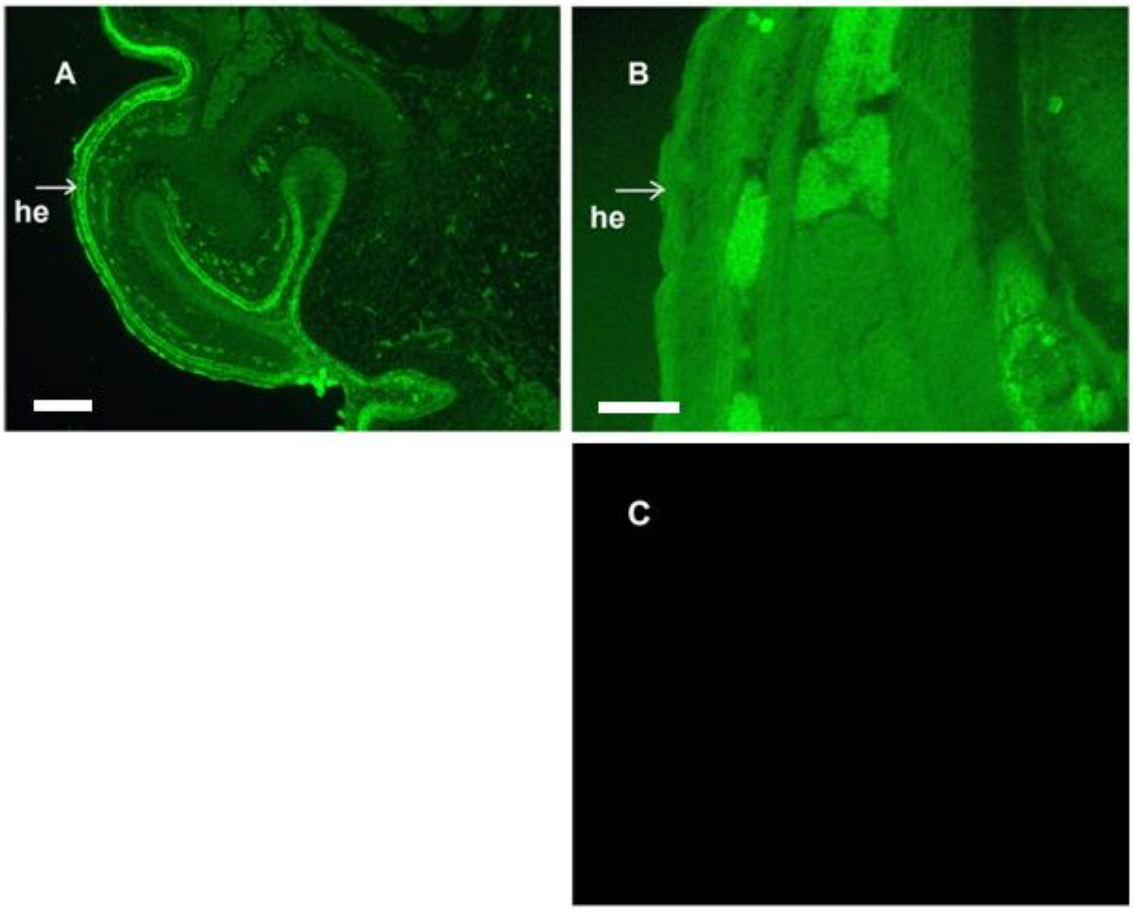


Figure 3.18 Head epidermis staining and its comparison with a no primary antibody control using wax sections at 15.5dpc. Head section incubated with both primary and secondary antibodies (A) and only secondary antibody as a control (B and C). Exposure in (C) is identical to (A) showing specificity of labelling. Extreme overexposure shown in (B). he: head epidermis. Scale bars: 100µm.

Perhaps then the absence of clusterin immunoreactivity in the inner ear reflected that the antibody that was raised against the C-terminus of the protein, and an inner ear isoform that has yet to be characterised, lacks these C-terminal sequences. To address this, a set of oligonucleotides, Clu9F and Clu9R (2.4.14) capable of amplifying a 164bp sequence from exon 8 to exon 9 of clusterin cDNA were designed that include the region that the peptide was derived from for raising this antibody (Appendix V.I).

Total RNA was extracted from 18.5dpc mouse ears, and subjected to RT-PCR analysis (2.1.7) with primers Clu9F and Clu9R. A clusterin plasmid dilution was used as a positive control and a no DNA sample was used as a negative control. The expected 164bp product was generated for both the 18.5dpc ear cDNA and for the clusterin plasmid control (Figure 3.19). but absent in the negative control demonstrating that this part of the clusterin gene is indeed transcribed into message in the inner ear.

Unfortunately there is a band in the negative control of unknown origin but the difference in size suggests it might be either from non-specific amplification or leakage from adjacent lane.

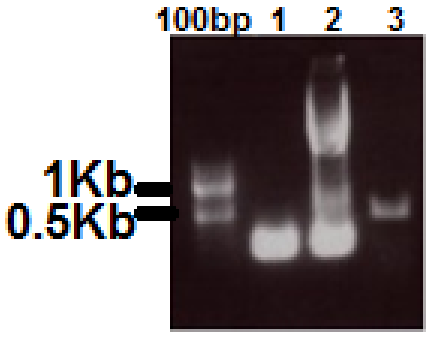


Figure 3.19 RT-PCR analysis of mouse clusterin cDNA at the C-terminus (1) amplification of a 164bp DNA fragment from the cDNA 18.5dpc mouse inner ear, (2) Clusterin plasmid as positive control, and (3) No DNA as negative control. The DNA band present in lane 3 is a non-specific band. 100bp: 100bp DNA ladder.

The mouse stop codon is located immediately after the antibody recognition site (Appendix V.I). Analysis of clusterin isoforms on the current genome browser does indicate some isoforms that do not include exons that encode the peptide used to raise this antibody, however, isoform clu001 is full length and should do so (Figure 3.20). One likely explanation for the lack of detection of immunoreactivity for the full length isoform could be the *in vivo* structure of the protein leading to unavailability of the

antigenic region, for instance by being hidden internally in the molecule, or even the inner ear isoform is one of the other species highlighted in the figure below. Arguing against the latter possibility is the RT-PCR analysis above. Alternatively, lack of immunoreactivity may be due to interspecific differences between the man and mouse sequences. It is interesting to note that only 11 out 14 amino acids are identical in both mouse and human in the sequence (Table 3.1) that was used to generate this antibody, which appears to be the most plausible explanation for failure to detect clusterin using this antibody.

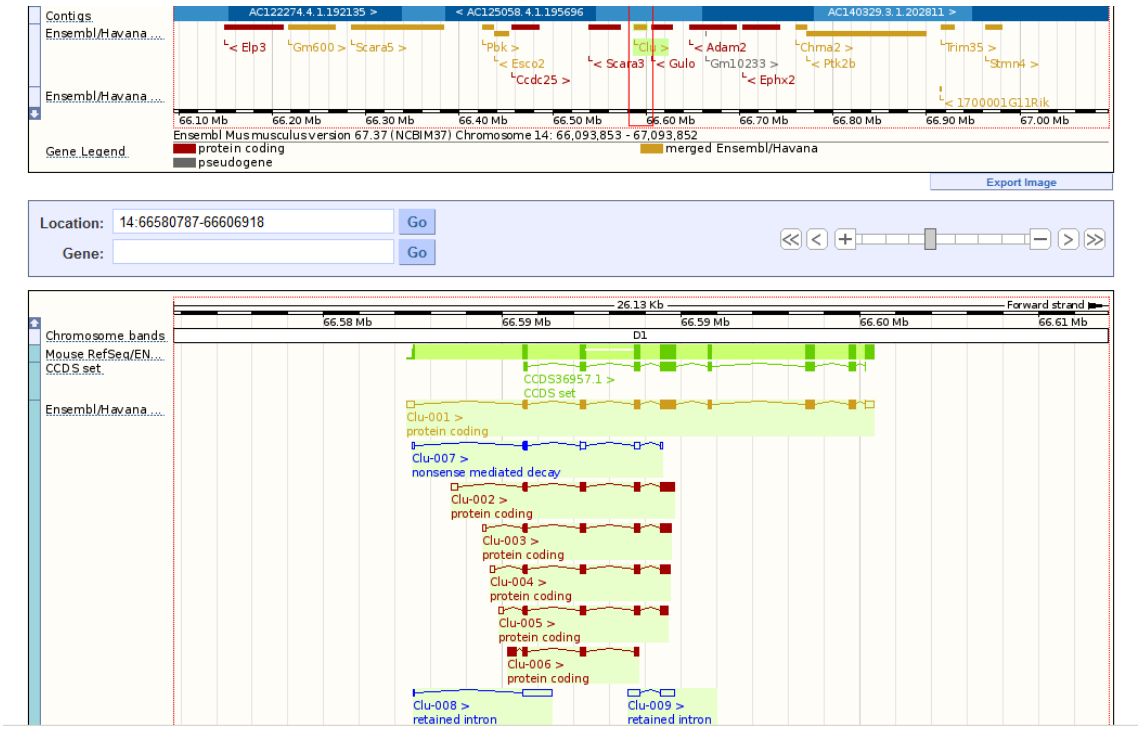


Figure 3.20 Mouse clusterin gene and its mRNA transcripts/isoforms - from ensemble.org (August 2012)

| | | | | | | | | | | | | | | |
|---|---|---|---|---|---|---|---|---|---|---|---|---|---|---|
| A) Human | GGAGAAAGCGCTGCAGGAATACCGCAAAAAGCACCGGGAGGA | | | | | | | | | | | | | |
| B) Mouse | GGAGAAGGCGCTACAGGAATACCGCAGGAAAAGCCGTGCGGA | | | | | | | | | | | | | |
| C) Mouse | | E | K | A | L | Q | E | Y | R | **R** | K | **S** | R | **A** | E |

Tabel 3.1 Sequence comparison of Human and mouse at the antibody recognition site. A) human sequence, B) corresponding mouse sequence and C) Mouse amino acid sequence. The underlined amino acids are different between mouse and human.

Therefore, a combined pubmed and internet (www.google.com) literature search for other clusterin antibodies was carried out, in particular for any antibodies that

recognizes larger regions of clusterin, or antibodies directed against the N-terminus. One antibody was found and purchased from Proteintech (ag2889- Rabbit polyclonal antibody) (2.3.1.5.1) that is generated against the last 350 amino acids of the human clusterin protein which should recognize the entire C-terminus (β-chain) and part of the N-terminus (α-chain) of mouse clusterin (Appendix V.I).

3.2.2.2 Immunohistochemistry using the clusterin antibody ag2889 (Proteintech): Only wax sections were analysed and prepared using heat-mediated antigen retrieval (2.3.1.2) (as recommended by the antibody provider). Titration of the antibody was carried out on 15.5dpc wax sections at 1/50, 1/100 and 1/200 dilutions. A goat anti rabbit fluorescent-conjugated secondary antibody (Invitrogen, Alexa fluor 488) at 1/500 dilution was used for detection. Clusterin immunoreactivity was detected at all dilutions (Figure 3.21), however the strongest fluorescence found was using a 1/50 dilution, and subsequent experiments were carried out at this dilution.

In this titration experiment, some immunofluorescence that previously was not detected by Abcam antibody was present. At this stage (15.5dpc) a low level of immunoreactivity was detected in the cochlea sensory epithelium, especially at the lesser epithelial ridge towards the strial edge (arrow in Figure 3.21 B). In some sections (3.23 F) low level immunoreactivity is also detected in the greater epithelial ridge (bigger arrow in 3.23 F). These two areas of immunoreactivity correspond to the areas of mRNA synthesis in the inner ear epithelium. However, much stronger immunoreactivity was also observed in the top wall of the developing cochlear duct (Figure 3.21). The lateral and central part of this wall will eventually develop as the stria vascularis and Reissner's membrane respectively and clusterin expression seems to be more centrally located on and around this wall (Figure 3.21). In addition, nearly the same level of immunoreactivity was also present in the periotic mesenchyme (Figure 3.21 A,D). Furthermore, isolated immunoreactive cells were detected in the developing otic capsule (Figure 3.21A).

As a next step the specificity of this staining was confirmed by using the following negative controls: (1) a non-specific primary antibody Rabbit IgG (1mg/ml, a gift from Prof Guy Richardson, University of Sussex) and secondary antibody (2) no antibody (3) secondary antibody only (4) primary antibody only controls all against 15.5dpc wax

sections. There was no specific immunoreactivity detected in these controls for any (Figure 3.22). Although in (B) rabbit IgG gives some low level fluorescence in the cochlear epithelium, this is not split into two domains. Nevertheless this confirms strong immunofluorescence in the nonsensory wall and periotic mesenchyme, and perhaps genuine but low levels in the cochlear sensory epithelium.

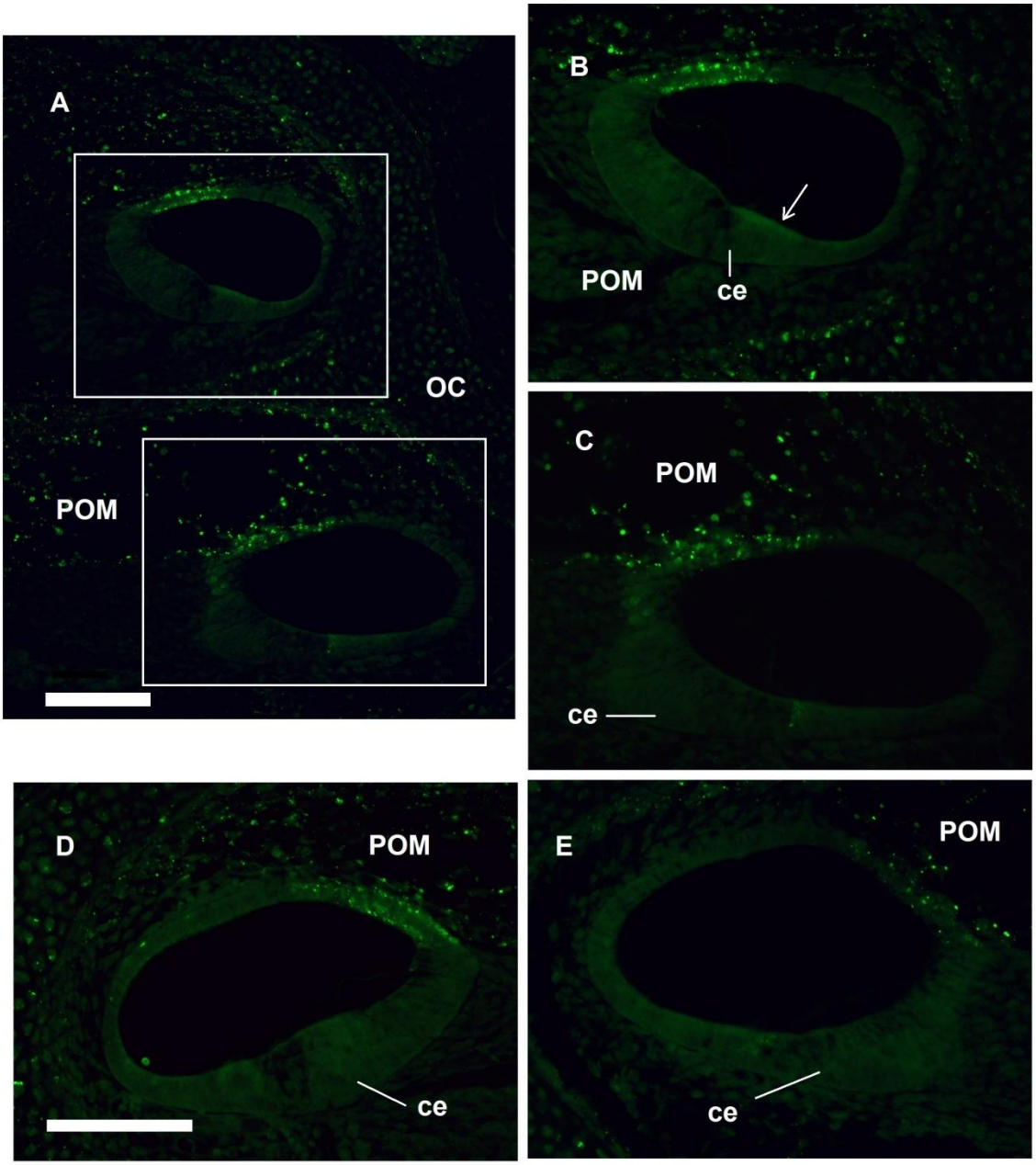


Figure 3.21 Titration of ag2889- Rabbit polyclonal primary antibody against 15.5dpc wax sections through the cochlea at dilutions 1/50 for (A, B and C), 1/100 (D) and 1/200 (E). B and C are the higher magnification of highlighted sections in A for middle and basal turns respectively. Scale bars: 100μm.

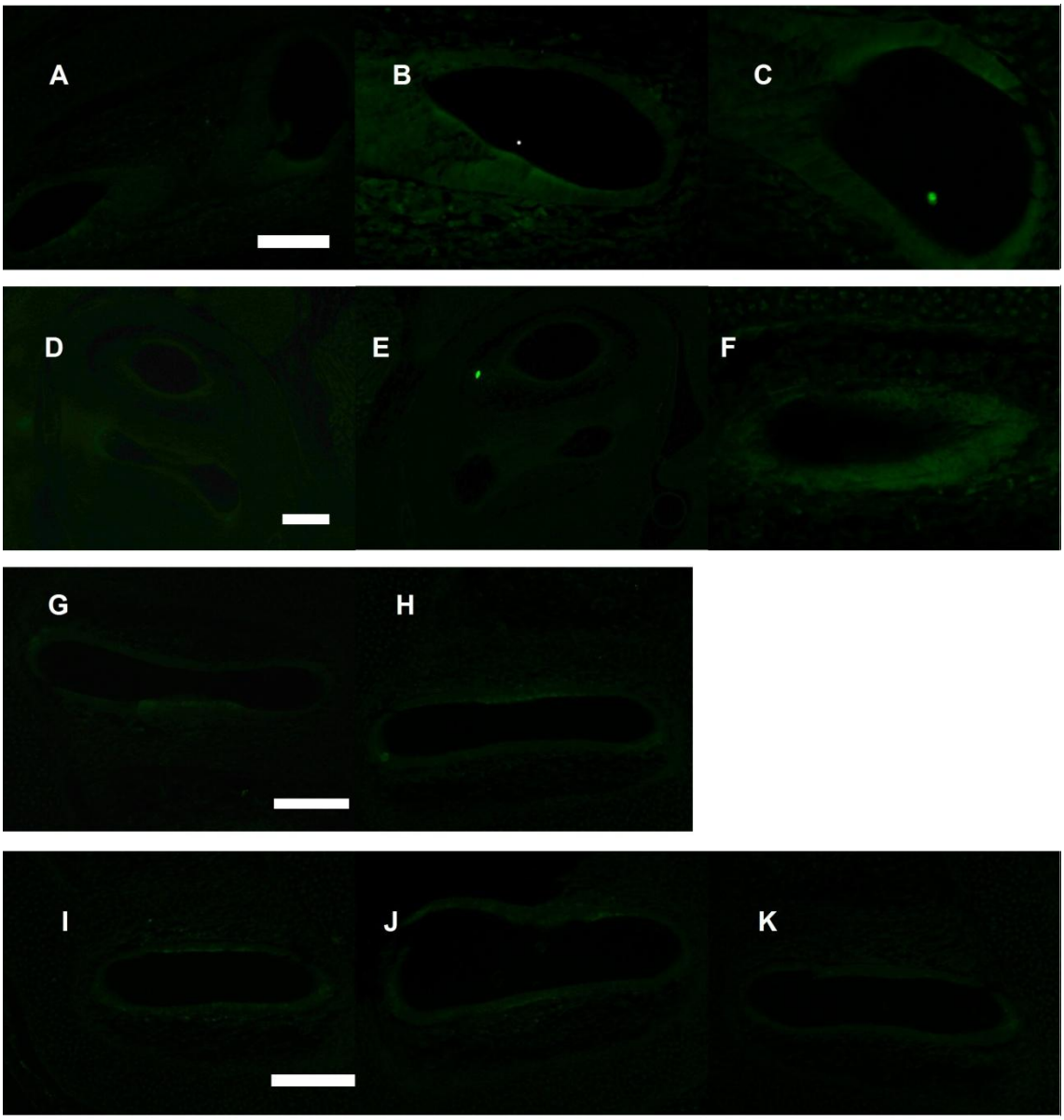


Figure 3.22 Controls for clusterin antibody (ag2889- Rabbit polyclonal antibody) using 15.5dpc cochlea wax sections. A-C: Rabbit IgG as primary and goat anti-rabbit as secondary antibody. D-F: no antibody. G and H: Primary antibody (ag2889- Rabbit polyclonal antibody) only. I-K: Secondary antibody (goat anti-rabbit) only. Scale bars: 100μm.

So in order to look at a time course of protein production, the antibody was examined again in wax sections across the whole 15.5dpc inner ear as well as at 13.5, 14.5 and 17.5dpc mouse heads (Figure 3.23-3.27). As found with the titration clear transient expression was found in periotic mesenchyme and Reissner's membrane in addition to the cochlear sensory epithelial expression, whilst still not as strong as these other domains, was clearly reflecting mRNA expression.

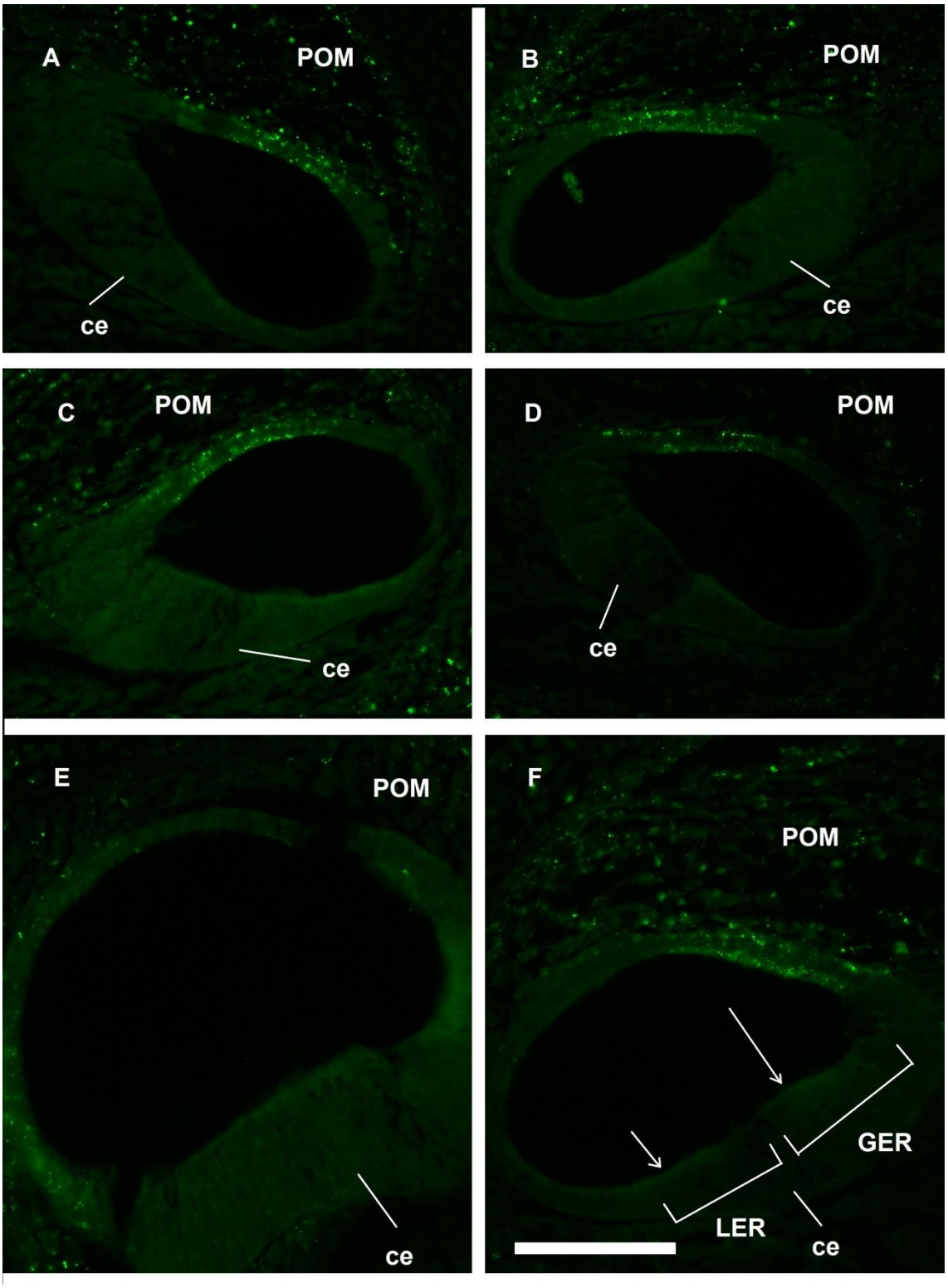


Figure 3.23 Mouse wax sections from 15.5dpc and detection of clusterin using ag2889- Rabbit polyclonal antibody. Basal and middle turns of the cochlea duct (A-F). GER: greater epithelial ridge, LER: lesser epithelial ridge, ce: cochlear epithelium and POM: periotic mesenchyme. Scale bars: 100μm.

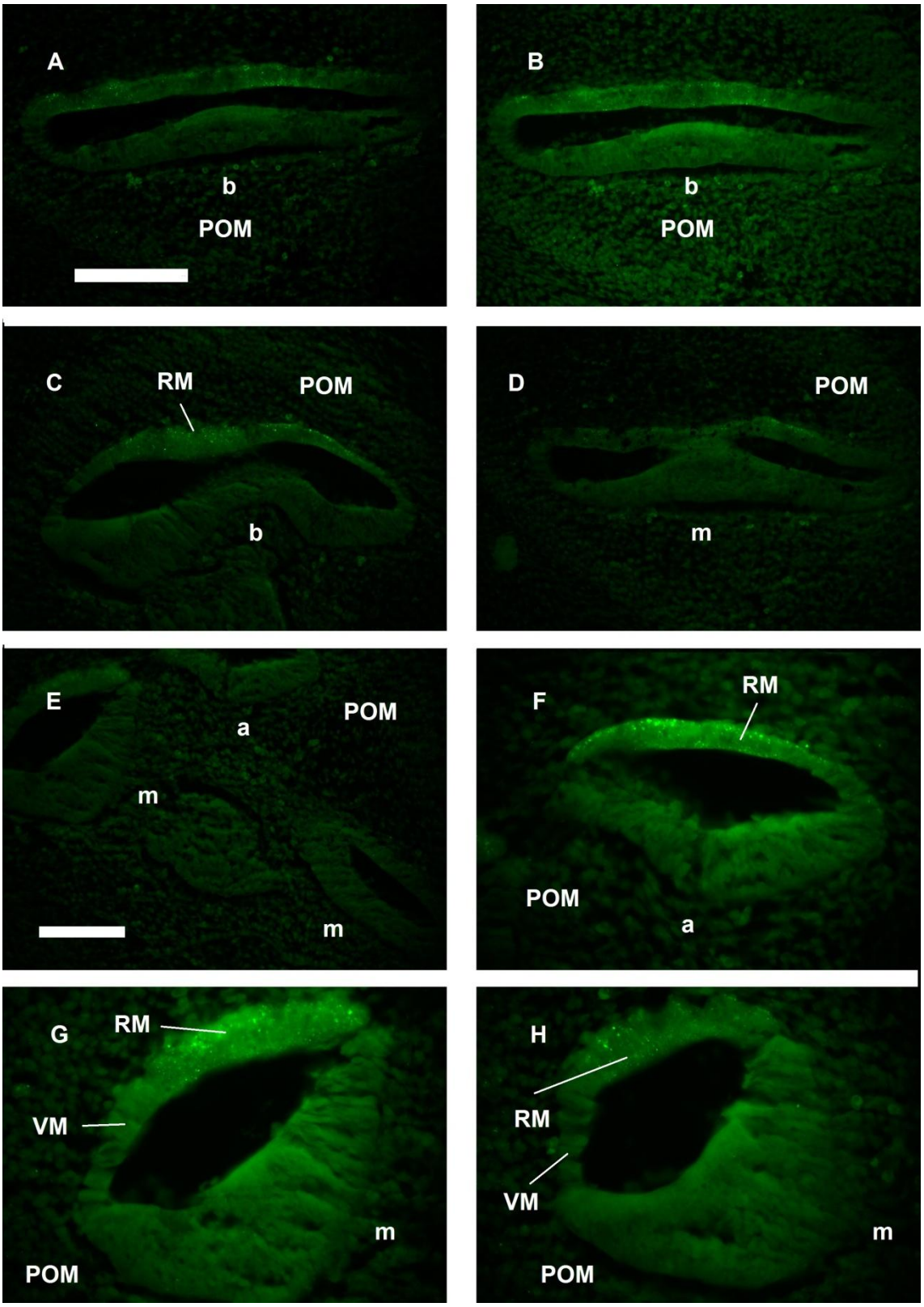


Figure 3.24 Mouse head wax sections from 13.5dpc and detection of clusterin using ag2889- Rabbit polyclonal antibody. Serial sections through the base of the cochlea (A-C), middle turns of the cochlea (D and E), apical turn of the cochlea (F) and higher magnification of basal turns of the cochlea (G and H). RM: Reissner's membrane, VM: vestibular membrane, POM: periotic mesenchyme, a: apical turn, b: basal turn and m: middle turn. Scale bars: 100μm.

At 13.5dpc the low level of immunoreactivity that was detected with the titration of 15.5dpc was also detectable along the length of the developing cochlea sensory epithelium (arrows in Figure 3.24) but only one patch of expression is detectable not two like 15.5-17.5dpc (Figure 3.23 and 3.27). The non-sensory epithelial cells at the top wall of the cochlea duct corresponding to the developing Reissner's membrane, in some of the basal (Figure 3.24 C) and all of the middle (Figure 3.24 G,H) and apical turns (Figure 3.24 F) also showed some immunoreactivity similar to 15.5dpc sections but clusterin immunoreactivity was not detected in the periotic mesenchyme (Figure 3.24 A-H) or otic capsule.

One day later at 14.5dpc clusterin protein expression was still present in the presumptive Reissner's membrane along the length of the cochlea (arrows in 3.25 B-D) and in addition some immunoreactivity was detectable in the periotic mesenchyme (Figure 3.25 B,D) and otic capsule (Figure 3.25 B and 3.26 B). The detected immunorectivity in the periotic mesenchyme was not only present surrounding the developing Reissner's membrane but also scattered randomly throughout the entire periotic mesenchyme (Figure 3.26 A). A low level of expression in the developing cochlea sensory epithelium was also detected which, similar to 13.5dpc, is still one continuous patch of expression.

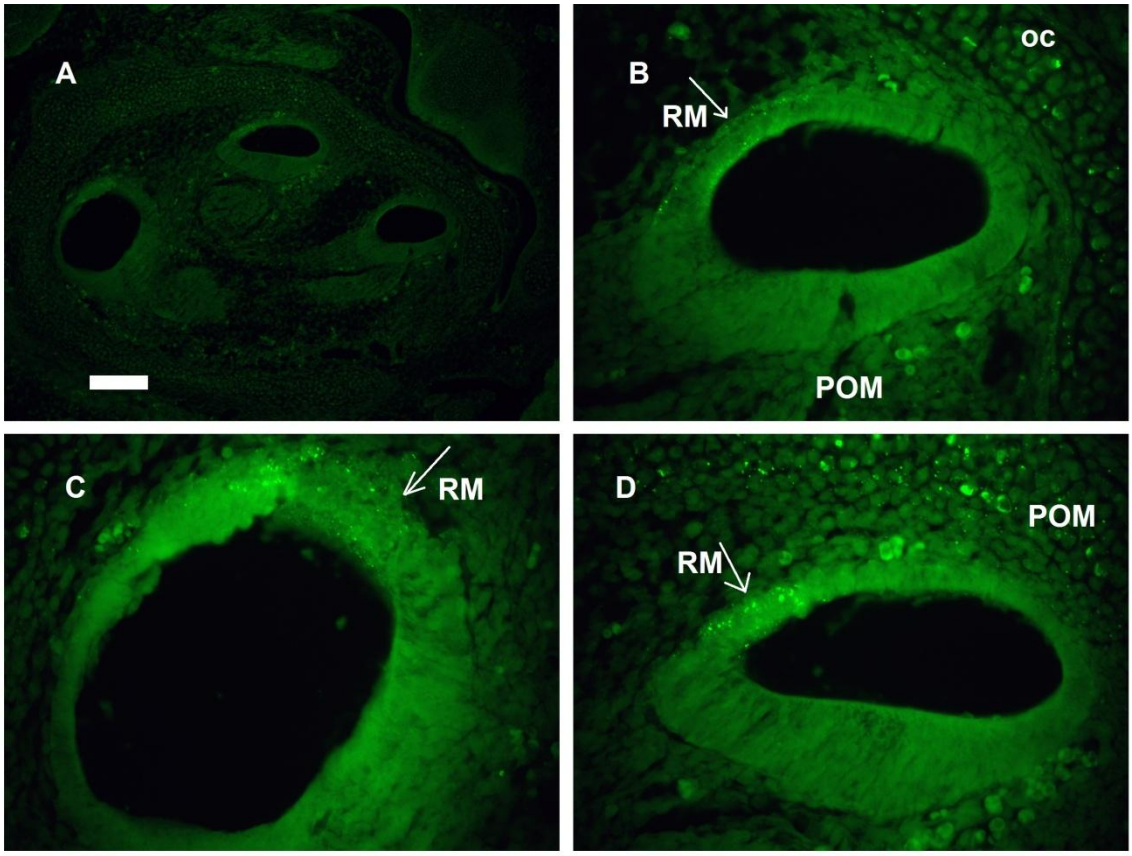


Figure 3.25 Clusterin immunohistochemistry of sections at 14.5dpc. Overview of the cochlea (A) and higher magnification of middle turns (B and C) and apex (D). Arrows point to the area of immunoreactivity in the Reissner's membrane. RM: Reissner's membrane, and POM: periotic mesenchyme. Scale bar: 100μm.

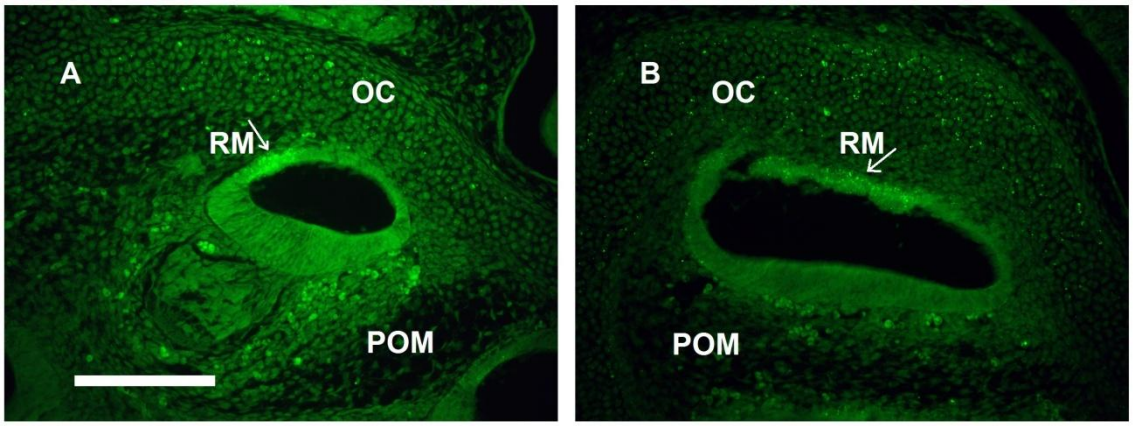


Figure 3.26 Clusterin immunohistochemistry against sections at 14.5dpc demonstrating immunoreactivity in developing Reissner's membrane and periotic mesenchyme (A) and otic capsule (B). Arrows point to the area of immunoreactivity in the Reissner's membrane. RM: Reissner's membrane, OC: otic capsule, and POM: periotic mesenchyme. Scale Bar: 100μm.

Similar to protein expression 15.5dpc, at 17.5dpc as well, the two areas of low immunoreactivity at the greater and lesser epithelial ridge were detected along the length of the cochlea (arrows in 3.27 B-D).

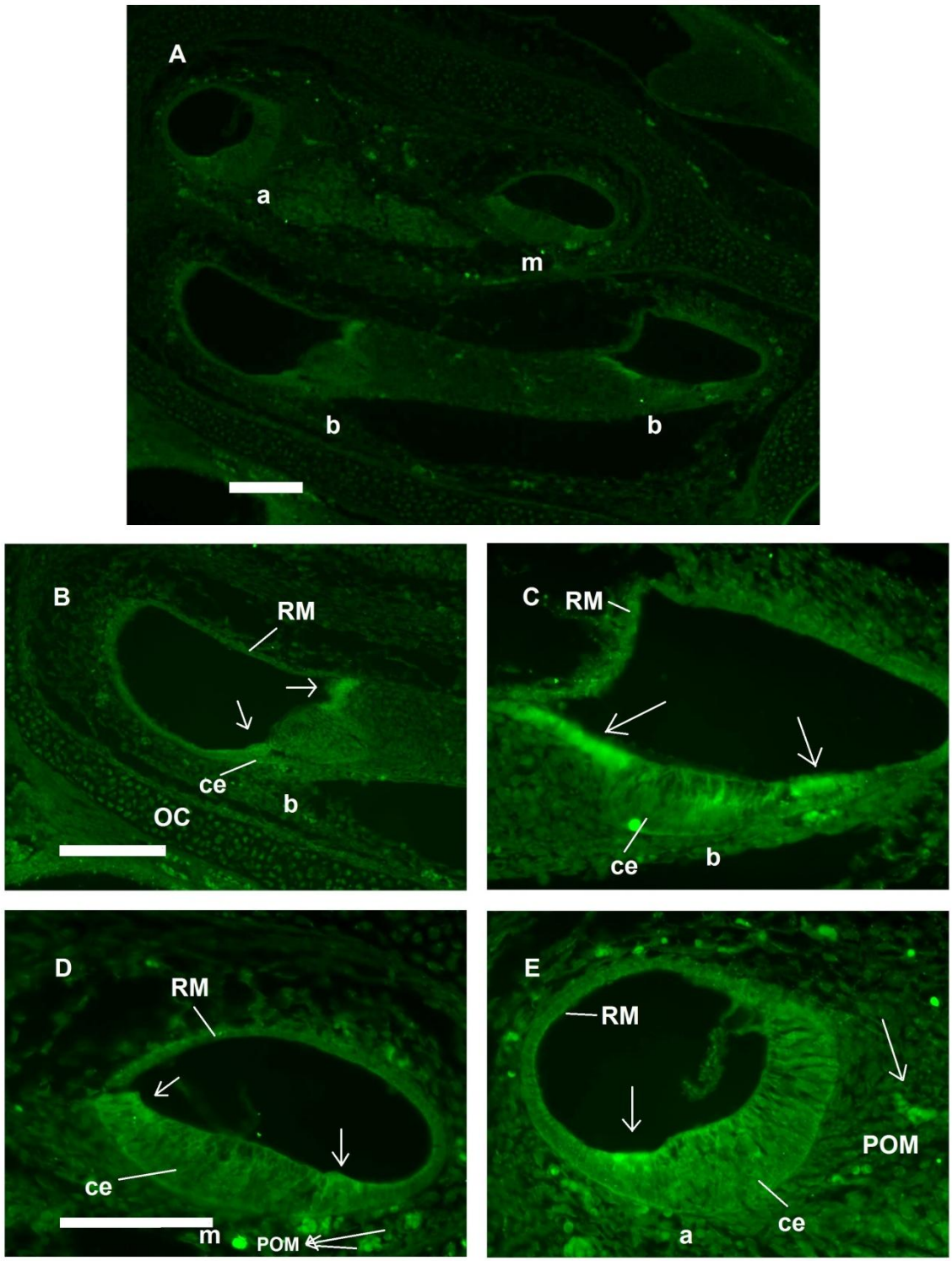


Figure 3.27 Mouse wax sections from 17.5dpc and detection of clusterin using ag2889- Rabbit polyclonal antibody. An overview of cochlea turns (A), higher magnification of cochlea turns (B-E), basal (B and C), middle (D) and apical (E). The arrows point to the area of strong immunoreactivity. a: apical b: basal, m: middle, ce: cochlea epithelium, POM: periotic mesenchyme, RM: Reissner's membrane, and OC: otic capsule. Scale bars: 100μm.

The immunoreactivity that was observed in the region of developing Reissner's membrane from 13.5-15.5dpc seems to become downregulated for clusterin expression at this stage (Figure 3.27 B-E). This is also the case with the observed areas of immunoreactivity in the periotic mesenchyme which appears to be much less detectable (Figure 3.27 D and E). In addition, no immunoreactivity was detected in the developing otic capsule (Figure 3.27 B).

### 3.2.3 Comparative localisation of clusterin mRNA in the developing inner ear with tectorin mRNA markers

The dynamic expression of clusterin mRNA expression in the developing cochlear epithelium from an initial broad domain across the entire sensory epithelium to two distinct lateral and medial domains were next localised with reference to other established cellular markers in the inner ear. In this study, the expression of two well defined supporting cells markers, tectorin α and tectorin β, were analysed by ISH in alternative sections with clusterin riboprobes. The tectorin α and tectorin β plasmids (a gift from Prof Guy Richardson, University of Sussex) were used to generate approximately 4.5Kb and 2.7Kb probes respectively (Legan, Rau et al. 1997) (Appendix V.VII and V.VIII).

Analysis of mouse head sections of 10-µm thick at stage 15.5 and 17.5dpc were used for tectorin α. For tectorin β also mouse head sections of 10-µm thick at 18.5 were used.

#### 3.2.3.1 Comparative expression of clusterin and Tectorin α at 15.5dpc

Alternate sections through the developing vestibular system of the mouse inner ear at 15.5dpc for clusterin and tectorin α confirm the absence of clusterin expression (Figure 3.28 A,C,E and G). In contrast, expression of α-tectorin expression is detected in the vestibular sensory epithelia, in the utriclar macula (um) and saccular macula (sm) (Figure 3.28 B,D,F and H). α-tectorin mRNA expression is first detected in the utricle at 12.5dpc and by 13.5dpc, the expression has been reported in both saccule and utricle (Rau, Legan et al. 1999).

In the developing auditory system, the expression of α-tectorin was first detected at 12.5dpc in basal turns, extends further along the cochlear duct at 13.5dpc, but is still absent from the apex; however is found throughout the entire length of the cochlear duct by 14.5dpc (Rau, Legan et al. 1999). At 14.5dpc the pattern of expression of α-tectorin mRNA, characteristic of neonatal animals first becomes visible in the basal turn of the cochlea. Using radioactive *in situ* hybridisation this has been defined as two bands of expression, a broader region that is inclusive of most of the greater epithelial ridge and a narrow band within the lesser epithelial ridge (Rau, Legan et al. 1999). Detailed cellular analysis revealed the greater epithelial ridge domain of expression extends and includes the immature inner phalangeal and border cells that surround the inner hair cells, whereas the lesser epithelial expression domain corresponds to the first two rows of presumptive Hensen's cells that are located alongside the third row of Deiter's cells (Rau, Legan et al. 1999) and this is illustrated diagrammatically (Figure 3.29). In this non-radioactive ISH analysis using α-tectorin the broader GER domain only is visible in most occasions, due to the reduced sensitivity in using non-radioactive probes (Figure 3.30)

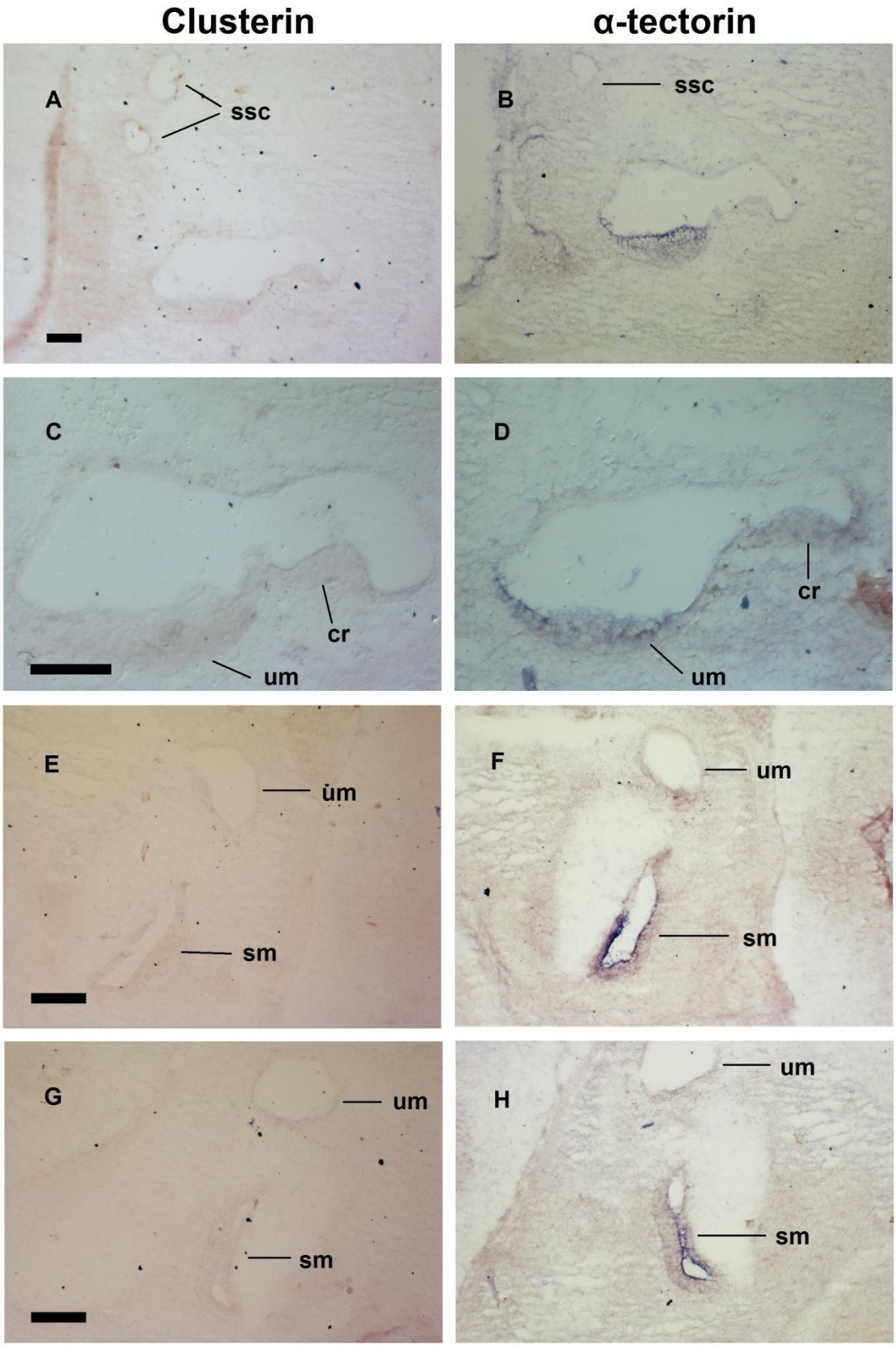


Figure 3.28 *In situ* hybridisation of alternate sections for mouse clusterin and α-tectorin gene marker on developing mouse vestibular system at 15.5dpc.

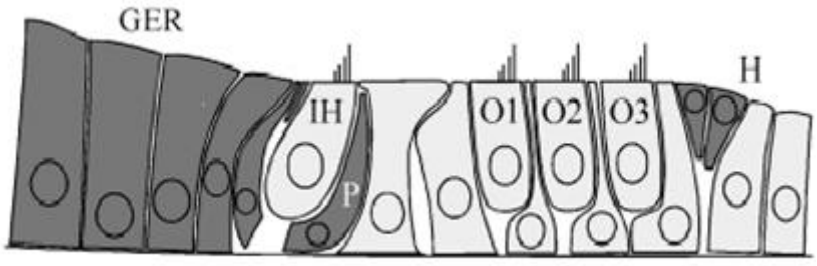


Figure 3.29 Schematic diagrams demonstrating the expression patterns of α-tectorin mRNA in the early postnatal organ of Corti. GER: greater epithelial ridge, IH: inner hair cells, O1-O3: outer hair cells 1,2, and 3, P:phalangeal cells, H:Hensen's cells. Adapted from Rau et al. (Rau, Legan et al. 1999). α-tectorin mRNA expressing cells are highlighted in dark gray.

Comparison of sections at the base of the cochlea for clusterin and α-tectorin expression shows that both share a wide central region of staining in the middle, with the lateral regions at the strial edge positive for clusterin and only for some of the sections of α-tectorin (Figure 3.30) (note the lower level expressing domain of α-tectorin is not detectable in this particular figure). However, Rau et al. 1999 shows this second domain (Rau, Legan et al. 1999) which is predicted to be at some cellular distance from the clusterin lateral domain. The wider region of staining present for clusterin seems to extend more for α-tectorin (Figure 3.30 compare C with D) covering some parts of the region in which clusterin expression is downregulated as was explained previously (Arrowheads in 3.6 J-L). However, the expression of clusterin and α-tectorin in this area overlaps greatly. In order to illustrate this more clearly, alternate sections of clusterin and α-tectorin mRNA *in situ* hybridisation pictures were false painted and overlaid on top of each other and their expression was compared (Figure 3.32).

For clusterin at the strial edges in the base of the cochlea, a narrow region of expression is detected (arrows in Figure 3.30 C). Expression analysis at approximately mid-way along the cochlear duct revealed expression in Hensen's cells for α-tectorin in sections evident as a very narrow and faint area of staining (smaller arrow in 3.31 B). Clusterin expression appears to be more broadly distributed, further laterally located and does not seem to overlap with α-tectorin (Figure 3.32).

Clusterin expression thus appears to be expressed by some of the supporting cells adjacent to Hensen's cells but is not expressed in Hensen's cells themselves (Figure

3.31 and 3.32). Expression may be in the supporting cells of Claudius and clearly in cells of the lateral wall of cochlear duct. However, without the use of stria vascularis markers it is not possible to say lateral wall expression overlaps with presumptive stria vasularis cells.

Both clusterin, and α-tectorin are expressed the full length of the cochlea (Figure 3.33).

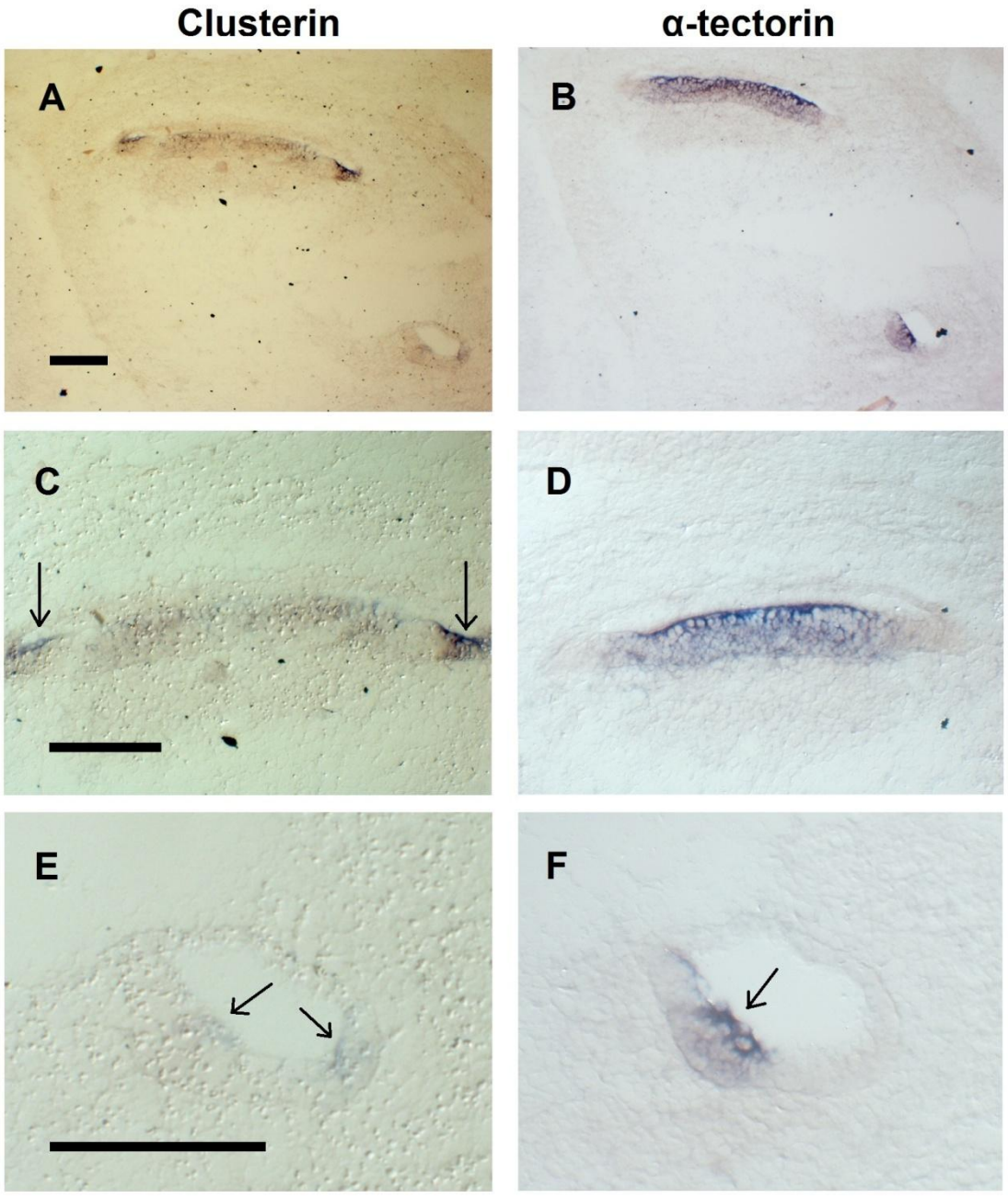


Figure 3.30 Comparative analysis of clusterin and α-tectorin mRNA expression during cochlea development by RNA *in situ* hybridisation on alternate cross sections at 15.5dpc. A and B: Overview of the cochlea section. C and D: basal turns, E and F: basal turns. Arrows point to the area of specific staining. Scale bars: 100μm.

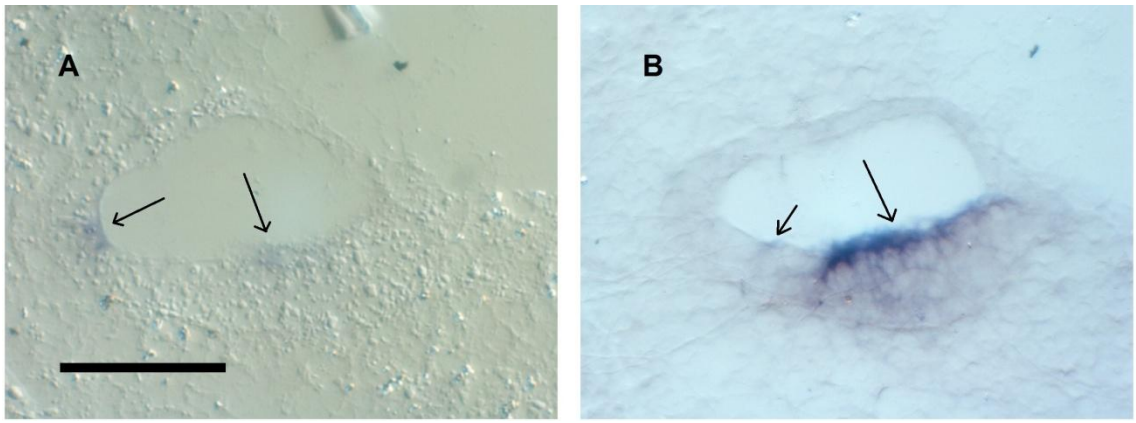


Figure 3.31 Comparative analysis of clusterin (A) and α-tectorin (B) expression during cochlea development by RNA *in situ* hybridisation on alternate cross sections at 15.5dpc. Expression in the middle basal turns. This figure demonstrates the expression of clusterin and α-tectorin in adjacent sections at the middle turns of the cochlea. In B the narrower band of α-tectorin is detectable (smaller arrow). Scale bar: 100μm.

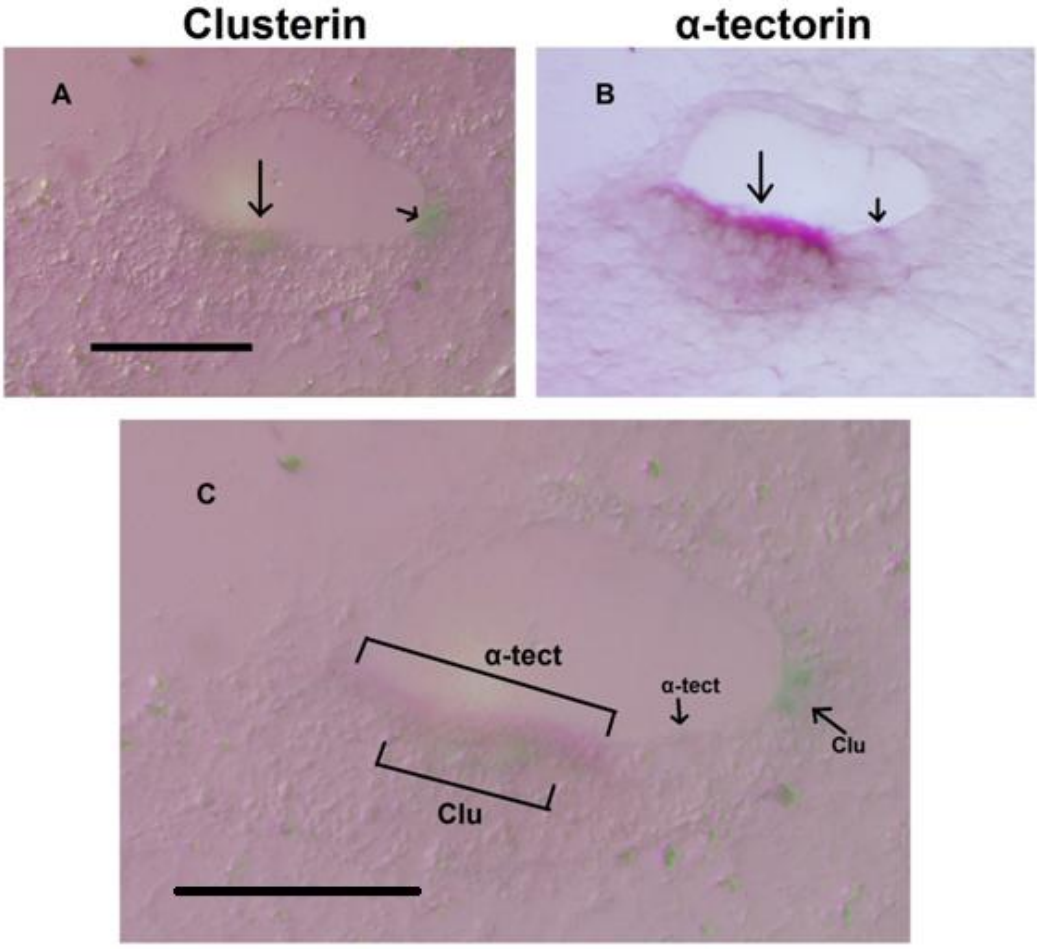


Figure 3.32 Comparison of clusterin mRNA expression with α-tectorin by false painting and overlaying the alternate sections at 15.5dpc. Clusterin and α-tectorin mRNA expression in the middle turns of cochlea respectively (A and B). The overlaid sections of clusterin and α-tectorin for comparison (C). Smaller arrows in A, B and C point to narrower region of clusterin and α-tectorin expression at the lateral side. Scale bar: 100μm.

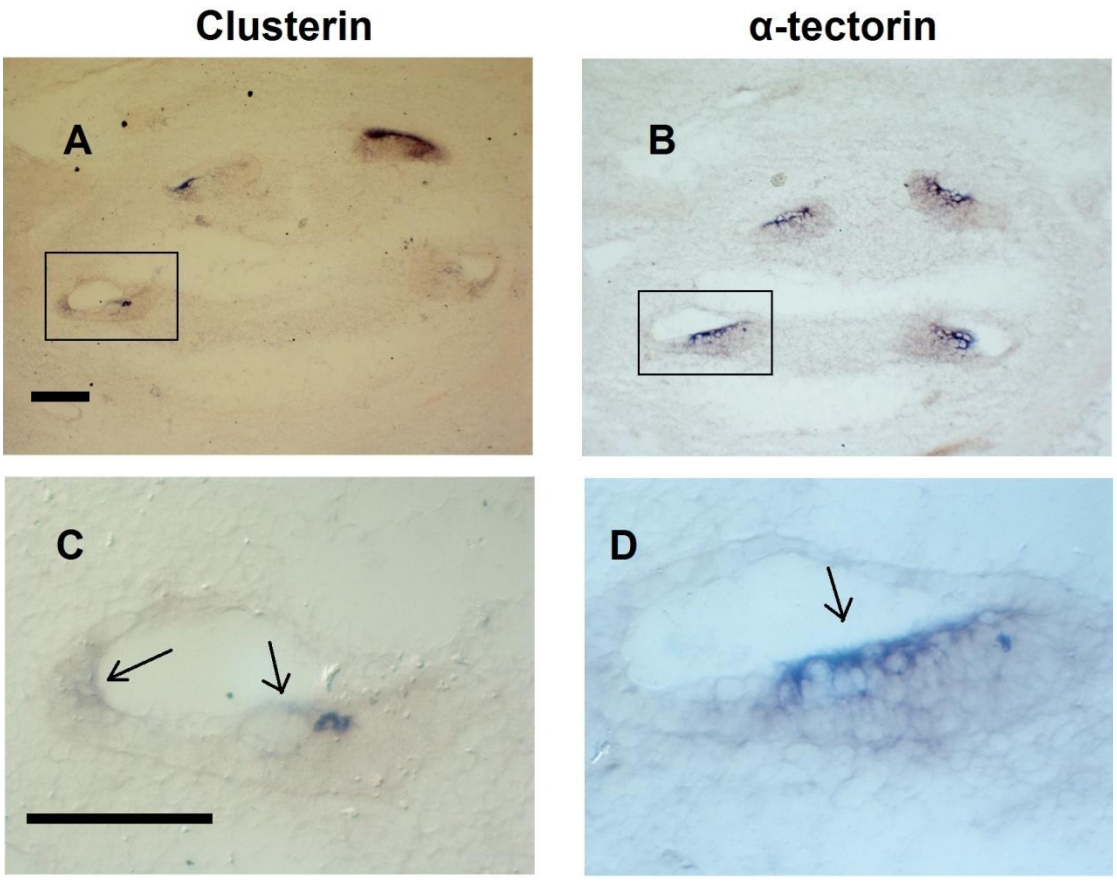


Figure 3.33 Comparative analysis of clusterin and α-tectorin expression during cochlea development by RNA in situ hybridisation on alternate cross sections at 15.5dpc in the mid-basal turns of the cochlea. Clusterin and α-tectorin mRNA in panel A and B respectively are expressed the full length of the cochlea**.** Expression is detected in mid-cochlear turns (C and D). Scale bars: 100μm.

### 3.2.3.2 Comparative expression of clusterin and α-tectorin at 17.5dpc

A comparative *in situ* hybridisation analysis was also carried out on alternate cross sections at 17.5dpc for clusterin and α-tectorin riboprobes. Both genes are again expressed the full length of the cochlea (Figure 3.35).

Comparison of clusterin and α-tectorin mRNA expression at the base of cochlea (compare Figure 3.34 A with B) demonstrates overlap of the broad patch of clusterin expression with α-tectorin. However, α-tectorin expression is more extensive and stretches further across the sensory epithelium towards the strial edge (Figure 3.34 A,B).

As the cochlea sensory epithelium divides into two separate part of two turns, the expression of both clusterin and α-tectorin are both downregulated where the ducts separate (arrow heads in Figure 3.34 C-F), leaving two opposite coils, each with a broad and narrow strip of clusterin expression. As at the start of the cochlea, the wider strip of α-tectorin expression extends further in the strial direction (longer arrow in Figure 3.35). Clusterin expression seems to be localised beyond where Hensen's cells can be anticipated (although not detected under non-radioactive conditions on some occasions) (smaller arrow in Figure 3.35). Clusterin may or may not include the Hensen's cells but it seems to cover the adjacent cells of Claudius and outer sulcus. Similar to 15.5dpc, alternate sections of clusterin and α-tectorin mRNA *in situ* hybridisation pictures were false painted and overlaid on top of each other and their expression at the basal and middle turns was compared which further confirmed the above descriptions (Figure 3.36).

In the middle sections, there is no difference to the above described comparative expression of the two genes at the cochlear base (Figure 3.35).

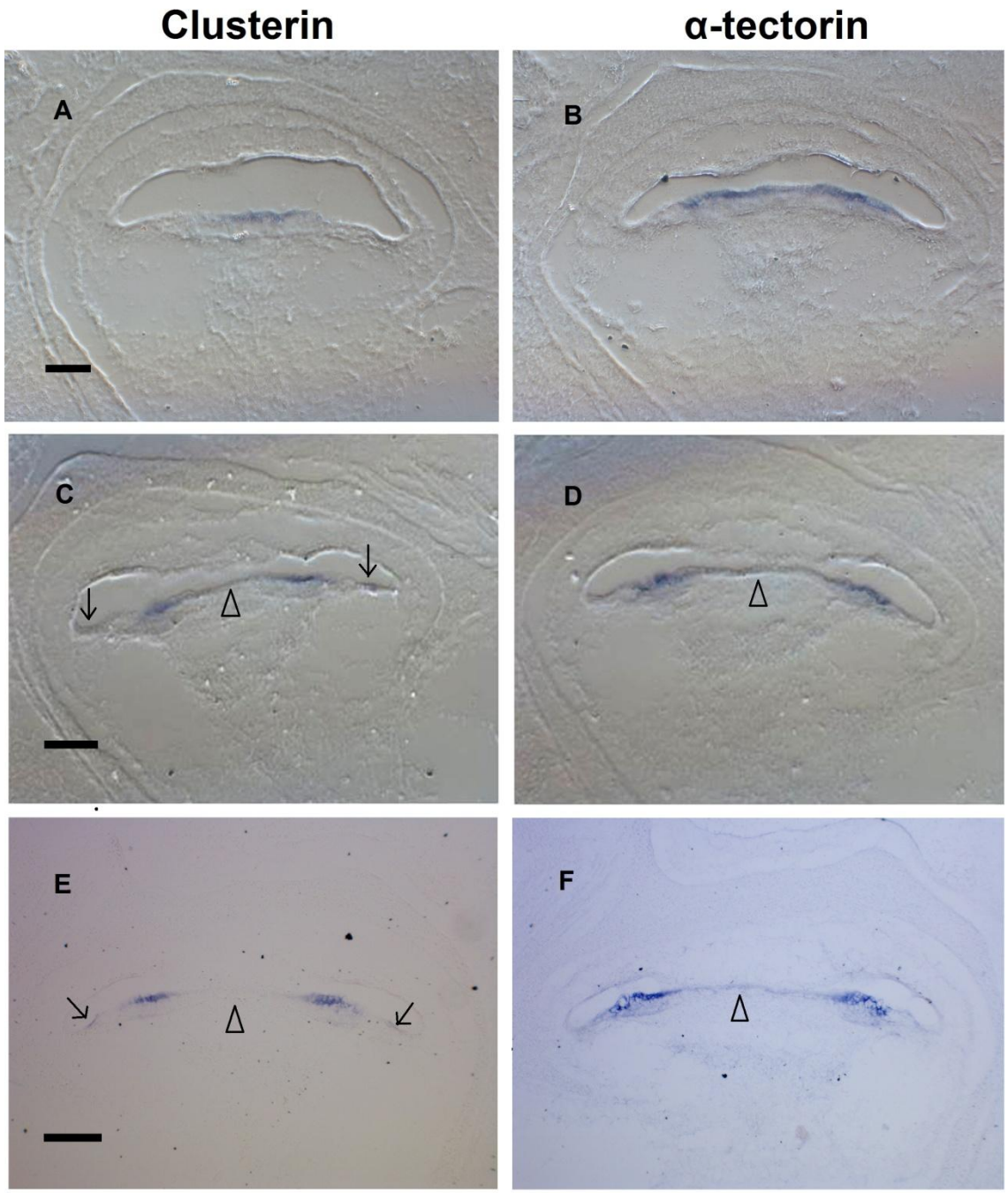


Figure 3.34 Comparative analysis of clusterin and α-tectorin expression during the cochlea development by RNA *in situ* hybridisation on alternate cross sections at 17.5dpc. Arrows point to the second stripe of expression of clusterin mRNA. Arrow heads in C-F demonstrate the clusterin downregulation regions. Scale bars: 100μm.

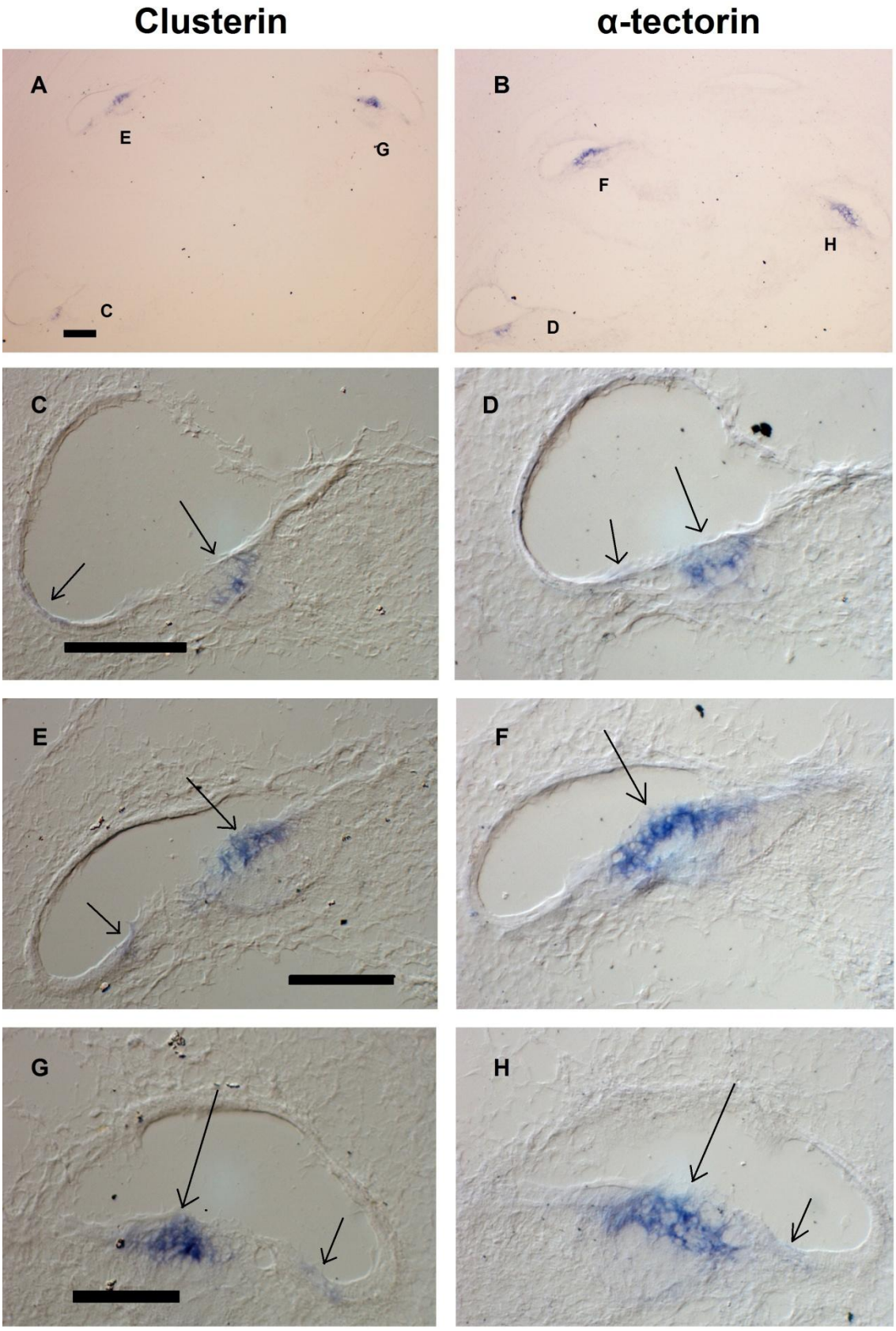


Figure 3.35 Comparative analysis of clusterin and α-tectorin expression during the cochlea development by RNA *in situ* hybridisation on alternate cross sections at 17.5dpc. All three profiles of cochlea (basal, middle, and apical) are compared. Overview of clusterin and α-tectorin expression in the cochlea A and B respectively. Basal turns for clusterin and α-tectorin C and D respectively. Apical turns for clusterin and α-tectorin E and F respectively. Middle turns for clusterin and α-tectorin G and H respectively. Arrows point to the specific labelling patterns. Scale bars: 100μm.

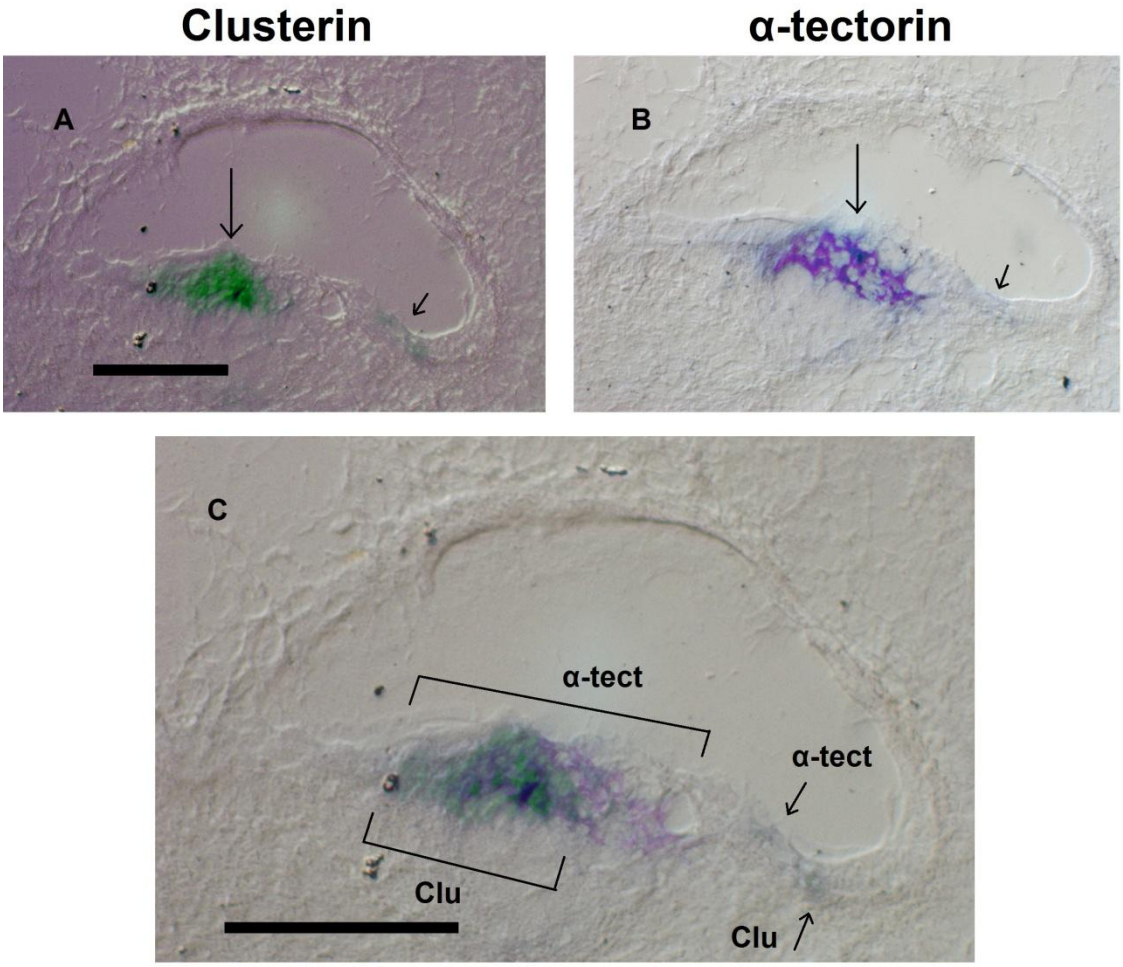


Figure 3.36 Comparison of Clusterin mRNA expression with α-tectorin by false painting and overlaying the alternate sections at 17.5dpc. A and B: Clusterin and α-tectorin mRNA expression in the basal turns of cochlea respectively. C: the overlaid sections of clusterin and α-tectorin for comparison. Smaller arrows in A, B and C point to narrower region of clusterin or α-tectorin expression at the lateral side. Scale bars: 100μm.

### 3.2.3.3 Comparative analysis of clusterin and β-tectorin at 18.5dpc

Clusterin mRNA expression was also compared to the expression of a second gene expressed in the developing sensory epithelium, β-tectorin, by analysing alternate sections at 18.5dpc. β-tectorin expression is first detected in the base of the cochlea at 12.5dpc but then extends over the ensuing 48hours to become expressed the full length of the cochlea (Rau, Legan et al. 1999). From 14.5dpc onwards the characteristic pattern of β-tectorin mRNA is established, as three distinct bands of expression. The first domain of expression is a narrow strip of expression in the greater epithelial ridge that lies adjacent to the inner hair cells and includes the developing border cells, this is

followed by a second stripe of expression in between the other two stripes that corresponds to the inner and outer pillar cells, and the final domain at the lateral margin of the lesser epithelial ridge corresponds to the third row of Deiter's cells (Figure 3.37) (Rau, Legan et al. 1999).

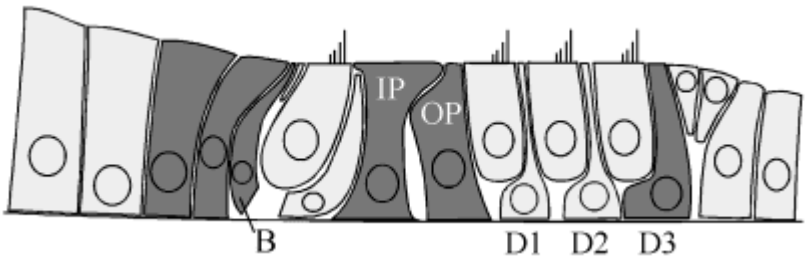


Figure 3.37 Schematic diagram demonstrating the expression patterns of β-tectorin mRNA in the early postnatal organ of Corti. B:border cell, IP:inner pillar cell, OP: outer pillar cell, D1-D3: Deiters' cells 1,2, and 3. Adapted from (Rau, Legan et al. 1999). β-tectorin mRNA expressing cells are highlighted in dark gray.

Clusterin expression overlaps with the β-tectorin in some but not all cochlear regions across the sensory epithelium (Figure 3.38 and 3.39).

The first stripe of β-tectorin expression in the greater epithelial ridge coincides with the broader medial clusterin expression domain that extends more towards the internal sulcus edge. There seems to be some overlap of expression where β-tectorin mRNA is expressed adjacent to the inner hair cells and the border cells (Figure 3.39 multiple asterisks).

The second stripe of β-tectorin expression in inner and outer pillar cells is not coincident with any clusterin expression.

However, the final stripe of β-tectorin expression, corresponding to the third row of Deiters' cells, does appear to overlap with clusterin expression (Figure 3.39 single asterisks). Detailed comparative analysis using false painted and overlaid figures (Figure 3.40) shows that this narrow clusterin expression domain lies just adjacent to the β-tectorin domain, closer to the outer sulcus but not in Deiter's cells and probably not in Hensen's cells and thus confirming this with two independent markers.

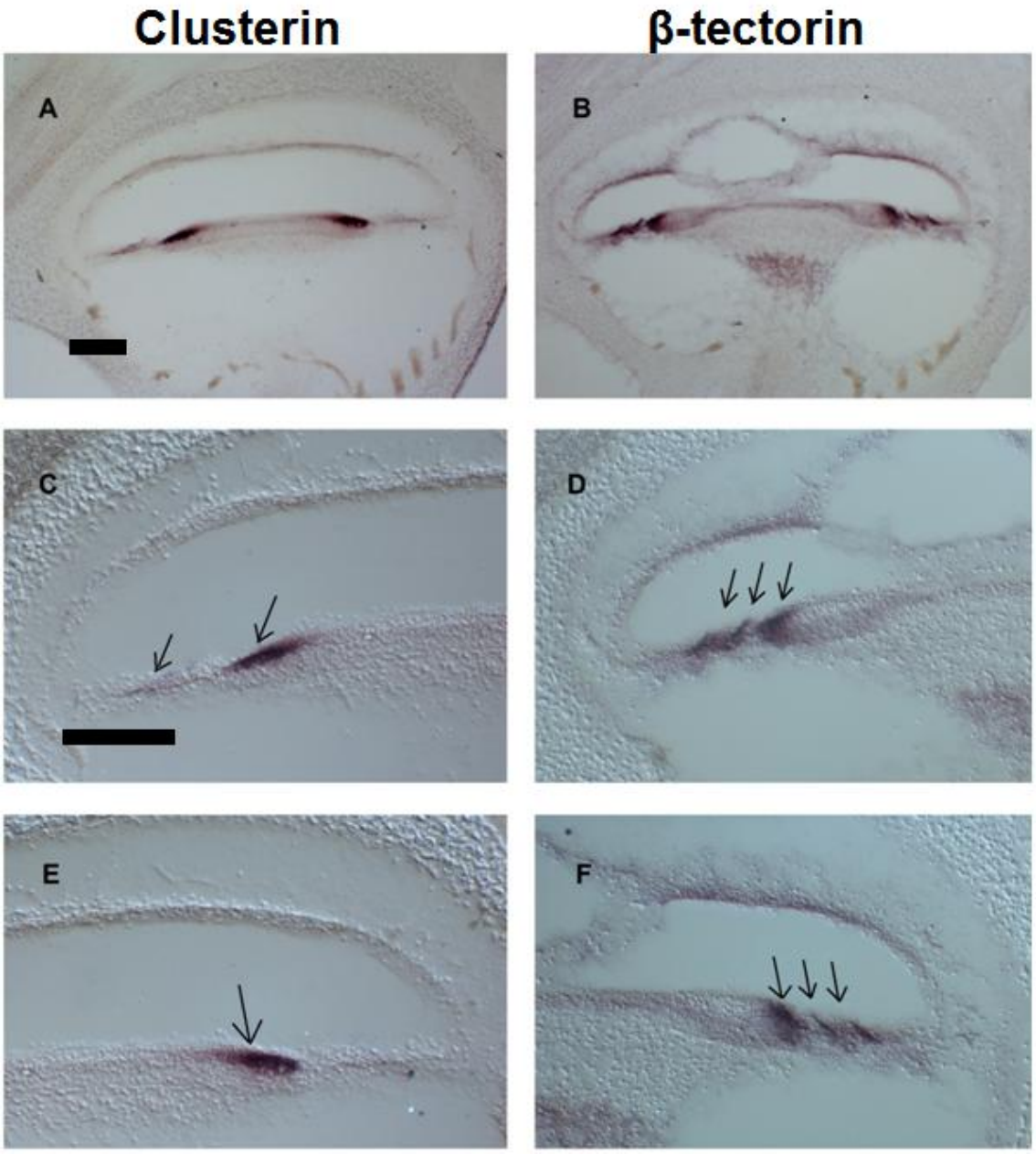


Figure 3.38 Comparison of clusterin and β-tectorin mRNA expression in the base of the cochlea at 18.5dpc. Overview of the expression of clusterin and β-tectorin respectively using cross sections through the base of the cochlea (A and B)**.** Higher magnification of cochlea parts in A (C and D). Higher magnification of cochlea parts in B (D and F). Arrows point to areas of specific labelling of each expression domain for each gene. Scale bars: 100μm.

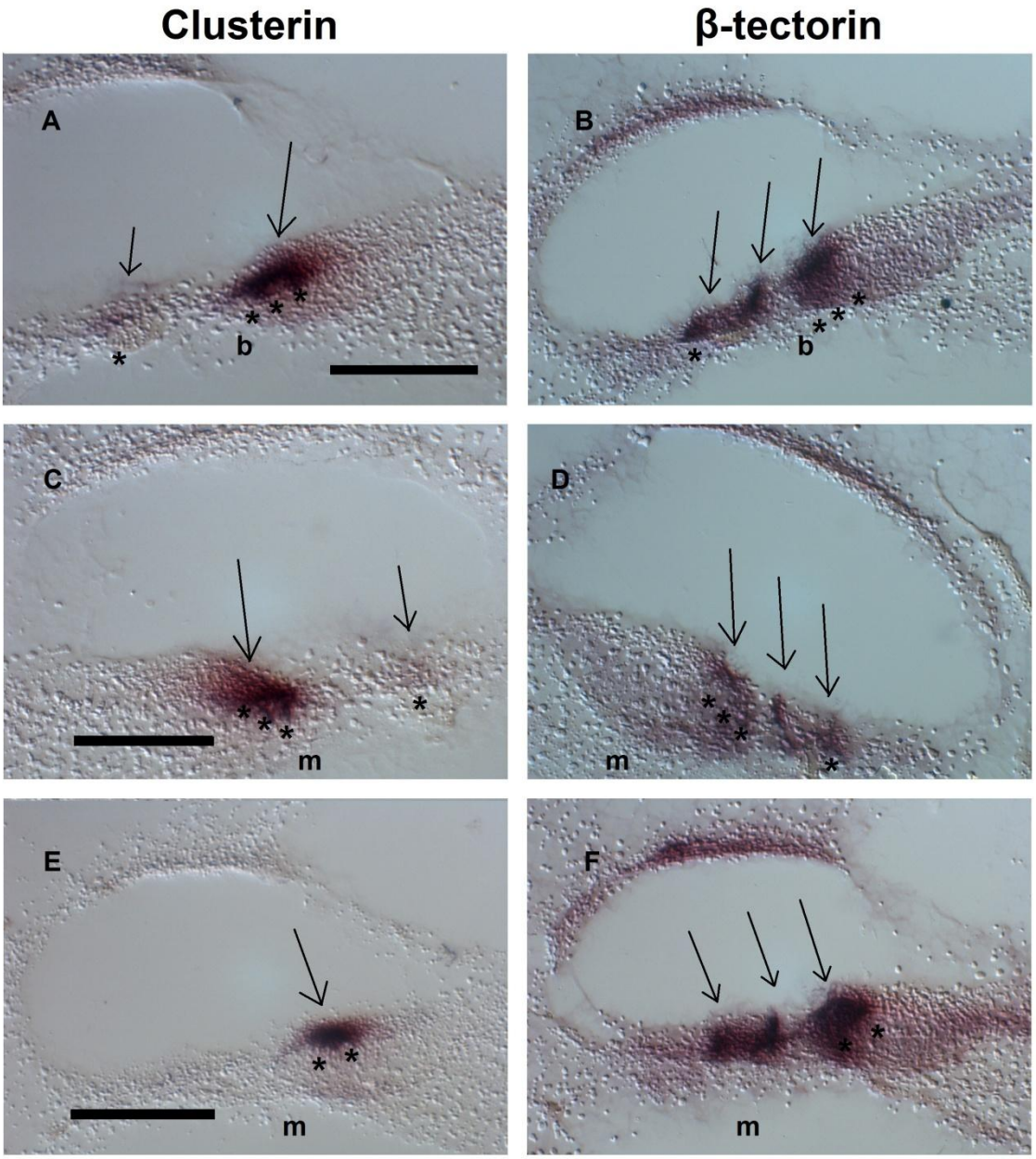


Figure 3.39 Comparison of clusterin and β-tectorin mRNA expression in the basal and middle turns of the cochlea at 18.5dpc. A and B: basal turns. C-F: medial turns. The area of overlap for clusterin and β-tectorin at the greater epithelial ridge is marked with multiple asterisks and clearly clusterin expression extends beyond this overlap towards the internal sulcus edge. The area of overlap for clusterin and β-tectorin at the lesser epithelial ridge is marked with a single star. b: base and m: middle**.** Arrows point to specific labelling patterns. Scale bars: 100μm.

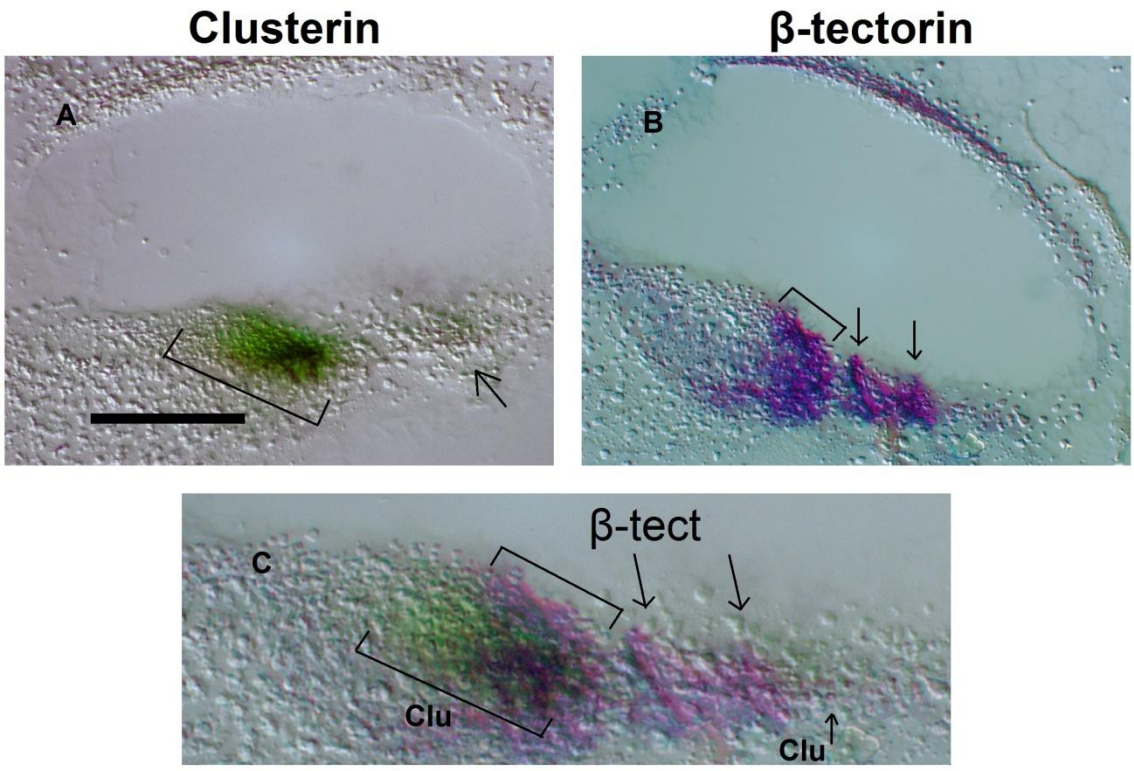


Figure 3.40 Comparison of clusterin mRNA expression with β-tectorin by false painting and overlaying the alternate sections at 18.5dpc. Clusterin and β-tectorin mRNA expression in the basal turns of cochlea respectively (A and B). The overlaid sections of clusterin and β-tectorin for comparison (C). Scale bar: 100μm.

### 3.2.4 Comparative localisation of clusterin protein in the developing inner ear with supporting cell and hair cell protein markers

To better understand the cellular localisation of the clusterin protein and determine which cell types of the developing sensory cochlea contain clusterin protein, sections were analysed for expression of hair cell and supporting cell markers. Myosin VIIA and Prox1 antibodies (both gifts from Prof Guy Richardson, University of Sussex) were used for the detection of hair cells and supporting cells respectively.

#### 3.2.4.1 Comparative analysis of Myosin VIIA and clusterin protein localisation

The expression of clusterin protein was compared to Myosin VIIA protein expression on alternate mouse head sections at 17.5dpc. The heat-mediated antigen retrieval was carried out on wax sections using Citrate buffer pH 6.0 (Appendix IV) followed by the

detection of Myosin VIIA using rabbit anti mouse primary antibody (from Abcam) at 1/100 dilution and goat anti rabbit fluorescent-conjugated secondary antibody (goat anti rabbit Alexa fluor 488) at 1/500 dilutions.

Myosin VIIA mRNA, one of the earliest known hair cell specific markers begins to be expressed at the base of the cochlea at E15 (14.5dpc) (Bermingham-McDonogh, Oesterle et al. 2006) and Myo VIIIA protein can be first detected at E16 (15.5dpc) when the differentiating sensory hair cells become morphologically recognizable (Chen and Segil 1999). The expression of clusterin seems to overlap greatly with the expression of Myosin VIIA protein in cochlear sensory epithelium in the basal, middle and apical turns (Figure 3.41 compare clusterin sections of C,E and G with B,D and F for Myosin VIIA). For a better comparison these sections were overlaid and it was further confirmed that clusterin expression overlaps greatly with Myosin VIIA as well as in adjacent supporting cells (Figure 3.42). At 15.5dpc and 17.5dpc when cochlear hair cells are differentiating, clusterin mRNA expression was detected as two distinct regions of expression with the wider region being located at the greater epithelial ridge and the narrower one at the lesser epithelial ridge. Both of these domains of mRNA expression were positioned away from the developing organ of Corti where hair cells are differentiating. However the overlap of clusterin and Myosin VIIA protein expression in hair cells in some parts of the cochlea is an interesting and unexpected finding.

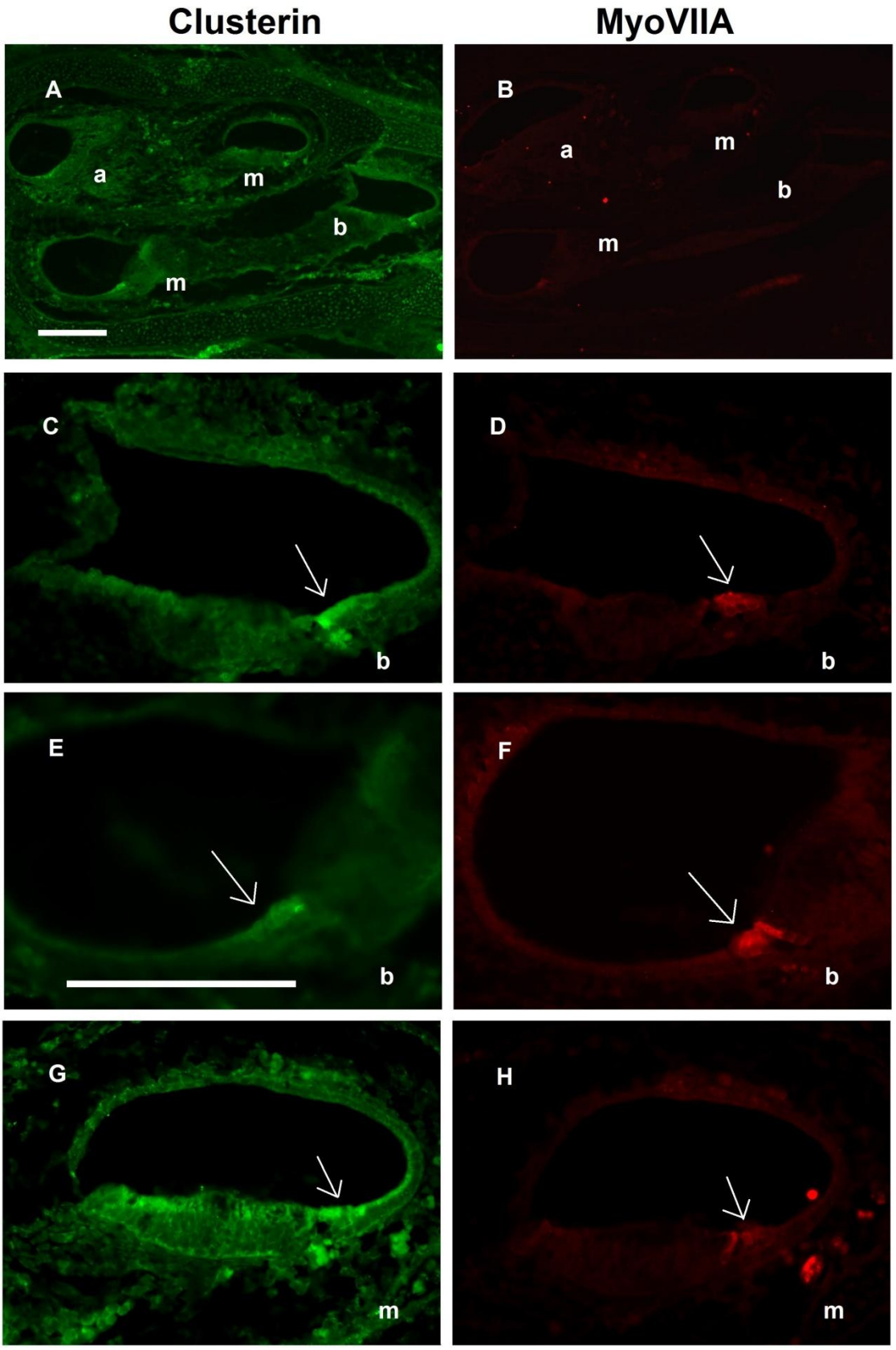


Figure 3.41 Comparison of clusterin and Myosin VIIA protein expression in the mouse cochlea sections at 17.5dpc. A and B: Overview of cochlea sections demonstrating all the three cochlea profiles for clusterin and Myosin VIIA respectively, C and D basal turns, E and F middle turns and, G and H middle turns for clusterin and Myosin VIIA respectively. Arrows point to the areas of overlap. a: apical turn, b: basal turn, m: medial turn. Scale bars: 150μm.

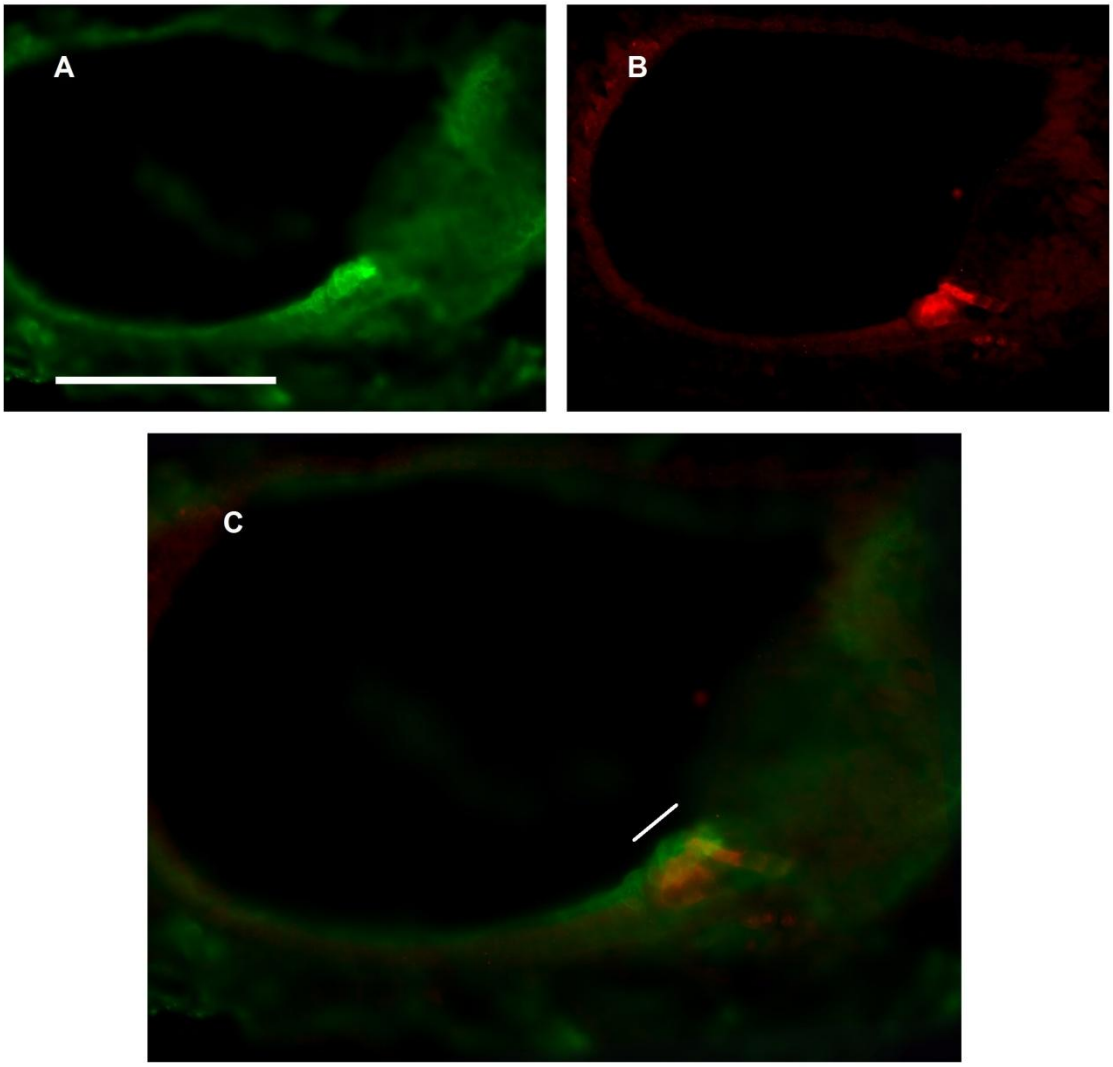


Figure 3.42 Comparison of clusterin (A) and Myosin VIIA (B) protein expression by overlaying the sections (C). The area of overlap between clusterin and Myo VIIA is marked with a line in C. Scale bar: 150μm.

### 3.2.4.2 Comparative analysis of Prox1 and clusterin expression in the inner ear

Clusterin protein expression was also compared to Prox1 protein localisation at 18.5dpc. The heat-mediated antigen retrieval was carried out on wax sections as described (2.3.12) and Prox1 rabbit anti mouse primary antibody (Chemicon at 1/1000 dilution) was incubated followed by goat anti rabbit fluorescent-conjugated secondary antibody (goat anti rabbit Alexa fluor 488) at 1/500 dilution. No immunoreactivity was found with the Prox1 antibody. Therefore the immunohistochemistry was repeated but using the antibody against cryosections of 18.5dpc (2.3.1.4).

Prox1 is a transcription factor and its protein expression is first detected in the base of the cochlea sensory epithelium at E14.5. The expression then spreads to apex and becomes restricted to the supporting cells – in particular Deiter's cells and pillar cells.

Clusterin immunoreactivity in the lesser epithelial ridge seems to overlap with Prox1 in the basal (Figure 3.43 compare A with B) and middle turns (Figure 3.43 compare C,E with D,F).

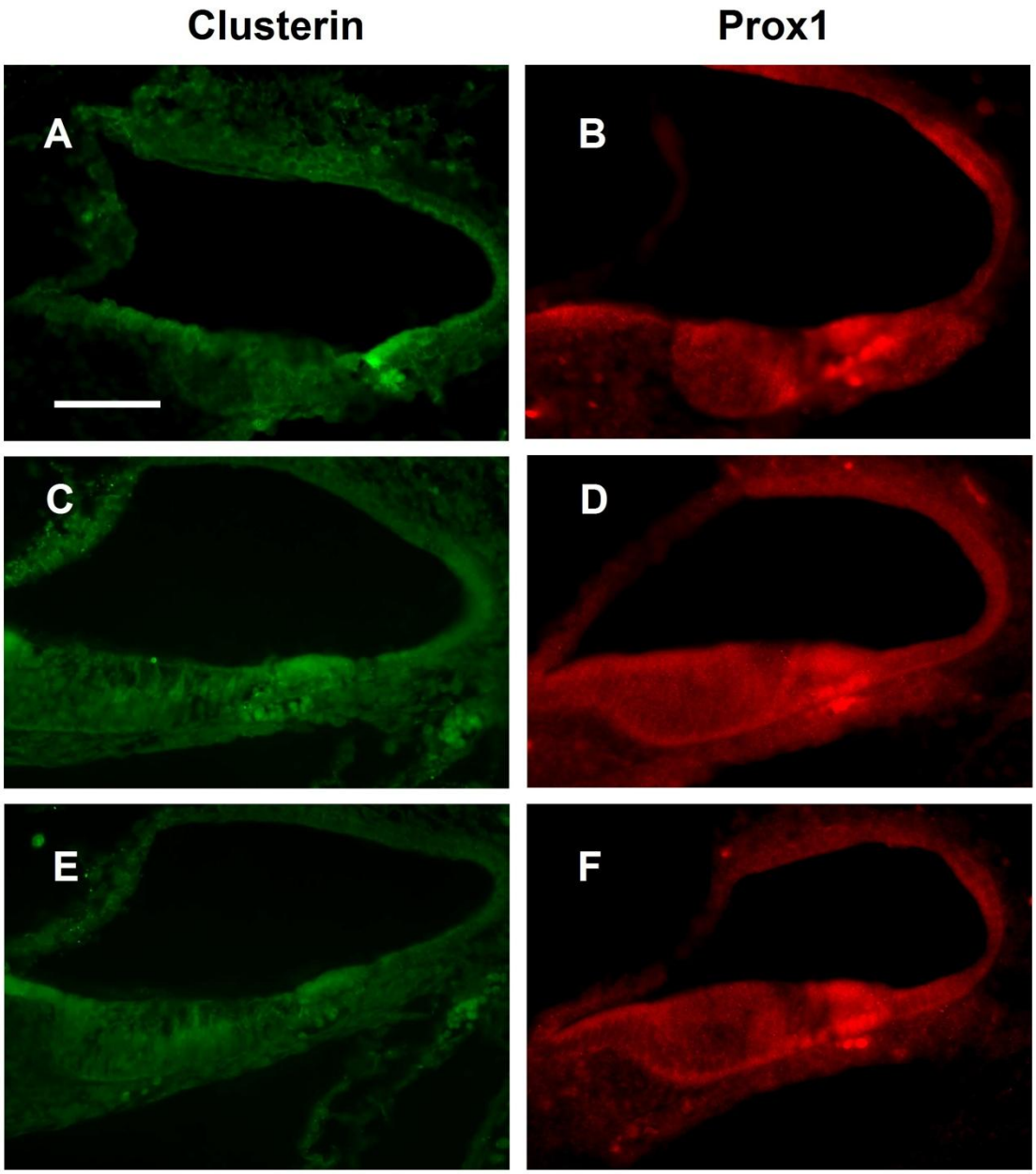


Figure 3.43 Comparison of clusterin and Prox1 protein expression in the mouse cochlea sections at 18.5dpc. A and B: basal turns, C, E and F middle turns for clusterin and, D and F middle turns for Prox1. Scale bar: 100μm.

Considering that clusterin also overlaps with regions of Myosin VIIA expression, this suggests that clusterin protein expression in the lesser epithelial ridge maps to an area between pillar cells and up to the Deiter's cells. As clusterin immunoreactivity in the greater epithelial ridge has no corresponding region for Prox1, it is not possible to comment on the exact identity of cells of this region.

The different tissue fixations required between antibodies precluded the possibility of overlaying consecutive sections. However instead, an approximation was made by selecting similar looking sections from separate experiments, and these data are thus more approximate. Nevertheless, when overlaying similar clusterin and Prox1 sections for comparison, expression partly overlaps with Prox1 (Figure 3.44). When partly overlaps, clusterin seems to extend towards the lateral side probably labelling the supporting cells next to the Deiter's cells e.g Claudius cells.

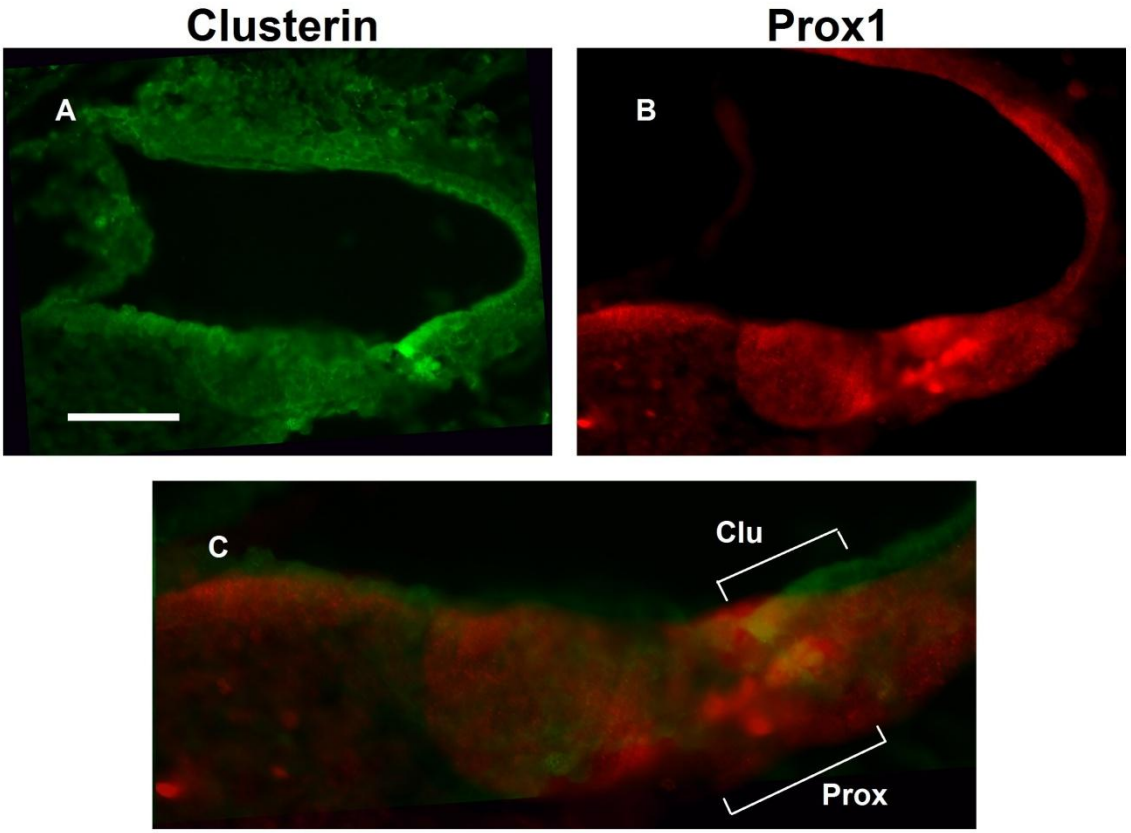


Figure 3.44 Comparison of clusterin (A) and Prox1 (B) protein expression by overlaying the sections (C). Scale bar: 100μm.

## 3.3 Discussion

Clusterin mRNA expression is initiated at 12.5dpc and by 13.5dpc extends across the whole length of cochlear epithelium. However, during further development, expression is downregulated in the central region of the cochlea sensory epithelium, leaving two domains of mRNA expression, in the greater epithelial ridge and a minor lateral domain extending into the lateral wall towards the stria vascularis (Figure 3.45). mRNA is always absent from the vestibular epithelium throughout development. Clusterin protein expression, curiously, is found surrounding the sensory epithelium, in the (nonsensory) developing Reissner's membrane and in periotic mesenchyme inside the developing capsule. Attempts were made to localise the exact cellular context of clusterin expression (protein and mRNA) in the cochlear sensory epithelium.

### 3.3.1 Clusterin mRNA localisation in the inner ear

Comparison of clusterin expression at 15.5dpc and 17.5dpc for α-tectorin and at 18.5dpc for the same comparative domains of β-tectorin provided further information with regards to the cells that express clusterin.

At both 15.5dpc and 17.5dpc two stripes of expression for both clusterin and α-tectorin are expected (1) a wider stripe in the greater epithelial ridge and (2) a narrower stripe of expression at the lesser epithelial ridge and towards the strial edge. These are illustrated in Figure 3.46.

GER expression: This stripe of expression seems to extend more towards the strial edge for α-tectorin. Therefore clusterin may be present in fewer cells in the greater epithelial ridge than α-tectorin (bigger arrows in Figure 3.35 E and F).

LER expression: This narrow stripe of clusterin expression is however wider and located further from the Hensen's cells compared to cells labelled by the α-tectorin riboprobe (Figure 3.35 compare A with B). Clusterin seems to label the neighbouring cells of Hensen's cells probably outer sulcus (which includes Claudius cells), spiral prominence and stria vascularis cells.

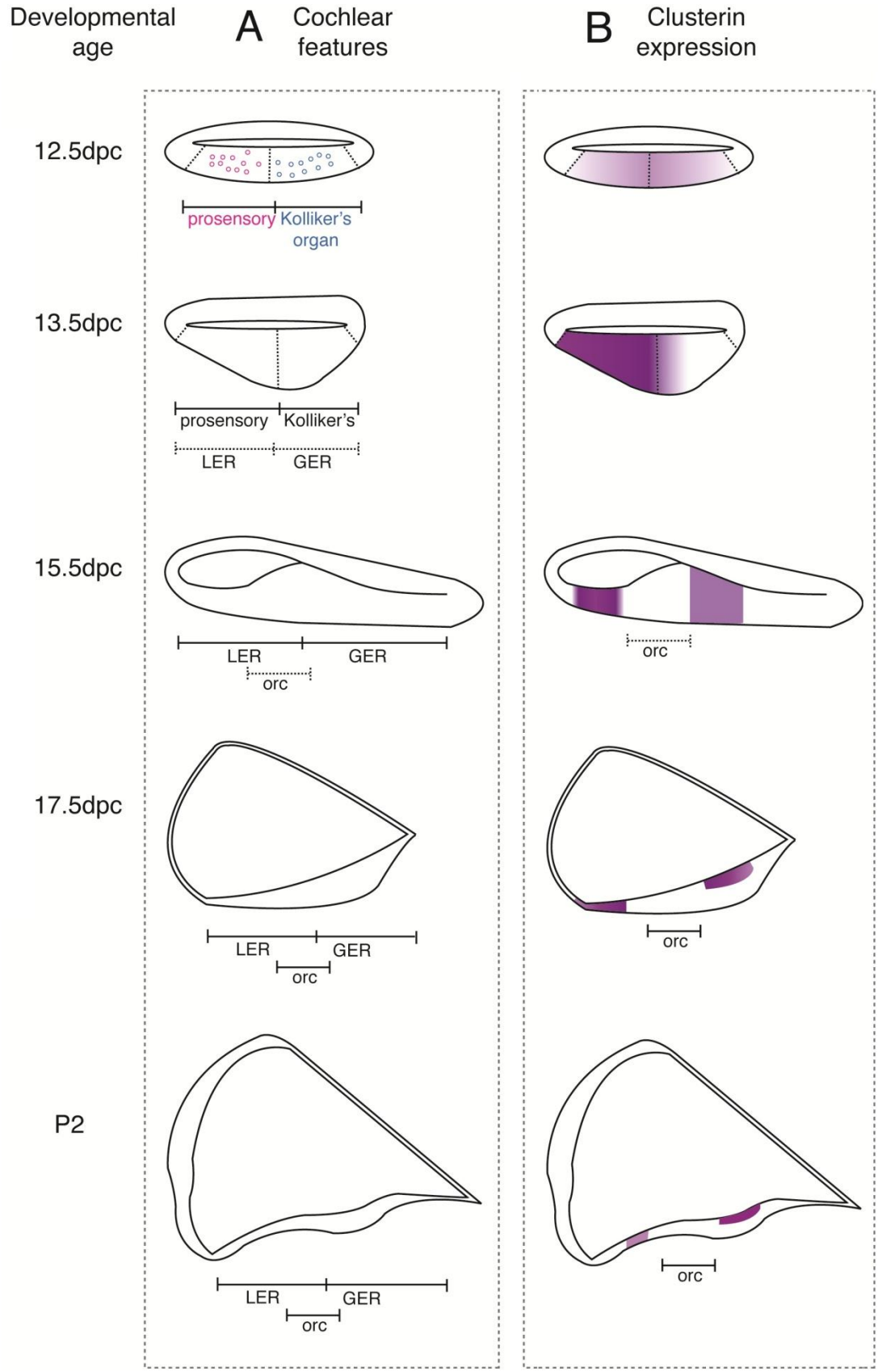


Figure 3.45 Summary of clusterin mRNA expression during the mouse inner ear development. **A**: Illustrates the features of developing cochlea epithelium from 12.5dpc to P2. **B:** Illustrates the pattern of clusterin mRNA expression in the developing cochlea from 12.5dpc to P2. Kollikers: Kolliker's organ, LER: lesser epithelial ridge, GER: greater epithelial ridge, orc: organ of Corti.

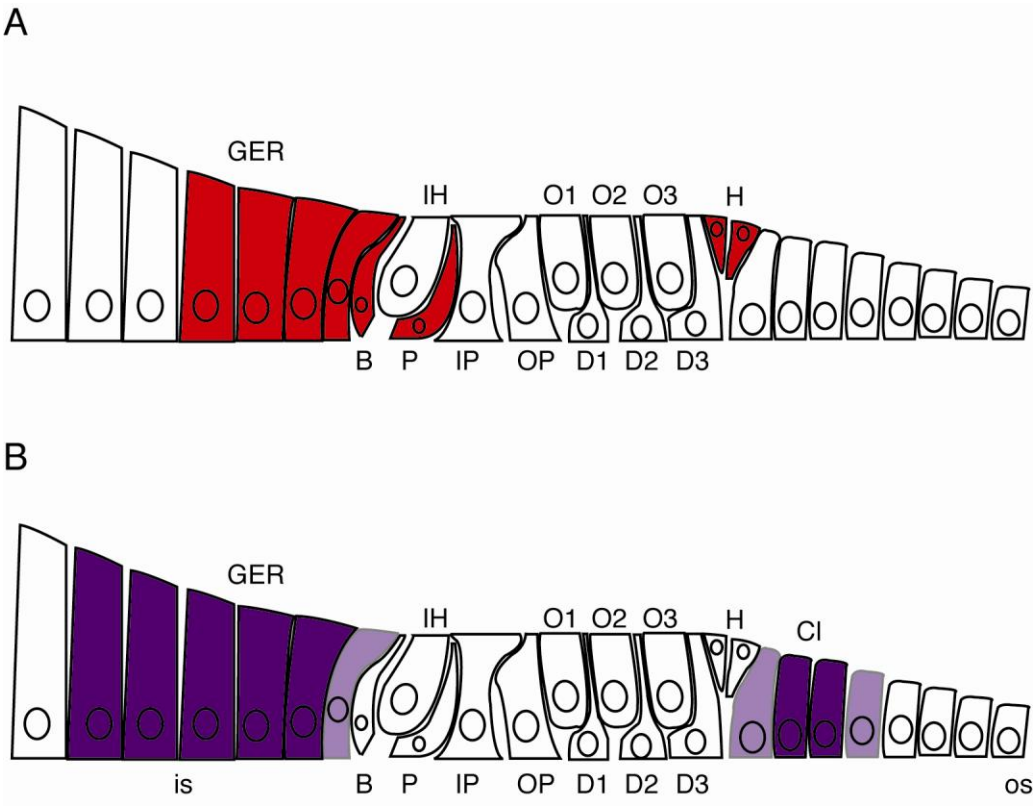


Figure 3.46 Comparative summary of clusterin and α-tectorin expression. Cellular details of early postnatal sensory epithelium, (A) early postnatal α-tectorin expression (Rau, Legan et al. 1999) (B) clusterin expression just prior to birth (17.5dpc). Lighter purple corresponds to lower levels of expression.

β-tectorin expression identified three cellular regions in the sensory epithelium of the mature cochlea; (1) cells that lie adjacent to the inner hair cells including the border cell, (2) the pillar cells and (3) the outer Dieter's cells.

Clusterin expression in the greater epithelial ridge overlaps with β-tectorin to a great extent, however clusterin extends further towards the internal sulcus but less towards the medial side (Multiple asterisks in Figure 3.38). Clusterin expression therefore appears to be absent from the border cells (Figure 3.47).

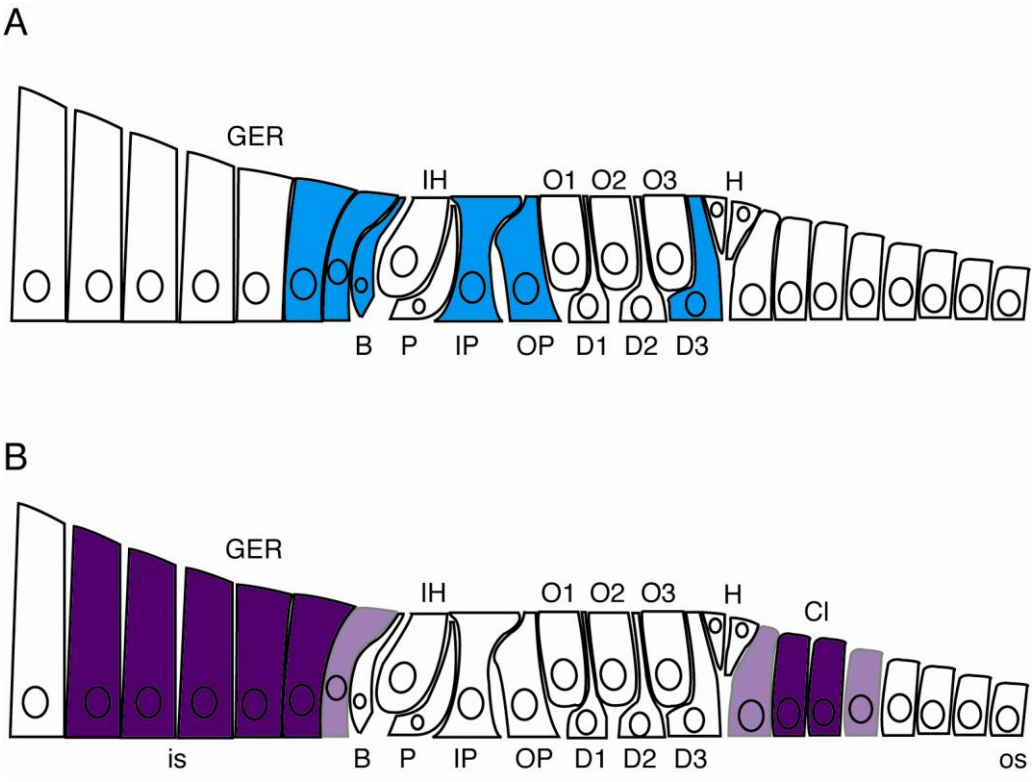


Figure 3.47 Comparative summary of clusterin and β-tectorin expression. Cellular details of early postnatal sensory epithelium, (A) early postnatal β-tectorin expression (Rau, Legan et al. 1999) (B) clusterin expression just prior to birth (18.5dpc). Lighter purple corresponds to lower levels of expression.

The second stripe of β-tectorin expression does not label with the clusterin riboprobe, confirming the absence of clusterin from inner and outer pillar cells (Figure 3.47).

The third stripe of β-tectorin labels the third row of Deiters' cells, and whilst the lateral clusterin domain is located close, it does not overlap with it (Single asterisks in Figure 3.38). This narrow strip of clusterin expression is located closer to the outer sulcus but not in Deiter's cells and probably not in the Hensen's cells as well (Figure 3.47). BMP4 which is a marker for Hensen's and claudius' cells of the outer sulcus could also have been used in alternate sections with clusterin to further localise clusterin expression in this region. Alternatively, clusterin, α-tectorin and β-tectorin expression can be studied and compared using three alternate sections.

In summary the data from the clusterin *in situ* hybridisation experiments and the comparison of its expression with α and β-tectorin suggests that the two stripes of clusterin mRNA expression detected between 15.5dpc to 17.5dpc corresponds to the inner sulcus for the wide stripe in greater epithelia ridge domain of expression and the

outer sulcus (Claudius cells) and, possibly, spiral prominence for the narrower domain of expression localised in the lesser epithelia ridge.

### 3.3.2 Correlation of expression with ongoing cellular processes in the developing inner ear

The study of clusterin mRNA expression during development of the mouse inner ear provides some novel insight into the potential roles it may play. At 11.5dpc the cochlea analge that has already emerged from the otocyst is expanding ventrally. At this stage, the progenitor cells in the presumptive organ of Corti that will eventually give rise to hair cells and supporting cells are still dividing and have not exited the cell cycle. Clusterin is not yet expressed at this stage in the developing auditory or vestibular system. This suggests that clusterin does not play an obvious role in the early cell proliferation in the inner ear.

However, the cells of the primordial organ of Corti located in the prosensory region begin their exit from the cell cycle at 11.5dpc onwards (Ruben 1967), and whilst this process can go on until 15.5dpc, more than 80% of these cells exit the cell cycle between 12.5–13.5dpc (Ruben 1967). Clusterin mRNA expression is initiated across the entire cochlear sensory epithelium at this stage (12.5dpc), and this region appears to roughly coincide with the cell cycle exit of many of the progenitor cells of the cochlea sensory epithelium, although levels of expression are not high.

One day later, at 13.5dpc, a robust and dramatic upregulation of clusterin mRNA expression in the developing cochlea sensory epithelium was detected. This strong clusterin mRNA expression again coincides with the cell cycle exit of most of the progenitor cells, and occurs just before the onset of terminal differentiation of cells that will give rise to either prosensory hair cells or supporting cells of the organ of Corti. At 14.5dpc from the mid-basal region of the cochlea, a gradient of differentiation that radiates in both directions begins. The differentiation of postmitotic progenitor cells of the organ of Corti turns leads to the development of the specialised sensory hair cells and their associated supporting cells. The strong clusterin mRNA expression observed

in the cochlea sensory epithelium at this stage therefore, may be related to cell cycle exit and onset of terminal differentiation of the cells in this organ.

At 13.5dpc the expression is in entire length, width and thickness of the cochlea in the base and in the mid turns in the prosensory domain from where the inner and outer hair cells and some of the supporting cells develop. Clusterin expression in the hair cell precursors therefore is suggestive of a role for clusterin in development and differentiation of hair cells.

In the middle turns of the cochlea, clusterin expression become more localised to the prosensory domain (Figure 3.48). Similar to $p27^{Kip1}$ protein localisation, clusterin mRNA is expressed very early in cells that will likely end up in the organ of Corti and at a time when the progenitors of hair cells and supporting cells are exiting the cell cycle. This finding once more suggests that similar to $p27^{Kip1}$, clusterin may have a role in inhibiting the cell cycle progression of cells of primordial organ of Corti. However, clusterin expression is absent from the cells of vestibular sensory organ during their exit from the cell cycle that takes place from E14 to postnatal day 3 (P3) (Ruben 1967). This also argues against a generic role in hair cell terminal differentiation in the inner ear if the same mechanisms are recruited. Although p27kip expression is in both developing vestibular and cochlear epithelia, the expression is lower in the vestibular epithelia and does not precisely correlate with cessation of cell division in this organ (Chen and Segil 1999).

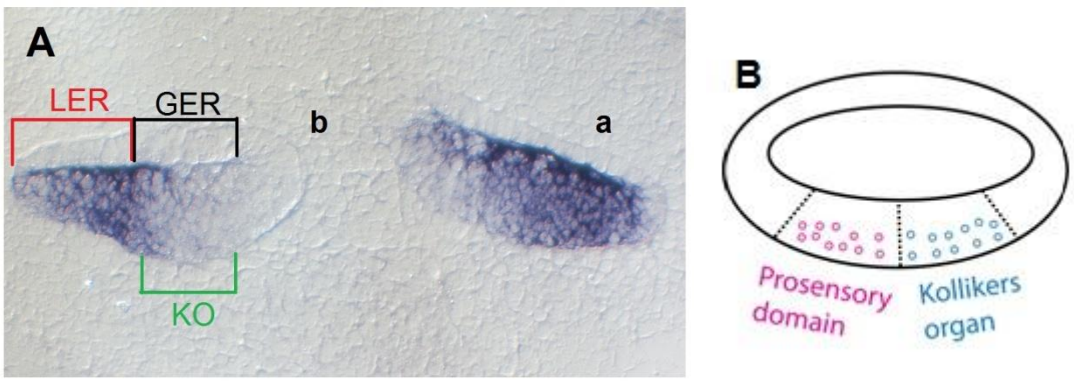


Figure 3.48 A: Clusterin expression is localised to the prosensory domain in the middle turns of the cochlea at 13.5dpc. B: Schematic representation of the developing cochlea epithelium at 13.5dpc. a: apex, b: base, GER: greater epithelial ridge, LER: lesser epithelial ridge, KO: Kolliker's organ.

Another argument against a role for clusterin as a general growth inhibitor/cell cycle progression inhibitor is that it's expression along the cochlea does not follow the apex to base pattern of cell cycle exit (Ruben 1967).

Clusterin is expressed the full length of the cochlea, however the details of expression varies. Whereas at apical and basal regions expression is across the entire width of epithelium, in mid-cochlear regions expression begins to become restricted (Figure 3.5 compare A with B). This change of expression in clusterin expression may be related to the onset of differentiation in the mid-basal region of the cochlea which takes place a day later at 14.5dpc. This is similar to the wave of differentiation (Ruben 1967) and therefore consistent with a role in, or associated with, this event.

The downregulation of expression in the sensory epithelium in mid cochlear turns was found to presage downregulation along the entire cochlear length when 15.5dpc sections were analysed. Two regions of expression result following the initial onset of clusterin downregulation, where a central region, corresponding to the presumptive developing organ of Corti, is first downregulated (Figure 3.6 J-L). Clusterin expression, therefore, demonstrates very dynamic expression between 13.5 and 15.5dpc. The initial expression of clusterin in prosensory cells that will eventually form the organ of Corti is downregulated in this organ some two days later and instead is detected in the cells surrounding this organ. At this stage the progenitor cells of organ of Corti that are post mitotic begin differentiating into hair cells and supporting cells. Differentiation starts at 14.5dpc and will continue for a few days until differentiation is complete at 17.5dpc (Lee, Liu et al. 2006).

Therefore, downregulation of clusterin in the developing organ of Corti coincides with the onset of differentiation of cells in this organ. Although clusterin expression at this stage suggests its association with the differentiation of prosensory cells (hair cells and supporting cells), its downregulation at the site where hair cells are differentiating may suggest a role for clusterin in the development of cells other than hair cells such as supporting cells. Clusterin may also have an inhibitory role in differentiation of the organ of Corti and therefore its inhibition maybe required to permit differentiation to occur. Another possibility is that clusterin may inhibit the cells neighbouring the organ

of Corti from adopting a hair cell fate by inhibiting their differentiation and this would require further studies to explore.

However arguing against a role for clusterin in differentiation, is that clusterin expression was detected outside the time frame or location of differentiation in the sensoy epithelium as well; for instance, clusterin expression persists at P2 when the differentiation in the organ of Corti has already ceased, and between 15.5dpc – P2 clusterin is expressed in non-differentiating cells.

Considering the association of clusterin with apoptosis, particularly during development and involution (Tenniswood, Guenette et al. 1992; Ahuja, Tenniswood et al. 1994; Witte, Aronow et al. 1994; Brown, Moulton et al. 1996; French, Soriano et al. 1996; Min, Jeong et al. 1998) clusterin expression could be related to the apoptosis taking place in inner ear and may mark the areas of surviving cells in areas of active cell death. Indeed TUNEL labelled cells have been detected in the precursor of cochlea duct sensory epithelium in rat between 11.5-15.5dpc (Nikolic, Jarlebark et al. 2000). The onset of clusterin expression coincides roughly with the appearance of these hot spots of cell death in the cochlea epithelium; however clusterin expression extends well beyond 15.5dpc. Furthermore, clusterin expression was not detected in vestibular system which also goes through programmed cell death during its development, so if a role in apoptosis, it would be organ-specific.

The innervation of the cochlear and vestibular epithelia is reported to happen simultaneously with their differentiation, Using tubulin immunostaining, it has been shown that cochlea epithelium in mice first receives a nerve supply from the vestibuloacoustic ganglion at E14 (Nishikori, Hatta et al. 1999) which is coupled with the observation of apoptotic cells in the cochlear epithelium and within migrating cells found in the vestibuloacoustic ganglion. In the vestibular division of the inner ear, this event takes place from E10.5 onwards. At these sites of innervation, some changes in the epithelium was reported such as the disappearance of the basement membrane, the differentiation of luminal cells and the presence of apoptotic cells at the basal side of innervating epithelium (Nishikori, Hatta et al. 1999).

Thus the upregulation of clusterin at 13.5dpc coincides with the cochlea epithelium receiving the first nerve supplies from the vestibuloacoustic ganglion. Clusterin expression at this stage may be related to the events that take place during the innervation, particularly differentiation and cell death. Apoptotic cells are also observed in the greater epithelial ridge during the first postnatal week that is related to synaptogenesis of auditory nerve fibers (Nishikori, Hatta et al. 1999). This is also in line with the observation of continued clusterin expression at postnatal day 2 (P2). However, clusterin is not expressed in the vestibular organ that also undergoes innervation, although it cannot be ruled out that it plays an auditory-specific role. Furthermore, with clusterin not being detected in the migrating vestibuloacoustic ganglion (an area with apoptotic hot spots at 13.5dpc), it seems unlikely that clusterin expression at this stage is related to apoptosis involved in innervating the cochlear sensory epithelium.

Unlike 13.5 and 15.5dpc, the expression of clusterin at 17.5dpc-P2 does not seem to cover the entire depth of the cochlea sensory epithelium. However expression does appear to become more apically localised.

The persistence of clusterin expression in mature supporting cells at postnatal stage P2 may demonstrate a role for clusterin in maintenance of quiescence in this tissue and may even contribute to the inability of this tissue to regenerate. However, there are other non-clusterin expressing cells that are also in this state. Furthermore, this quiescent role is unlikely since clusterin is no longer present after the onset of hearing since, at postnatal day 17 and 18 clusterin, expression was no longer detected in the inner ear. The absence of clusterin in adult inner ear may support clusterin association with cell death as adult cochlea cells are at postmitotic states and under normal conditions do not go through apoptosis.

### 3.3.3 Clusterin protein localisation in the inner ear

In order to detect clusterin protein two different antibodies were tried but immunoreactivity in the inner ear was only clearly detected by one. It is not quite clear why, but this could be related to the presence of an inner ear specific isoform that is not

recognised by this antibody. However RT-PCR has shown that isoforms including the peptide region raised for this first antibody are generated in the inner ear (Figure 3.19). Alternatively the clusterin peptide could be at different stages of maturation and/or present in different subcellular locations. The most probable explanation however may lie with the divergence of sequence of the mouse/human from the sequence recogniseable by the antibody as was argued before (3.2.2.1 and Table 3.1).

A curious bipartite pattern of clusterin protein expression was observed, as bright cellular/acellular immunoreactivity outside the epithelium, and lower levels in the epithelium itself.

(1) Non-sensory epithelial clusterin immunonoreactivity: clusterin protein seems to be expressed over a short period of time in the developing Reissner's epithelium, periotic mesenchyme and otic capsule. Simultaneous expression of clusterin in these regions maybe of some kind of importance. For instance, clusterin may be produced by the cells of Reissner's membrane and other epithlia and then secreted in the periotic mesenchyme and otic capsule to carry out some unknown function. In support of this, clusterin protein was detected in the Reissner's membrane a day earlier than the other two domains, and although clusterin immunoreactivity is spread throughout the entire periotic mesenchyme, it is more localised to around the developing Reissner's membrane. Furthermore, clusterin immunoreactivity was stronger in the Reissner's membrane. However, it is possible that clusterin is produced completely away from the inner ear and becomes translocated here. As outlined in the introduction, clusterin is present in all body fluids at different concentrations. Thus its expression in the periotic mesenchyme might be related to its expression in blood plasma.

The detection of clusterin protein expression in the developing Reissner's membrane was an unexpected finding. Although the expression in this region begins early, it is only transiently expressed and not detectable after 15.5dpc, at a stage when this membrane is still forming (Figure 3.49). Therefore, the expression of clusterin does not seem to be related to the morphogenesis of this membrane. It is possible that clusterin is related to the differentiation of Reissner's membrane. However, very little is known about the differentiation of this organ.

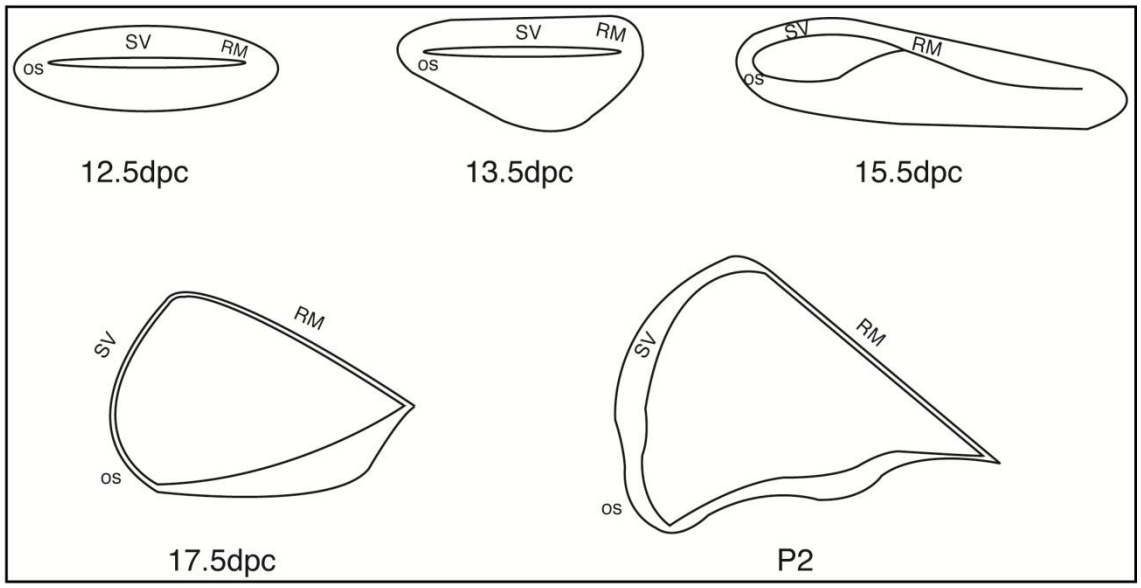


Figure 3.49 Cochlear development from 12.5dpc to P2. These developmental stages illustrate the morphogenesis of Reissner's membrane which is not complete yet at 17.5dpc when clusterin expression is absent. SV: stria vascularis, os: outer sulcus, RM: Reissner's membrane. Adapted from (Kim and Wangemann 2010)

The transient expression of clusterin protein (from 14.5-15.5dpc) in the developing otic capsule at the time of cartilage formation may illustrate clusterin involvement in capsule development. Reciprocal signals from the cochlear epithelium and surrounding mesenchyme is required for the correct formation of the otic capsule. Cartilage formation is initiated around 13.5dpc, and cartilage is present throughout the capsule at 15.5dpc (Ficker, Powles et al. 2004). This further supports the secretory pathway of clusterin from Reissner's membrane or from the cochlear sensory epithelium into the Reissner's membrane and then into the mesenchyme and otic capsule. Clusterin may play a role in condensing mesenchyme and the chondrogenesis process. However it will require specific experiments to resolve all of these issues, as well as to explain the origin of extracellular clusterin, as it is by no means certain that this originates from inner ear epithelium.

The immunoreactivity detected in non-sensory epithelial cells (presumptive Reissner's membrane), in periotic mesenchyme and otic capsule mesenchyme, does not overlap with the mRNA expression detected by *in situ* hybridisation. The discrepancy in the data at the mRNA and protein levels could be due to the mRNA riboprobes not being able to detect the clusterin transcript isoform produced in these cells, ie. an isoform that

lacks the sequences (end of exon7 to mid exon9, Figure 3.20) recognisable by the probe. As previously shown (Figure 3.20) a number of isoforms that lack C-terminal sequences are identified in the genome browser. However these have not been thoroughly validated beyond random sequencing of cDNA libraries, and could simply reflect artefacts of cloning and/or sequencing procedures. Indeed the absence of clear ORFs and 3'UTR regions would suggest if such isoforms do exist, they are unlikely to generate functional clusterin protein, and any functional role, would require fundamentally different interactions.

(2) Sensory epithelial clusterin immunoreactivity: a lower level of clusterin expression was also detected in the cochlear sensory epithelium. These regions roughly correspond to the mRNA locations in the greater and lesser epithelial ridge (Figure 3.27 C). The comparison of clusterin expression with Myosin VIIA and Prox1 protein markers demonstrated some surprising results as there seemed to be some overlap between the clusterin immunoreactivity in the lesser epithelial ridge with both markers.

The lower level of immunoreactivity in the sensory epithelia in comparison to the nonsensory epithelial cells could be due to the presence of a different form of clusterin protein in the non-sensory and sensory epithelia cells, either a different isoform or the same major isoform that has been processed differently leading to differences in availabity of the antigenic sites. Although the structural detail of the nuclear form of the clusterin is still unknown, based on the available information, both protein isoforms (produced as a result of alternative transcription initiation site or by alternative splicing, in which exon 2 is spliced out), share the region that is recognisable by the antibody (ag2889, Proteintech). Therefore, the antibody may detect both the nuclear form in the cochlear epithelium and the secretory form in the extra-sensory epithelial regions but with different affinity.

The overlap between clusterin and Myosin VIIA immunostaining was an unexpected finding, as at this stage when the hair cells are differentiating, clusterin mRNA showed downregulation in some of these cells. Therefore, the presence of clusterin protein in these cells might suggest that clusterin mRNA is expressed in supporting cells outside the organ of Corti but the protein is transported or secreted into the adjacent hair cells to

support their differentiation and/or morphogenesis in the cochlear epithelium, or perform some other undefined role.

The presence of clusterin in Prox1 expressing cells may again indicate a role for clusterin in the development and differentiation of organ of Corti and/or may be prepared here for translocation elsewhere – possibly the neighbouring hair cells or into the periotic mesenchyme.

Clusterin immunoreactivity in the greater epithelial ridge however was further away from the Myosin VIIA or Prox1 expressing cells and therefore it is not possible to make any detailed comment on the identity of the cellular localisation of the protein in this region.

### 3.3.4 Relationship between clusterin protein expression in sensory and non-sensory epithelia

Clusterin mRNA has previously been reported to be expressed in differentiating epithelial cells in various parts of the body such as the developing skin, eye, kidney, vibrissae, as well as in ventricular cavities of the brain and liver (French, Chonn et al. 1993). Given that the clusterin mRNA is also expressed in cochlear epithelium, it is perhaps not surprising to detect clusterin protein in the epithelial cells of the inner ear. However, there remain two questions as to what is the functional significance of the transient protein expression in the non-sensory regions and how this expression relates to the expression detected in the sensory epithelium. As mentioned before, one possible explanation could be that clusterin protein is made and processed in the cochlea sensory epithelium and then is secreted in the periotic mesenchyme. Further investigation is necessary to find out the source of clusterin protein in the developing Reissner's membrane and to investigate if clusterin can be transported somehow from the sensory epithelium to this membrane, and then become secreted by these cells. However given that clusterin is not generally expressed throughout the different inner ear sensory epithelia, but is restricted to the cochlea and this suggests it may play an important role in the development of the hearing organ, the cochlea. Clearly the clusterin knockout mouse inner ear phenotype needs to be examined in detail to test whether the sense of

hearing is affected and if the morphology of Reissner's membrane epithelium is affected. Although researchers from different fields of clusterin biology have not mentioned the loss of balance in these mice, this would not be unexpected given the expression documented herein. As clusterin is not expressed in the vestibular system, defects in the development of this organ leading to loss of control and balance, is not expected. However, the hearing of the clusterin knockout mice needs to be tested to check if these mice are deaf. Recently the morphology of the cochlea in these mice were analysed by paint filling and gross cochlear morphology was reported to be normal (Monks and Morrow 2012). However, detailed analysis of sections is necessary to assess the development of the organ of Corti and other regions of the cochlea, especially Reissner's membrane.

The functional significance of clusterin expression in nonsensory regions is not clear but may be similar to the suggested cellular role of clusterin during development of sensory regions, one or more roles from cell cycle exit, differentiation, and/or apoptosis.

### 3.3.5 Expression and deducing possible function/s of clusterin

The detection of clusterin expression in the cochlear sensory epithelium at a time that cochlea is going under major morphogenetic changes as well as its upregulation at the time of hair cell differentiation suggests a role for clusterin in either the morphogenesis of the cochlea and/or the differentiation of the organ of Corti.

Clusterin expression has also been associated with cell death – particularly the nuclear form (nClu). Localised apoptotic cell spots has also been detected during the inner ear development. Clusterin protein and mRNA upregulation in the cochlea sensory epithelium at the time of cochlea innervation and differentiation could be related to the apoptotic role of clusterin. Clusterin might trigger apoptosis in these regions in order to assist with the removal of inappropriate cells or the ganglion cells that are not formed normally. However this would represent an unusual role since clusterin expression has been associated with cell survival – perhaps it helps fulfil this role here as well. Assuming a role for clusterin in triggering apoptosis, raises the question as to why clusterin is not expressed in the developing CVG itself which undergoes localised

apoptosis, and why the innervation of the vestibular epithelium is not accompanied with the expression of clusterin. Maybe its apoptotic role is epithelial and other factors perform a related function in the developing neurons. The other argument against an apoptotic role for clusterin during innervation would be the non-sensory expression areas of clusterin, assumed to be the secretory form. What is the point of isolated periotic mesenchyme cells surviving apoptosis where apoptosis has not been demonstrated? It is however possible that the sensory non- epithelial regions have a different clusterin source and different forms with distinct roles.

Another possibility is that clusterin functions as an extracellular chaperone in the ear. Generally, clusterin expression has been associated with the cellular stress response (heat shock response). Chaperones are responsible, for the detection and response to environmental changes such as oxidative stress, heavy metals, developmental processes, growth factor stimulation and pathological conditions such as infection and tissue damage. These changes give rise to the misfolding and aggregation of intracellular proteins and leads to a heat shock response that initiates the production of heat shock proteins (HSPs). These proteins repair the stressed proteins via chaperone and protease functions. Clusterin is hypothesized to be a HSP and its upregulation during the development of the inner ear therefore could indicate a role for clusterin as an extracellular chaperon assisting with the removal of the stressed proteins (partially unfolded) produced during the development. For instance, the disruption of the cochlear basement membrane during innervation may give rise to the production of stressed proteins and ultimately result in clusterin synthesis that functions as an extracellular chaperone to remove the stressed proteins. The detection of clusterin protein in this study and its receptor megalin in a separate study (1.7) in the Reissner's membrane further supports a role for clusterin as an extracellular chaperone that assists with clearance of stressed proteins via receptor-mediated endocytosis.

The secretory form of clusterin is believed to be cytoprotective. As discussed before, sClu expression is upregulated in regions undergoing apoptosis and injury. However, it is not detectable in the dying cells, but instead in the surrounding cells that are going to survive (1.11). Clusterin has a protective role in the surviving cells by assisting with the clearance of debris from dying cells. Clusterin has also been suggested to clear lipid-based tissue debris during tissue remodelling. This may explain the downregulation of

clusterin mRNA from the differentiating hair cells of the organ of Corti and its strong expression in the neighbouring cells. Therefore, clusterin protein might be synthesised in the neighbouring cells of organ of Corti and then secreted into the differentiating cells of organ of Corti to remove any un-needed cells, cell debris and misfolded proteins, and therefore protect these neighbouring cells. This hypothesis is further supported by the observation of overlaps between the MyoVII A expressing cells and those that express clusterin protein. This however neither explain the presence of clusterin immunoreactivity in other inner ear regions, particularly the non-sensory regions, nor explain why this role of clusterin is only restricted to the cochlear sensory epithelium and not the other sensory regions of the inner ear.

# 4. Results: Recombineering of a clusterin bacterial artificial chromosome for regulatory studies in vivo

## 4.1 Introduction and aims

There are different approaches for studying gene regulation and screening for enhancer activity. Computational and bioinformatic analystical tools such as evolutionary conserved region (ECR) browser (Ovcharenko, Nobrega et al. 2004), http://ecrbrowser.dcode.org/, are useful in identifying highly conserved sequences across species that may be functionally important. *In vitro* approaches such as Chromatin immunoprecipitation (ChIP) based technology (i.e., ChIP-sequencing) (Robertson, Hirst et al. 2007) allows DNA that interact with proteins to be identified. The ENCODE project (Thomas, Rosenbloom et al. 2007) represents a recent attempt to centralize these comparative and *in vitro* experimental approaches under one umbrella, thereby providing a starting point to examine the gene regulatory landscape. In ChIP-sequencing, chromatin immunopercipitation (ChIP) and massively parallel sequencing is combined to identify the DNA sequences bound by transcription factors *in vivo* (Robertson, Hirst et al. 2007). Whilst extremely powerful and rapid, these technologies do not in any way test the function of any supposed protein-DNA interaction.

A longer standing approach where functional significance can be assayed, however, is to link genomic fragments of interest in vector constructs to a reporter cassette and monitor reporter activities in transgenic animals. The cis-regulatory elements that control spatiotemporal expression of genes can be positioned far upstream, downstream or within introns of the genes themselves or even in introns of neighbouring genes. Powles et al. identified a 5.7Kb enhancer only 5-6Kb upstream of Fgf3 promoter. This enhancer contains all the cis regulatory elements required to drive reporter expressoion in the endogenous Fgf3 expressing domain (Powles, Marshall et al. 2004). However enhancers can be positioned far away from promoter. For instance, Ahn et al identified an enhancer in Brn4/Pou3f4 gene approximately a megabase upstream of the open reading frame that directs expression to the otic mesenchyme (Ahn, Passero et al. 2009). Therefore, in order to maximise the chances of being able to study the normal regulation of clusterin, a large genomic region was obtained to try and ensure regulatory sequence for clusterin is readily available.

BAC vectors have proven to be very useful for generating reporter gene constructs to survey the broader cis-regulatory landscape in mouse (Jeong, El-Jaick et al. 2006;

Carvajal, Keith et al. 2008; Inoue, Inoue et al. 2008). BACs are able to accept large foreign DNA inserts (up to 300Kb) and their propagation is based on the F-factor replication system of *E. Coli.* Replication is through a low copy number replicon allowing the stable propagation of cloned DNA down to a single copy per bacterial cell in a supercoiled circular form (Asami, Inoue et al. 2011). The high clonal stability of BACs, together with their relative ease of handling has made BAC-based cloning strategies more popular than other vectors with large cloning capacity, such as P1-derived artificial chromosomes (PACs) and yeast artificial chromosomes (YACs) (Gong, Kus et al. 2010).

The aim of the first part of this chapter was to generate a clusterin reporter BAC construct that should contain regulatory elements responsible for controlling endogenous expression of the gene. In order to achieve this, Red/ET recombination technology (recombineering) was used to modify a clusterin BAC by insertion of Bglobin-ZsGreen reporter gene into a clusterin genomic region. The idea is all regulatory regions should recapitulate endogenous expression of clusterin in the inner ear as defined in chapter 3.

As discussed in chapter 3, the expression of clusterin mRNA ceases at some stage between P2 and P17 in the developing mouse cochlea. Therefore, in order to determine the fate of the clusterin expressing cells after P2 in the adult inner ear, in the second part of this investigation, the same clusterin BAC was modified by the insertion of the Cre recombinase coding region into the same clusterin genomic region. This construct will be used for the generation of a Cre transgenic mouse that will express Cre under the control of clusterin regulatory sequences. This potential cochlea-specific Cre recombinase expressing mouse strain will then be crossed with a silent reporter transgenic line to track the fate of cell populations expressing clusterin for fate mapping studies. In this mouse strain, floxed transcriptional stop sequences are removed upon the activation of Clu driven Cre recombinase leading to constitutive expression of the reporter gene in cells expressing Cre recombinase, as well as their daughter cells.

## 4.2 BAC selection

Using the ensemble suite of programmes (www.ensembl.org) to browse the mouse genome for large contiguous pieces of DNA from the BAC locus (Version September 2009), two bacterial artificial chromosomes (BACs), bMQ70i04 and bMQ377e19, containing the entire mouse clusterin gene together with 5' and 3' flanking sequences were identified. Both BACs are cloned in the 11.6Kb pBACe3.6 vector (Appendix VI.I) and contain the full sequence of the mouse clusterin gene (9 Exons and 8 introns, 13.065Kb) (Figure 4.1 and 4.16). The difference between these two BACs is in the size of their flanking sequence.

The bMQ377e19 BAC contains 45Kb flanking sequences; 18.164 and 27.147Kb upstream and downstream respectively (Figure 4.1). The total size of this BAC is 71.0Kb including the entire mouse clusterin gene (Figure 4.1). The 18.1Kb 5' upstream region also includes 3.4Kb of the 3' end of the Scara3 (scavenger receptor class A, member 3) gene and the 27.1Kb downstream 3' region contains nearly the entire Gulo [gulonolactone (L-) oxidase] gene (21.9Kb out of 22.4Kb) (Figure 4.1).

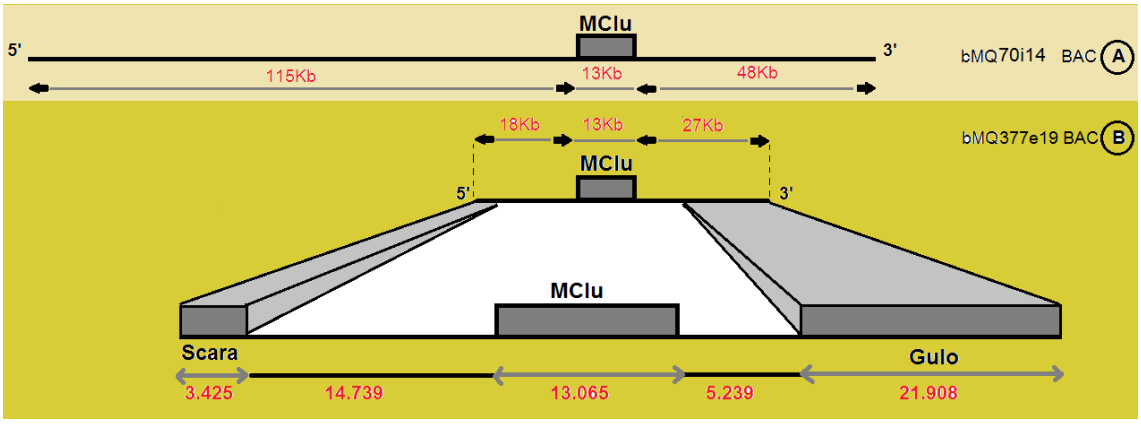


Figure 4.1 Schematic drawing of entire length of bMQ377e19 and bMQ70i04 BACs and the position of clusterin gene and its neighbouring genes in E19 BAC. On the top the bMQ70i04 BAC with the clusterin gene, and its 5' and 3' flanking regions and their sizes are shown. At the bottom the bMQ377e19 BAC with the clusterin gene, its 5' and 3' flanking regions together with the Scara and Gulo neighbouring genes is demonstrated. The demonstrated sizes are in Kb. Only some part of Scara gene and nearly all Gulo gene is included in the bMQ70i14 BAC.

The bMQ70i04 BAC contains 164.309Kb of flanking sequences, consisting of 115.941Kb 5' upstream and 48.368Kb 3' flanking regions. The total size of this BAC is 188Kb including the entire mouse clusterin gene (Figure 4.1).

### 4.3 Design of clusterin reporter BAC

The mouse clusterin transcription start site precedes exon 1 and there is only one transcript variant reported for mouse clusterin on the NCBI database (NM_013492.2). There are two in frame ATG translation initiation sites in exon 2 for mouse and none in exon 1 and 3. The first ATG is believed to be used for the production of sClu (1.4). It is still not clear whether in mice the intracellular form of the clusterin is truly produced and the molecular mechanisms leading to its production is also still unknown. There are regulatory sequences (androgen response elements) reported in intron 1 of human clusterin (Cochrane, Wang et al. 2007). Therefore in the design of a clusterin reporter BAC, reporter gene insertion was targeted to intron 2 so that it is positioned after the ATG sites in exon 2 and the regulatory elements of intron 1. It is however important to note that the reporter cassette (human Bglobin-Zsgreen-SV40) has its own minimal promoter, and thus will come under transcriptional control of clusterin regions, independent of the endogenous clusterin basic transcriptional (core promoter) and translation sequences.

The ZsGreen reporter cassette to be introduced contained a 120bp human beta-globin minimal promoter, about 1Kb ZsGreen reporter gene coding region and a polyadenylation signal (pA) from simian virus 40 (SV40). The ZsGreen reporter gene is a human codon-optimized variant of wild-type *Zoanthus* sp.Green Fluorescent Protein (ZsGreen1) gene. The minimal promoter is able to interact with the cells basal transcriptional machinery, but is not sufficient to initiate expression. However, in combination with enhancers, the regulatory sequences that control the spatiotemporal transcription activities of the gene, reporter expression is initiated and therefore this cassette can be used to test for regulatory elements.

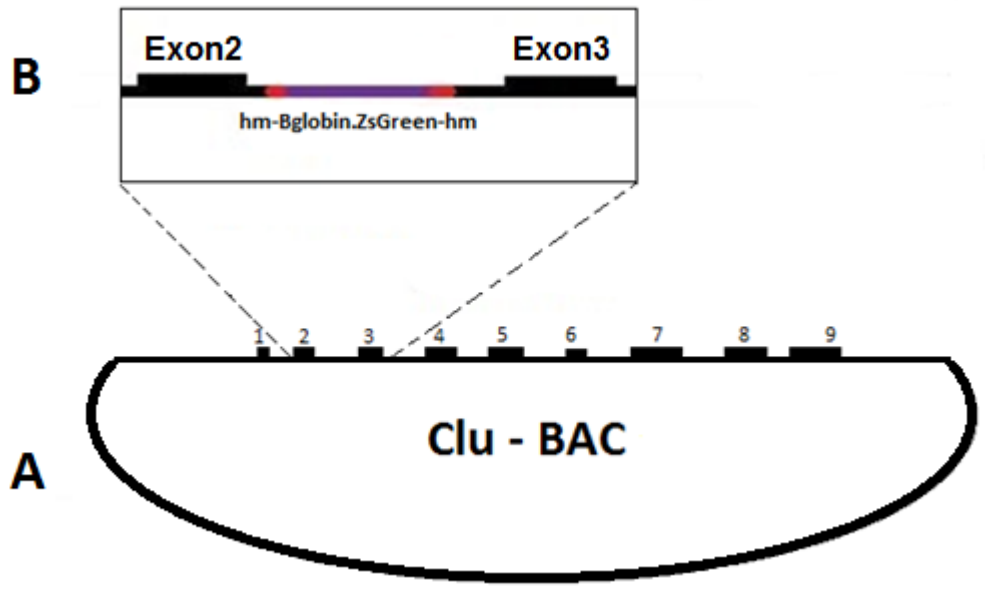


Figure 4.2 Overview of construct design. Schematic representation of clusterin BAC before modification (A) and after modification by insertion of human Bglobin-ZsGreen reporter cassette into the intron 2 using "Counter selection BAC modification Kit" (B). hm: homology arms.

### 4.4 Overview of the recombineering process

Recombineering is an efficient method of *in vivo* genetic engineering in *E. Coli* and relies on the homologous recombination using Red/ET recombination system. Homologous recombination occurs through homology regions, which are stretches of DNA shared by the two molecules that recombine (linear DNA PCR products and BAC in this case).

Using the "Counter-Selection BAC Modification Kit" from Gene Bridges, BAC modifications are carried out through three main steps (Figure 4.3).

In the first step of recombineering, DH10ß *E. Coli* cells carrying the BAC is transformed with the Red/ET expression plasmid, pSC101-BAD-gbaA$^{tet}$, (Appendix VI.IV) that contains all the necessary genes required for homologous recombination *in vivo* (Figure 4.3, step 1). pRed/ET carries the λ phage redγβα operon expressed under the control of the arabinose-inducible pBAD promoter (Guzman, Belin et al. 1995) and also confers Tetracycline resistance. Redα processes linear dsDNA and provides 3' overhangs, and Redβ, is a DNA annealing protein and mediates strand annealing. The λ encoded Gam protein inhibits the RecBCD exonuclease activity of *E. Coli.* The pBAD

promoter is both positively and negatively regulated by the product of the *ara*C gene (Schleif 1992). AraC is a transcriptional regulator that forms a complex with L-arabinose. Arabinose binds to AraC and allows transcription to begin. In presence of glucose and the absence of arabinose transcription is blocked by the AraC dimer (GENEBRIDGES technical protocol Feb 2005).

The pRed/ET plasmid derives from plasmid pSC101 which is a low copy number plasmid. The repA protein encoded in pSC101 is required for plasmid DNA replication and the partitioning of plasmids during division (Miller, Ingmer et al. 1995). This plasmid is temperature-sensitive; whilst stable at 30ºC, it is ejected from cells at non-permissive temperatures of 37ºC or more (GENEBRIDGES technical protocol Feb 2005). The selection and counter selection system in the recombineering kit is partly based on the properties of the *rpsL* gene and Streptomycin selection. The *rpsL* gene encodes for S12 ribosomal protein which is a target of Streptomycin and therefore makes the cells Streptomycin sensitive. Most commonly used *E. Coli* strains, including DH10B, carry a mutated *rpsL* gene resulting in Streptomycin resistance, which is a prerequisite for this technology to be useful. Introduction of wild type rpsL into such Streptomycin resistant *E. Coli* strain will make the strain Streptomycin sensitive again.

In the second step of recombineering, after induction of pRedET recombineering genes (by adding L-arabinose together with a temperature shift from 30ºC to 37ºC), the rpsL-neo counter selection/selection cassette flanked by 50bp homology arms is electroporated into these cells (Figure 4.3, step 2). Red/ET recombination inserts the rpsL-neo cassette into the target locus via the homology arms. The modified colonies will survive Kanamycin selection on agar plates and will be Streptomycin sensitive. The BAC intermediate clones at this step will be referred to as rpsLneo Clu-BAC.

In the third step of recombineering, after induction of pRed/ET genes once again, the rpsL-neo cassette will be replaced by the non-selectable Bglobin-ZsGreen cassette with 50bp homology arms (Figure 4.3, step 3). Only colonies which lost the selection/counter-selection cassette will now grow on Streptomycin containing plates. Clones at this step will be referred to as ZsGreen Clu-BAC and represents the final construct.

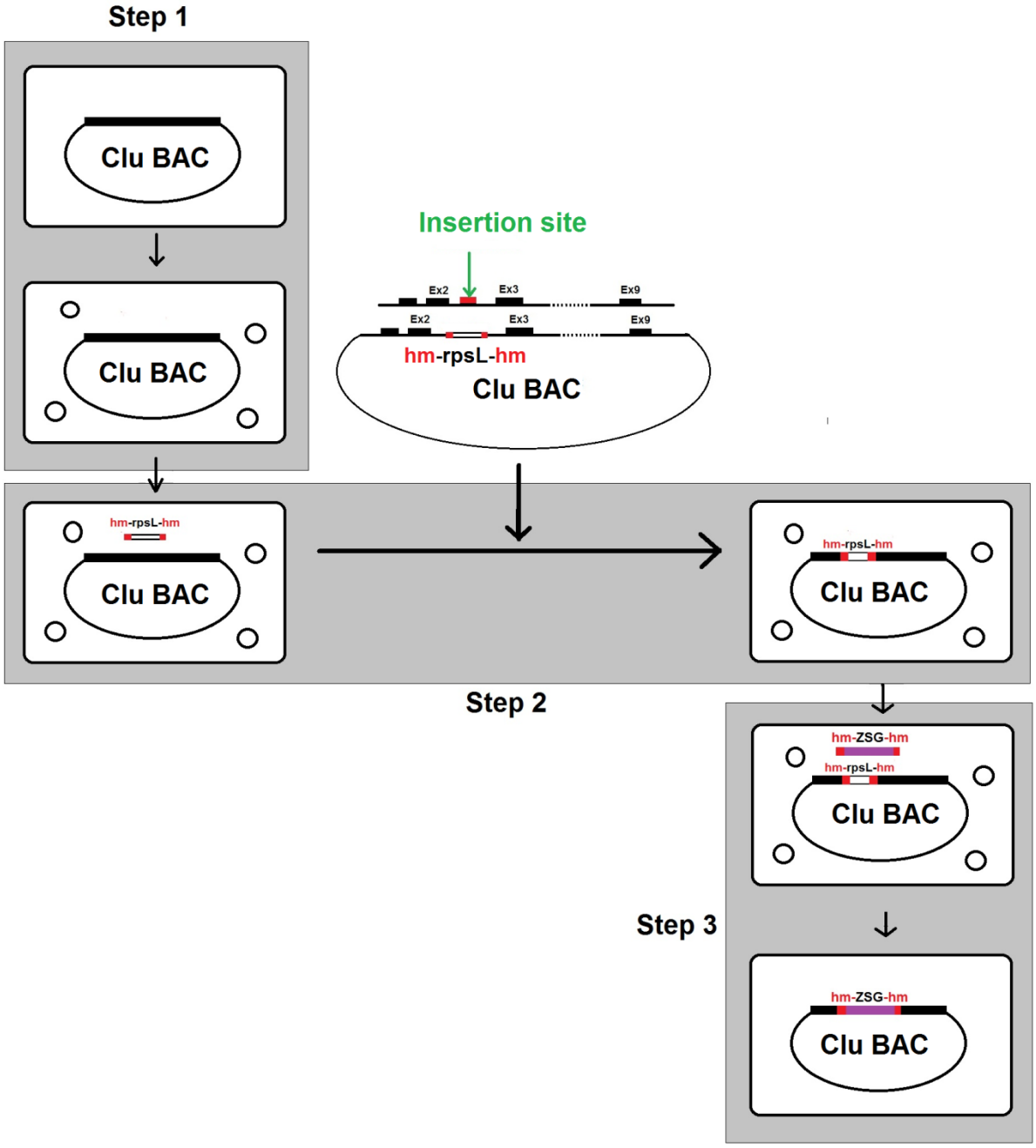


Figure 4.3 Using "Counter selection BAC modification Kit" clusterin BAC will be modified in 3 steps. Step 1: introduction of pRedET into the BAC containing DH10ß *E Coli* cells. Step 2: The rpsL-neo cassette flanked by homology arms will be inserted into the intron 2 of the clusterin gene through homologous recombination. Step 3: The rpsL-neo cassette will be replaced by the PCR amplified ZsGreen cassette (flanked by the same homology arms as rpsl-neo). In step 2 and 3 homologous recombination will happen between the homology arms and by induction of the red/et genes through temperature shift and addition of L-arabinose. Small circles in step 1-3 represent Red/Et plasmid.

## 4.5 Generation of a clusterin-ZsGreen reporter BAC by recombineering

### 4.5.1 BAC clone characterization

A glycerol sample of bMQ70i04 and bMQ377e19 BAC (will be referred to as 70i04 Clu-BAC and E19 Clu-BAC respectively) was obtained from Geneservice (http;//www.lifesciences.sourcebioscience.com/).

**E19 Clu-BAC**: In order to analyse whether the received BAC contains the entire clusterin gene, a PCR analysis was carried out using primer pairs that allow to amplify the entire coding region of the gene. Initially primer pair 1 was designed to amplify a 1542bp fragment from exon 1–intron 1 of the mouse clusterin gene (2.4.1 and Figure 4.6). In addition the PCR was also carried out on mouse genomic DNA as a positive control.

Two of the E19 Clu-BAC clones (E19/4 and E19/5) successfully produced the expected 1542bp band (Figure 4.4, lane 4 and 6), but the positive control (genomic DNA) failed to produce any bands (Fig 4.4, lane5).

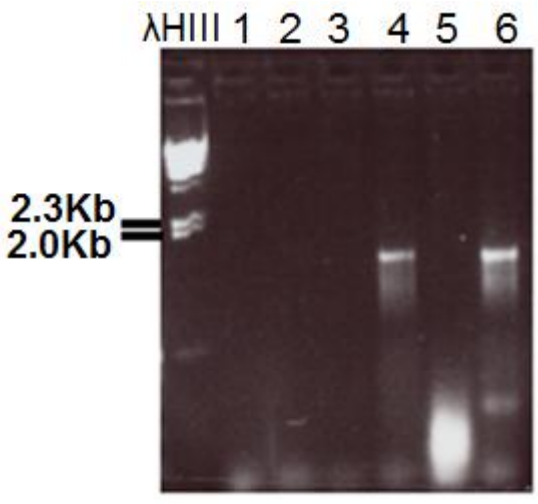


Figure 4.4 Characterisation of E19 Clu-BAC using primer pair 1. *Lane 1-4:* Clone E19/1- E19/4. *Lane 5*: mouse genomic DNA as a positive control. *Lane 6*: Clone E19/5. λHIII: the HindIII digest of lambda DNA used as a DNA ladder.

The E19/4 and E19/5 clones were further analysed using a second set of primers (primer pair 2) to amplify 1390bp of clusterin intron 2 (2.4.1). Both clones gave the expected band size (Figure 4.5 and 4.6). Thus the expected bands are generated in the 5' region of the gene.

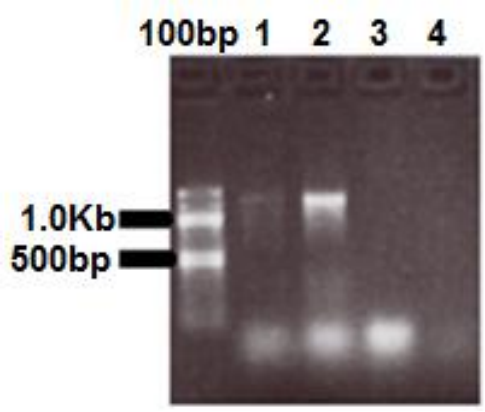


Figure 4.5 Characterisation of E19 Clu-BAC using primer pair 2. *Lane 1 and 2*: Clone E19/4 and E19/5. *Lane 3*: mouse genomic DNA as a positive control. *Lane 4*: No DNA negative control. 100bp: the 100bp DNA ladder.

However it was thought to further analyse the integrity of the complete coding region of the clusterin gene in this BAC. Therefore, nine sets of primers capable of amplifying about every 1Kb of the entire clusterin gene (Figure 4.6 and 2.4.1) were designed and used with the E19/5 Clu-BAC. Mouse genomic DNA and primer pair 2 were also used as positive control and mouse genomic DNA with no primers as a negative control. Apart from primer pair 8, all the primers generated the expected bands (Figure 4.7 A). Another PCR reaction was carried out for primer pairs 8 and on this occasion the expected band was generated (Figure 4.7 B). Mouse genomic DNA and primer pairs 8 also were used as positive control in this PCR.

**70i14 Clu-BAC**: This BAC that contains larger flanking sequences generated some nonspecific bands when analysed as above by PCR using integrity oligos, suggesting possible rearrangements and/or deletions of the clusterin gene in this BAC (Figure 4.7 C). Therefore, only E19 Clu-BAC was used for the generation of clusterin reporter construct.

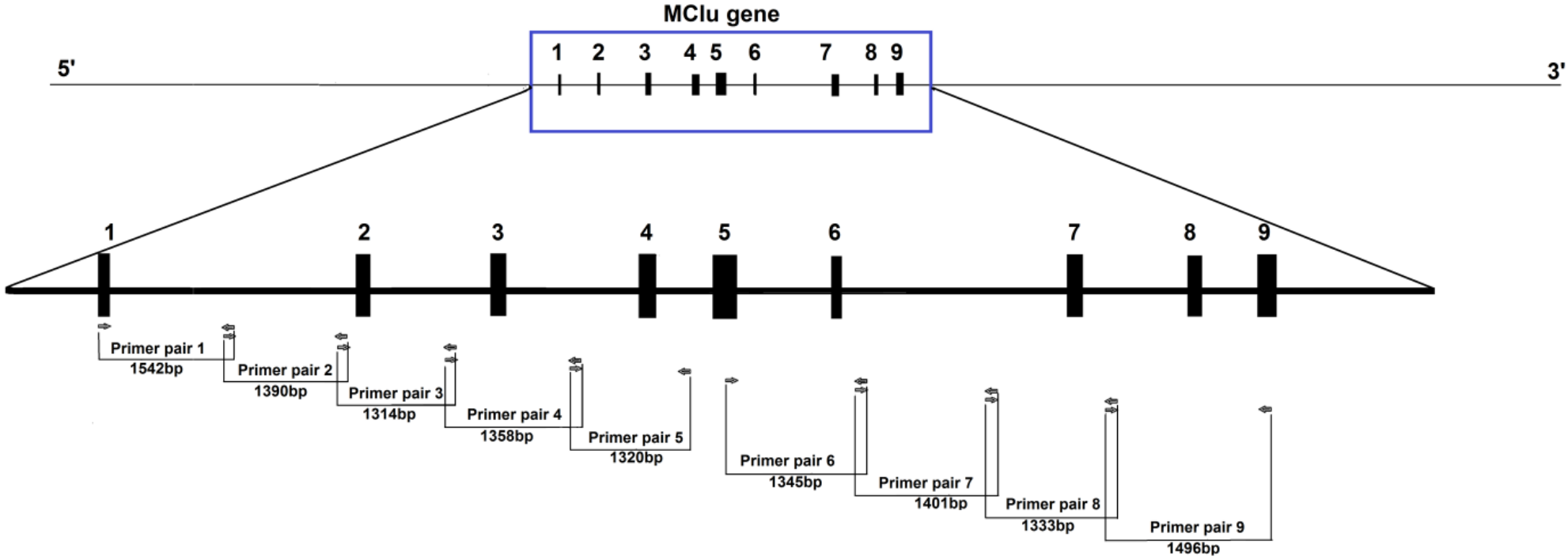


Figure 4.6 Schematic illustration of location of primers used to characterise the integrity of intron/exon structure of the clustein gene in the E19 BAC. Primer pairs are numbered to denote pairs used in combination. Note: roughly drawn to scale. See 2.4.1 for primer sequences.

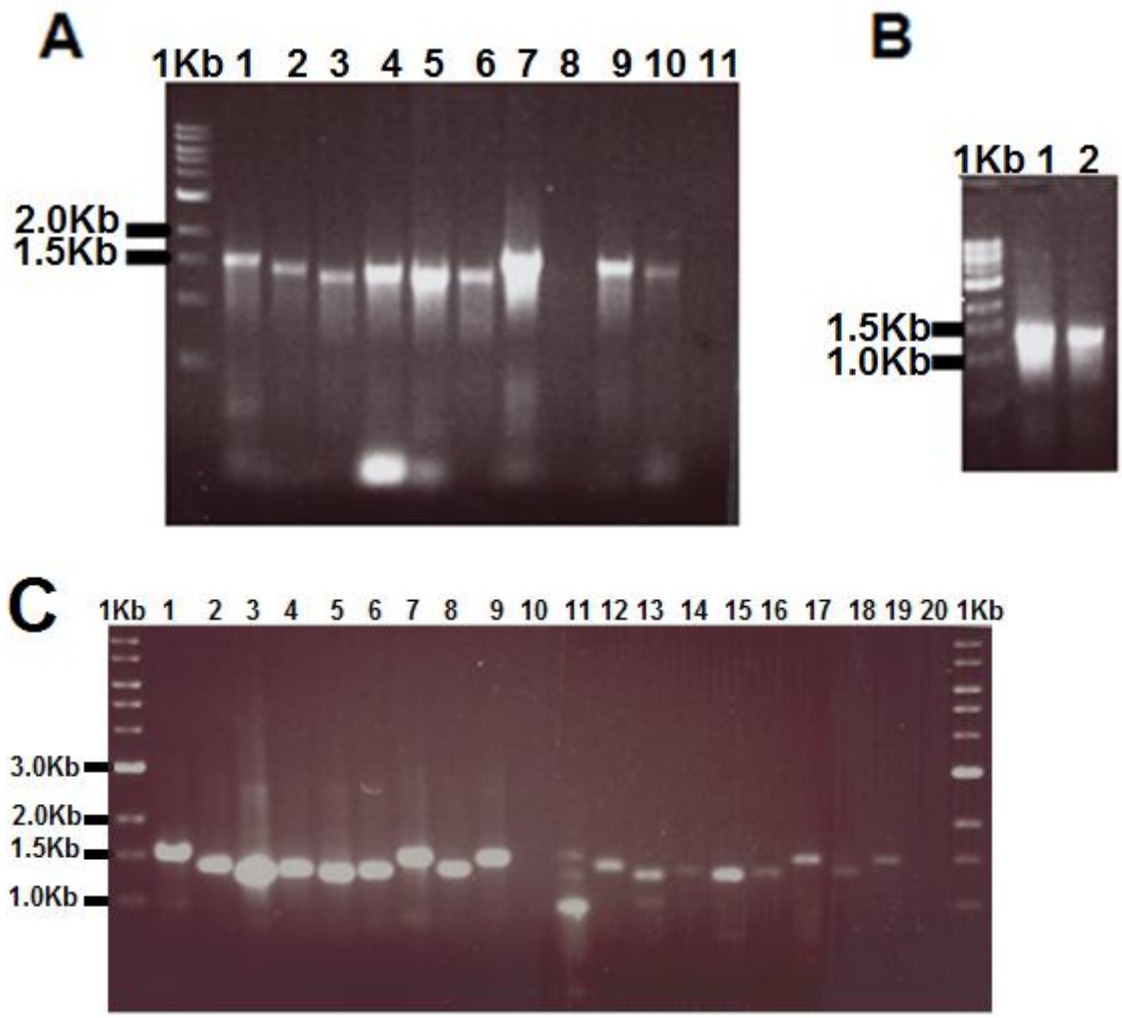


Figure 4.7 Gene walking PCR for analysis of the integrity of clusterin coding region in bMQ377e19 (A and B) and bMQ70i04 BACs (C). 1Kb: 1Kb DNA ladder.

**A:** *Lane 1-9:* Oligo pair 1-9 against bMQ377e19 BAC. *Lane 10*: Mouse genomic DNA and oligo pair 2 as a control. *Lane 11*: No DNA negative control. All the expected bands are present for oligo pair 1-9 and also for the mouse genomic control DNA except pair 8.

**B:** The production of the expected band (1333bp) from bMQ377e19 BAC using oligo pair 8 (lane 1) and also from the mouse genomic DNA (lane 2). *Lane 1:* Oligo pair 8 against E19 Clu-BAC. *Lane 2:* Mouse genomic DNA and oligo pair 8 as a control.

**C:** *Lane 11-19:* Oligo pair 1-9 against bMQ70i04 BAC and comparison with bMQ377e19 BAC (*lane 1-9). Lane 10 and 20*: Blank. This analysis revealed that the bMQ70i04 BAC that contains larger flanking sequences might have gone under some rearrangements or deletions.

### 4.5.2 BAC modification by insertion of Bglobin-ZsGreen gene

In order to confirm that the *E. Coli* containing the clusterin BAC are Streptomycin resistant, the E19/5 Clu-BAC clone was streaked on agar plates containing Streptomycin and Chloramphenicol. The growth of clones on these plates confirmed that the E19/5 Clu-BAC clones are Streptomycin resistant.

#### 4.5.2.1 Introduction of the pRed/ET plasmid

Fresh culture was used to prepare electrocompetent cells (2.1.18.3) containing the clusterin BAC, and the pRed/ET plasmid was introduced by electroporation (2.1.18.7) and selected on agar plates containing Tetracycline plus Chloramphenicol to select for both the pRed/ET plasmid and BAC respectively.

#### 4.5.2.2 Recombineering of rpsL-neo in the clusterin BAC

**Induction of the Red/ET recombination genes:** Clones containing the pRed/ET plasmid were next induced to express the recombination enzymes (2.1.18.4)

**Preparation of linear rpsl-neo cassette:** The amplification of a 1320bp of rpsL-neo gene together with 50bp homology arms to clusterin (Figure 4.8) the right and left of rpsL-neo cassette was carried out using HRrpsl-for and HRneo-rev oligos (2.4.2) and amplification was with using high fidelity Phusion Taq DNA polymerase (New England Biolabs). The homology arms are the 50bp regions homologous to the right and left of the mouse clusterin in the middle of intron 2 and represent the insertion point for the Bglobin-ZsGreen reporter gene. The rpsL-neo plasmid provided in the kit was used as DNA template for the above PCR reaction.

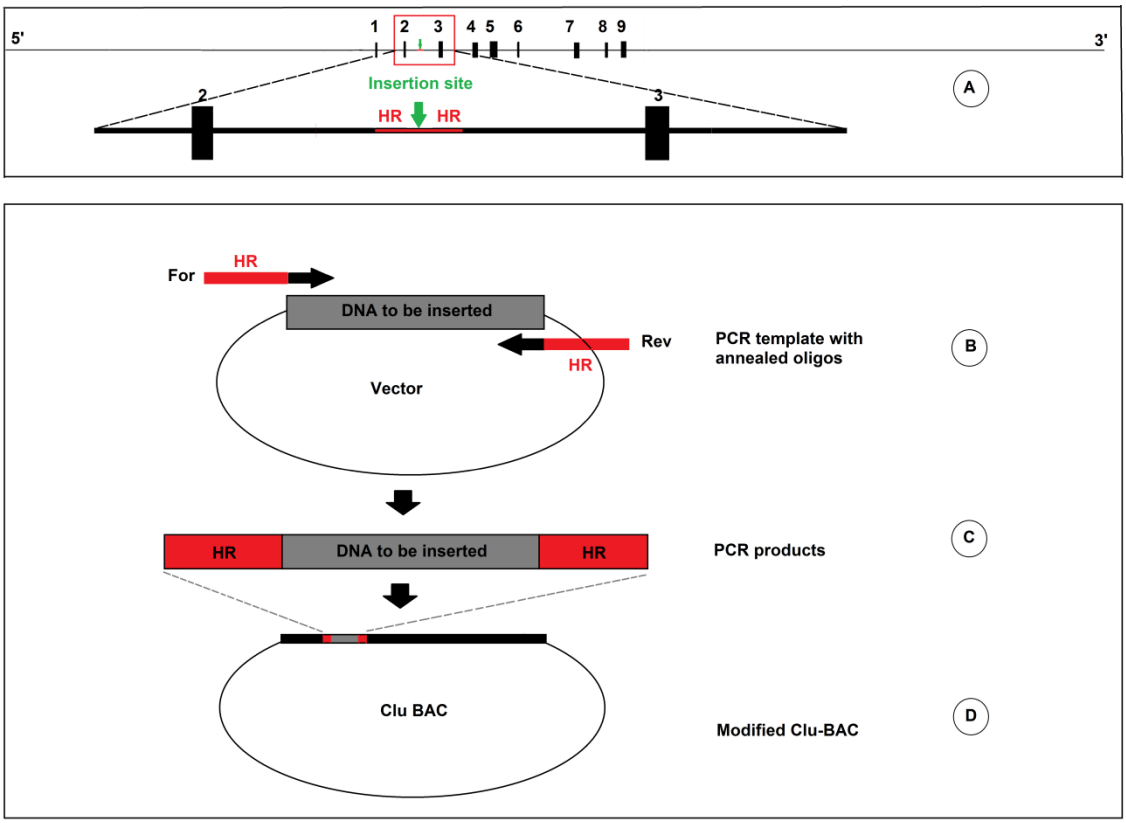


Figure 4.8 Schematic representation of the practical steps for the production of PCR products with homology arms to clusterin gene is demonstrated. A: clusterin gene insert into the E19 BAC (Clu gene with the 5' and 3' flanking regions) and the insertion point in mid intron 2 is demonstrated. B: Forward and reverse oligos are designed so that they anneal to the gene to be inserted, with 50bp flanking regions that are homologous to the right and left of insertion point. C: The produced PCR products contain the homology arm (HR) sequence. D: The incorporation of PCR product into the Clu-BAC is shown. Not drawn to scale.

**Electroporation of the linear targeting substrate DNA:** Both induced and uninduced cells were made electrocompetent (2.1.18.4). Linear PCR product was introduced into both induced and uninduced cells by electroporation (2.1.18.7) and subsequently plated on LB agar plates containing Chloramphenicol, Kanamycin and Tetracycline and incubated at 30ºC for 20-40 hours. The "uninduced cells plus DNA" is a control to estimate the number of background colonies produced as a result of electroporation of intact plasmid template from a PCR reaction (Shyam K. Sharan 2009).

**Identification and confirmation of the recombined clones:** After 24-40 hours 12 colonies from induced plates were picked and grown in LB conditioned with Chloramphenicol, Kanamycin and Tetracycline. The tubes were incubated at 30 $^{o}$C with shaking at 1100rpm for 1-2 hours and used for the steps below:

- Culture streaked on LB plates conditioned with Streptomycin, Kanamycin plus Chloramphenicol to test the function of the rpsL-neo cassette.

- Culture grown into 2ml of fresh LB culture with Kanamycin and Chloramphenicol for preparing BAC DNA and for PCR verification.

- Growth in Chloramphenicol, Kanamycin and Tetracycline at 30$^{o}$C overnight for use in the second round of Red/ET recombination.

The first few attempts for the insertion of rpsL-neo were unsuccessful, and PCR analysis of clones obtained at this step generated either no band or some non-specific bands (data not shown). On each occasion the same numbers of colonies were obtained on the induced and uninduced plates. Therefore, the recommended protocol was revisited with a view to optimise conditions.

#### 4.5.2.3 Optimisation of recombineering parameters

The following conditions in the recombineering protocol were addressed:

- Incubation period following plating
- Kanamycin resistance
- Design of additional controls
- Improvement of Transformation frequency through variation of electroporation settings
- Dpn1 digestion of rpsL-neo PCR products
- Increasing DNA concentration

**The incubation period following plating:** The plating time (up to 48 hours) was reduced to a maximum of 28 hours following personal communication with the company, who confirmed large colonies were expected to grow within 24 hours of incubation at 30$^{o}$C. Indeed, it has been believed that most if not all clones will have some amount of revertants that have become Streptomycin resistant (Hyman Lab).

**Kanamycin selection:** Uptake of the neo gene will confer Kanamycin resistance to colonies. Therefore, one explanation for equal number of colonies on induced and uninduced plates could be that the E19 Clu-BAC vector backbone itself was carrying a Kanamycin resistant gene and therefore supporting its growth on LB agar Kanamycin containing plates. This was tested by streaking the Clu-BAC.pRedET cells on LB agar plates containing Kanamycin, Chloramphenicol and Tetracycline. As a positive control E19.Red/ET cells were streaked on LB agar plates containing Chloramphenicol and Tetracycline. There was no growth on Kanamycin containing plates demonstrating that the E19 Clu-BAC was Kanamycine sensitive as required for the positive selection system to work.

**Addition of further controls:** Apart from the uninduced cells plus DNA control, another control was introduced into the experiment which was "induced cells without DNA". If colonies are present on this plate either the selection system was failing, or the cells have a high reversion frequency for the property selected (Shyam K. Sharan 2009).

**Electroporation settings:** There are two factors crucial for efficient transformation of DNA into the cells by electroporation, voltage (V) and time constant (GENEBRIDGES technical protocol 2007). A time constant lower than 5 msec generally indicates impurities or salts in either the electrocompetent cells or in the DNA for transformation (Shyam K. Sharan 2009). However, the time constant is only revealed following the electric pulse. In order to attempt to improve the time constant, low salt LB medium (Appendix I) was used for the growth of cells (Genebridges, personal communication)
Voltage was however an obvious parameter that could be carefully altered. 0.01ng of pbluescriptSK$^{+}$ was electroporated into electrocompetent E19 Clu-BAC cells using a variety of voltages (Table 4.1). From these experiments, there was a slight improvement with increasing voltage, with optimum transformation frequencies achieved following electroporation using 2.5KV. Whilst this was chosen for subsequent experiments, it is worth bearing mind that these frequencies were using supercoiled plasmid DNA which may have different transformation characteristics compared to using linear DNA.

Table 4.1 Optimization of voltage for electroporation of E19 Clu-BAC containing cells with 1µg of plasmid DNA (pbluescriptSK$^{+}$)

| Voltage (KV) | Time constant | Transformation efficiency (per 1µg of DNA) |
|---|---|---|
| 1.35 | 5.20 | $8\times10^{9}$ |
| 1.6 | 5.16 | $9.2\times10^{9}$ |
| 2.0 | 5.12 | $1.8\times10^{10}$ |
| 2.5 | 5.06 | $2.1\times10^{10}$ |

It was decided that 2.5KV would be used in the subsequent experiments.

**Dpn1 digestion of rpsL-neo PCR products:** Dpn1 digestion can be used to eliminate the template plasmid DNA which, in BAC recombineering experiments would be useful to prevent plasmid templates remaining to be transformed and become stable episomes. Communication with the manufacturers of the BAC modification kit, confirmed that the rpsL-neo template provided in the kit is a plasmid but no restriction digestion is needed to linearise the plasmid before the electroporation of rpsL-neo PCR products because the plasmid is suicidal (personal communication). A literature search of BAC recombineering methods revealed that the rpsL-neo plasmid templates are usually linearised prior to PCR amplification (Muyrers 2001; Junping Wang 2006; Nakamura 2008; Shyam K. Sharan 2009). The plasmid form (of unamplified material) can present a considerable source of "carry over" and lead to high background levels of colonies. This is because any residual, intact, template plasmid present with the electroporated PCR product will also produce selectable colonies upon selection for the encoded antibiotic resistance gene (here neo for Km resistance). Background can be significantly reduced by digestion of the amplification reaction, with Dpn1 or with a restriction enzyme at sites present in the vector backbone but absent in the sequence to be amplified. Ideally the replication origin of the plasmid DNA should be destroyed (Shyam K. Sharan 2009). Unfortunately, the manufacturers refused to reveal the plasmid's sequence, but in the trouble shooting section of the manual provided, Dpn1 digestion of the PCR products prior to electroporation was recommended in cases where the same number of colonies on the induced and un-induced plates were found. Thus Dpn1 digestion was used to linearize the original methylated plasmid after amplification

and thereby eliminate the template plasmid leaving the amplified PCR product for homologous recombination.

Following transformations of Dpn1 digested amplified products and plating on LB agar plates with Kanamycin, Chloramphenicol and Tetracycline, again the same number of colonies were obtained for the induced and un-induced plates and the colonies either failed to grow in LB with Kanamycin and Chloramphenicol or failed to produce any product after PCR analysis indicating that recombineering had not been achieved. The time constant was checked after each electroporation and was found to be approximately 5msec or just below 5msec with a transformation efficiency of about $10^{10}$ per 1µg of bluescriptSK$^{+}$.

The company persisted that rpsL-neo plasmid template has a suicide backbone and is not capable of replicating itself in normal *E. Coli* cells and therefore there will not be any "carry-over" of the plasmid template in the PCR samples.

Wang *et al. (2006*) describe the generation of an rpsL-neo plasmid that has been successfully used in their recombineering experiments. A wild-type *rpsL* allele was amplified by PCR from *E. Coli* DH5α using primers that also added a ribosome-binding site, and then cloned in front of *Tn5-neo* in pR6K-Tn5-neo (Figure 4.9) (Junping Wang 2006).

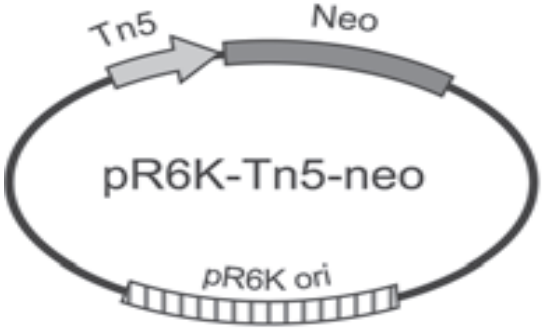


Figure 4.9 Schematic presentation of the pR6K-Tn5-neo used for the cloning of the rpsL cassette next to the Neo gene. Adopted from (Junping Wang 2006).

Wang *et al. (2006)* assert that cloning the Tn5-neo cassette into an R6K origin plasmid has eliminated the source of plasmid carry over, since plasmids based on this origin require expression of the Pir protein for replication. All *E. Coli* hosts lack the *pir* gene,

and thus use of this plasmid as the PCR template should completely eliminate the plasmid background following transformation and failure to replicate.

Whilst not confirmed, it seemed likely that the generation of the rpsL-neo plasmid included in the kit was carried out by Wang *et al*. (moreover they also describe the generation of a pRed/ET vector). It thus seemed likely that similar number of colonies on induced/un-induced might represent slow growing, false positive satellite colonies growing on the plates probably as the result of the long incubations (28-40 hours). Therefore in the subsequent experiments the incubation time was reduced to a maximum of 28 hours.

**DNA concentration**: As the electroporation of linear DNA is not very efficient ($10^4$ – fold less active than of circular DNA molecules) (GENEBRIDGES technical protocol 2007), attempts were made at increasing the amount of linear DNA in the electroporation. Following amplification, the product was concentrated by either precipitation (2.1.18.6) or via the gene clean protocol (2.1.2).

Following the incorporation of the above optimisations and electroporating 100ng of PCR products, colonies of different size were now noted on plates. Moreover, whilst the uninduced plus DNA plates had some colonies, the ratio of the colonies on induced/uninduced was 10:1. The functional test (2.1.18.9) was carried out and the Streptomycin resistant clones were used for miniprep and further analysis.

#### 4.5.2.4 Analysis of clones recovered following optimisation of the protocol

In order to analyse clones for successful recombineering, a variety of PCR assays were carried out:

- PCR analysis using internal neo oligonucleotides
- PCR analysis using Clu-rpsL oligonucleotides spanning the 5’ site of recombination
- PCR analysis using clusterin intron 2 oligos
- PCR analysis using oligos to monitor the integrity of the coding region

**PCR analysis using internal neo oligonucleotides:** neo forward and reverse oligos (F288-Neo1 and R289-Neo2) were designed to amplify a 152bp product from the neo gene (2.4.4 and Figure 4.15B) that should be present in all successfully integrated rpsL-neo recombinants. PCR analysis of colonies 1-12 generated the expected band size. pβglobin-ZsGreen 1:1 (Appendix VI.II) plasmid dilution was used as positive control as it also contains a Kanamycin resistance gene (Figure 4.10). This confirms the incorporation of the neo gene in the clusterin BAC, but does not address the fidelity of the recombination event.

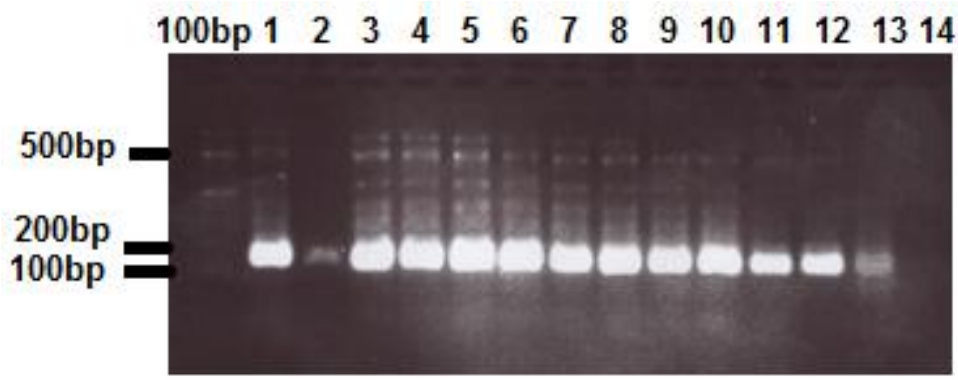


Figure 4.10 PCR analysis of clones from rpsL-neo insertion step using neo oligos. *Lanes 1-12*: clone 1-12. *Lane 13*: pβglobin-ZsGreen 1:1 plasmid as positive control. *Lane 14*: No DNA negative control. 100bp: the 100bp DNA ladder.

**PCR analysis using Clu-rpsL oligonucleotides:** in order to analyse the fidelity of recombination at the 5' end of the rpsL-neo cassette, oligonucleotides were designed against clusterin intron 2 (outside the homology region) and a second oligonucleotide against the rpsL gene in a reverse orientation (F321-Clu int2 and R322-rpsl oligos) (2.4.4 and Figure 4.15B). The predicted PCR product of 591bp was obtained for all the colonies examined (Figure 4.11). The negative control did not produce any product in this PCR (Figure 4.11, lane 14). In a separate PCR reaction E19 unmodified BAC was used and similarly failed to demonstrate a PCR product confirming the specificity of the PCR products for clones 1-12 (Figure 4.12).

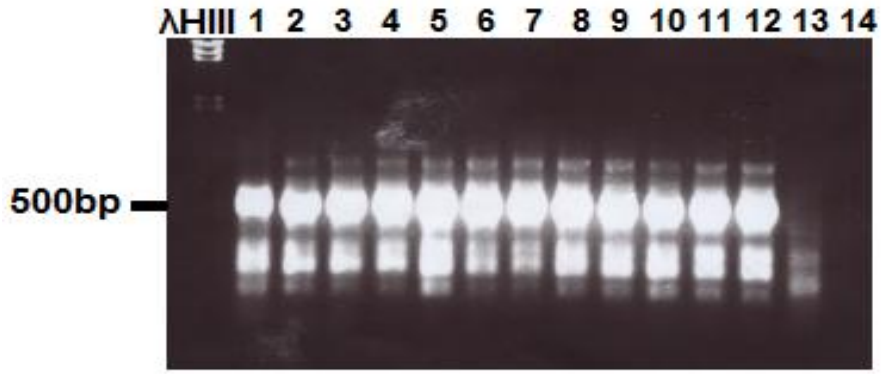


Figure 4.11 PCR amplification across the 5' arm of the rpsL-neo insertion using F321-Clu int2 and R322-rpsl oligos. *Lanes 1-12*: Recombinant BAC clones 1-12. *Lane 13*: pβglobin-ZsGreen 1:1 plasmid as negative control. *Lane 14*: No DNA negative control. λHIII: the HindIII digest of lambda DNA used as a DNA ladder.

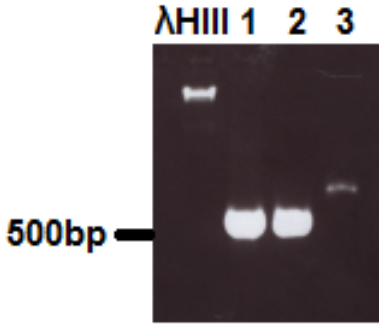


Figure 4.12 Control E19 Clu-BAC and two of the successfully modified BACs by insertion of rpsLneo are checked by using left arm oligos. *Lane 1*: Clone 1, *Lane 2*: Clone 2, *Lane 3*: Unmodified E19 Clu-BAC. λHIII: the HindIII digest of lambda DNA used as a DNA ladder.

**PCR analysis using clusterin intron 2 oligos**: forward and reverse oligos (F321-Clu int2 and R221-Clu int2) (2.4.4 and Figure 4.15B) from outside of the homology region and spanning the designed insertion site were used to amplify either a 536bp DNA band (in the case of no insertion) or a PCR product of 1856bp following successful rpsL-neo insertion. Figure 4.13 showed clones 1-4 all have the correct sized band indicating insertion of rpsL-neo cassette into intron 2.

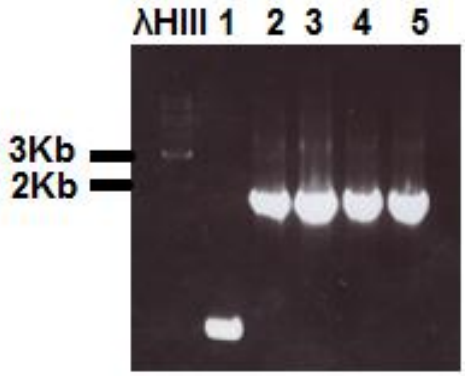


Figure 4.13 PCR analysis of clones 1-4 using outside homology oligos. *Lane1:* Unmodified E19 Clu-BAC. *Lane 2-5*: Successfully modified BACs by insertion of rpsL-neo into their clusterin intron 2. λHIII: the HindIII digest of lambda DNA used as a DNA ladder.

**Integrity oligos:** Following identification of successful integration of the rpsL-neo cassette, the recombined BAC was also assayed with oligonucleotide primer pairs ("integrity oligos") to assay for the correct maintenance of intron-exon structure of the clusterin gene, in a similar manner to the initial BAC characterisation as previously described (4.5.1). As positive control the oligos from outside homology arms (F321-Clu int2 and R221-Clu int2), capable of amplifying a 1856bp bands were also used. Also oligo pair 3 (F220-Clu int1 and R221-Clu int2) and no DNA was used as negative control (Figure 4.15B).

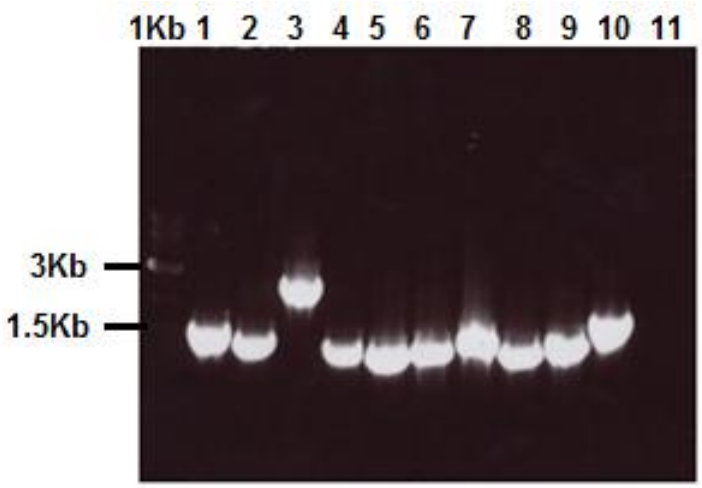


Figure 4.14 Gene walking PCR of clusterin insert in rpsl-neo Clu-BAC. *Lane 1-9*: Oligo pair 1-9. *Lane 10*: oligos "F321-Clu int2" and "R221- Clu int2" that are oligos from outside homology arms as positive control. *Lane 11*: oligo pair 3 and no DNA negative control. 1Kb: 1Kb DNA ladder

The expected bands for all the oligo pairs used are present and produce identical products as described for the unaltered E19 BAC (Figure 4.14) except for oligo pair 3. The 2634bp band for oligo pair 3 confirms again the successful insertion of rpsL-neo cassette into clusterin intron 2 (lane 3). The oligos from outside homology arms also amplify the expected band of 1856bp (lane 10). A summary of the oligos used is detailed in Figure 4.6 and 4.15B.

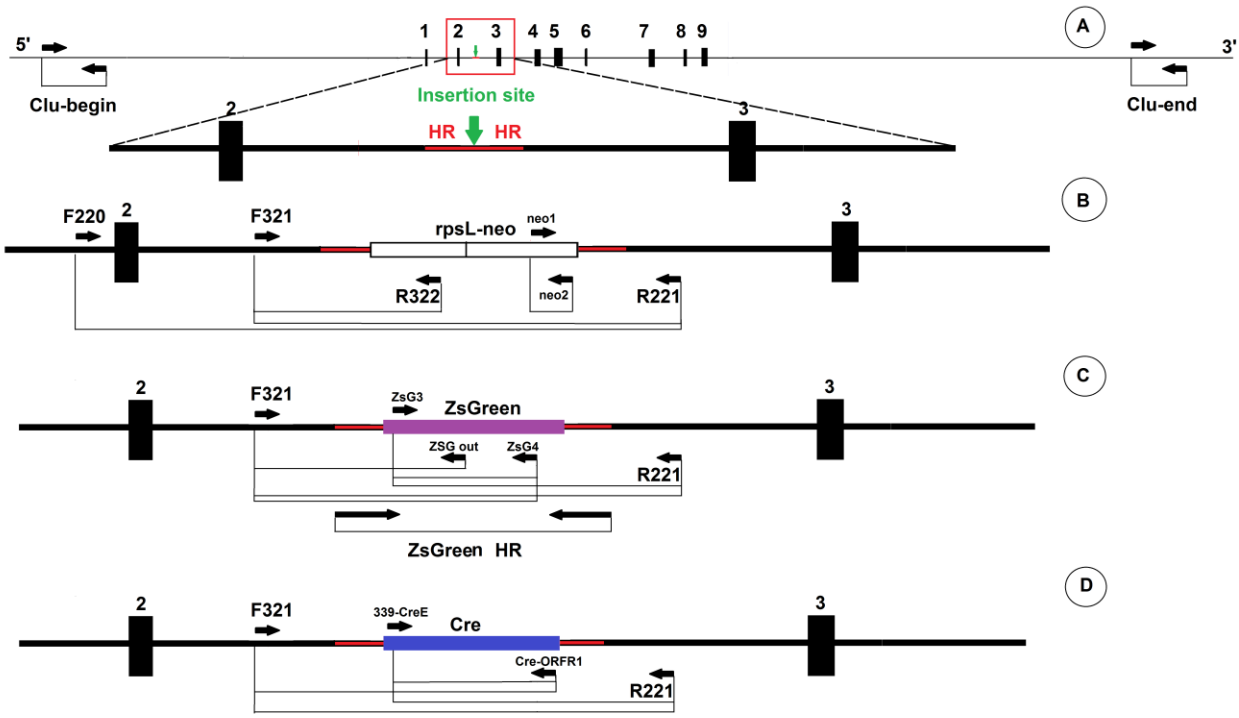


Figure 4.15 Schematic drawing overviewing the PCR analysis of Clu-BAC during the recombineering processes. A: unmodified Clu-BAC. The exons, introns, 5' and 3' flanking regions are shown. The insertion site between exon 2–exon 3 is demonstrated below with the HR representing the 50bp homology region used for the amplification of rpsL-neo and ZsGreen genes for subsequent insertion at the insertion site in intron 2. B, C and D: demonstrates the variety of primers used for the analysis of rpsL-neo, Bglobin-ZsGreen and Cre recombinase cassette insertion respectively in intron 2. The extreme beginning and end of "ZsGreen Clu-BAC" was checked by two sets of primers and are shown in A as Clu-being and Clu-end. The drawing is roughly to the scale. For the primers' list and their sequence see section 2.4. F321: F321-Clu int2 oligo, R221: R221-Clu int2 oligo.

### 4.5.3 Replacement of rpsL-neo with ZsGreen by recombineering

In order to replace the rpsL-neo cassette with the fluorescent reporter cassette, first a linear PCR product of the cassette was prepared. A 5' oligonucleotide was designed using the same 5' clusterin homology arm as above but followed by nucleotides corresponding to the Bglobin promoter (ZsGreen-HR forward). The 3' oligonucleotide was similarly designed using the identical 3' clusterin homology arm followed by sequence from the SV40 poly adenylation signal (ZsGreen-HR reverse). These oligonucleotides were used to amplify linearised Bglobin-ZsGreen-SV40 pA cassette flanked by 5' and 3' clusterin arms of homology (2.4.3 and Figure 4.8).

Using the optimised parameters described above (4.5.2.3) this was used to generate clones in an identical manner as described above. However in this case, rpsl-neo will be replaced by a 1186bp PCR product containing the Bglobin-ZsGreen cassette. The PCR products were electroporated into the cells and different dilutions of the culture were grown on agar plates containing Chloramphenicol and Streptomycin. The ratio of induced to uninduced bacterial colonies was between 10:10 to a maximum of 10:8 and almost never 10:1 as the protocol described.

#### 4.5.3.1 Identification and confirmation of recombined clones

Clones were analysed either only by PCR or by a combination of southern blot, dot blot or colony blot hybridisation and then followed by PCR analysis.

For PCR analysis, 12 colonies were analysed in each batch. In the first 3 recombineering attempts, analysis of the clones did not lead to the detection of the expected PCR products, and sometimes non-specific bands were produced (data not shown).

Therefore, in order to screen a large number of colonies unequivocally, a Southern blot approach was adopted. 110 recombinant clone minipreps were digested with *Hind* III. Bioinformatic analysis of the clusterin BAC predicts that *Hind* III would cut the E19 Clu-BAC 16 times but does not cut the Bglobin-ZsGreen-SV40 insert. Either side of the site of insertion, *Hind* III is predicted to cut at 15190bp and 24349bp releasing a band of about 10Kb that also includes a Bglobin-ZsGreen-SV40 cassette (Figure 4.16). The digested samples were run on a 0.8% agarose gel followed by transfer to Hybond nitrocellulose membranes and hybridised against a 720bp $^{32}$P labelled DNA probe from ZSGreen and visualised through autoradiography. None of the clones examined revealed a clear band of about 10Kb for the ZsGreen (Data not shown).

In addition a dot blot and colony blot approach was also taken. The colony blot and dot blot hybridisation membranes were also hybridised with $^{32}$P labelled ZsGreen DNA probe and similarly visualised using autoradiography (Figure 4.17, data not shown for dot blot analysis). Potentially positive clones were identified by autoradiography and grown up for PCR analysis.

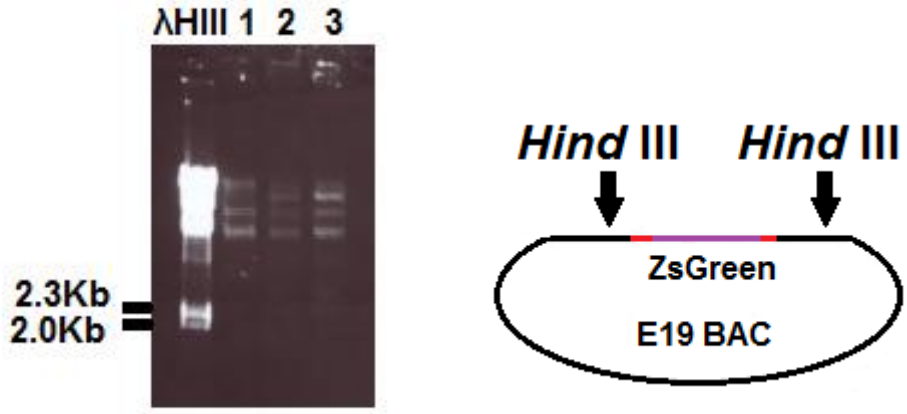


Figure 4.16 The drawing demonstrates the position of *Hind* III restriction site that will release a 10Kb band including the approximate 1Kb band of ZsGreen cassette for further analysis by blotting. *Hind* III cuts the E19 Clu-BAC 16 times but does not cut the ZsGreen cassette. The gel picture on the left demonstrates 3 *Hind* III BAC DNA digests (lane 1-3) on gels. λHIII: the HindIII digest of lambda DNA used as a DNA ladder.

From the dot blot membrane some colonies were chosen for further analysis by PCR, but again no positive clones were detected. However, the colony hybridisation membranes looked more promising and some of the clones produced strong signals which again were collected and analysed by PCR (Figure 4.17).

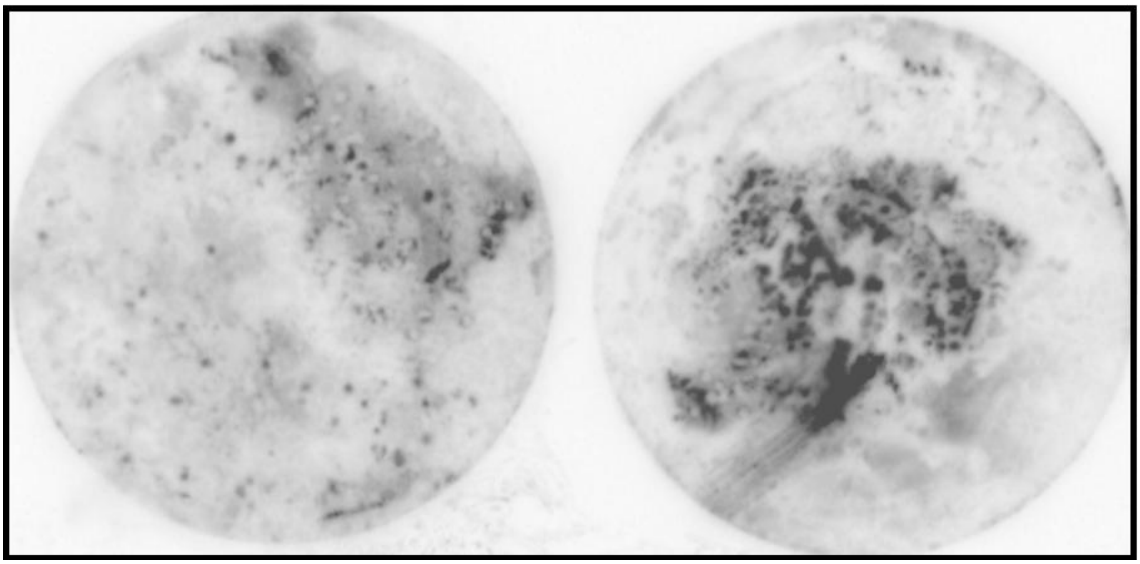

Figure 4.17 Colony blot analysis of clones collected from step 3 of recombineering which are hybridised against a ZsGreen $^{32}$P labelled probe. Only 2 out of 12 membranes are shown.

**PCR analysis of recombineeing clones from step "Recombineering of ZsGreen in the clusterin BAC"**

Miniprep DNA was prepared from 24 clones showing stronger hybridisation signals in the dot blot screen followed by PCR analysis listed below:

- PCR analysis across the 3' arm of homology
- PCR analysis using clusterin intron 2 oligonucleotides
- PCR analysis across the 5' arm of homology
- PCR analysis of Bglobin-ZsGreen insert using oligos containing the 50bp homology arms
- PCR analysis at the extreme ends of the ZsGreen Clu BAC

**PCR analysis of the 3' arm of homology**: oligonucleotides were designed to amplify a 1245bp product across a correctly integrated 3' arm of homology. Oligonucleotides were from the clusterin intron 2 (R221-Clu int2) and a forward oligonucleotide from the ZsGreen ORF (ZsG3) (2.4.4 and Figure 4.15C). Clones 509 and 511 from first colony blot screen, and clones 514-521 from the second colony blot screen produced the expected band size of 1245bp (Figure 4.18 and 4.19).

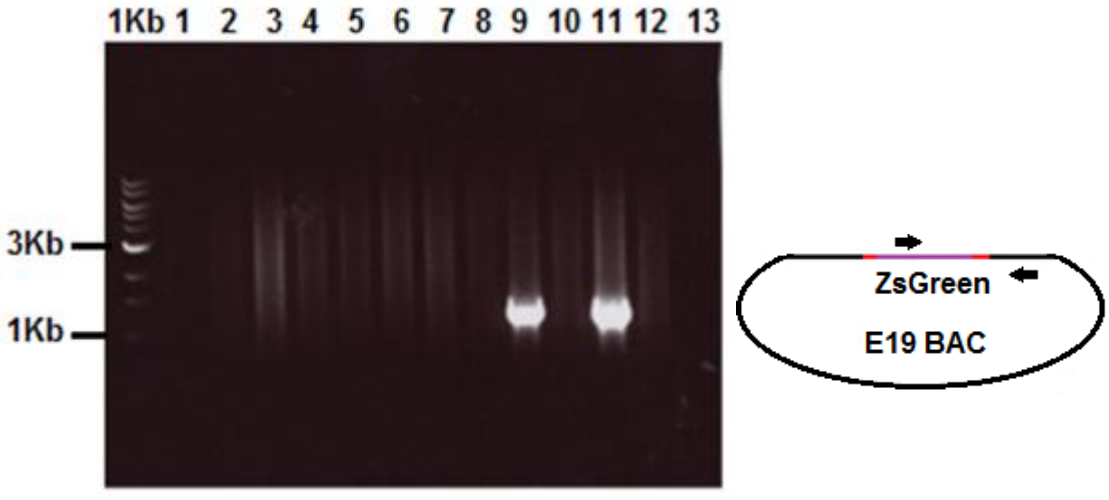


Figure 4.18 PCR analysis of 3' arm of homology using ZsG3 forward and R22-Clu int2 reverse oligos. *Lane 1-12*: clone 501-512. *Lane 13*: No DNA negative control. Clones 509 and 511 generated the expected band of 1245bp. The thumbnail shows the oligonucleotides positioned across the 3' arm. 1Kb: the 1Kb DNA ladder.

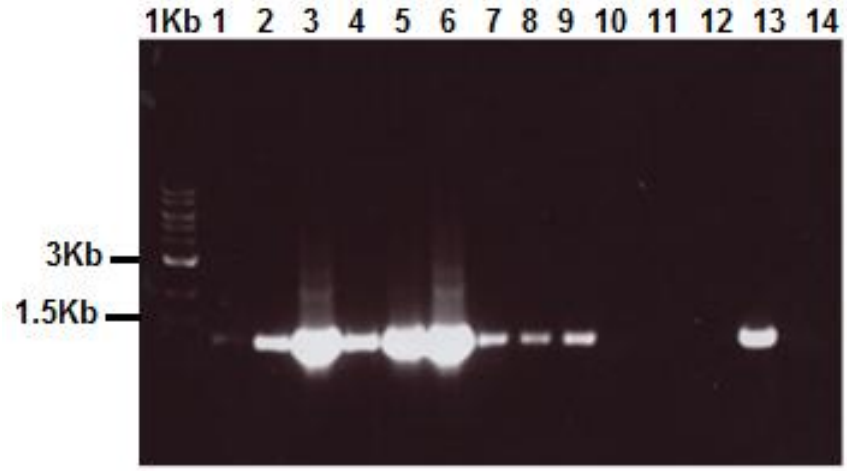


Figure 4.19 PCR analysis of clones collected from the replica plates after colony blot analysis using ZsG3 forward and R22-Clu int2 reverse oligos. *Lane 1-12*: clone 513-524. *Lane 13*: Clone 509 from the previous gel as positive control. *Lane 14*: No DNA negative control. The strong bands (3,5 and 6) were potential successfully recombined clones. The other lanes also demonstrated the same size but less intense band which either represent successfully recombined clones or contamination from clones of lane 3,5 and 6. 1Kb: the 1Kb DNA ladder.

**PCR analysis using clusterin intron 2 oligonucleotides:** Clu intron 2 forward and reverse oligos (F321-Clu int2 and R221-Clu int2) (2.4.4) from outside of the homology arms were used to analyse clones 509 and 511 previously identified as possible ZsGreen replacements (Figure 4.16C and 4.18). Clone 510 that failed to generate the diagnostic band was used as a negative control. These oligonucleotides are predicted to amplify either a 1622 (replacement) or 1856bp (non-replacement but containing rpsL-neo) PCR products (Figure 4.20 and 4.21).

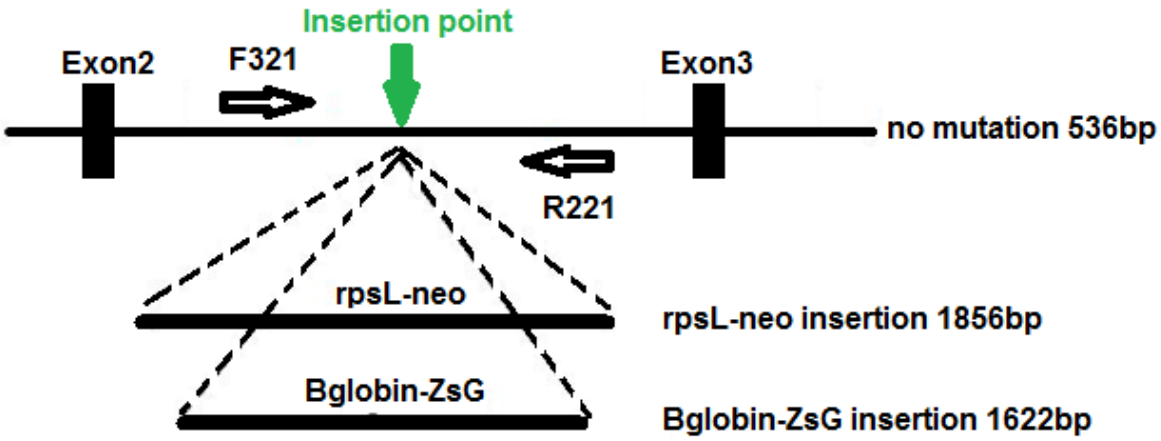


Figure 4.20 Schematic of PCR analysis using oligonucleotide intron 2 forward and reverse. When oligos outside the homology arms were used different band size were expected. For the un-modified E19 Clu-BAC this is 536bp, for the rpsl-neo Clu-BAC this is 1856 and for rpsl-neo ZsGreen Clu-BAC this is 1622bp. The green arrow indicates the insertion point for either rpsL-neo or Bglobin-ZsGreen cassette.

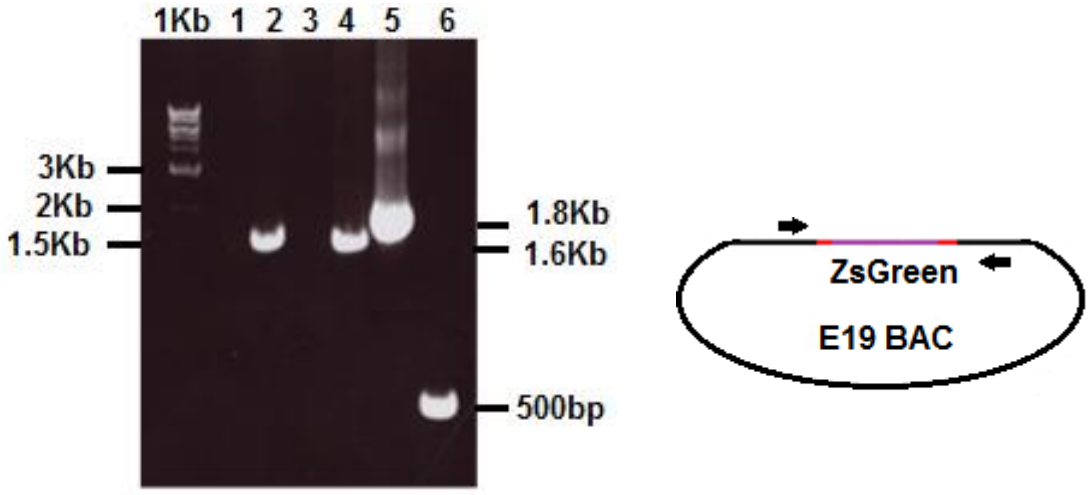


Figure 4.21 PCR analysis using oligos from outside the homology arms. *Lane 1*: No DNA negative control. *Lane 2, 3 and 4*: Clone 509, 510 and 511 respectively. *Lane 5*: rpsL-neo Clu-BAC. *Lane 6*: Unmodified E19 Clu-BAC. The expected band of about 1.6Kb is present for clones 509 and 511 which indicate the successful insertion of Bglobin-ZsGreen-SV40 cassette. 1Kb: the 1Kb DNA ladder.

**PCR analysis across the 5' arm of homology:** "F321-Clu int2" oligonucleotide that binds to clusterin intron 2 outside the homology arm and ZsG4 reverse oligo (2.4.4) that binds ZsGreen gene were used to analyse recombinant clones (Figure 4.15C). Insertion of ZsGreen would lead to amplification of a 950bp DNA fragment; no fragment would be amplified without insertion. The expected band of 950bp was present for clones 509 and 511 (Figure 4.22).

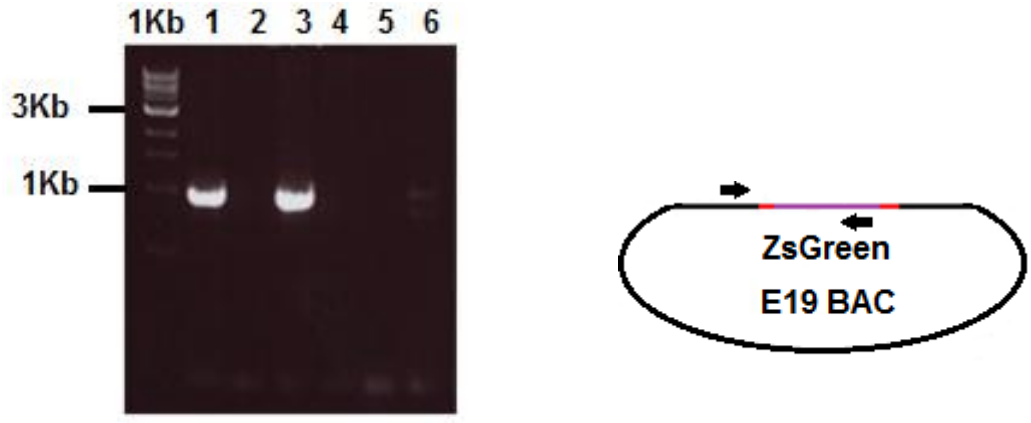


Figure 4.22 PCR analysis of 5' arm of insertion using "F321-Clu int2" and "ZsG4" oligos. *Lane 1*: Clone 509. *Lane 2*: Clone 510. *Lane 3*: Clone 511. *Lane 4*: Unmodified E19 Clu-BAC. *Lane 5*: No DNA negative control. *Lane 6*: rpsL-neo Clu-BAC. 1Kb: 1Kb DNA ladder

**PCR analysis across the entire Bglobin-ZsGreen insert using oligos including the 50bp homology arms**: Next using ZsGreen-HR forward and ZsGreen-HR reverse

oligos (used to amplify ZsGreen cassette for preparing linear insert), The entire predicted 1186bp Bglobin-ZsGreen band was amplified (2.4.3, Figure 4.23 and Figure 4.15C) for clone 509 and 511 but not clone 510.

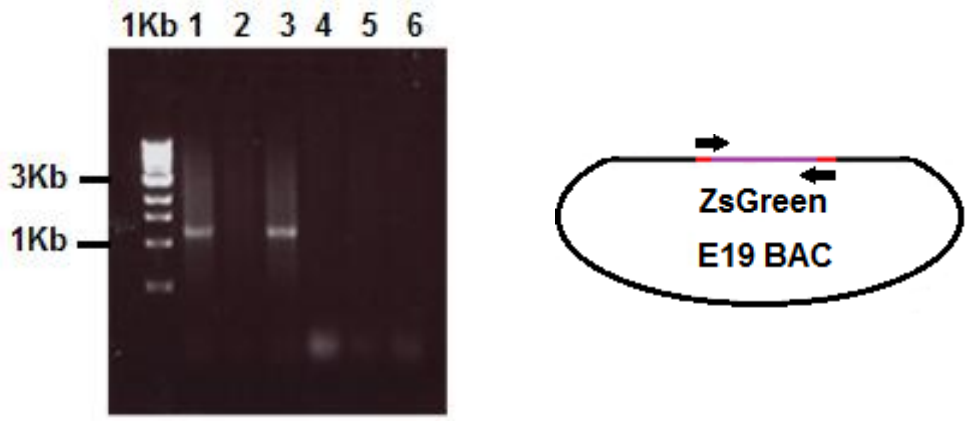


Figure 4.23 PCR analysis of clones using oligos with 50bp homology arms. *Lane 1-3*: clone 509-511. *Lane 4*: Unmodified E19 Clu-BAC. *Lane 5*: rpsL-neo Clu-BAC. *Lane 6:* No DNA negative control. 1Kb: 1Kb DNA ladder.

**PCR analysis at the extreme ends of the ZsGreen Clu-BAC:** In order to ensure that the entire 5' and 3' BAC sequences were still present in ZsGreen Clu-BAC and had not been rearranged/lost, oligonucleotides pairs (FClu-begin/RClu-begin) and (FClu-end/RClu-end) were used (2.4.5) and the predicted products of 1234bp from the 5' end and 742bp from the 3' end of the clusterin BAC were generated for clones 509 and 511 (Figure 4.15A and 4.24).

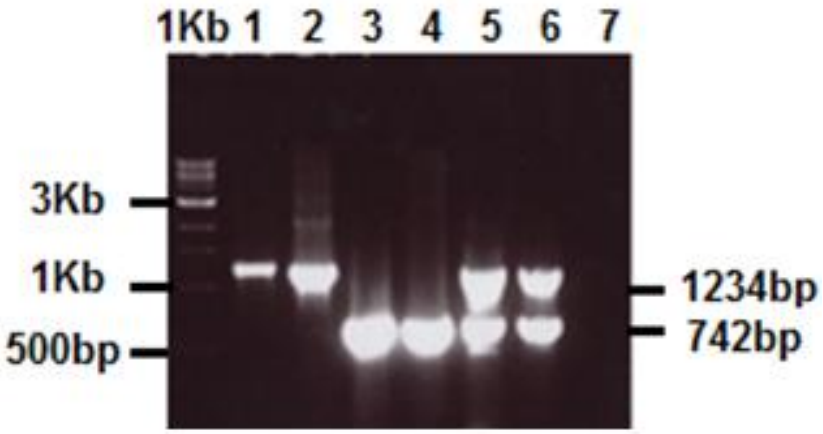


Figure 4.24 Checking the extreme ends of the ZsGreen Clu BAC. *Lane 1*: clone 509 and 5' end oligos. *Lane 2*: Clone 511 and 5' end oligos. *Lane 3*: Clone 509 and 3' end oligos. *Lane 4*: Clone 511 and 3' end oligos. *Lane 5*: Unmodified E19 Clu-BAC and 5' and 3' end oligos in a multiplex PCR. *Lane 6*: rpsL-neo Clu-BAC and 5' and 3' end oligos in a multiplex PCR. *Lane 7*: No DNA negative control. 1Kb: 1Kb DNA ladder.

Although the correct band sizes were produced, sequencing was also used to confirm the correct sequence-specific integration of the Zsgreen cassette. Clones 509 and 511 were sent for sequencing to MWG-operon. However the sequencing reactions failed on three separate occasions using the R221-Clu int2, F321-Clu int2, and R221-Clu int2 oligonucleotides as sequencing primers (2.4.4). Next a larger scale prep sent for sequencing was once again assayed using the "integrity oligos" used for confirming intron-exon structure, but this revealed that this larger scale preparation had undergone some rearrangement (Figure 4.25 compare to Figure 4.7 A and B) since multiple bands were formed for some primer pairs.

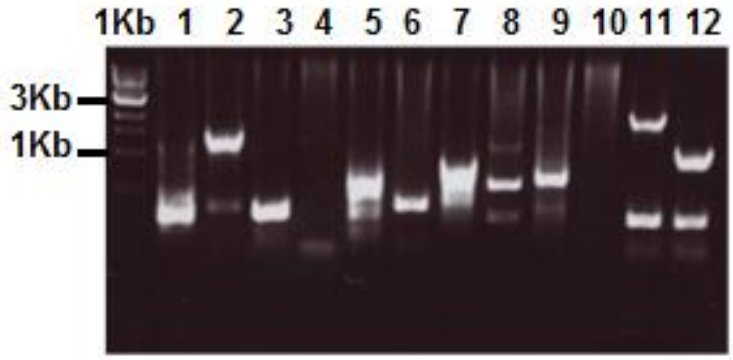


Figure 4.25.PCR analysis of integrity of clusterin gene insert of clone 509. *Lane 1-9*: Integrity oligo pair 1-9. *Lane 10*: No DNA negative control and oligo pair 3. *Lane 11*: rpsL-neo Clu-BAC and oligo pair 3. *Lane 12*: Unmodified E19 Clu-BAC and oligo pair 3. 1Kb: 1Kb DNA ladder.

Therefore, an additional 12 clones were rescued from glycerol stocks and analysed using a variety of PCR analysis prior to sequencing (data not shown but using primer pairs presented above). One clone (clone 527) that constantly produced the expected band was chosen and assayed with the "integrity oligos" before (data not shown) and after (Figure 4.26) large scale preparation of BAC DNA for sequencing. Expected bands were amplified (Figure 4.26) as in the original BAC (Figure 4.7 A and B) but without the spurious amplicons generated from clones 509/511 (Figure 4.25).

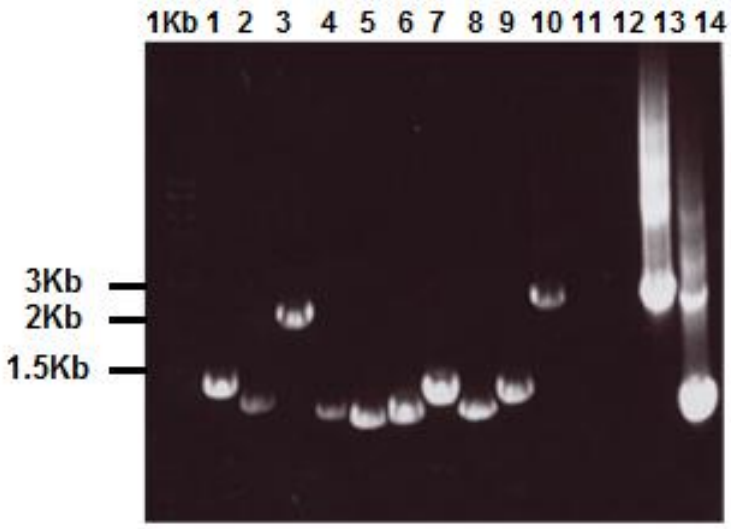


Figure 4.26 PCR analysis of integrity of clusterin gene insert of clone 527. *Lane 1-9*: Integrity oligo pair 1-9. *Lane 10*: rpsL-neo Clu-BAC and oligo pair 3. *Lane 11*: No DNA negative control. *Lane 12*: Blank. *Lane 13*: rpsL-neo Clu-BAC and oligo pair 3. *Lane 14*: Unmodified E19 Clu-BAC and oligo pair 3. 1Kb: 1Kb DNA ladder.

The left arm of insertion was again checked using "F321-Clu int2 and ZsG out" and "F321-Clu int2 and ZsG4" sets of oligos and the expected band of 527bp and 950bp were present respectively for the midiprep of clone 527 (Figure 4.15C and 4.27).

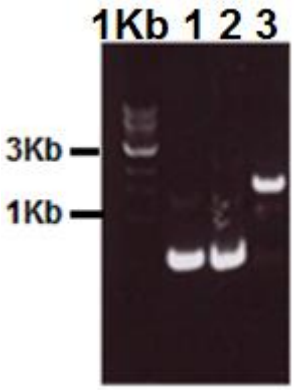


Figure 4.27 PCR analysis of clone 527 after midiprep. *Lane 1*: Midiprep of clone 527 and oligos F321-Clu int2 and ZsG out. *Lane 2*: Miniprep of clone 527 and oligos F321-Clu int2 and ZsG out as a control. *Lane 3*: Midiprep of clone 527 and oligos F321-Clu int2 and ZsG4. 1Kb: 1Kb DNA ladder.

Finally, using oligos outside the right homology arm (For-seq int2 and Rev-seq int2) (2.4.15) ZsGreen Clu-BAC clone 527 was successfully sequenced and the correct and precise insertion of ZsGreen reporter cassette into intron 2 of clusterin was confirmed and DNA was prepared for egg microinjection as detailed in 2.1.17.

## 4.6 Generation of a clusterin-Cre recombinase BAC by recombineering

The reporter BAC generated above is designed to potentially capture all regulatory elements responsible for inner ear expression of clusterin. As shown in chapter 3, clusterin mRNA expression is downregulated in the inner ear after postnatal day 2. Therefore simply following reporter expression will not permit the adult cells that have expressed clusterin during their development to be identified. However, such lineage tracing can be carried out by genetically marking cells using the Cre-lox system with a silent reporter mouse. In order to use this technology for clusterin the design of this particular experiment was to insert the Cre recombinase coding region into the clusterin BAC at the identical location to where the ZsGreen reporter was inserted as detailed above. Integration in intron 2 would however not lead to expression since first a basal promoter needed to be positioned upstream of the Cre recombinase ORF as well as downstram polyadenylation signals and these transcriptional control sequences were first added to Cre recombinase.

### 4.6.1 Generation of the "Bglobin promoter-Cre recombinase-SV40 polyA cassette"

The intermediate BAC for insertion of the Cre cassette had already been generated above (4.5.2.2) where rpsL-neo was inserted into intron 2.

In order to prepare Bglobin-Cre-SV40 template, the 120bp "human Bglobin minimal promoter" and 1.1Kb "Cre" cassette were separately sub-cloned into Spe-β-globinZsgreen vector (Appendix VI.II) next to the SV40 pA (Figure 4.28). This vector was then used as template in the PCR reactions for the preparation of Bglobin-Cre-SV40 pA cassette with homology arms.

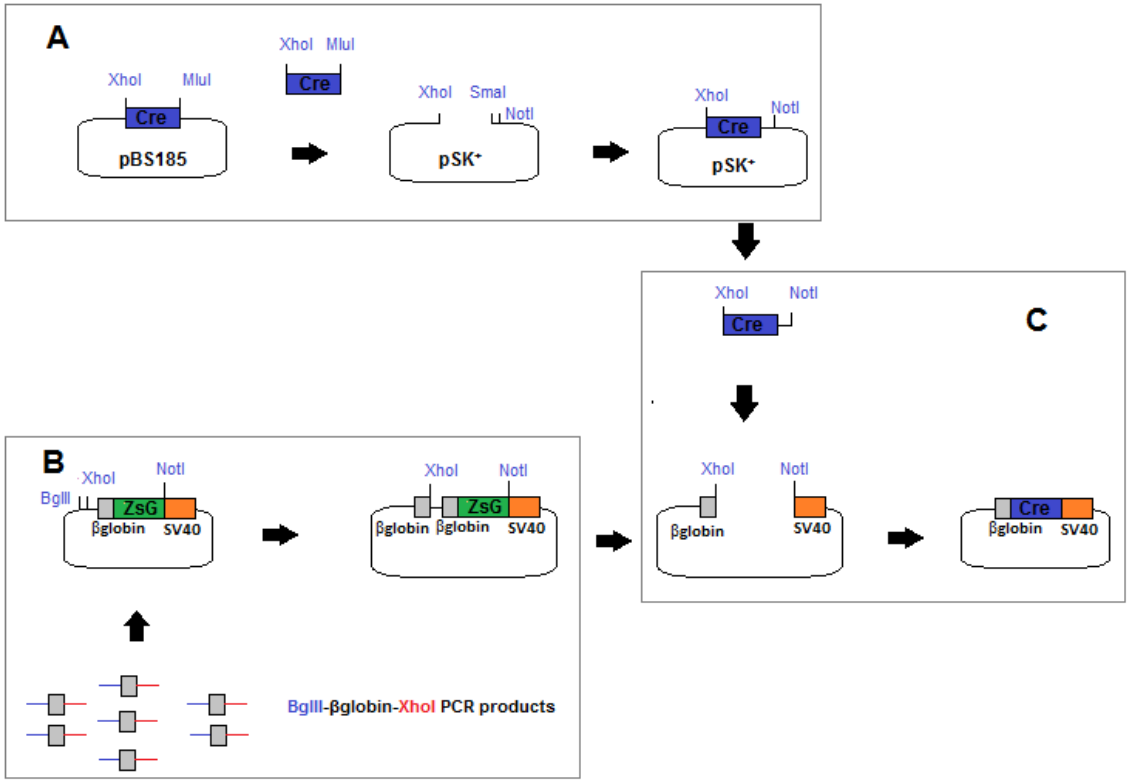


Figure 4.28 Schematic representation of cloning steps for preparation of human beta-globin-Cre-SV40 cassette. **(A)** Plasmid pBS185 (Cre Expression vector) was digested with MluI and blunt ended by end filling of the ends and then was digested with XhoI to release the 1.1Kb Cre fragment and then was cloned into pSK$^{+}$. **(B)** PCR amplification of human βglobin minimal promoter and introduction of BglII and XhoI sites to the beginning and end of PCR products followed by cloning into Spe-β-globinZsgreen vector **(C)** The double digested Cre was cloned into the XhoI-NotI sites of the clone from step B.

### 4.6.1.1 Cloning of the Bglobin-Cre cassette into a Spe-β-globinZsgreen vector

The strategy adopted was to isolate the Cre ORF using XhoI and MluI sites (with the latter filled in) and this was first cloned into bluescript. Next, PCR mutagenesis was carried out to generate 120bp BglII-Bglobin-XhoI promoter and then subcloning this promoter into Spe-β-globinZsgreen vector. This vector was then used for subcloning of Cre ORF between the newly introduced Bglobin and the existing SV40 pA of Spe-β-globinZsgreen (Figure 4.28).

**Step 1:** A XhoI- MluI(blunted) 1Kb fragment of pBS185 containing Cre was cloned at XhoI- SmaI sites of a pBluescript SK$^{+}$ (Figure 4.28A).

pBS185 Cre (Appendix VI.III) was digested with MluI restriction enzyme and run on a gel to confirm digestion was complete (data not shown). The MluI ends were end-filled using T4 DNA polymerase (2.1.1) and purified by gel extraction. Next the MluI filled in fragments was digested with XhoI and once again purified by isolating a 1Kb fragment from an agarose gel. This Cre ORF was cloned into pBluescript $Sk^+$. pBluescript was digested with SmaI (a blunt-end producing endonuclease) and XhoI and purified from an agarose gel. Concentrations of vector and insert were determined (2.1.3.3) and ligations were set up in vector:insert ratios 1:1, 1:3, 1:5 and a vector only control (1:0).

Ligations were transformed into super competent DH5α *E. Coli* cells (2.1.3.5) and plated on LB Ampicillin. 12 single colonies were picked and DNA prepared (2.1.14). For screening clones, miniprep DNAs were digested with *EcoR* V since *EcoR* V cuts the Cre ORF once, to linearise a fragment of 4.1Kb if successfully cloned. The pBluescript $Sk^+$ will also be cut only once with *EcoR* V (but is lost in the Cre-pBluescript $Sk^+$). From this analysis, 9 clones demonstrated a 4.1Kb band (Figure 4.29).

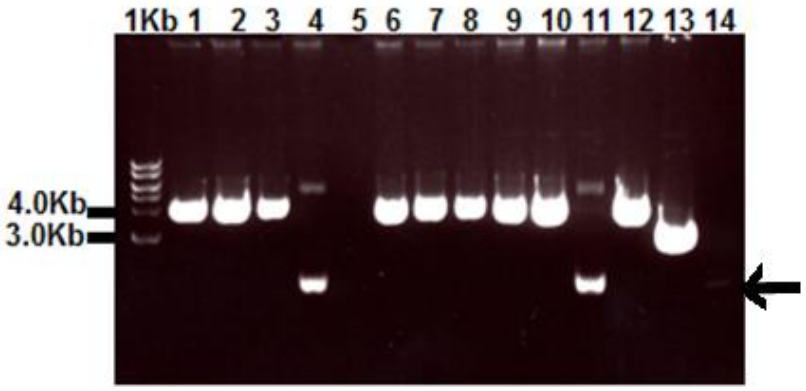


Figure 4.29 Analysis of clones from insertion of Cre ORF into pBluescript $SK^+$ (step 1 of cloning of the Bglobin-Cre casstte into a Spe-β-globinZsgreen vector) by restriction digestion with *EcoR* V. *Lane 1-12*: Digested clone 66-77. *Lane 13: EcoR* V digested pBluescript $Sk^+$. *Lane 14:* Undigested pBluescript $Sk^+$. Clone 66, 67, 68, 71, 72, 73, 74, 75 and 77 produced a 4Kb band. The black line at the right side of the gel points to the uncut pBluescript $Sk^+$ band. 1Kb: 1Kb DNA ladder.

At the next step towards analysis of the miniprep samples, 5 of the samples were digested with XhoI to linearise the vector. As a control pBluescript $SK^+$ was also digested (Figure 4.30). XhoI cuts the Cre- pBluescript $SK^+$ and the pBluescript $SK^+$ only

once and respectively a band of about 4.0Kb and about 3.0Kb is expected and confirms the recombinant clones.

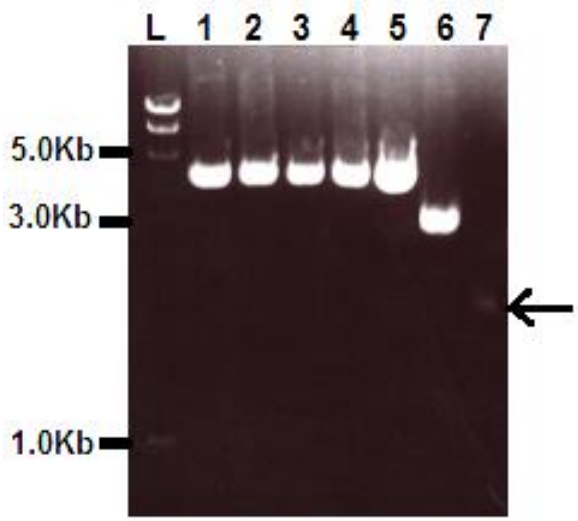


Figure 4.30 Analysis of positive clones from step1, by digestion with XhoI restriction enzyme. *Lane 1-5*: Clone 71-74 and 77 respectively. *Lane 6 and 7*: XhoI digested and undigested pBluescript $SK^+$ respectively. Clone 71-74 and 77 are linearised with *EcoR V* restriction enzyme and have a larger band than the XhoI digested pBluescript $SK^+$. The undigested band is highlighted with an arrow. L: Mass Ruler "Express forward DNA ladder mix".

A large scale midipreparation was made of the Cre-ORF intermediate clone 71. Then a XhoI- NotI double digestion was carried out to prepare enough DNA insert for the next step of cloning (step 3).

**Step 2**: 102bp Bglobin PCR products were cloned into BglII-XhoI Spe-β-globinZsgreen vector (Figure 4.28B).

A Spe-β-globinZsgreen vector containing the human Bglobin minimal promoter was used as template in a "mutagenesis" PCR. Forward and reverse oligos (Bglobin-BglII and Bglobin-XhoI, 2.4.6) were designed so that BglII and XhoI are introduced to the 5' and 3' ends of Bglobin PCR products respectively. Phusion high-fidelity DNA polymerase was used to amplify ~122bp BglII-Bglobin-XhoI PCR products. PCR products were checked on agarose gel before double digestion with BglII and XhoI followed by gel extraction.

Spe-β-globinZsgreen vector was also double digested with BglII and XhoI followed by gel extraction. Ligation reactions were then set up between BglII-Bglobin-XhoI PCR

products and BglII-XhoI Spe-β-globinZsgreen vector for 1:1, 1:3, 1:5, 1:10 and a vector only control (1:0).

Ligations were transformed into super competent DH5α *E. Coli* cells (2.1.3.5) and plated on LB Kanamycin. 12 single colonies were picked and DNA prepared (2.1.15). For screening clones, miniprep DNAs were double digested with BglII and NotI restriction enzymes. Spe-β-globinZsgreen vector was also double digested as a control. The expected bands are 3.2Kb and either 985bp in case of successful cloning of an additional copy of the promoter, or 885 if there is no insert. Only one of the clones demonstrated the 3.2Kb and the 985bp bands (Figure 4.31 lane 2). The rest of the clones had the 3.2Kb band and a band smaller than 985 (probably the 885).

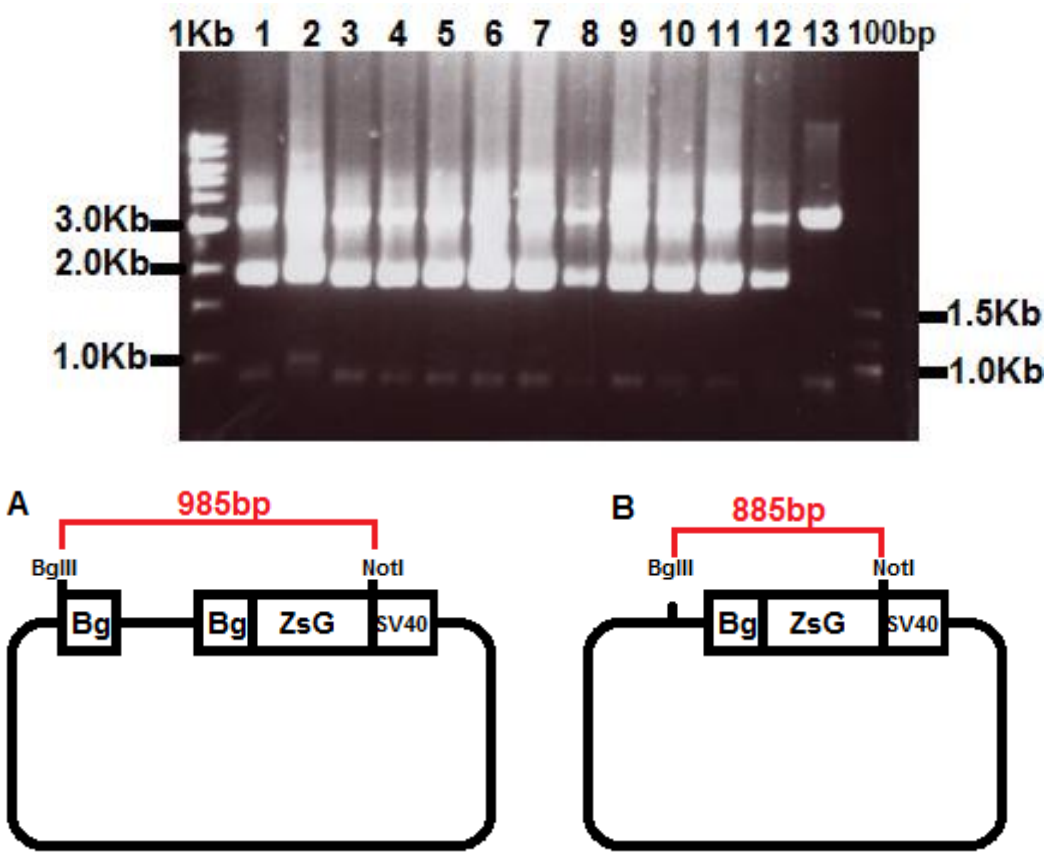


Figure 4.31 Analysis of clones by digestion with BglII and NotI restriction enzymes. *Lane 1-12:* Clone 1-12. *Lane 13*: BglII and NotI digested Spe-β-globinZsgreen vector as a control. All the clones released the same band of about 1.0Kb as control apart from clone 2 that released a larger band closer to 1.0Kb than the control. The drawings illustrate the band sizes released after double digestion with BglII and NotI restriction enzymes in case of second β-globin insertion (A) or no insertion (B). Bg: Human Bglobin minimal promoter. There is a band of about 2.0Kb in lane 1-12 which is a non-specific band probably representing the undigested supercoiled plasmid. 1Kb and 100bp: the 1Kb and the 100bp DNA ladder respectively.

This clone was further analysed by PCR using the forward and reverse oligos (**Bglobin-BglII** and **Bglobin-XhoI**, 2.4.6) (oligo also used for introducing BglII and XhoI restriction sites into Bglobin cassette). Spe-β-globinZsgreen vector together with another two miniprep DNAs which failed to generate the expected band sizes in previous digestion were used as controls. Clone 2 again successfully generated the expected two 102 and 271bp bands whereas the control (Spe-β-globinZsgreen vector) did not generate the 271bp band (Figure 4.32) but only the 102 amplicon.

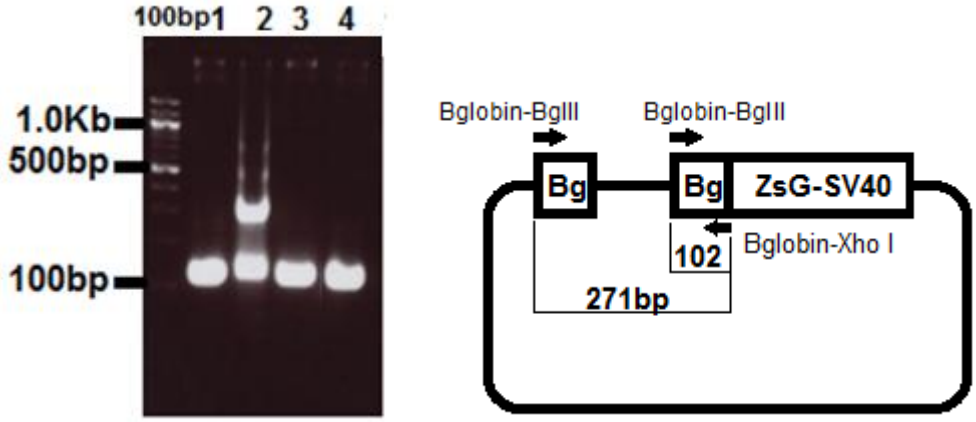


Figure 4.32 PCR analysis of "BglII-Bglobin-XhoI" insertion into the Spe-β-globinZsgreen vector using Bglobin-BglII and Bglobin-XhoI as respectively forward and reverse oligos. *Lane 1-3:* Clone 1-3. *Lane 4:* Spe-β-globinZsgreen vector as a control. Only clone 2 produced the 271bp band demonstrating the Bglobin insertion. The drawing illustrates the production of 102 and 271bp bands in this PCR. 100bp: the 100bp DNA ladder.

Final confirmatory analysis of this clone was carried out by double digestion of this clone with BglII and XhoI restriction enzymes to release the newly introduced Bglobin insert. The Spe-β-globinZsgreen vector control again was included. The expected band of 102bp again was generated only by clone 2 (Figure 4.33).

A midiprep was then carried out to prepare enough vector DNA for the next step of cloning.

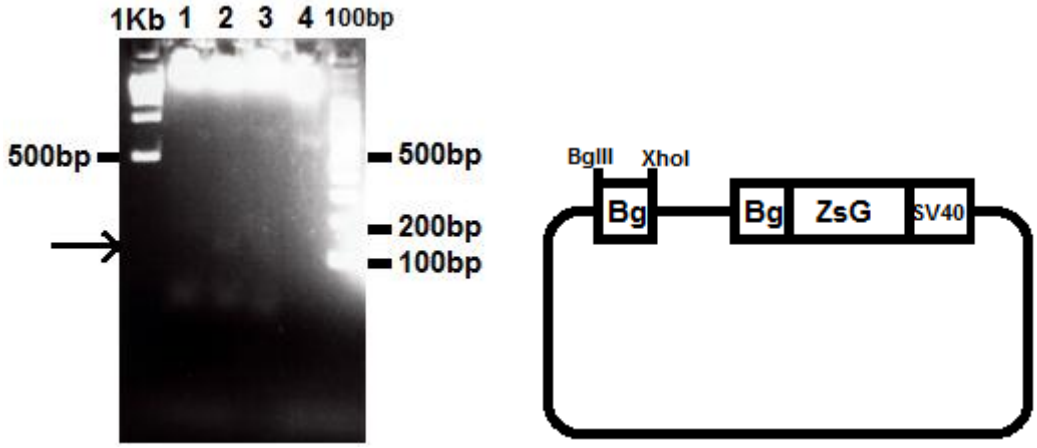


Figure 4.33 Analysis of clones by digestion with BglII and XhoI restriction enzymes that will release the BglII-Bglobin-XhoI insert. *Lane 1-3*: Clone 1-3. *Lane 4*: Digested Spe-β-globinZsgreen vector as a control. Note the released about 102bp band for clone 2 which is not present for the control vector or other clones examined (this band is highlighted with an arrow). 1Kb and 100bp: the 1Kb and the 100bp DNA ladder respectively.

**Step 3**: Cloning of XhoI-Cre-NotI into XhoI-NotI vector obtained from step 2 (Figure 4.28C).

The pBluescript $SK^+$.Cre clone from step 1 was double digested with XhoI and NotI restriction enzymes and gel extracted. Also, the clone from step 2 was similarly double digested with XhoI and NotI followed by gel extraction of the vector backbone. The ligation reactions were then set up between the 1123bp XhoI-Cre-NotI products and the 3215bp XhoI-NotI vector for 1:1, 1:3, 1:5 and a vector only control (1:0). Ligations were transformed into super competent DH5α *E. Coli* cells (2.1.3.5) and plated on LB Kanamycin.

12 single colonies were picked and DNA prepared (2.1.14). For screening clones, miniprep DNAs were double digested with XhoI and NotI to release the Cre insert. The expected bands are 3215bp for the vector and 1123bp for the Cre insert (Figure 4.34). 10 of the clones generated the expected bands thus confirming the Cre insertion.

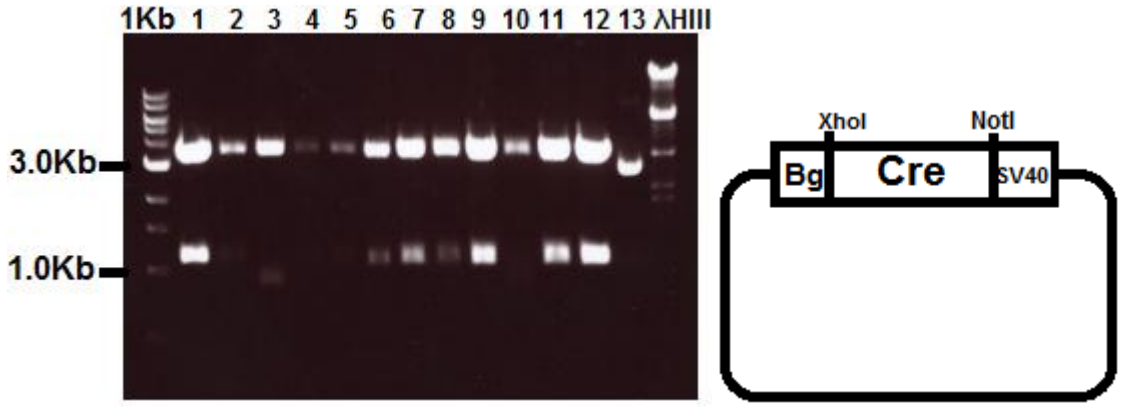


Figure 4.34 Analysis of clones obtained from step 3 by digestion with XhoI and NotI restriction enzymes which releases the Cre insert. *Lane 1-12:* Clone 1-12. *Lane 13*: Undigested clone 1 as a control. Clone 1,2,4,5,6,7,8,9,11 and 12 produced the expected band of about 1.1Kb for Cre. The drawing illustrates the XhoI and NotI restriction sites. 1Kb: the 1Kb DNA ladder. λHII: the λHindIII digest of lambda DNA.

These clones were further analysed by PCR using a forward oligonucleotide that binds to the Bglobin promoter (**bglobin-BglII**) and a reverse oligonucleotide (**CreORFR1**) that binds to Cre to generate 1192bp DNA fragments. Obtained clone from step 2 was used in this experiment as a negative control (2.4.7 and Figure 4.35). 5/7 clones produced the expected band confirming the insertion of XhoI-Cre-NotI into XhoI-NotI vector obtained from step 2. These vectors now contain "Bglobin-Cre-SV40 pA" cassette necessary for the recombineering of Cre.

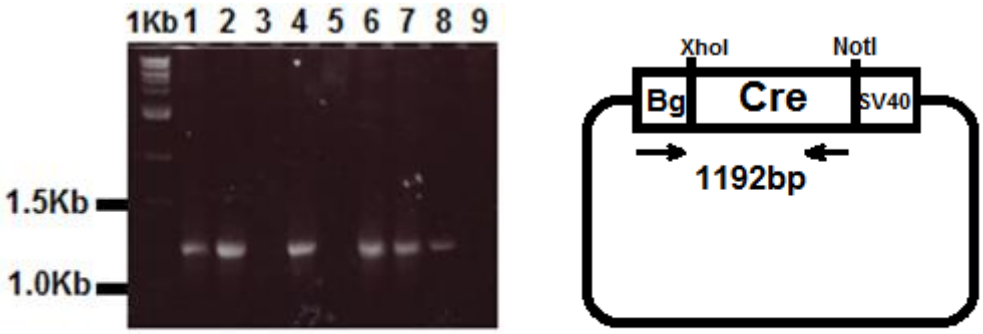


Figure 4.35 PCR analysis of clones obtained from step 3 using Bglobin-BglII and CreORFR1 oligos. *Lane 1-7*: clone 1-3 and 9-12 respectively. *Lane 8:* No DNA negative control. *Lane 9:* A clone from step 2 as a control. Clone 1,2,9,11 and 12 produced the expected band of about 1.2Kb. 1Kb: the 1Kb DNA ladder.

The DNA midiprep was carried out, the clone was sequenced and verified and used as template in PCR reactions to produce a linear "Bglobin-Cre-SV40 pA" with 50bp homology arms for the Cre recombineering.

### 4.6.2 Recombineering of Cre recombinase into the clusterin BAC

Oligonucleotides (HRCre-for and HRCre-rev) were designed that contained the same 50bp homology arms to clusterin intron 2 as successfully used earlier, together with Bglobin and SV40 sequences. These were used to amplify a linearised product from the Bglobin-Cre-SV40 plasmid generated above. Using the optimised protocol defined in 4.5.2.3 this was used for recombineering experiments as optimised earlier in this chapter.

#### 4.6.2.1 Induction of the Red/ET recombination genes

Single colonies of rpsL-neo Clu-BAC intermediate (4.5.2.4) were obtained by streaking a glycerol stock on LB agar plates containing Chloramphenicol, Kanamycin and Tetracycline. Cultures were grown and either induced or uninduced with arabinose (2.1.18.4) and were made electrocompetent (2.1.18.4).

Linear Bglobin-Cre-SV40 cassette was prepared using Phusion High fidelity DNA polymerase. The 1.2Kb linearised product was purified by gel electrophoresis and its concentration determined (2.1.3.3). 2-4µl (100-200ng) was electroporated into induced and uninduced electrocompetent cells and following the optimisation steps described in 4.5.2.3 was grown and subsequently plated on LB agar plates containing Chloramphenicol, Streptomycin and Tetracycline. Plates were incubated at 30ºC overnight.

#### 4.6.2.2 Identification and confirmation of recombined clones

The experiment was conducted twice. In the first attempt the ratio of induced to uninduced clones was approximately 1:1 but in the second attempt this ratio exceeded 5:1. Colonies from induced plates were grown in LB medium with Chloramphenicol, Streptomycin and Tetracycline. Small scale DNA preparations were carried out. PCR analysis was used to identify correctly engineered recombinant clones from a total of 100 clones.

**Clusterin intron 2 oligos (F321-Clu int2 and R221-Clu int2)** oligos were used as the first line of screening since these oligonucleotides bind to clusterin sequence outside the Bglobin-Cre cassette insertion point and either side of the clusterin homology arms (2.4.9 and Figure 4.39D). The predicted PCR products are 551bp for the unmodified Clu-BAC, 1800bp for the rpsL-neo intermediate BAC and 1772bp for correctly replaced Bglobin-Cre clusterin recombineered BAC.

Most of the clones examined by this PCR screen produced a band of about 1700-1800bp (Figure 4.36 data is shown only for 28 clones). This excluded any rearranged BACs or unmodified BACs from further analysis. However the 28bp size difference could not be determined from this analysis so additional PCR assays were carried out on these clones.

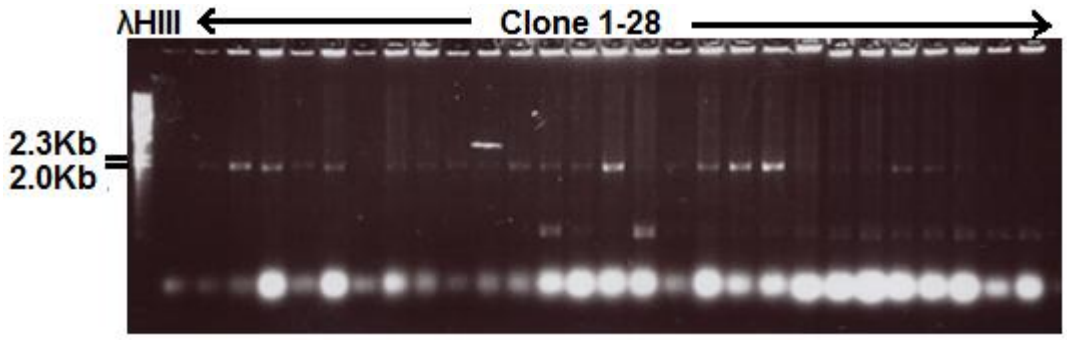


Figure 4.36 PCR analysis of clones obtained from recombineering of Cre recombinase in the clusterin BAC using F321-Clu int2 and R221-Clu int2 oligos. *Lane 1-28*: Clone 1-28. The clones with a band of about 2.0Kb were selected for further analysis. λHIII: the HindIII digest of lambda DNA.

Next, a combination of clusterin and insert-specific oligonucleotides were used.

**F321-Clu int2 and CreORFR1** oligonucleotides were used that will amplify across the 5' arm of recombination with an anchor in the Cre insert (Figure 4.16D). For successfully recombineered clones, the expected PCR product is 1442bp whereas no bands are predicted without Cre insertion. As can be seen from the gel (2.4.9 and Figure 4.37- data is shown only for some of the clones) there were multiple non-specific bands present for the clones examined. Therefore, attempts were made to adjust the PCR conditions including increasing the annealing temperature in an attempt to eliminate the non-specific bands but this did not prove successful (data not shown).

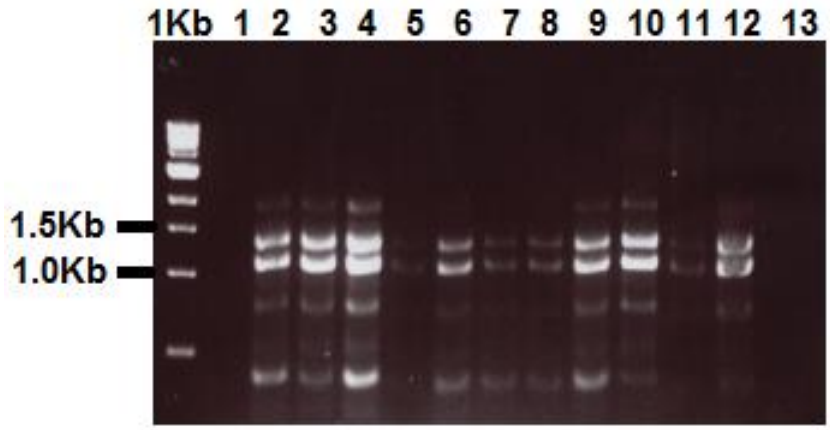


Figure 4.37 PCR analysis of some of the clones that produced the expected band from previous PCR analysis were further analysed using F321-Clu int2 and CreORFR1 oligos. Clones in lane 1-12 demonstrated some non-specific bands. 1Kb: the 1Kb DNA ladder.

A second recombineering experiment was carried out and 50 clones were examined again by PCR using a different set of oligos.

At this point it was noticed that the reverse primers that were designed for the amplification of "Bglobin-Cre-SV40 pA" linear DNA, were incorrectly designed and do not contain the SV40 sequence but rather contain the end of Cre ORF. The designed forward and reverse oligos therefore only amplify the"Bglobin-Cre" and not the "SV40 pA" and as a result the modified BAC contains the "Bglobin-Cre" rather than "Bglobin-Cre-SV40 pA". However, analyses of clones that had been recovered were carried out, bearing in mind that another recombineering experiment was later required to enter the "SV40 pA" next to the Bglobin-Cre cassette. The SV40 pA has 245bp (from 795-1040 in Spe-Bglobin-ZsGreen plasmid).

**Oligonucleotides 339-CreE** (designed against 3' region of the Cre ORF), and **R221-Clu int2**: were used to analyse the 3' recombineering event (2.4.9 and Figure 4.39D). These oligos are predicted to amplify a 1350bp band in correctly engineered BACs. 3 out of 50 clones demonstrated the correctly generated fragment (Figure 4.38). Positive clones, 75, 94 and 112 were further examined below.

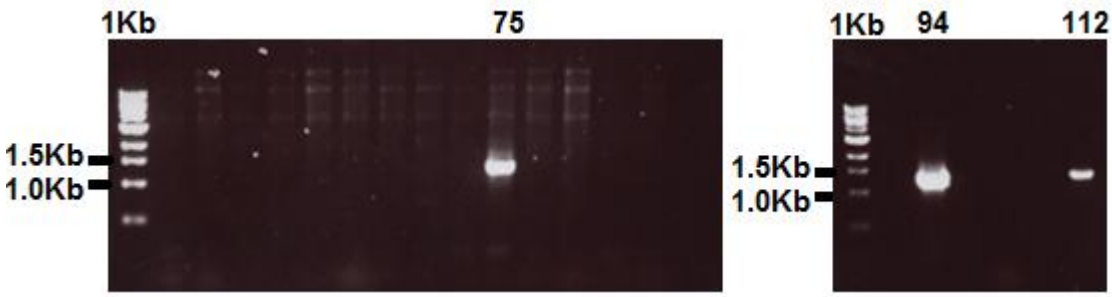


Figure 4.38 PCR analysis of Cre recombineering clones using 339-CreE and R221-Clu int2 oligos. Only clone 75, 94 and 112 generated the expected band size of about 1.3Kb. 1Kb: the 1Kb DNA ladder.

**339-CreE, CreORFR1** and **F321-Clu int2, CreORFR1 oligos** were used in a multiplex PCR reaction (2.4.9 and Figure 4.39D): in a single PCR reaction oligos were used for analysis of DNA miniprep of clone numbers 75 and 94. The expected bands of 1023bp and 1442bp (Figure 4.40) were present for both 75 and 94 clones. For the final confirmation of correctly inserted Bglobin-Cre another PCR using oligo **F321-Clu int2** and **R221-Clu int2** was carried out (2.4.9 and Figure 4.39D) and again the expected band of 1772bp was present for both 75 and 94 clones although very faint for clone 94 (Figure 4.41). The rpsL-neo Clu-BAC was also used in this PCR as a control however the expected band is about 1856Kb and therefore hard to distinguish from the generated band of 1772bp of Cre Clu-BAC. The expected band of 500bp was also generated from unmodified E19 Clu-BAC which was used as a control in this PCR.

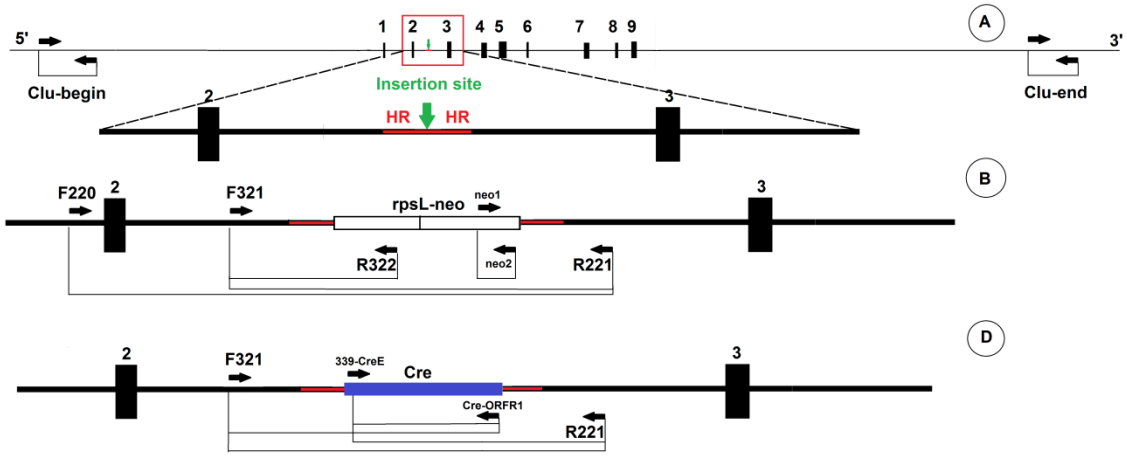


Figure 4.39 Schematic drawing overviewing the PCR analysis of Clu-BAC during the recombineering processes. A and B: unmodified Clu-BAC and rpsL Clu-BAC respectively (both are described in details in Figure 4.16). C: demonstrates the variety of primers used for the analysis of Cre recombinase cassette insertion in intron 2. The drawing is roughly to the scale. For the primer list and sequence see section 2.4. F321: F321-Clu int2 oligo, R221: R221-Clu int2 oligo.

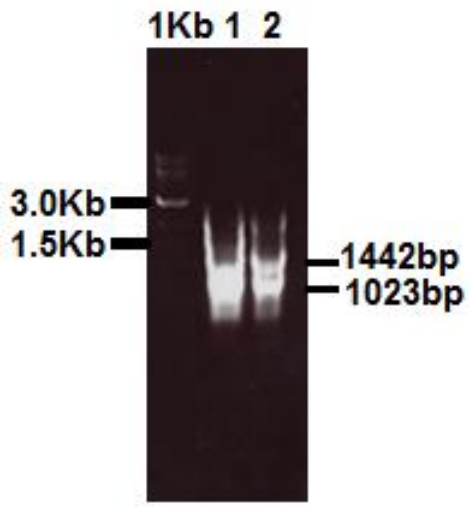


Figure 4.40 PCR analysis of clones 75 and 112 (Clu-Cre BAC) using F321-Clu int2 and 339-CreE as forward and CreORFR1 as reverse oligo in a multiplex PCR. *Lane 1 and 2*: Clone 57 and 94 respectively. The expected band sizes of about 1442 and 1023bp were produced for both clones. 1Kb: the 1Kb DNA ladder.

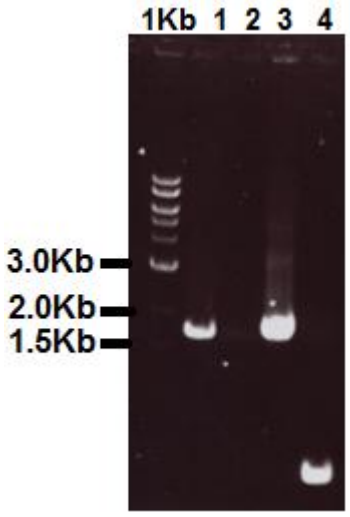


Figure 4.41 PCR analysis of clone 75 and 94 (Cre Clu-BAC) using oligo F321-Clu int2 and R221-Clu int2. *Lane 1 and 2*: Clone 75 and 94 respectively. *Lane 3*: rpsl-neo Clu-BAC. *Lane 4*: Unmodified E19 Clu-BAC which has generated the expected band of about 556bp. 1Kb: the 1Kb DNA ladder.

To test clones for any other rearrangement, the **"integrity oligos"** (2.4.1) were used to amplify products across the clusterin coding region at approximately 1Kb intervals (Figure 4.42). For some of the oligo pairs some non-specific products were present and increasing the annealing temperature for these oligos did not lead to the loss of these bands (Data not shown). Therefore, one conclusion could be that the two clones under analysis had undergone some additional rearrangement. Therefore, clone 112 was next

analysed as above. Clone 112 generated the predicted fragments for successful recombineering but also all predicted bands using the "integrity" oligonucleotide pairs to scan the clusterin gene (Figure 4.43).

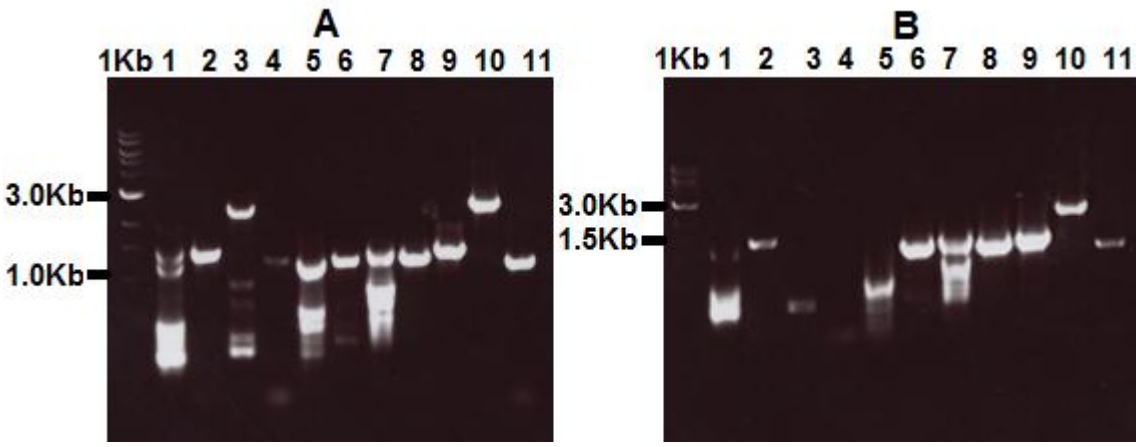


Figure 4.42 PCR analysis of clone 75 (A) and 94 (B) for the clusterin gene integrity using integrity oligos. *Lane 1-9* in A and B: represent DNA bands produced by primer pairs 1-9 respectively. *Lane 10* in A and B: rpsL Clu-BAC and oligo pair 3. *Lane 11* in A and B: Unmodified Clu-BAC and oligo pair 3. Some non-specific band for both clones is present. 1Kb: the 1Kb DNA ladder.

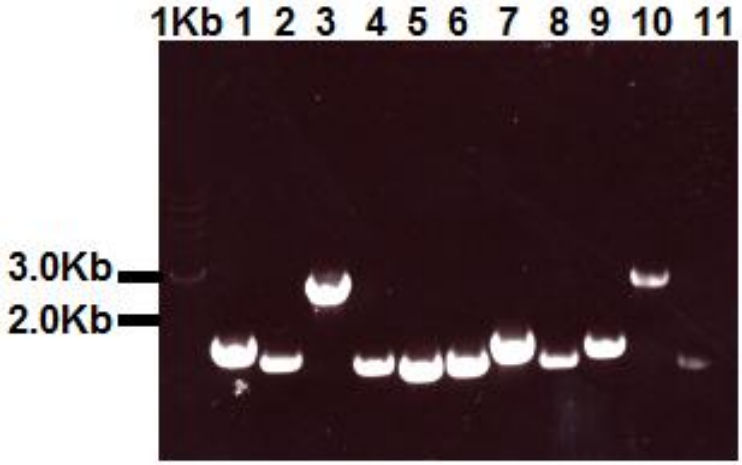


Figure 4.43 PCR analysis of clone 112 (Cre Clu-BAC) for the clusterin gene integrity using integrity oligos. *Lane 1-9*: Primer pairs 1-9 respectively. *Lane 10*: rpsL Clu-BAC and oligo pair 3. *Lane 11*: Unmodified Clu-BAC and oligo pair 3. All the expected bands are produced for clone 211. 1Kb: the 1Kb DNA ladder.

The fidelity of successful replacement of rpsl-neo cassette by Bglobin-Cre in clone 112 was finally confirmed by sequencing across the modified region, both 5' and 3' arms (data not shown).

### 4.6.3 Removal of loxP sites from BAC backbone and their replacement with selectable markers

Unfortunately it became apparent that the vector used in construction of the bMQ BAC library, pBACe3.6 also includes loxP sites. It was reasoned that these could be removed in *cis* by clusterin control of Cre recombinase and this could result in loss of the transgene upon activation of Cre. This would potentially complicate at best any lineage tracing of Cre-expressing cells and at worst, lead to failure to faithfully follow the fate of Cre lineage. Therefore, attempts were made to remove these loxP sites by additional modifications of the BAC sequentially *in vitro* using homologous recombination. The loxP site (at 4831-4864bp) was first replaced with a rpsl-neo cassette flanked by 50bp homology arms complementary to the vector sequence adjacent to the loxP site (Appendix VI.I). Subsequently, the mutant loxP site, (loxP511 site, at 11408-11441bp) in the pBACe3.6 vector backbone (Appendix VI.I) was to be replaced with another selectable marker such a LacZ gene flanked by 50bp homology arms complementary to the sequence adjacent to the loxP511 site. As will be explained below, the removal of loxP511 was not carried out as we still do not know whether E19 Clu-BAC contains the regulatory sequences necessary to drive the genes expression.

#### 4.6.3.1 Removal of loxP sites from pBACe3.6 vector backbone

Homologous recombination was carried out in an identical manner to the earlier recombineering events. The clusterin-Cre BAC was grown and induced and uninduced electrocompenet cells were prepared (2.1.18.4).

**A linear rpsl-neo cassette was prepared**: oligos were designed to include 50bp homology arms to either side of the loxP site, together with sequence from the 5’ end of rpsL and 3’ end of neo (2.4.10 and Figure 4.8B-D) and used to amplify a 1320bp rpsL-neo cassette using the supplied rpsL-neo plasmid (Counter selection BAC modification kit, Gene Bridges) as template and Phusion DNA polymerase. PCR products were purified by gel extraction and the concentration was determined.

100-200ng of the linear rpsl-neo cassette was electroporated and 24 colonies from induced plates were picked, DNA prepared and analysed by a variety of PCR assays.

### 4.6.3.2 PCR analysis of recombineeing clones following removal of loxP site

Oligonucleotides **pBACe95 and pBACe96** (2.4.11) were designed as flanking oligos from outside of the homology region used in recombination, and are predicted to amplify a 2020bp fragment following a successful insertion of rpsL-neo, or 734bp DNA band where an insert is not integrated between the oligonucleotides. In 8/24 clones, the 2020bp fragment was amplified (Figure 4.44). Although there are some non-specific bands present for some of the clones, however, clone 3,7,8,16,19,25,26, and 27 have clearly produced a band of about 2.0Kb.

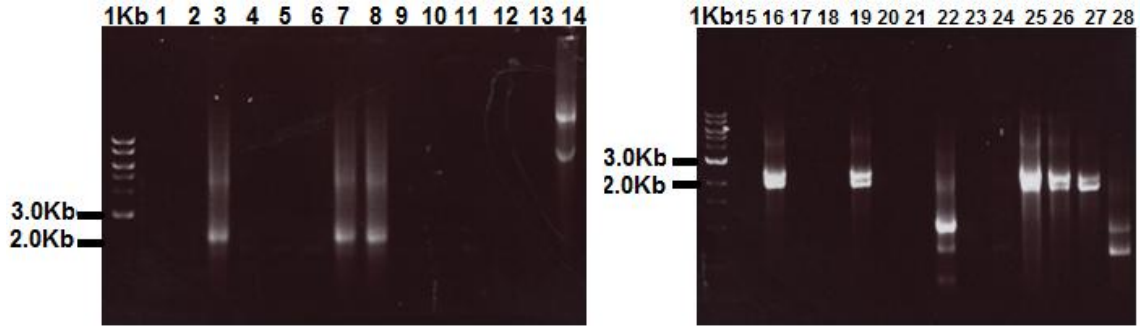


Figure 4.44 PCR analysis of clones for confirmation of loxP removal and its replacement with rpsL-neo cassette using pBACe95 and pBACe96 oligos. *Lane 1-13*: Clone 1-13. *Lane 15-27:* Clone 15-27. *Lane 14 and 28*: Cre Clu-BAC before loxP removal. Clone 3,7,8,16,19,25,26, and 27 have produced the expected band of about 2.0Kb band. 1Kb: the 1Kb DNA ladder.

Additional analysis involved the use of internal neo oligonucleotides, **F288-Neo1 and 289-Neo2**. These are predicted to amplify a 152bp neo fragment and this was detected in clones 3,7,8,16,19,25,26, and 27 (Figure 4.45).

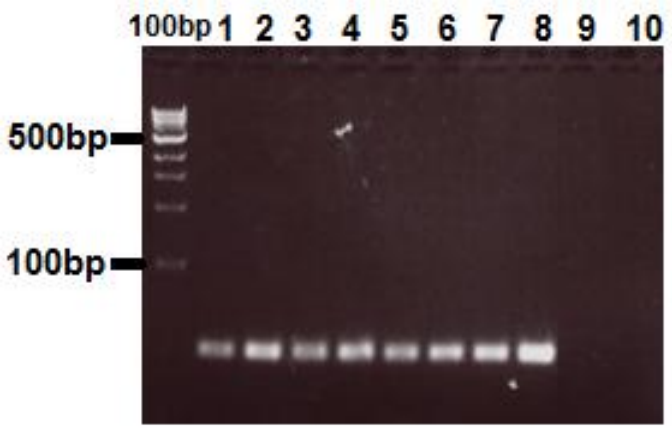


Figure 4.45 PCR analysis of clones for confirmation of loxP removal and its replacement with rpsL-neo cassette using F288-Neo1 and 289-Neo2 oligos. *Lane 1-8*: Clone 3,7,8,16,19,25,26, and 27 respectively. *Lane 9*: Cre Clu-BAC before loxP removal. *Lane 10:* No DNA negative control. 100bp: the 100bp DNA ladder.

Finally, oligonucleotides **pBACe95** and **R322-rpsL** were used to analyse the 5' arm of recombination. The expected PCR product will be 767bp. This was confirmed in clones 3,7,8,16,25,26, and 27 but not in clone 13 (Figure 4.46). Clone 3 that constantly produced the expected band in different PCR analysis was used for the next step (loxP511 removal).

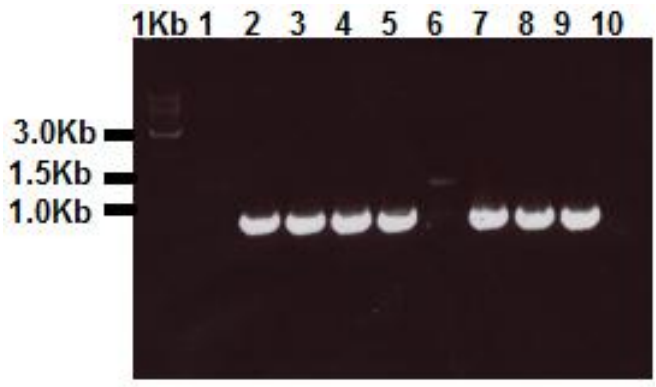


Figure 4.46 PCR analysis of clones for confirmation of loxP removal and its replacement with rpsL-neo cassette using pBACe95 and R322-rpsL. *Lane 1*: Cre Clu-BAC before loxP removal. *Lane 2-9:* Clone 3,7,8,16,19,25,26, and 27 respectively. *Lane 10:* No DNA negative control. 1Kb: the 1Kb DNA ladder.

### 4.6.3.3 Towards the replacement of loxP511 with a lacZ marker and replacement of Bglobin-Cre cassette with Bglobin-Cre-SV40 pA

As it is not reasonable to prepare the Cre Clu-BAC while we are not sure whether the E19 Clu-BAC contains the regulatory sequences to derive the expression of recombined genes (ZsGreen or Cre), the loxP511 was not removed. Once a pronuclear injection is successfully carried out and the transgenic mice are generated, the analysis of the mice will be carried to find out whether the reporter gene is activated in the inner ear and if so then the Cre recombineering would be useful for the generation of Cre transgenic mice and further experiments.

A strategy for the removal of the second loxP site in the pBACe3.6 vector backbone, LoxP511 (Appendix VI.I) could be to replace it with the lacZ (not selectable) marker. Confirmation of the ability of the different plasmids and host cells to not encode β galactosidase was tested by plating cells on LB agar plates with Chloramphenicol, Kanamycin, Tetracycline as well as Xgal/IPTG (Appendix I). Only white colonies were found demonstrating that the cells are not capable of bgalactosidase production.

HRloxP511-for and HRloxP511-rev oligonucleotides (2.4.12) and pBluescript II $SK^+$ vector DNA could be used to amplify 579bp lacZ gene and its promoter with 50bp homology arms complementary to the sequence adjacent to loxP511 site.

## 4.7 Discussion

### 4.7.1 Recombineering, its advantages and the available recombineering kits

Recombineering is a powerful new technique that uses phage derived recombination proteins to make genetic manipulation possible *in vivo*. Having many advantages over classical *in vitro* cloning methods, recombineering has become a popular tool for deletion, insertion and point mutation of genomic DNA in BACs and PACs for the subsequent generation of transgenic and knockout animals. Unlike traditional cloning methods there is no need for restriction enzymes or DNA ligases and therefore the availability of unique restriction sites in both genomic DNA and cloning vector is not a limiting factor. Using standard cloning methods, the size of DNA segment subject to manipulation is another limiting factor, as most cloning vectors either do not have the capacity or do not tolerate large DNA inserts whereas in recombineering large pieces of DNA can easily be manipulated *in vivo* (GENEBRIDGES technical protocol Feb 2005). In addition, unlike plasmid clones, BAC transgenes are more independent of positional effect variegation that can lead to undesirable expression patterns (Tian, James et al. 2006), since BACs/PACs carrying larger DNA fragments that can contain the entire gene and its flanking regulatory sequences to recapitulate endogenous expression pattern (Margaret L. Van Keuren and Saunders 2009).

The other advantage of recombineering is short homology requirements, and the technique can be used for the insertion of selectable or non-selectable markers (Shyam K. Sharan 2009). There are however some limitations of the technology for instance, manipulation within sequences that contain repeat sequences with short homology arms are difficult. Another limiting factor is that the sequence of the target area needs to be known, although this is not normally a limiting factor for most organisms that are commonly used. In addition, most of the substrate DNA is produced by PCR, and these

products can sometimes acquire mutations through amplification (Shyam K. Sharan 2009). Although this can be verified by sequencing to check the integrity of the amplicon, when the integrity of the entire insert is crucial (in this case the 5' upstream, Clu gene and the 3' downstream) this can become rather unwieldy to sequence a whole BAC. In addition, the high efficiency of the lambda recombinase system may lead to BAC DNA instability (Sparwasser, Gong et al. 2004).

Apart from Red/ET recombination system used in this study, another method of BAC modification is the use of a shuttle vector that contains both the recombinase RecA gene and DNA sequence to be inserted/mutated flanked by homologous genomic segments (<1Kb) (Yang, Model et al. 1997). Electroporation of this vector into BAC containing cells will lead to RecA directed homologous recombination taking place between the shuttle vector and the BAC DNA and thus insertion of modified sequence. The advantage of recombineering (Red/ET recombination system), however, is that the linear DNA is produced by PCR without the need for a separate cloning step to generate the shuttle vector.

Although the recombineering technique is not as easy and fast as it is marketed, it seemed to be the best option for the generation of the ZsGreen Clu-BAC due to the cloning vector size and the advantages of this technique. However, there are two different BAC modification kits available which are based on this Red/ET cloning strategy. The more "advanced" kit, the "Counter selection BAC modification kit" (GENE BRIDGES) is preferred over "Quick and easy BAC modification kit". Both are based on homologous recombination between homology arms using λ phage recombinant genes. However, in order to select colonies carrying successfully modified BACs using the "Quick and easy BAC modification kit", a selectable marker (e.g a drug marker for instance neo gene) needs to be inserted in the DNA target site (in this case ZsGreen-neo DNA cassette) and this may be an undesirable modification which can complicate reporter gene expression in transgenic animals. In contrast using the "Quick and easy BAC modification kit" any non-selectable DNA (e.g ZsGreen reporter gene) can be efficiently inserted into the target region without leaving any genetic scar. Furthermore, the "Counter selection BAC modification kit" will obviate the need for cloning a selectable marker next to the reporter gene prior to PCR amplification of reporter-selectable marker gene cassette. The only advantages of "Quick and easy BAC

modification kit" however is that only one round of recombineering is needed. Therefore, based on these advantages the two steps "Counter selection BAC modification kit" was selected and used for Clu BAC modification.

### 4.7.2 Critical parameters for a successful recombineering

Recombineering is generally believed to be a very efficient and fast approach for the generation of large transgenic constructs. However, there are some parameters that play a critical role in successful generation of modified, BAC construct. These factors include the $OD_{600}$ of the BAC containing bacterial cells, which is optimal at just below 0.3 (2.1.18.4), and electroporation settings, particularly voltage which needs to be adjusted for each experiment based on the bacterial species used (e.g. DH5α, DH10α, HB101 etc), volume and concentration of DNA subject to electroporation, and the kind of electroporation apparatus used.

Another important factor is the concentration and the purity of the linear DNA cassette. The DNA sample should contain minimum salt and should be at a high concentration (100-200ng/µl). Once all these critical parameters are adjusted properly, the recombineering technique can become a routine technique in the laboratory. However, the success of modification is believed to vary from one BAC to another BAC (GENEBRIDGES technical protocol 2007) probably based on the BAC's stability, size and the target area. Larger BACs tend to be less stable, and manipulation of areas with repetitive sequences can be problematic and may increase the rate of rearrangement/deletion within the BAC.

### 4.7.3 Examples of recombineered transgenic constructs

Using recombineering technology, BAC transgenes that contain the necessary regulatory sequences to drive cell-specific gene expression can be modified to express proteins (physiologically relevant proteins or exogenous proteins such as Cre) or reporters (LacZ, eGFP or ZsGreen) in defined cell populations. For example Kim et al. (2007) used recombineering to modify *ephA8* BAC DNA by inserting a lacZ reporter

downstream of the *ephA8* promoter in exon 1. This BAC DNA was used to generate BAC transgenic mouse by pronuclear injection and was shown to express the reporter in the developing midbrain in a similar pattern to the endogenous ephA8 gene (Kim, Song et al. 2007). Zou et al. (1999) also used BAC technology to recapitulate the endogenous expression pattern of $\alpha$9 acetylcholine receptor ($\alpha$9 AChR) which is specifically expressed in hair cells of the inner ear. In this study homologous recombination based technology (RecA-mediated recombination) was used to modify a BAC that contained the entire $\alpha$9 AChR gene with its 5' and 3' sequences. The modified BAC also contained an internal ribosomal entry site (IRES) and a gene coding the enhanced GFP cassette in the $\alpha$9 AChR gene locus (just after stop codon) with a copy of c-myc tag just before the stop codon at the 3' end of the gene (Zuo, Treadaway et al. 1999).

One example of Cre BAC transgenesis is from the work of Cohen-Salmon et al. (2002) who generated an Otog-Cre transgene again via homologous recombination technology using a RecA shuttle vector. This construct contains the Cre gene under the control of mouse Otog promoter. The Otog-Cre mouse line expresses Cre at E10 in the otocyst and at E18 its expression is detected in all cells of the gap junction epithelial network. This mouse line was crossed with floxed connexin26 (Cx26) mice for the generation of targeted deletion of Cx26 in the epithelial gap junction network (Cohen-Salmon, Ott et al. 2002).

### 4.7.4 The choice of reporter gene

The ZsGreen reporter gene was chosen because of its availability in the lab and also based on some of its advantages over other reporter genes.

The ZsGreen gene is a popular choice as a reporter gene for *in vivo* studies and produces a green fluorescent protein which has been reported to be like GFP but brighter and more photostable (J. Chuck Harrell 2007). Furthermore, ZsGreen is capable of tolerating fixation without significant effects on fluorescence. In addition, no staining reaction is required for ZsGreen and the tissues can be readily sectioned and directly visualised using a fluorescent microscope. Thus an ideal reporter for Clu regulation studies *in vivo*.

### 4.7.5 The ZsGreen Clu-BAC and its applications

The strong expression of clusterin which is spatially and temporally restricted in the developing inner ear to a subset of cells in the cochlea sensory epithelium is suggestive of an enhancer that could be useful for driving expression of heterologous genes in the inner ear. The spatio-temporal gene expression is controlled by regulatory sequences, or enhancer, that can be positioned either close or far away from the transcription start site. Towards the initial steps for determining the enhancer sequence of clusterin, the clusterin BAC reporter construct was generated for the subsequent production of transgenic mice.

It would have been ideal to modify the BAC that contains the larger flanking sequences (bMQ70i14 BAC) to increase the possibility of capturing the Clu regulatory sequences. However, this BAC showed some rearrangement and/or deletion in the genomic regions (Figure 4.7 C) thus the modification of smaller BAC (bMQ377e19 BAC) was undertaken as the PCR analysis indicated an intact BAC.

Upon generation of ZsGreen Clu-BAC transgenic mice, the expression of reporter gene will be studied in the developing mouse inner ear. If the reporter gene becomes activated in the developing cochlear epithelium in an identical manner to endogenous mRNA as described in chapter 3, this would demonstrate the enhancer is localised within this genomic sequence.

The enhancer of the E19 Clu-BAC can subsequently be further narrowed down by sequential cloning of clusterin gene flanking sequences present in the E19 Clu-BAC into a plasmid vector that contains a reporter gene to generate enhancer reporter constructs for the subsequent generation of transgenic mice containing smaller test sequences.

An alternative approach, however, could be sequential deletion of genomic sequences from the ZsGreen Clu-BAC for the subsequent generation of transgenic mice. This latter approach is preferred as less constructs and transgenesis are needed. Up to this point however, the injection of ZsGreen Clu-BAC construct into the mouse fertilised eggs have been unsuccessful and thus it is still not clear whether the regulatory

sequences required to drive the expression of clusterin in the mouse cochlea epithelium is present in this construct or not. In case of these regulatory sequences not being present in this construct, the larger bMQ70i14 BAC could be reconsidered. The flanking sequences present in this BAC but not in the E19 Clu-BAC can be cloned into the ZsGreen Clu-BAC or into a plasmid vector containing a reporter gene for the subsequent generation of transgenic mouse. Alternatively alternate overlapping BACs could be obtained.

### 4.7.6 The Cre Clu-BAC and its possible applications

The generation of a Cre Clu-BAC transgenic line is also useful for gene function studies in the inner ear at embryonic stages in addition to fate mapping studies at postnatal stages. A Clu-Cre mouse line that contains all the clusterin regulatory sequences required to drive its expression, is a suitable tool for conditional gene deletion in Clu expressing cells of the cochlea sensory epithelium from about 13.5dpc to P2 as outlined in (Figure 4.47).

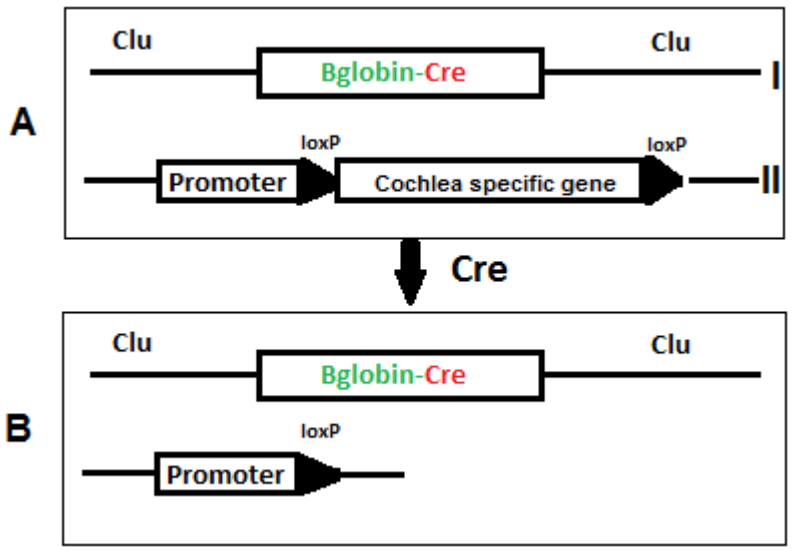


Figure 4.47 The Cre Clu-BAC mouse line can be used in conditional gene knock out studies. A: after the generation of Clu Cre-BAC mouse line that express Cre under the regulation of mouse clusterin regulatory sequences in clusterin expressing cells of inner ear (I), this mice line can be crossed with a floxed cochlea specific gene (II). Upon activation of Cre in clusterin expressing cells in the inner ear, the floxed gene will be deleted in the clusterin expressing cells of the cochlea.

After P2, however, when clusterin expression ceases in the cochlea sensory epithelium, this mouse line is also useful for fate mapping studies to track the fate of clusterin expressing cells in the inner ear and identify what these cells give rise to adult ear. To achieve this, the Cre Clu-transgenic mouse will be crossed with a silent reporter mouse line (R26R), which upon activation by Cre in clustrein expressing cells, the loxp-floxed stop codon is deleted and the reporter gene becomes permanently active in these cells (Figure 4.48).

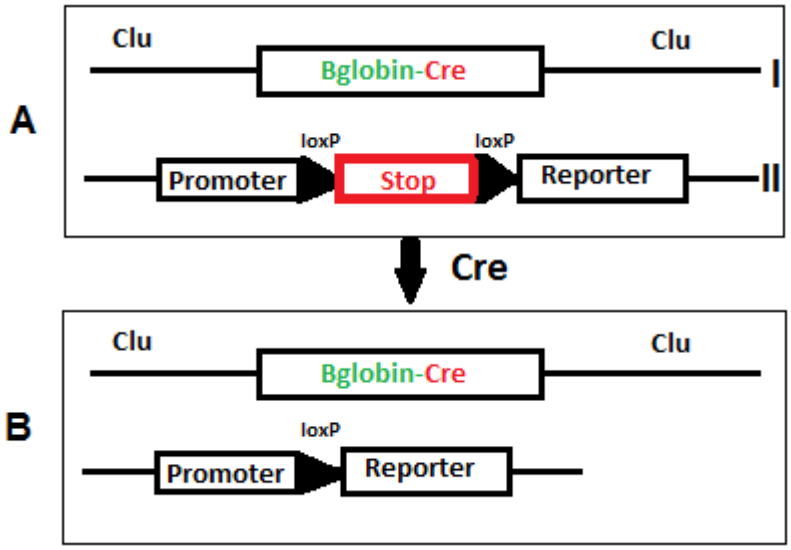


Figure 4.48 The generation of a reporter mouse line that permanently express reporter gene in Cre expressing cells. A: after the generation of Clu Cre-BAC mouse line that express Cre under the regulation of mouse clusterin regulatory sequences in clusterin expressing cells of inner ear (I), this mice line can be crossed with a silent reporter mice line (II) for the generation of a mice line that permanently express reporter gene upon activation of Cre in clusterin expressing cells in the inner ear (B) for fate mapping studies.

### 4.7.7 Possible complication with the ZsGreen Clu-BAC construct

The existence of other genes (Scara3 and Gulo) in the ZsGreen Clu-BAC construct can potentially affect the reporter gene expression. The entire 5' regulatory sequence of Scara3 and 3' regulatory sequence of Gulo gene together with half of the Scara3 and nearly the entire Gulo genes are present in the ZsGreen Clu-BAC construct. The regulatory sequences of these genes if present in the BAC can result in increase or decrease of reporter gene expression. However given there is no change to the

endogenous organisation of these genes in the BAC, it is unlikely they will interfere with reporter expression.

However, these additional genes, if expressed in the transgenic mouse might lead to an unwanted phenotype. In such cases, however, a smaller BAC that does not contain these genes can be chosen for generating the construct or alternatively these genes could be removed from the BAC by recombineering, although there is a possibility of losing some of the Clu regulatory sequences.

### 4.7.8 Future plans

The first goal is to generate Clu-ZsGreen reporter mice. A careful developmental analysis will be required to compare to the expression patterns reported in this study that will reveal whether all or some of the cis-acting regulatory sequences are located within the 58Kb genomic sequence. Should this prove to be the case, the Clu-Cre construct will be completed and used for lineage tracing studies, and this will reveal the ultimate utility of the transgene for functional studies.

If the regulatory sequences are present in the above construct then the Clu Cre-BAC construct that has been partly modified will be fully modified by removal of the second loxP site (loxP511) and insertion of the SV40 pA next to the Cre sequences by recombineering for the subsequent generation of Cre mice line.

# 5. General Discussion

# 5. General Discussion

## 5.1 Clusterin mRNA and protein expression during mouse inner ear development

Clusterin mRNA demonstrated a dynamic and cochlea-specific expression between 12.5dpc–P2 (Figure 3.45). Expression became progressively restricted to a subset of supporting cells either side of the organ of Corti, in the inner and outer sulcus, and possibly spiral prominence before its complete downregulation at some stage between P2-P17. The restricted expression of clusterin in the inner ear within cochlear sensory epithelium is suggestive of involvement of clusterin specifically in the development of the auditory system in mouse. The dynamic and transient expression of clusterin makes it hard to judge on its biological importance, its function and the fate of clusterin expressing cells. Clusterin however may play different roles at different times and in different cells during the development of mouse cochlea. For instance while its expression in the prosensory domain of cochlea at 13.5dpc (Figure 3.48) may suggest a role for clusterin in inhibiting cell cycle progression, its downregulation from the central region of the cochlea epithelium where the presumptive organ of Corti is developing (Figure 3.6 J-L) may be related to the differentiation of cells of organ of Corti or even the differentiation of surrounding supporting cells.

Proposing a role for clusterin during the mouse inner ear development becomes even more complicated by the observed clusterin protein expression patterns in this study. Surprisingly clusterin protein expression was not only transiently detected in the developing cochlear sensory epithelium but also in periotic mesenchyme, otic capsule and in non-sensory epithelia such as Reissner's membrane.

The low level of immunoreactivity detected in the cochlear epithelium may represent an intracellular (nuclear or cytoplasmic) form of clusterin. However, it may have been produced as a result of antibody detecting a non-specific antigen and therefore may does not represent clusterin expression at all. This can also be true for the clusterin protein expression observed in the non-sensory regions. All the available clusterin antibodies are unable to distinguish between the nuclear and secretory form, as they recognize an epitope of the protein which is common to both isoforms. Therefore the usage of a

different antibody cannot rule out the first possibility, but may help with the other possibility (e.g. non-specific detection). The usage of a different antibody may also help to confirm the specificity of immunoreactivity detected in the non-sensory regions. Alternatively, clusterin protein patterns can be studied in Clu knockout mice for comparison.

The auditory clusterin protein in the sensory and nonsensory epithelia, otic capsule and periotic mesenchyme, seems to be produced as a result of its local synthesis rather than plasma contamination/transportation as is evident from its abundant mRNA presence in the cochlear sensory epithelium. Therefore, assuming that all the detected clusterin protein expression in the sensory and non-sensory epithelium is due to specific labelling, then the non-sensory protein must have been produced as a result of clusterin secretion from the cochlear sensory epithelium. Further investigation needs to be carried out to confirm this route and also the mechanisms of clusterin transport from cochlear epithelium to the periotic mesenchyme, otic capsule and Reissner's membrane. The biological significance and the role of clusterin in tissues other than cochlear sensory epithelium also need to be investigated.

### 5.2 Clusterin function during the mouse inner ear development

Considering the many attributed biological functions of clusterin, its function during the development of cochlea can be speculated on based on its specific spatio-temporal expression pattern. However as discussed in chapter 3 and above, there is discrepancy between clusterin mRNA and protein expression in the developing inner ear, making speculation of roles more hazardous. Nevertheless, based on mRNA expression patterns, the transient clusterin expression at a time that cochlea sensory epithelium is undergoing differentiation and elaborate morphological changes (or morphogenesis) so that individual cell types is generated is indeed suggestive of a role specifically in differentiation and/or morphogenesis of cochlear epithelium. This is consistent with the French et al. (1993) report that demonstrated a clear relationship/correlation between clusterin gene expression during mouse embryogenesis and epithelial cell differentiation (French, Chonn et al. 1993). However, it is still unclear how clusterin may affect cellular differentiation, but some reports suggest that "it could confer adhesive

properties to certain states of differentiation, enabling morphogenic rearrangements of cells" (Seiberg and Marthinuss 1995). In addition, it has been suggested that "cell coat-bound clusterin is involved in binding, via its predicted heparin binding domain, of other cell surface proteoglycans, creating a molecular bridge between adjacent cells" (French, Chonn et al. 1993).

These roles (cellular differentiation and morphogenesis) and many other suggested roles of clusterin (1.10) demonstrate that clusterin can be a cytoprotective molecule, and it plays this role as a result of being an extracellular chaperone. Clusterin assists with protein homeostasis and as a result supports cell survival during the development and differentiation of cochlear sensory epithelium. The extracellular chaperone role of clusterin, which is currently at the centre of attention of many researchers in the clusterin field, seems to represent the unifying role of clusterin that may explain its wide tissue distribution and its varied biological and pathological functions *in vivo*.

The experiments in this study do not address potential roles of clusterin, and it is not possible to rule out other roles that clusterin may play e.g. apoptosis, cell-interaction and cell cycle progression inhibition. It is however important to note that each of these roles could again fall within the cytoprotective role of clusterin. Clusterin upregulation is believed to assist cell-cell and cell-substratum interactions to maintain tissue integrity. For instance, during renal tissue injury and remodelling, clusterin is induced by stressed cells to promote cell interactions (cell-cell and cell-matrix) which are profoundly affected. Also during development as well, maintaining the correct set of cell-cell/matrix interactions is vital.

All in all, most of the cellular events happening during the development of auditory and vestibular system such as proliferation, differentiation, morphogenesis, and apoptosis appear essentially identical. The restriction of clusterin expression to the auditory system demonstrates a specific role for clusterin in the development or specification of the cochlear sensory epithelium, the organ of Corti. Furthermore it may suggest a role for clusterin in the homeostasis of endolymph hence its mRNA expression in the outer sulcus and its protein expression in the Reissner's membrane. These two areas are involved in endolymph ion homeostasis.

It would be interesting to investigate the effect of clusterin overexpression on cultured cells derived from the inner ear (to check whether Clu can induce cell differentiation of cultured cells) or *in vivo* and/or its knockdown via anti-clusterin antibody or via interfering RNA (siRNA) to see what effect/s it may have on cochlear epithelial cell differentiation and development. The knockdown effects however are more readily accessible by studying the cell morphology and development of the inner ear of clusterin knockout mice. However, clusterin loss of function might be compensated by other gene/s, although it does not appear to be a member of an extended gene family.

### 5.3 Clu reporter BAC and its applications

The generation of a clusterin reporter BAC is useful in the search for the enhancer sequences that control clusterin expression during inner ear development. Once the minimal genomic regions required to drive expression of the ZsGreen reporter gene to endogenous regions of clusterin expression, this enhancer can be used to locate the upstream transcription factor binding sites. The other applications of this enhancer/construct would be for its use in misexpression of exogenous genes for functional analysis as well in gene therapy.

Furthermore, the Clu enhancer can be used for recombining with other inner ear/cochlea specific genes to drive the expression of gene/s in inner ear for gene therapy (Figure 5.1). This potentially may offer some benefits for deafness treatment/hearing impairment.


Figure 5.1 Recombining Clu enhancer with inner ear/cochlea specific genes

### 5.4 Clu Cre BAC and its applications

Assuming that all the required regulatory sequences are present in the recombineered Clu-Cre BAC construct, it can be used for many purposes upon generation of Cre

transgenic mice. Apart from a clusterin fate mapping study that was described before (4.6), Cre transgenic mice can be used to further confirm clusterin mRNA expression patterns observed in the mouse inner ear, by *in situ* hybridisation using a Cre riboprobe.

Another application of the Clu-Cre transgenic mouse would be for the generation of cochlea-specific knockout mutants. This could be used to delete any other gene in the clusterin expressing cells of inner ear for gene functional studies. For this, the gene subject to deletion needs to first be flanked by loxP sites. The tissue specific and temporally restricted Cre expression will delete the loxP-floxed gene. This is particularly useful for the genes that are expressed in the inner ear and that their systemic deletions demonstrate embryonic lethality. The utility remains to be determined by the full extent of regulatory regions found in the BAC, since regulatory regions for domains of clusterin outside the inner ear may also be localised with the BAC.

In addition the Clu-Cre BAC can be used for Cre-mediated misexpression of exogenous genes in clusterin expressing cells for the purpose of gene function studies. This is also called "ectopic gene expression" or "conditional gain of function upon Cre-mediated recombination" which are potentially useful for "Cre mediated gene therapy" (Figure 5.2).

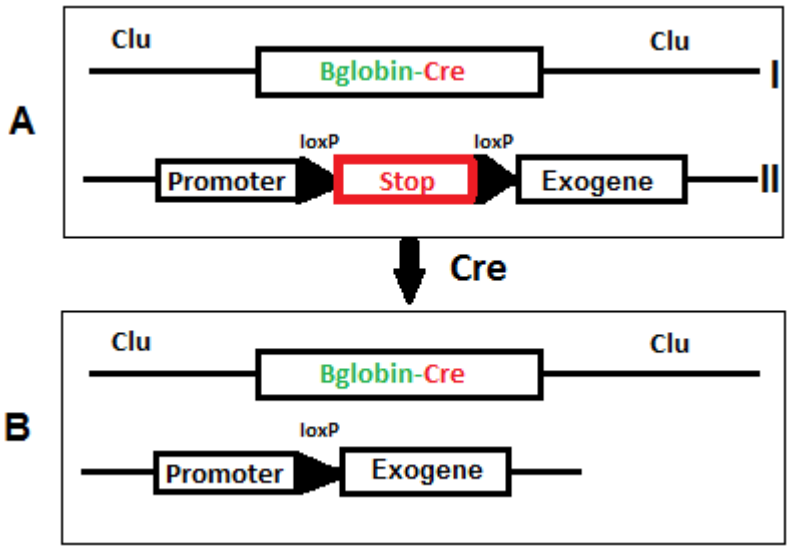


Figure 5.2 The Cre mouse line can be potentially used for ectopic gene expression. A: after the generation of Clu Cre-BAC mouse line that express Cre under the regulation of mouse clusterin regulatory sequences in clusterin expressing cells of inner ear (I), this mice line can be crossed with a silent exogene mice line (II) for the generation of a mice line that expresses the exogene upon activation of Cre in clusterin expressing cells in the inner ear (B) for Cre mediated gene therapy.

## 5.5 Summary and concluding remarks

In this study, clusterin was shown to exhibit transient and dynamic expression during mouse inner ear development. From initial expression across the cochlear sensory epithelium, expression becomes progressively localised to the inner and outer sulcus supporting cells. Its auditory restricted expression coincides with the differentiation and morphogenesis of this organ and therefore is suggestive of a distinct role for clusterin in the development and differentiation of cochlear sensory epithelium. Its functional role in the inner ear has yet to be demonstrated, but it is possibly induced as a result of developmental stress and is likely to play cytoprotective role to maintain cell interactions during tissue remodelling during morphogenesis. It may achieve this by acting as an extracellular chaperone to remove cell debris and unwanted cells produced during the development of cochlea sensory epithelium.

The generation of a clusterin reporter BAC firstly demonstrated the feasibility of recombineering technique for BAC modification. Secondly, the testing of this BAC *in vivo* will be the first critical step towards the identification of clusterin regulatory sequences by testing a large flanking region of the mouse clusterin gene. Thirdly, the eventual identification of a mouse inner ear clusterin enhancer will be a useful experimental tool to induce the expression of other genes in the cochlea sensory epithelium for misexpression studies, as well as for gene therapy for treatments of hearing impairment. The generation of a Clu Cre-BAC furthermore will be useful not only for clusterin fate mapping studies but also for generating cochlea-specific gene knockouts.

Further investigation however needs to be carried out to explain the discrepancy in the clusterin mRNA and protein expression observed in the developing cochlea and to find the source of non-sensory epithelia clusterin. It will be particularly interesting to see which aspects of clusterin expression, the protein and/or mRNA patterns are reproduced by the clusterin ZsGreen reporter BAC in transgenic animals throughout development.

# Appendixes

## Appendix I - Growth media

| | |
|---|---|
| LB: Per litre | 10g NaCl (Fisher Scientific)<br>10g Tryptone (Fisher Bioreagents)<br>5g Yeast extract (Oxoid)<br>pH 7.0 with $5_N$ NaOH<br>(15g Bacto agar was added for LB agar)<br>(For low salt LB NaCl was reduced to 5g) |
| Xgal/IPTG agar plates | 20µl of Xgal<br>4µl IPTG<br>Spread on each agar plate and air dried. |
| S.O.C: Per litre | 0.5g NaCl<br>20g Tryptone<br>5g Yeast extract<br>10ml of 250mM KCl<br>5ml of 2M $MgCl_2$<br>20ml of 1M Glucose<br>pH 7.0 with 5M NaOH |

Media is autoclaved for at 120ºC for 20 minutes at 15 lb/sq. in.

## Appendix II - Southern analysis solutions

| | |
|---|---|
| Southern hybridisation buffer | 6x SSC<br>0.5% SDS<br>100µg/ml denatured salmon sperm DNA<br>5x Denhardt's solution |
| 50X Denhardt's solution | 1% Ficoll<br>1% mg/ml polyvinylpyrolidone (PVP)<br>1% mg/ml bovin serum albumin (BSA)<br>Dissolved in $H_2O$ and sterilised by filtration through a 0.2 micron filter<br><br>5g Ficoll<br>5g polyvinylpyrolidone (PVP)<br>5g bovin serum albumin (BSA)<br>$H_2O$ to 500ml<br>Sterilised by filtration through a 0.2µ filter |

| | |
|---|---|
| Gel loading buffer | 0.25% bromophenol blue<br>0.25% xylene cyanol FF<br>30% glycerol |

**Appendix III - *In situ hybridisation* reagents**

| | |
|---|---|
| *In situ hybridisation* buffer | 50% formamide<br>5x SSC<br>1% SDS<br>50µg/ml yeast RNA (tRNA)<br>50µg/ml heparin<br>5mM EDTA<br>0.2% Tween-20<br>0.5% CHAPS |
| 10XTBST | 1.4M NaCl<br>27mM KCl<br>0.25M Tris-HCl (pH 7.5)<br>1% Tween-20 |
| NTMT | 100mM Tris (pH 9.5)<br>100mM NaCl<br>50mM $MgCl_2$<br>0.1% Tween-20 |
| PBS | 140mM NaCl<br>3mM KCl<br>10 mM $Na_2HPO_4$<br>0.2mM $KH_2PO_4$<br>pH 7.4 with HCl |

**Appendix IV - Buffers**

| | |
|---|---|
| 20x SSC | 3M NaCl<br>0.3M Sodium citrate<br>pH 7.0 with 10M NaOH |
| 10X TE | 0.1M Tris (pH7.5)<br>10mM EDTA |

| | |
|---|---|
| 50X TAE | 2M Tris-HCl<br>1M Glacial acetic Acid<br>50mM EDTA pH 8.0 |
| Frozen Storage Buffer (FSB) | 7.4g KCl<br>8.9g $MnCl_2.4H_2O$<br>1.5g $CaCl_2.2H_2O$<br>0.8g $HACoCl_3$<br>10ml of a 1M stock (pH 7.5) of KAc<br>100g Redistilled glycerol<br>pH 6.4 with 0.1M HCl<br>Sterilised by filtration through a 0.22µ filter |
| 10X TBS buffer pH 7.6 | 24g Tris base<br>88g NaCl<br>pH 7.6 with 12M HC |
| Citrate-EDTA Buffer pH 6.2 | 10mM Citric Acid<br>2mM EDTA<br>0.05% Tween 20<br>pH 6.2 with 1M NaOH |
| Citrate buffer pH 6.0 | 10mM Citric Acid<br>0.05% Tween 20<br>pH 6.0 with 1M NaOH |

## Appendix V - Sequences

### Appendix V.I - Mouse clusterin cDNA and amino acid

From (www.ensemble.org)

```
   1 GCTGGGTGCTGCGCCTCTTACCCCCACCTCTAGGCTTCCAGAAAGCTCCTGGTGCATTCT
     ............................................................
     ............................................................

  61 CCGGCATTCTCTGGGCGTGAGTCACGCAGGTTTGCAGCCAGCCCCAAAGGGGGTGTACTT
     ............................................................
     ............................................................

 121 GAGCAGAGCGCTATAAATAGGGCGCTTCCCCGGTGCTCACCACCCGCGTCACCAGGAGGA
     ............................................................
     ............................................................

                                                            R
 181 GCGCACTGGAGCCAAGCCGCAGACCGGACTCCAGATTCCAAGGAGGCCACGCCATGAAGA
     ..........................................................ATGAAGA
     ..........................................................-M--K--

 241 TTCTCCTGCTGTGCGTGGCACTGCTGCTGATCTGGGACAATGGCATGGTCCTGGGAGAGC
   8 TTCTCCTGCTGTGCGTGGCACTGCTGCTGATCTGGGACAATGGCATGGTCCTGGGAGAGC
   3 I--L--L--L--C--V--A--L--L--L--I--W--D--N--G--M--V--L--G--E--

 301 AGGAGGTCTCTGACAATGAGCTCCAAGAACTGTCCACTCAAGGGAGTAGGTATATTAATA
  68 AGGAGGTCTCTGACAATGAGCTCCAAGAACTGTCCACTCAAGGGAGTAGGTATATTAATA
  23 Q--E--V--S--D--N--E--L--Q--E--L--S--T--Q--G--S--R--Y--I--N--

 361 AGGAGATTCAGAACGCCGTCCAGGGAGTGAAGCACATAAAAACTCTCATAGAAAAACCA
 128 AGGAGATTCAGAACGCCGTCCAGGGAGTGAAGCACATAAAAACTCTCATAGAAAAACCA
  43 K--E--I--Q--N--A--V--Q--G--V--K--H--I--K--T--L--I--E--K--T--

 421 ACGCAGAGCGCAAGTCCTTGCTCAACAGTTTAGAGGAAGCCAAGAAGAAGAAAGAGGATG
 188 ACGCAGAGCGCAAGTCCTTGCTCAACAGTTTAGAGGAAGCCAAGAAGAAGAAAGAGGATG
  63 N--A--E--R--K--S--L--L--N--S--L--E--E--A--K--K--K--K--E--D--

                Y
 481 CTCTGGAGGACACTAGGGATTCTGAAATGAAGCTGAAGGCATTCCCGGAAGTGTGTAACG
 248 CTCTGGAGGACACTAGGGATTCTGAAATGAAGCTGAAGGCATTCCCGGAAGTGTGTAACG
  83 A--L--E--D--T--R--D--S--E--M--K--L--K--A--F--P--E--V--C--N--

 541 AGACCATGATGGCCCTCTGGGAGGAGTGCAAGCCCTGCCTGAAGCATACCTGCATGAAGT
 308 AGACCATGATGGCCCTCTGGGAGGAGTGCAAGCCCTGCCTGAAGCATACCTGCATGAAGT
 103 E--T--M--M--A--L--W--E--E--C--K--P--C--L--K--H--T--C--M--K--

 601 TCTATGCACGTGTCTGCAGGAGCGGCTCAGGGCTGGTCGGCCAGCAGCTAGAGGAGTTTC
 368 TCTATGCACGTGTCTGCAGGAGCGGCTCAGGGCTGGTCGGCCAGCAGCTAGAGGAGTTTC
 123 F--Y--A--R--V--C--R--S--G--S--G--L--V--G--Q--Q--L--E--E--F--
```

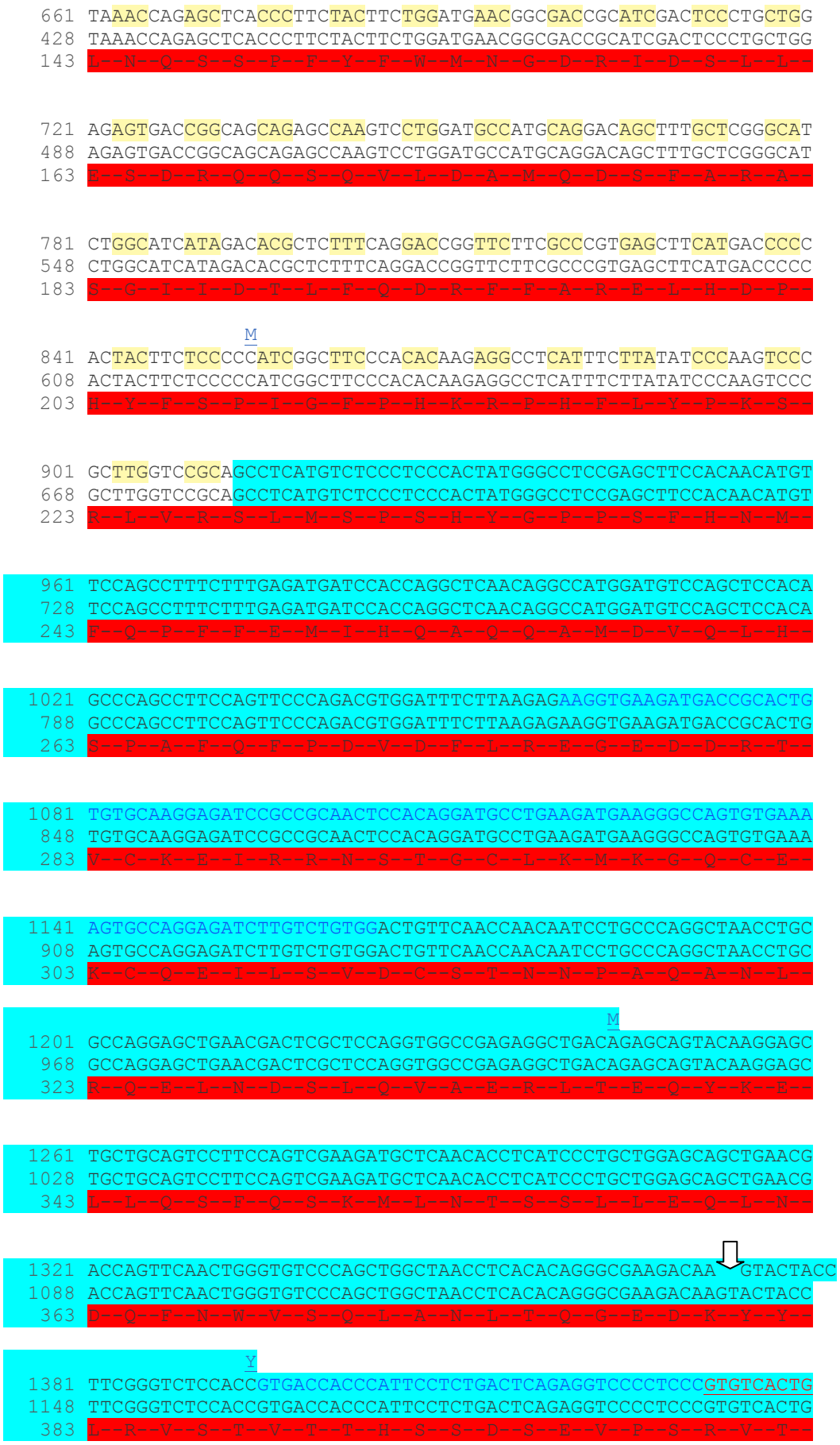
661 TAAACCAGAGCTCACCCTTCTACTTCTGGATGAACGGCGACCGCATCGACTCCCTGCTGG
428 TAAACCAGAGCTCACCCTTCTACTTCTGGATGAACGGCGACCGCATCGACTCCCTGCTGG
143 L--N--Q--S--S--P--F--Y--F--W--M--N--G--D--R--I--D--S--L--L--
721 AGAGTGACCGGCAGCAGAGCCAAGTCCTGGATGCCATGCAGGACAGCTTTGCTCGGGCAT
488 AGAGTGACCGGCAGCAGAGCCAAGTCCTGGATGCCATGCAGGACAGCTTTGCTCGGGCAT
163 E--S--D--R--Q--Q--S--Q--V--L--D--A--M--Q--D--S--F--A--R--A--
781 CTGGCATCATAGACACGCTCTTTCAGGACCGGTTCTTCGCCCGTGAGCTTCATGACCCCC
548 CTGGCATCATAGACACGCTCTTTCAGGACCGGTTCTTCGCCCGTGAGCTTCATGACCCCC
183 S--G--I--I--D--T--L--F--Q--D--R--F--F--A--R--E--L--H--D--P--
M
841 ACTACTTCTCCCCCATCGGCTTCCCACACAAGAGGCCTCATTTCTTATATCCCAAGTCCC
608 ACTACTTCTCCCCCATCGGCTTCCCACACAAGAGGCCTCATTTCTTATATCCCAAGTCCC
203 H--Y--F--S--P--I--G--F--P--H--K--R--P--H--F--L--Y--P--K--S--
901 GCTTGGTCCGCAGCCTCATGTCTCCCTCCCACTATGGGCCTCCGAGCTTCCACAACATGT
668 GCTTGGTCCGCAGCCTCATGTCTCCCTCCCACTATGGGCCTCCGAGCTTCCACAACATGT
223 R--L--V--R--S--L--M--S--P--S--H--Y--G--P--P--S--F--H--N--M--
961 TCCAGCCTTTCTTTGAGATGATCCACCAGGCTCAACAGGCCATGGATGTCCAGCTCCACA
728 TCCAGCCTTTCTTTGAGATGATCCACCAGGCTCAACAGGCCATGGATGTCCAGCTCCACA
243 F--Q--P--F--F--E--M--I--H--Q--A--Q--Q--A--M--D--V--Q--L--H--
1021 GCCCAGCCTTCCAGTTCCCAGACGTGGATTTCTTAAGAGAAGGTGAAGATGACCGCACTG
788 GCCCAGCCTTCCAGTTCCCAGACGTGGATTTCTTAAGAGAAGGTGAAGATGACCGCACTG
263 S--P--A--F--Q--F--P--D--V--D--F--L--R--E--G--E--D--D--R--T--
1081 TGTGCAAGGAGATCCGCCGCAACTCCACAGGATGCCTGAAGATGAAGGGCCAGTGTGAAA
848 TGTGCAAGGAGATCCGCCGCAACTCCACAGGATGCCTGAAGATGAAGGGCCAGTGTGAAA
283 V--C--K--E--I--R--R--N--S--T--G--C--L--K--M--K--G--Q--C--E--
1141 AGTGCCAGGAGATCTTGTCTGTGGACTGTTCAACCAACAATCCTGCCCAGGCTAACCTGC
908 AGTGCCAGGAGATCTTGTCTGTGGACTGTTCAACCAACAATCCTGCCCAGGCTAACCTGC
303 K--C--Q--E--I--L--S--V--D--C--S--T--N--N--P--A--Q--A--N--L--
M
1201 GCCAGGAGCTGAACGACTCGCTCCAGGTGGCCGAGAGGCTGACAGAGCAGTACAAGGAGC
968 GCCAGGAGCTGAACGACTCGCTCCAGGTGGCCGAGAGGCTGACAGAGCAGTACAAGGAGC
323 R--Q--E--L--N--D--S--L--Q--V--A--E--R--L--T--E--Q--Y--K--E--
1261 TGCTGCAGTCCTTCCAGTCGAAGATGCTCAACACCTCATCCCTGCTGGAGCAGCTGAACG
1028 TGCTGCAGTCCTTCCAGTCGAAGATGCTCAACACCTCATCCCTGCTGGAGCAGCTGAACG
343 L--L--Q--S--F--Q--S--K--M--L--N--T--S--S--L--L--E--Q--L--N--
1321 ACCAGTTCAACTGGGTGTCCCAGCTGGCTAACCTCACACAGGGCGAAGACAAGTACTACC
1088 ACCAGTTCAACTGGGTGTCCCAGCTGGCTAACCTCACACAGGGCGAAGACAAGTACTACC
363 D--Q--F--N--W--V--S--Q--L--A--N--L--T--Q--G--E--D--K--Y--Y--
Y
1381 TTCGGGTCTCCACCGTGACCACCCATTCCTCTGACTCAGAGGTCCCCTCCCGTGTCACTG
1148 TTCGGGTCTCCACCGTGACCACCCATTCCTCTGACTCAGAGGTCCCCTCCCGTGTCACTG
383 L--R--V--S--T--V--T--T--H--S--S--D--S--E--V--P--S--R--V--T--


Amino acid 22-226 (clusterin N-terminus) representing α subunit of clusterin is not highlighted while amino acid 227-442 (clusterin C-terminus) for β subunit is highlighted in light blue. The conserved nuclear localisation signal (1.6), amino acid 73-79, is highlighted in purple. Amino acids 99-449 (corresponding to the last 350 human amino acids) that is recognised by the Proteintech antibody is highlighted in red. At the end of this sequence, the amino acid sequences recognised by Abcam antibody, amin acids 435-449, are labelled with yellow letters. Arrows point to the mouse clusterin riboprobe sequence. Oligonucleotides Clu9F and Clu9R (2.4.14), used in IHC analysis to check the C-terminus of mouse clusterin gene are underlined and in red letters. Also note the keys below from ensemble:

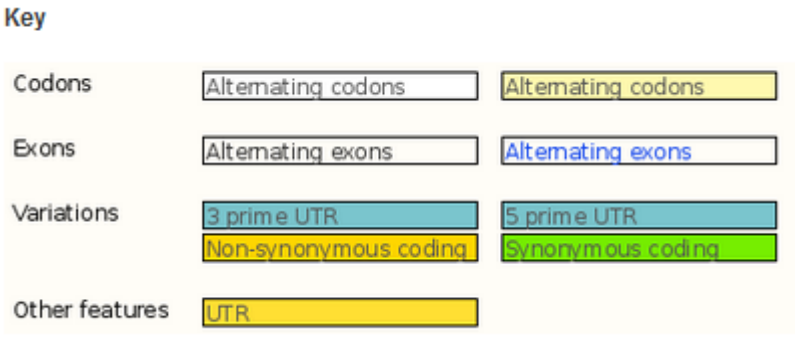

## Appendix V.II - Mouse clusterin riboprobe sequence

```
                                                          1369 gtactacc
1381 ttcgggtctc caccgtgacc acccattcct ctgactcaga ggtcccctcc cgtgtcactg
1441 aggtggtggt gaagctgttt gactctgacc ccatcacagt ggtgttacca gaagaagtct
1501 ctaaggataa ccctaagttt atggacacag tggcggagaa ggcgctacag gaataccgca
1561 ggaaaagccg tgcggaatga gatagaagca tcaccttcct atatgtagga gtgtctggga
1621 gggaatctcc cagctccccg aggtggctgc agacccctag agaactccac atgtctccag
1681 gcgagtaggc ctcacccaag cagcctgccc ttcctctgga ttctgtac
```

## Appendix V.III - Mouse clusterin genomic sequence exon2-3

GACTCCAGATTCCAAGGAGGCCACGCCATGAAGATTCTCCTGCTGTGCGTGGCACTGCTG
CTGATCTGGGACAATGGCATGGTCCTGGGAGAGCAGGAGGTCTCTGACAATGAGCTCCAA
GGTAGGTAGGCTGAGACTGTTCCTCTGGTGGATGCTATAGGGCCCAGGGCAGGGCCATTC
CTCAAAGCTCAGTCCCCAAGTGCTGAGGGCTGTTTTCATTCTACATCCTGGGTCTGTCCA
TGCCCTCTGCCCTCTCTAGGTCCTGTCTTGATGTTTTTGTGGTCAGGTGACTTCTAGACA
TTGCCCTCTGTCTCAAGCCCCTCTGTTGGCTGCCTGTCATTCCTTTGTCATTACTGGTCC
CCTCACCTGGCTCTCTTACTCTTCTCCCAAAGCCGTGCCCTAGACCCTTTGAAACTTTGT
CAGTCTTCCCTTTGTGTGACATCCAGGGTTCTTACCGATGTGTCTCCACACCAACCCCTC
CTGGAAAGCCATATCCACCAATTTCCTCCTCTGGAAAAAGGGCAATGCAATTTGACATGA
AGTAGTCACCTGAGAGCACCCTCTCCCTTCCTCCCCATCTTCCAAGGCTTTTCTGGAAAC
CCACCTTTTCTCCCTTCTTCTCTCCTAACCTCTTGCTCATAGCTGACCAGTTCTGGGGGG
GGGGGTCTTCGTTAAAGACAATGTGATCAGATTCTTTGATGTGGATACACACGGTGAAAT
GATTGCTGTTGTCAAGCTATTAGCTGTCCATCACCTCAACTTATCATTGGGTTCAGACAC
TTAAAATATGTTCTCTCAGCACACTTCAAGGGTAGAACACATTATCAACCACGAGCTCTG
CTTGGACCATTGACCTTCGGGCTTACTTGTGTTGCTACATCATTGAAGCTCTTGCCCTTG
GCTCAGCAGTCCCCCCTCCCGCTTCTCTTTGGATGTGTCTGGCAACCGCATCAGGTAGAA
AACAGCAGAGGTGTGGGAAATGGCACTTGACACAGGATAAGTAAGTGGTACCACCGTGAC
ATGATGTGTCATTGCCTTCGTCACCTGGGGCCGTGTCATGGCTATGGTCTCCATGGTGAA
TGCAGCTCTTCATTTATCGTCCCGTCTCCATGGTGTCTGGTGCTATCCTGTCACCTGACC
CTGTGCGTTGTAGCAAAGAAGTGCCAGGATTGGGTTAACCTGAGCTTCACAGAGATAATT
TCCAAAAGAGCACTTTTATTACACCTTGATGCTTAGGAGGTTGTTTTGTTTTGTTTTCTG
TTTTCCTTGAAATATTCTCTGTGGCTGTTGGCTCTCCAGGGTGGCATGGTGGGGTCAGTC
ATAGTATGGCTGCCCCTCTCTGCACCACTCACTCCTGAGTTTCTGAGCTGTGACTTGGAG
TCTACCATGAGCCCTTTGATGGGACATAGAGGCAGGACTGAGGCCATAAGGACTGCCACA
GGCTTGGGGTAATAGTGATGGTGTCTCAGCTTGACGCCCCCAGCACTCCCCATCAAAGCA
TGGCTTTCTCACCGTCCCCCTGGCACCCAGGCTATTTCTCCAGCCATTCCTCCCCGCCCC
CCTCAACTCACTGTACCTTCCTCTCTCTCACAGAACTGTCCACTCAAGGGAGTAGGTATA
TTAATAAGGAGATTCAGAACGCCGTCCAGGGAGTGAAGCACATAAAAACTCTCATAGAAA
AAACCAACGCAGAGCGCAAGTCCTTGCTCAACAGTTTAGAGGAAGCCAAGAAGAAGAAAG
AG

Exons 2 and 3 are highlighted in purple and are pointed with arrows on the top and the bottom of the sequence. 3' right arm of homology for recombination is highlighted in yellow and 5' left arm in green. The broken arrow between the blue and yellow highlights point to the insertion poing in the mid intron 2.

## Appendix V.IV - Predicted modified mouse clusterin sequence exon 2-3 modified by insertion of the rpsL-neo cassette

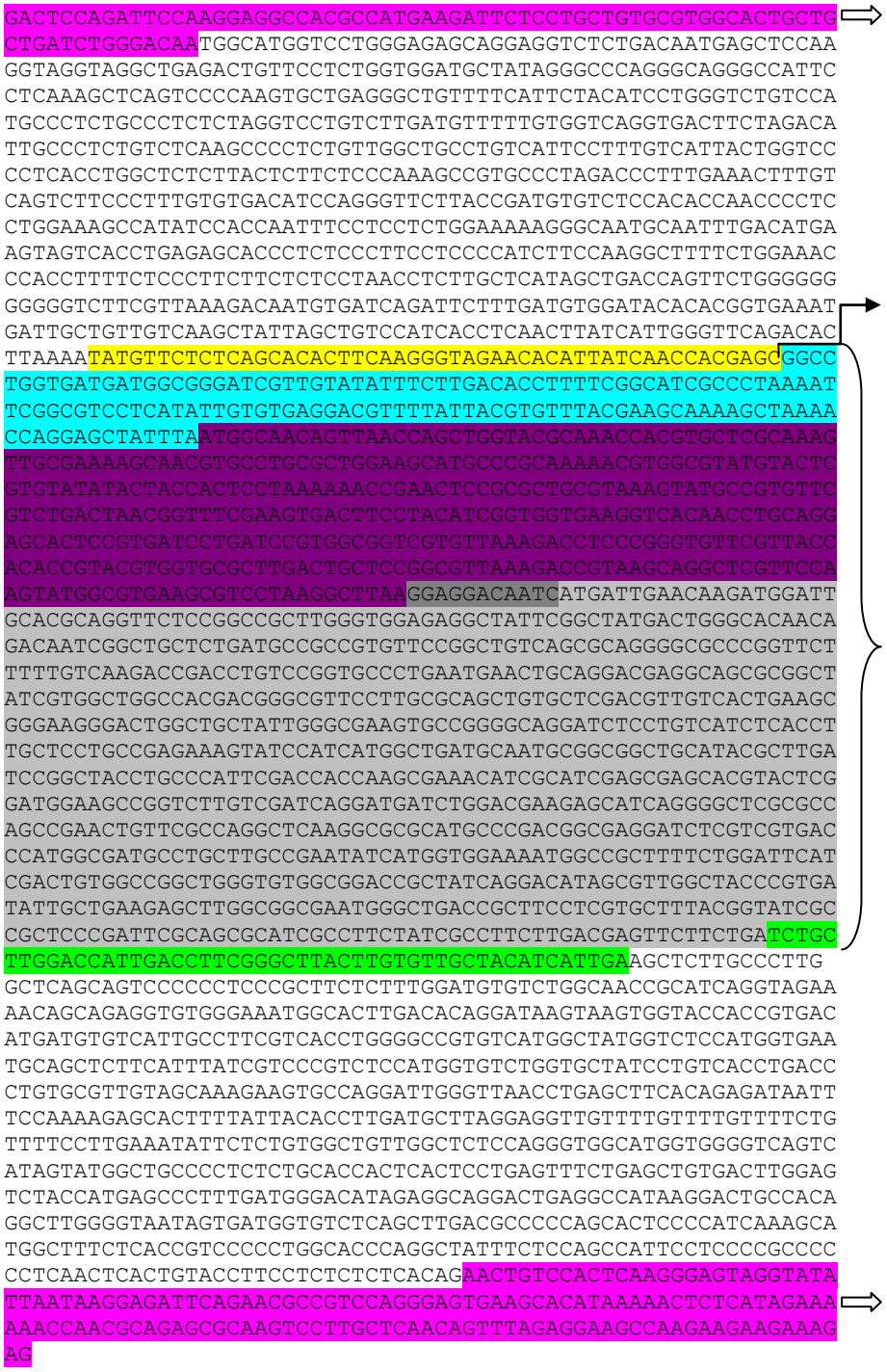


Exons 2 and 3 are highlighted in purple are pointed with arrows on the top and the bottom of the sequence. Right arm of homology is highlighted in yellow and left arm in green. The rpsL-neo insert consists of 4 different elements highlighted in different colours between the homology arms (green and yellow highlights). Promoter of the rpsL gene is highlighted in blue. The rpsL gene is highlighted in dark purple, the neo gene is highlighted in light gray and the dark gray is some sequence from the vector backbone. The broken arrow between the blue and yellow highlights point to the insertion poing in the mid intron 2.

## Appendix V.V - Predicted mouse clusterin sequence exon 2-3 modified by replacement of rpsL-neo (appendix V.IV) with Bglobin-ZsGreen- SV40 pA

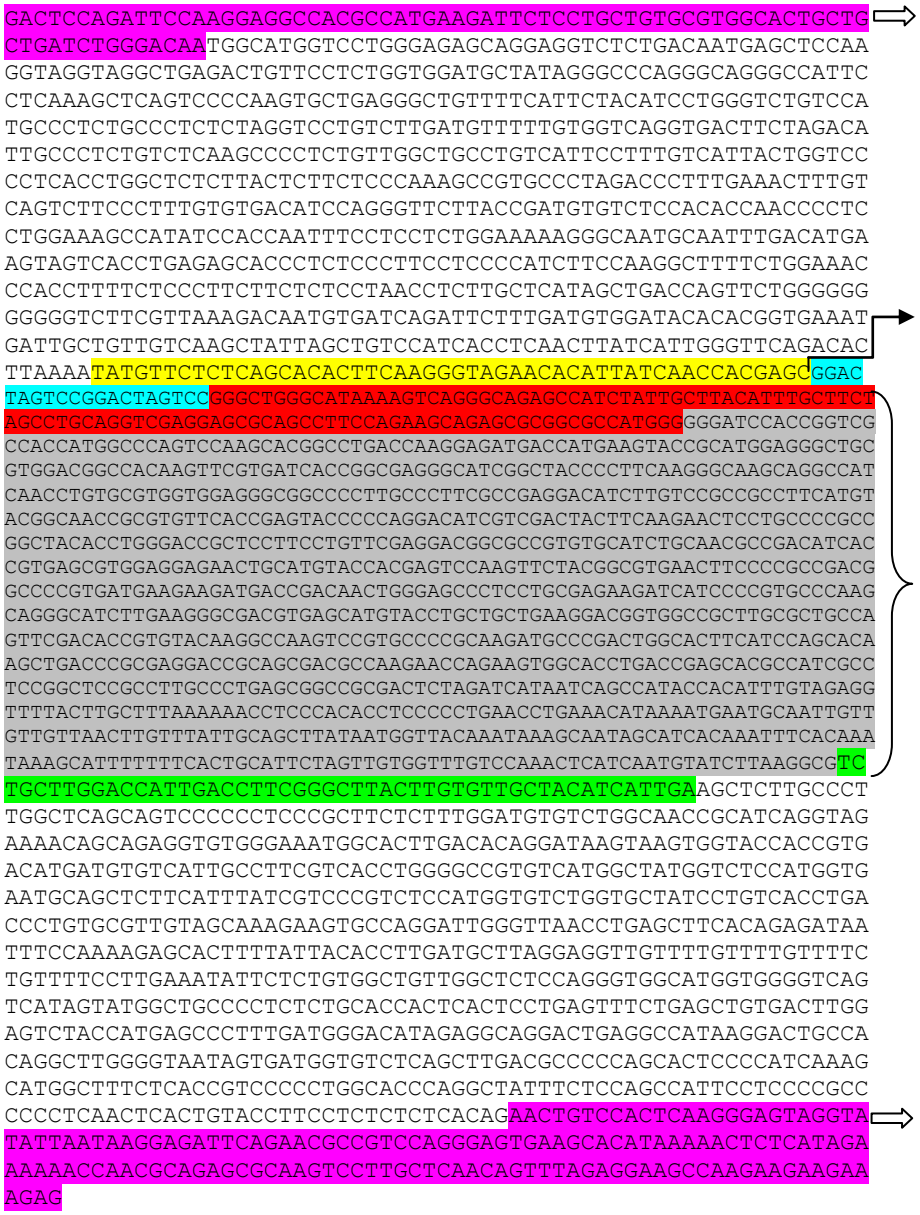


Exons 2 and 3 are highlighted in purple and are pointed with arrows on the top and the bottom of the sequence. 5' right arm of homology is highlighted in yellow and 3' left arm in green. Bglobin-ZsGreen insert cassette consists of 2 Spe linkers highlighted in blue, 105bp of human Bglobin promoter highlighted in red, 961bp of ZsGreen gene together with SV40 pA highlighted in light gray. The broken arrow between the blue and yellow highlights point to the insertion poing in the mid intron 2.

## Appendix V.VI - Predicted mouse clusterin sequence exon 2-3 modified by replacement of rpsL-neo with Bglobin-Cre-SV40 pA

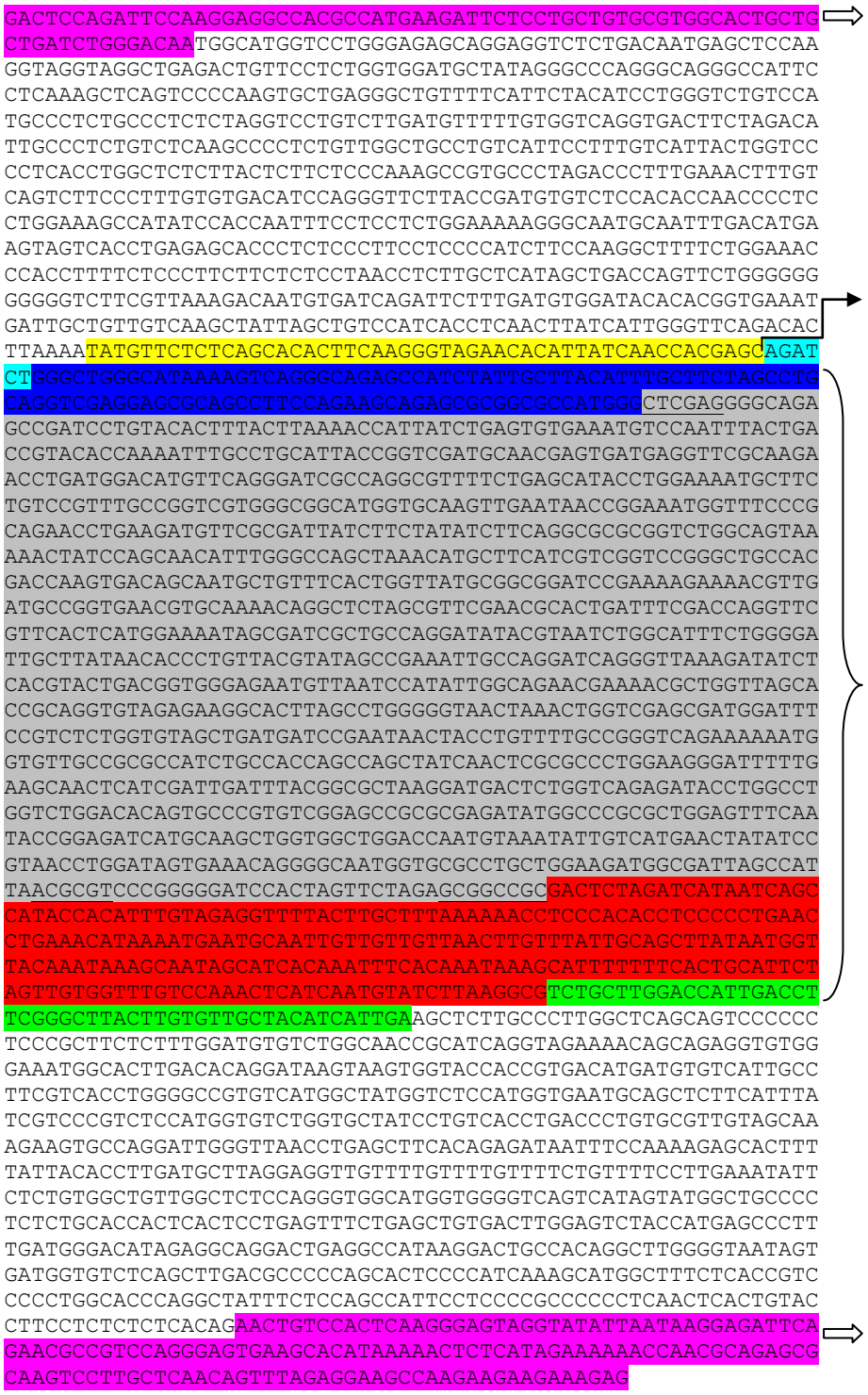


Exons 2 and 3 are highlighted in purple and are pointed with arrows on the top and the bottom of the sequence. 5' Right arm of homology is highlighted in yellow and 3' left arm in green. Bglobin is highlighted in blue. Cre sequence is in gray and the CTCGAG XhoI unique site that marks the beginning and ACGCGT MluI and GCGGCCGC NotI sites that mark the end of the Cre are underlined. The AGATCT between the left homology arm and Bglobin sequence, highlighted in light blue is BglII site. The SV40 pA is highlighted in red. Note that the SV40 pA sequence is not inserted into the Clu Cre-BAC construct (4.5.2). The broken arrow between the blue and yellow highlights point to the insertion poing in the mid intron 2.

**Appendix V.VII - Tectorin α transcript sequence – used to prepare α-tectorin probe**

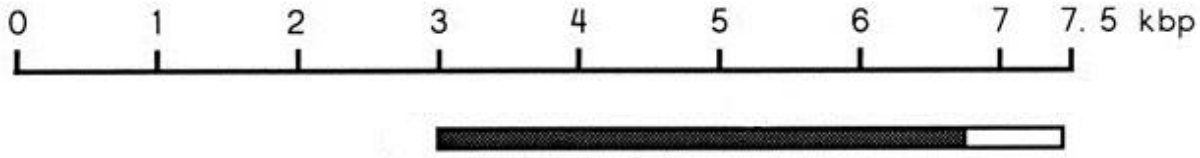


ENSMUST00000042190 cdna:KNOWN_protein_coding

TGTGGTATCATCAACGACCCCTCCAACAGCTCCTTCCTGGAGTGCCATGGGGTGGTTAAT
GTCACCGCCTACTACCGCACCTGCCTGTTTCGCCTGTGCCAGAGCGGAGGCAATGAGTCA
GAGCTGTGTGATTCTGTGGCCCGCTATGCCAGTGCTTGCAAGAATGCAGATGTGGAGGTG
GGCCCCTGGAGGACCTATGACTTCTGCCCTCTAGAATGCCCGGAGAACAGCCATTTTGAG
GAGTGTATGACATGTACAGAGACCTGCGAGACCCTGGCCTTGGGCCCCATCTGTGTGGAC
AGCTGCTCTGAGGGATGCCAGTGTGATGAAGGTTATGCCCTGCAGGGCAGCCAGTGTGTC
CCTCGGAGCGAGTGCGGCTGCAACTTTGAGGGGCATCAACTTGCCACCAATGAGACCTTC
TGGGTAGACCAGGACTGCCAGATCTTCTGCTACTGCAATGGCACAGACAACAGTGTCCAC
TGTGAGACCATTCCCTGCAGGGACGATGAATACTGTATGGAAGAGAGTGGCTTGTACTAC
TGCCAGCCCCGTACTGATGCTTCCTGTATCGTCTCAGGCTATGGTCACTACCTCACCTTT
GATGGCTACCCATTTGACTTCCAGACCAGTTGTCCTCTTATCCTCTGCACCACAGGAAGC
AGACCAATCTCAGACTCTTTCCCCAAGTTCATTGTAACAGCCAAGAATGAGGACCGGGAC
CCATCTCTAGCCTTGTGGGTGAAGCAGGTGGACGTGAACGTGTTTGGCTACAGCATTGTG
ATACACCGGGCTTACAAGCACACTGTGTTGGTCAACAATGAGCGGTTGTACCTGCCCCTG
AAGTTAGGACAAGGGAAGATAAACATCTTTTCATTCGGCTTTCATGTGGTTGTGGAGACT
GACTTTGGCCTGAAGGTCGTGTATGACTGGAAGACCTTCCTGTCCATTACCGTCCCCCGG
AGCATGCAGAACGGCACCTATGGCCTCTGTGGACGCTACAATGGCAACCCCGATGATGAC
CTTGAGATGCCCATGGGGCTGCCTGCACTGAGTATCAACGAGTTTGGCCAGAGCTGGGTG
AAGAGAGACACCTTCTGCCAGGTGGGCTGTGGGGACCGCTGCCCATCCTGTGCCAAAGTG
GAAGGTTTCTCCAAAGTACAGCAGCTGTGCAGCCTGATCCCCAACCAGAATGCTGGCTTT
GCCAAATGTCACAGCAAAGTCAACCCCACCTTCTTCTACAAAAACTGCCTGTTTGACTCC
TGTATCGATGGGGGTGCCGTGCAGACAGCCTGCAGCTGGTTACAAAACTATGCCAGCACT
TGCCAGACTCAAGGAATCGCAGTGACCGGCTGGAGGAACTACACGTCCTGTTCGGTTACC
TGCCCCCCCAACAGCCACTATGAGAGCTGTGTGAGCGTCTGCCAGCCCCGCTGCGCAGCC
ATCCGCCTGAAGAGTGACTGTAATCACTACTGCGTAGAGGGCTGCCAGTGTGATGCAGGC
TACGTCCTCAATGGCAAGAGCTGCATCTTGCCCCACAACTGTGGCTGCTACTCAGATGGC
AAATACTATGAGCCCAAGCAGCTATTCTGGAATGGGGACTGCACGCGGCGCTGCCGCTGT
TTCAGGCGCAACCTGATCCAGTGTGACCCACGCCAATGCAAGTCAGATGAGGAGTGCGCC
CTGCGCAGTGGGGTGCGCGGCTGCTTCAGCACCAAAACCTCCTACTGCCTAGCGGCAGGG
GGTGGTGTCTTCCGCACGTTCGATGGTGCCTTCCTGCGCTTCCCTGCCAACTGCGCCTTC
GTGCTCTCAACCATCTGCCAGAAATTGCCAGACATCTCCTTCCAGCTCATCATCAACTTC
GACAAGTGGTCCTCGCCCAACCTCACTATCATCTCACCGGTCTATTTCTACATTAACGAA
GAGCAGATTCTCATCAACGATCGGAACACTGTCAAGGTGAATGGCACACAAGTAAATGTT
CCATTTATAACGGGCTTGGCAACCAAAATCTACAGCAGCGAGGGGTTTCTGGTGATCGAC
ACCAGTCCCGACATCCAGATATATTACAATGGTTTTAACGTCATTAAAATCAGCATCAGT
GAGAGGCTACAGAACAAAGTGTGTGGGCTCTGTGGGAACTTCAATGGAGACATGACTGAC
GACTACGTGACCTTGCGGGGGAAACCCGTGGTGAGCAGCGTGGTGCTGGCCCAGAGCTGG
AAGACCAATGGCATGCAGAAGAGACCTCTCGCCCCCAGCTGCAACGAGCTACAGTTCTCA
CAGTATGCAGCCACATGTGACAATGTGCACATCCAGGCCATGCAGGGTGACGGCTACTGC
CTGAAACTCACCGACATGAAGGGCTTCTTCCAGCCCTGCTATGGGCTCCTTGATCCCCTC
CCGTTCTACGAGTCCTGTTACCTGGATGGCTGCTACAACCACAAGAAGTTCCAGCTGTGT
GGCTCCCTGGCTGCCTACGGGGAGGCCTGCCGCTCCTTCGGCATCCTTAGCACCGAGTGG
ATTGAGAAAGAGAATTGCTCAGGAGTGGTTGAAGACCCTTGTGTGGGGGCGGATTGTCCC
AACAGGACCTGCGAGCTGGACAACGGAGGAGAATTATGTGGCTGCATTGAGCCACCCCCC
TATGGAAACAATTCCCATGACATCATCGACGCGGAGGTGACCTGCAAGGCAGCCCAGATG
GAAGTGTCCATATCTAAGTGCAAGCTCTTCCAGCTGGGCTTTGAGAGAGAGGGTGTGAGA
ATCAATGACCGGCAGTGCTCTGGCATCGAGGGCGAGGATTTTATCTCCTTTCAAATCAAC

AACACCAAAGGGAACTGTGGGAACATCGTGCAGTCCAATGGCACTCATATCATGTATAAA
AACACAATCTGGATTGAAAGTGCCAACAACACTGGCAACATCATCACGAGGGACCGCACG
ATCAATGTGGAATTTTCATGCGCTTATGAGCTAGATATCAAGATCTCCTTAGACTCTGTC
GTGAAGCCTATGCTAAGTGTCATCAACCTGACAGTTCCGACCCAGGAGGGCAGCTTCACC
ACCAAGATGGCACTCTATAAAAATGCTTCCTACAAACACCCTTACCGCCAAGGGGAAGTT
GTGCTGACAACTCGGGATGTGCTGTACGTGGGCGTCTTTGTGGTCGGAGCTGACTCTACA
CACTTGATTCTCACACTCAACAAATGCTACGCCACCCCCTCCCGAGACAGCAACGACAAG
CTTCGGTACTTCATCATCGAAGGAGGATGTCAGAACATCAAAGACAACACCATTGGCATA
GAGGAGAACGGAGTGTCCCTAACCTGTCGTTTCCACGTCACCGTCTTCAAGTTCATCGGA
GACTACGATGAAGTTCATCTTCACTGTGCAGTGTCCCTCTGTGACTCAGAGAAATACTCT
TGCAAGATTAATTGCCCACAAAATTCCAGGATCGCCACAGATTATTCAAAAGAGCACAAA
GAACAGATCATTTCAGTGGGACCCATTAGGAGAAAAAGGCTGGACTGGTGTGAAGACAAC
GGCGGCTGTGAGCAGATCTGCACCAGCCGGGTCGACGGGCCTCTGTGCAGCTGTGTGACC
GGATCCCTGCAAGAAGATGGAAGGAGCTGCAGAGCCTCTAATTCTTCAGTGGAACTTCAA
GTTTGGACACTTCTTCTCATCATGACCCAGATCTCACTGTGGCATTTGATCTATAAATCA
GGCGCAACCTCATAACGAACTCAGGGTGCTTTCTTCAGTCCCTGTAGGTATAAAAGTGTG
TGTCCCCAAGTCAAAACAGCCTCTCACACTCACGCCACCTTCCTCCAGCAGTCAGATCTG
GAGGACACCAACGTTCCTGGCTCCTCTTCCACAGTATGCAATAGTGGTTTCTCAAAGCCA
ATGGGAGGAAAGCACGCTCTTACCCTCAATGCCAAACAGCTGGCACTGGGTACCTAGGTT
CAGGCCAGAAGCCAGCCAGGGAAAGCTCTGGCTACAGAAGTCTGATGGGAAAGCTGGCCA
GAAAAGTTGGTCTGTCCCGCGCTGTTTCTGGAACACCGTGGTTATAGGCAAGGCTATTGC
TGTGACTTTGAATTAAAGTTGCGTCTCTCTCTGTGGAGCCTCGCCAACACTGCCCTCAGC
TCACTTTGCTTAGCTCCTCCCCCTCCTGCTGTGGCCTCCACCTTGCCGTGCCAGCTTCAG
TCACTGGAGATGATGTTTGTAGACCTGGAGAACCTCACCCTGCCCGTCCCGATCCTCAAA
CCCAGCCCTTCACATTTTACAAATCAACCAAATAATTTTTAATGTGTTTTATCCTTAAAT
AAACTTTGTGTTCAAGTA

**Appendix V.VIII - Tectorin β transcript sequence – used to prepare β-tectorin probe**

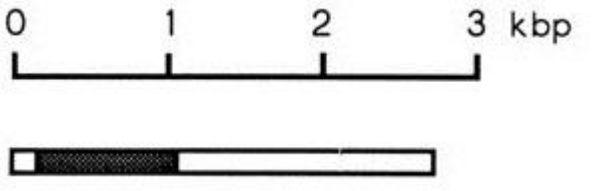


>ENSMUST00000025936 cdna:KNOWN_protein_coding
TCTAACCCTTGACTGTAACTTTTCCTTCATATTTCCGATACAGAACAACCGCGACCCGGG
GCCTGGAAGGAGCGTGAGCATTGAGCCAGTTTGGTTTGGCCACCTGGCAGAGATCGACTC
TAGAGGAGCGATGGTGGTCAGGGCCTTCGTTTTGCTGGCCCTCTTTGCAGAAGCCTCAGC
GAAATCATGCACTCCGAATAAAGCAGATGTCATCCTTGTGTTTTGTTATCCCAAGACCAT
CATCACTAAAATCCCCGAGTGTCCCTATGGATGGGAAGTACACCAGCTGGCACTCGGGGG
GCTGTGTTACAACGGGGTCCATGAAGGTGGCTATTACCAGTTTGTCATCCCTGATCTGTC
ACCTAAGAACAAGTCCTACTGTGGAACCCAGTCAGAGTACAAGCCCCCCATCTACCACTT
CTACAGCCACATCGTGTCCAACGACAGCACAGTGATCGTGAAGAACCAGCCCGTCAACTA
CTCCTTCTCCTGCACCTACCACTCCACCTACTTGGTGAACCAGGCTGCTTTTGACCAGAG
AGTGGCCACTGTTCACGTCAAGAACGGGAGCATGGGCACATTTGAAAGCCAGTTGTCCCT
CAACTTCTACACTAATGCCAAGTTTTCCACCAAAAAAGAAGCTCCCTTCGTTCTGGAAAC
GTCCGAAATCGGCTCAGATCTGTTTGCGGGAGTAGAAGCCAAAGGCCTAAGCGTTCGGTT
CAAAGTGGTCTTGAATAGCTGCTGGGCCACCCCCTCGGCTGACTTCATGTACCCCTTACA
GTGGCAGCTCATCAATAAGGGCTGCCCCACCGATGAGACAGTCCTCGTGCATGAGAACGG
CAAAGACCACAGGGCCACTTTCCAATTCAATGCCTTCCGGTTCCAGAACATCCCCAAACT
TTCCAAGGTTTGGTTACACTGTGAGACGTTCATCTGCGACAGTGAGAAGCTCTCCTGCCC
CGTGAACTGTGACAAACGGAAGCGCATGCTACGTGACCAGACAGGAGGTGTCCTGGTTGT
GGAGTTGTCCCTGAGGAGCAGGGCATTTTCCGGCCTCTGTGACTTCTCAGATGTTCTTCT
TCACCTCATCCTGATGCTGGGGACCTGGGCTGTGTTGTAGGAGACAGCTGGACAGCTGTA
GCAGCTCTCTCCAAGGCCACCCTGAACTATGACACATTCGTTTATTGTGCTGCCAAAAAA
AGAACAGACAGAAGACTGCATGGCTGGGGAGCTGGGAACAGCCCTTTGCCAAATATGTGT
TCCCCCATGTTTGTGTGTGGATGTGAATTTGGTGAACCTCTGCCTCAGAGCCACACTTCC
ACTTATTCCGTCCTGCGGCCGTTAGATCCTGATAATCTTCTCCATGAAGCCAGAGAGGAG
TGTTCTCTCCTCCGCTCAAATTAGAGCAGCATTTGGAAGCTACTTTCATTATAAAAGACT
CTCACACACTCATCACATGCAGCTTAACATTTGGAGGCAGAGACAGACAAACACCAAAAA
AAAAAAATCAATGCCAAATACAGAATCCACAGGAATAGCCAACTTTACCCAGCAGGCACT
CTGTCATTGAGACAGTACAGTTCTAAGGACCAGCATCGAGCCCCCAGGCAGGAAGTTCCA
GTCTTCAACCACGATGTGGAAGTCCAAGTTAAATACAATATATTTACTCAAACTTCTGTA
ATGGATGAGAAGGGGATCCTTGAGAGCCGCTAGTACCAGTCTGCTTTTATCATAGGGTTT
CTTAAATAGATATAATCATTAGGGAGGTATAGATGTCTTATCCTTACAAGAGATTCTATT
TCTTTAGTCACAAATAAATAGGAAATCGACTATGAACAAGTAAAACTCATCTCCATTTCA
CAGAAGAGTGTGGCATTGCCTCCGTGAACTGTATTTGCACGGGAGTGGAAAGACTCTGGC
CGAGCCGGTTCTCTGAGAGGTGAGAGCCGAGCTTCCCTCACACCTGTGGTGCCCTGTGCG
TTCAATAGCCTAGTGTGTGCTCTTGGAAGTCTTCCTGTCAGGATGGTGGGATGCGAACAT
CCAAGCCCTGTTCCTTCTTGGTCACTTGTGACTGTGGGGACTGAACCATCCACTCATCAG
AAATGTAATGCATACACAGTCAATGACATCACATGACAGCACACTCTCAGAACTGGCCAC
CCCTGTGACCCAGAGCATGCCAACGTCCGTAGGTCACATTTGGCAATGAGAAGCCAAGTG
AACACACCAATCCTGTGAGAGCATGAGCTGTGGTATGACAGGAGAGACCTTGTGCTAAGT
CTTTTTTTTTCCCCTTTGTCACTTTCACACTGGGCATTTGAAATCACATATCAGTTTGTC
CCTCTGTATTTCATGCCCTTGAGAGGTCTTGATGTCTGTGGTTTACCAATCCTTTTACAA
CTTGGGTAAATGAACTTAGAAATTGTGTTTGTTTAGCCGCAGGCTAGTGCACGGTGGTCC
CATGTATTCTAAACTTGGTATCTAGTTCATGCTCCAATCAGTTTGGAACCACTTCCTAAT
GTAACGTCAGAGTTTGTTGTAGCTGAGAATTACAGAAAACCTGCTTTCTTGATCCTAGTC
AGGAACTCTTACGAAGCACACATATAGCCAAGCTTATAGGTCTTTGGCTGTCAGACTAAA
AACAATGTTTGATCCTGATGTATGGTCTTGTATCTCAACCTGGTGCTATGGACTAAATAA
AATGTCTGGAGTAAGTAACCTGTGA

## Appendix VI - BACs and plasmid vector maps

## Appendix VI.I - pBACe3.6 map - Clusterin BAC backbone

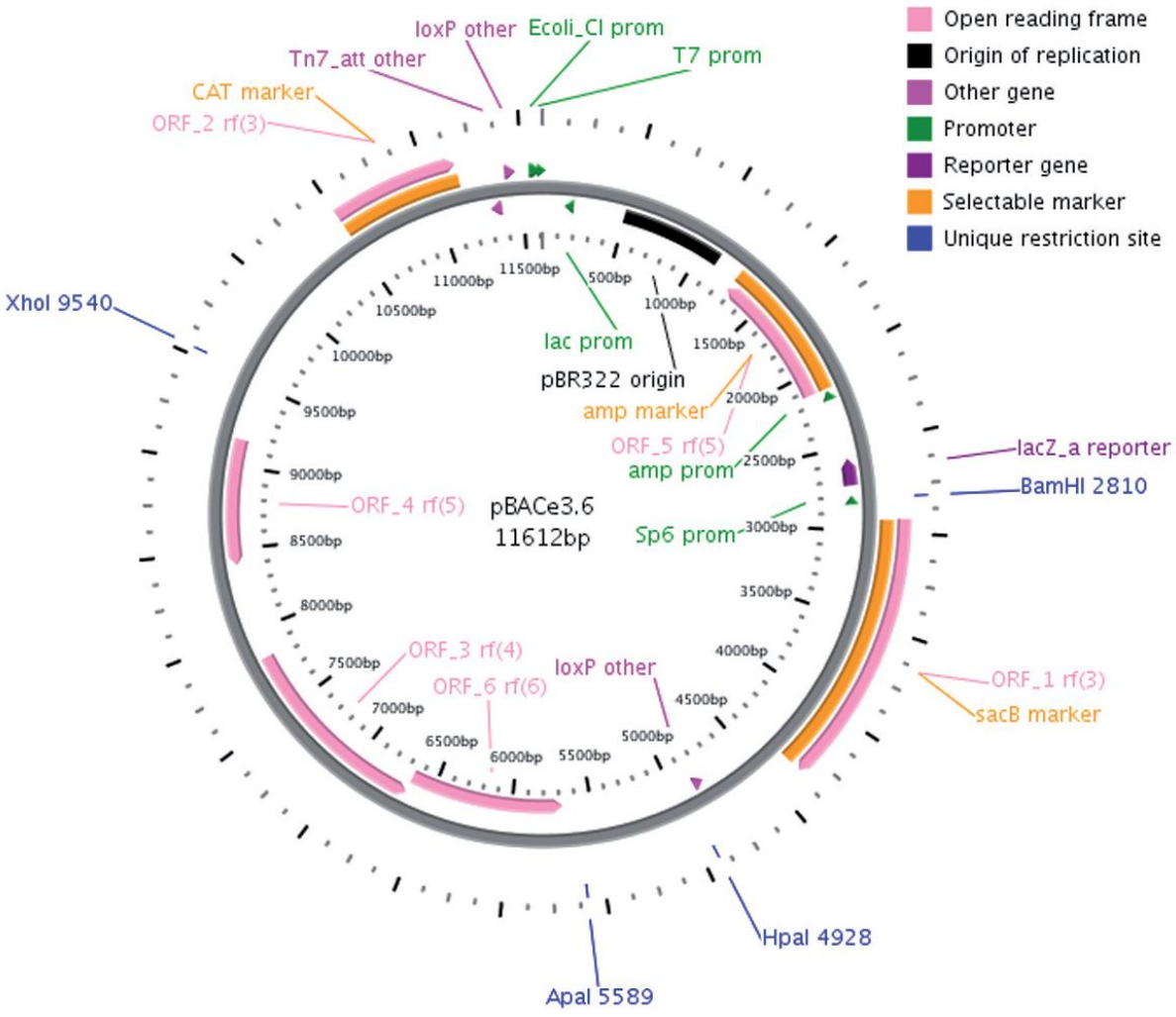


The clustrein gene and its flanking sequences are cloned into the pBACe3.6 vector at *EcoRI* sites (not shown in this figure but present at position 10 and 2801bp. The vector includes 2 loxP sites, a non-mutated loxP at 4831-4864bp and a mutated loxP (loxP511) at 11408-11441. Selectable markers include: Amp marker, CAT marker for Chloramphenicol resistance, and the "SacB marker which can be used as a positive selective marker for the recombinant clones against the non-insert colonies."

**Appendix VI.II - Plasmid "βglobin-ZsGreen 1:1" vector map**

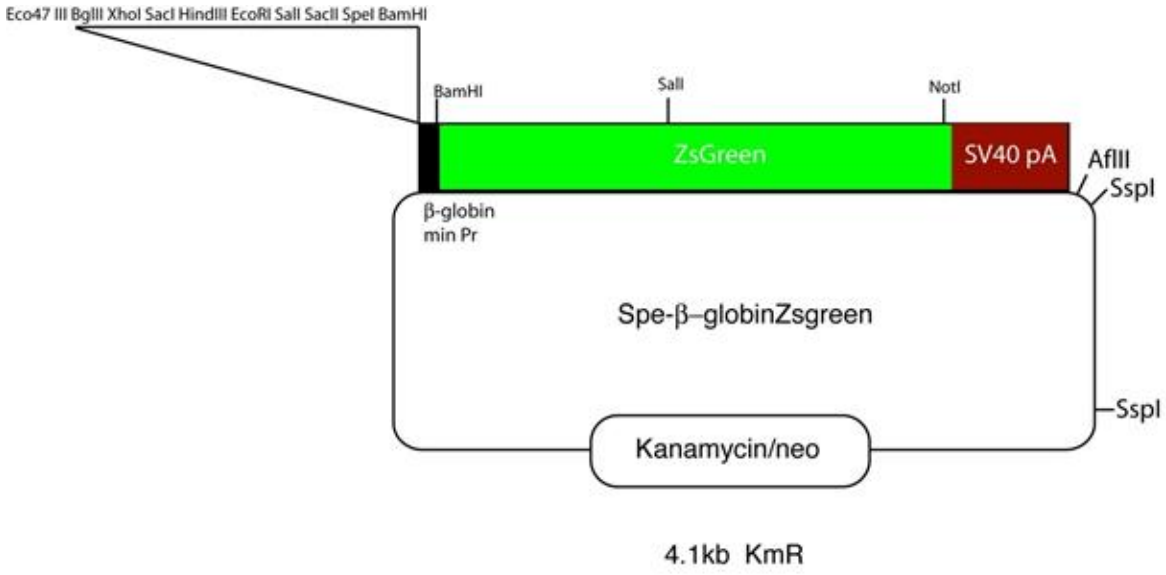


**Appedix VI.III - Cre expression plasmid**

Adapted from http://www.addgene.org

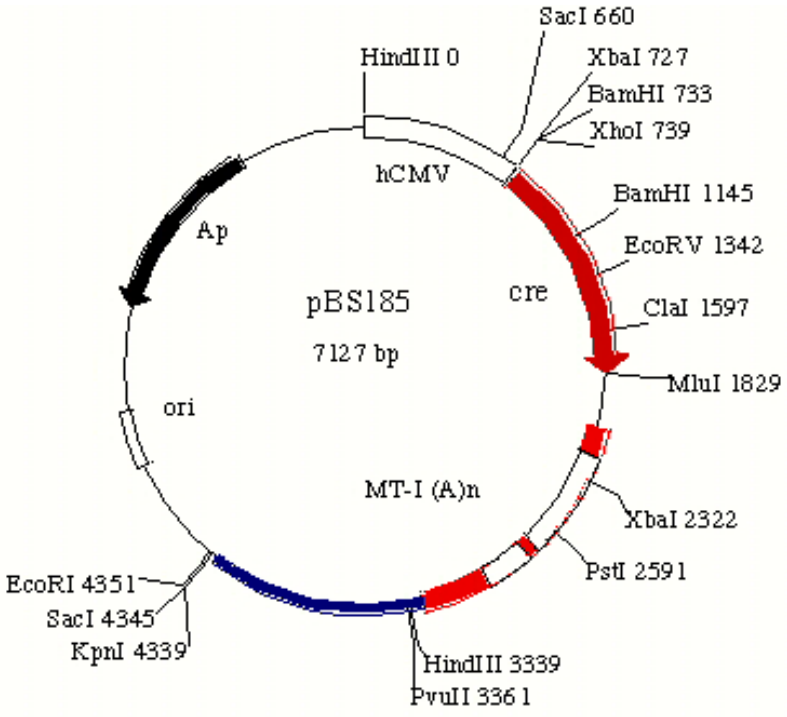

## Appendix VI.IV - Map of the Red/ET expression plasmid

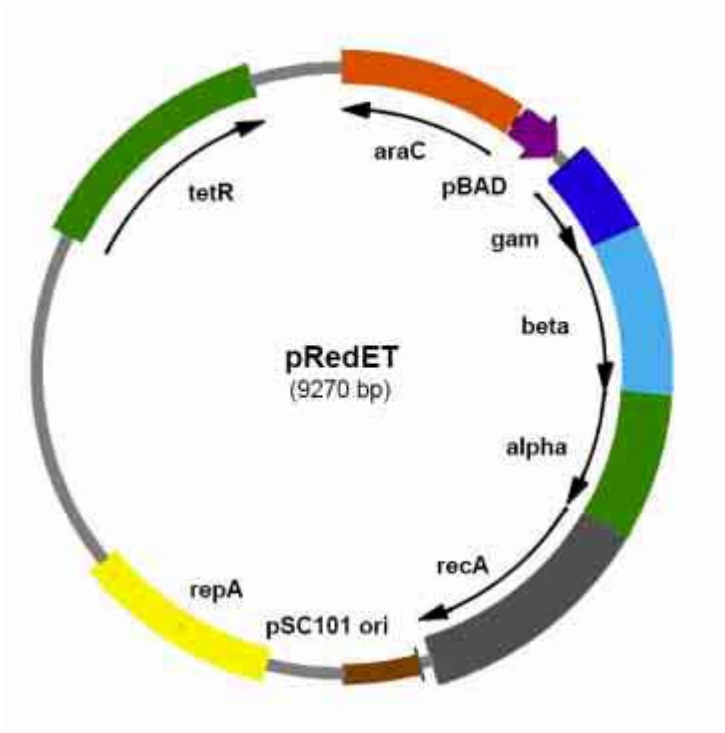


Map of the Red/ET plasmid (pSC101-BAD-gbaA$^{tet}$). Expression of the Red/ET recombination proteins is induced by L-arabinose, which activates the BAD promoter at 37ºC. Modified from (GENEBRIDGES technical protocol 2007).

# References

## References


Ahn, K. J., F. Passero, Jr., et al. (2009). "Otic mesenchyme expression of Cre recombinase directed by the inner ear enhancer of the Brn4/Pou3f4 gene." Genesis (New York, N.Y. : 2000) **47**(3): 137-141.

Ahuja, H. S., M. Tenniswood, et al. (1994). "EXPRESSION OF CLUSTERIN IN CELL-DIFFERENTIATION AND CELL-DEATH." Biochemistry and Cell Biology-Biochimie Et Biologie Cellulaire **72**(11-12): 523-530.

Alvarez, I. S. and J. Navascues (1990). "SHAPING, INVAGINATION, AND CLOSURE OF THE CHICK-EMBRYO OTIC VESICLE - SCANNING ELECTRON-MICROSCOPIC AND QUANTITATIVE STUDY." Anatomical Record **228**(3): 315-326.

Anniko, M. (1983). "CYTODIFFERENTIATION OF COCHLEAR HAIR-CELLS." American Journal of Otolaryngology **4**(6): 375-388.

Ard, M. D. and D. K. Morest (1984). "CELL-DEATH DURING DEVELOPMENT OF THE COCHLEAR AND VESTIBULAR GANGLIA OF THE CHICK." International Journal of Developmental Neuroscience **2**(6): 535-547.

Aronow, B. J., S. D. Lund, et al. (1993). "APOLIPOPROTEIN-J EXPRESSION AT FLUID-TISSUE INTERFACES - POTENTIAL ROLE IN BARRIER CYTOPROTECTION." Proceedings of the National Academy of Sciences of the United States of America **90**(2): 725-729.

Asami, J., Y. U. Inoue, et al. (2011). "Bacterial artificial chromosomes as analytical basis for gene transcriptional machineries." Transgenic Research **20**(4): 913-924.

Bach, U. C., M. Baiersdorfer, et al. (2001). "Apoptotic cell debris and phosphatidylserine-containing lipid vesicles induce apolipoprotein J (clusterin) gene expression in vital fibroblasts." Experimental Cell Research **265**(1): 11-20.

Bailey, R. and M. D. Griswold (1999). "Clusterin in the male reproductive system: localization and possible function." Molecular and Cellular Endocrinology **151**(1-2): 17-23.

Bailey, R. W., A. K. Dunker, et al. (2001). "Clusterin, a binding protein with a molten globule-like region." Biochemistry **40**(39): 11828-11840.

Bajari, T. M., Strasser, V., Nimpf, J., and Schneider, W. J. (2003). "A model for modulation of leptin activity by association with clusterin. ." FASEB J **17**: 1505-1507.

Barald, K. F. and M. W. Kelley (2004). "From placode to polarization: new tunes in inner ear development." Development **131**(17): 4119-4130.

Bell, R. D., A. P. Sagare, et al. (2007). "Transport pathways for clearance of human Alzheimer's amyloid beta-peptide and apolipoproteins E and J in the mouse central nervous system." Journal of Cerebral Blood Flow and Metabolism **27**(5): 909-918.

Bermingham-McDonogh, O., E. C. Oesterle, et al. (2006). "Expression of Prox1 during mouse cochlear development." Journal of Comparative Neurology **496**(2): 172-186.

Bettuzzi, S. (2009). "Chapter 1: Introduction." Adv Cancer Res **104**: 1-8.

Bettuzzi, S., R. A. Hiipakka, et al. (1989). "Identification of an androgen-repressed mRNA in rat ventral prostate as coding for sulphated glycoprotein 2 by cDNA cloning and sequence analysis." Biochem J **257**(1): 293-296.

Bettuzzi, S., F. Scorcioni, et al. (2002). "Clusterin (SGP-2) transient overexpression decreases proliferation rate of SV40-immortalized human prostate epithelial cells by slowing down cell cycle progression." Oncogene **21**(27): 4328-4334.

Bever, M. M. and D. M. Fekete (1999). "Ventromedial focus of cell death is absent during development of Xenopus and zebrafish inner ears." Journal of Neurocytology **28**(10-11): 781-793.

Bissonnette, J. P. and D. M. Fekete (1996). "Standard atlas of the gross anatomy of the developing inner ear of the chicken." Journal of Comparative Neurology **368**(4): 620-630.

Blaschuk, O., K. Burdzy, et al. (1983). "PURIFICATION AND CHARACTERIZATION OF A CELL-AGGREGATING FACTOR (CLUSTERIN), THE MAJOR GLYCOPROTEIN IN RAM RETE TESTIS FLUID." Journal of Biological Chemistry **258**(12): 7714-7720.

Bok, J., W. Chang, et al. (2007). "Patterning and morphogenesis of the vertebrate inner ear." International Journal of Developmental Biology **51**(6-7): 521-533.

Brooker, R., K. Hozumi, et al. (2006). "Notch ligands with contrasting functions: Jagged1 and Delta1 in the mouse inner ear." Development **133**(7): 1277-1286.

Brown, T. L., B. C. Moulton, et al. (1996). "Apolipoprotein J/clusterin expression defines distinct stages of blastocyst implantation in the mouse uterus." Biology of Reproduction **55**(4): 740-747.

Bursch, W., T. Gleeson, et al. (1995). "EXPRESSION OF CLUSTERIN (TESTOSTERONE-REPRESSED PROSTATE MESSAGE-2) MESSENGER-RNA DURING GROWTH AND REGENERATION OF RAT-LIVER." Archives of Toxicology **69**(4): 253-258.

Buttyan, R., C. A. Olsson, et al. (1989). "INDUCTION OF THE TRPM-2 GENE IN CELLS UNDERGOING PROGRAMMED DEATH." Molecular and Cellular Biology **9**(8): 3473-3481.

Caccamo, A. E., M. Scaltriti, et al. (2005). "Ca2+ depletion induces nuclear clusterin, a novel effector of apoptosis in immortalized human prostate cells." Cell Death Differ **12**(1): 101-104.

Calero, M., T. Tokuda, et al. (1999). "Functional and structural properties of lipid-associated apolipoprotein J (clusterin)." Biochemical Journal **344**: 375-383.

Cantos, R., L. K. Cole, et al. (2000). "Patterning of the mammalian cochlea." Proceedings of the National Academy of Sciences of the United States of America **97**(22): 11707-11713.

Carvajal, J. J., A. Keith, et al. (2008). "Global transcriptional regulation of the locus encoding the skeletal muscle determination genes Mrf4 and Myf5." Genes & Development **22**(2): 265-276.

Cervellera, M., G. Raschella, et al. (2000). "Direct transactivation of the anti-apoptotic gene apolipoprotein J (Clusterin) by B-MYB." Journal of Biological Chemistry **275**(28): 21055-21060.

Chang, W., L. Cole, et al. (2004). Molecular genetics of vestibular organ development. The vestibular system. S. M. F. R. R. P. A. N. Highstein. **Volume 19:** 11-56.

Chang, W., Z. Lin, et al. (2008). "Bmp4 is essential for the formation of the vestibular apparatus that detects angular head movements." Plos Genetics **4**(4).

Charnay Y, I. A., Vallet PG, Hakkoum D, Lathuiliere A, Poku N, Aronow B, Kovari E, Bouras C, Giannakopoulos P. (2008). "Clusterin expression during fetal and postnatal CNS development in mouse." Neuroscience. 2008 Aug 26;155(3):714-24. Epub 2008 Jun 17.

Chen, P., J. E. Johnson, et al. (2002). "The role of Math1 in inner ear development: Uncoupling the establishment of the sensory primordium from hair cell fate determination." Development **129**(10): 2495-2505.

Chen, P. and N. Segil (1999). "p27(Kip1) links cell proliferation to morphogenesis in the developing organ of Corti." Development **126**(8): 1581-1590.

Choi, N. H., T. Mazda, et al. (1989). "A SERUM-PROTEIN SP40,40 MODULATES THE FORMATION OF MEMBRANE ATTACK COMPLEX OF COMPLEMENT ON ERYTHROCYTES." Molecular Immunology **26**(9): 835-840.

Choimiura, N. H., Y. Takahashi, et al. (1992). "IDENTIFICATION OF THE DISULFIDE BONDS IN HUMAN PLASMA-PROTEIN SP-40,40 (APOLIPOPROTEIN-J)." Journal of Biochemistry **112**(4): 557-561.

Chun, J. T., L. Wang, et al. (1999). "Glycoprotein 330/megalin (LRP-2) has low prevalence as mRNA and protein in brain microvessels and choroid plexus." Experimental Neurology **157**(1): 194-201.

Ciuman, R. R. (2009). "Stria vascularis and vestibular dark cells: characterisation of main structures responsible for inner-ear homeostasis, and their pathophysiological relations." Journal of Laryngology and Otology **123**(2): 151-162.

Cochrane, D. R., Z. Wang, et al. (2007). "Differential regulation of clusterin and its Isoforms by androgens in prostate cells." Journal of Biological Chemistry **282**(4): 2278-2287.

Cohen-Salmon, M., T. Ott, et al. (2002). "Targeted ablation of connexin26 in the inner ear epithelial gap junction network causes hearing impairment and cell death." Current Biology **12**(13): 1106-1111.

Colvin, J. S., B. A. Bohne, et al. (1996). "Skeletal overgrowth and deafness in mice lacking fibroblast growth factor receptor 3." Nature Genetics **12**(4): 390-397.

Dabdoub, A., C. Puligilla, et al. (2008). "Sox2 signaling in prosensory domain specification and subsequent hair cell differentiation in the developing cochlea." Proceedings of the National Academy of Sciences of the United States of America **105**(47): 18396-18401.

Desilva, H. V., J. A. K. Harmony, et al. (1990). "APOLIPOPROTEIN-J - STRUCTURE AND TISSUE DISTRIBUTION." Biochemistry **29**(22): 5380-5389.

Desilva, H. V., W. D. Stuart, et al. (1990). "PURIFICATION AND CHARACTERIZATION OF APOLIPOPROTEIN-J." Journal of Biological Chemistry **265**(24): 14292-14297.

Driver, E. C. and M. W. Kelley (2009). "Specification of Cell Fate in the Mammalian Cochlea." Birth Defects Research Part C-Embryo Today-Reviews **87**(3): 212-221.

Erkman, L., R. J. McEvilly, et al. (1996). "Role of transcription factors Brn-3.1 and Brn-3.2 in auditory and visual system development." Nature **381**(6583): 603-606.

Fekete, D. M., S. A. Homburger, et al. (1997). "Involvement of programmed cell death in morphogenesis of the vertebrate inner ear." Development **124**(12): 2451-2461.

Fekete, D. M., S. Muthukumar, et al. (1998). "Hair cells and supporting cells share a common progenitor in the avian inner ear." Journal of Neuroscience **18**(19): 7811-7821.

Fettiplace, R. and C. M. Hackney (2006). "The sensory and motor roles of auditory hair cells." Nature Reviews Neuroscience **7**(1): 19-29.

Ficker, M., N. Powles, et al. (2004). "Analysis of genes from inner ear developmental-stage cDNA subtraction reveals molecular regionalization of the otic capsule." Developmental Biology **268**(1): 7-23.

Fischercolbrie, R., R. Zangerle, et al. (1984). "ISOLATION AND IMMUNOLOGICAL CHARACTERIZATION OF A GLYCOPROTEIN FROM ADRENAL CHROMAFFIN GRANULES." Journal of Neurochemistry **42**(4): 1008-1016.

French, L. E., A. Chonn, et al. (1993). "MURINE CLUSTERIN - MOLECULAR-CLONING AND MESSENGER-RNA LOCALIZATION OF A GENE ASSOCIATED WITH EPITHELIAL DIFFERENTIATION PROCESSES DURING EMBRYOGENESIS." Journal of Cell Biology **122**(5): 1119-1130.

French, L. E., J. V. Soriano, et al. (1996). "Modulation of clusterin gene expression in the rat mammary gland during pregnancy, lactation, and involution." Biology of Reproduction **55**(6): 1213-1220.

French, L. E., A. Wohlwend, et al. (1994). "HUMAN CLUSTERIN GENE-EXPRESSION IS CONFINED TO SURVIVING CELLS DURING IN-VITRO PROGRAMMED CELL-DEATH." Journal of Clinical Investigation **93**(2): 877-884.

Freyer, L., V. Aggarwal, et al. (2011). "Dual embryonic origin of the mammalian otic vesicle forming the inner ear." Development **138**(24): 5403-5414.

Fritz, I. B., K. Burdzy, et al. (1983). "RAM RETE TESTIS FLUID CONTAINS A PROTEIN (CLUSTERIN) WHICH INFLUENCES CELL-CELL INTERACTIONS INVITRO." Biology of Reproduction **28**(5): 1173-1188.

Furlong, E. E. M., N. K. Keon, et al. (1996). "Expression of a 74-kDa nuclear factor 1 (NF1) protein is induced in mouse mammary gland involution - Involution-enhanced occupation of a twin NF1 binding element in the testosterone-repressed prostate message-2/clustertin promoter." Journal of Biological Chemistry **271**(47): 29688-29697.

Garden, G. A., M. Bothwell, et al. (1991). "LACK OF CORRESPONDENCE BETWEEN MESSENGER-RNA EXPRESSION FOR A PUTATIVE CELL-DEATH MOLECULE (SGP-2) AND NEURONAL CELL-DEATH IN THE CENTRAL-NERVOUS-SYSTEM." Journal of Neurobiology **22**(6): 590-604.

Gavara, N. and R. S. Chadwick (2009). "Collagen-Based Mechanical Anisotropy of the Tectorial Membrane: Implications for Inter-Row Coupling of Outer Hair Cell Bundles." PLoS One **4**(3).

Gelissen, I. C., T. Hochgrebe, et al. (1998). "Apolipoprotein J (clusterin) induces cholesterol export from macrophage-foam cells: a potential anti-atherogenic function?" Biochem J **331 ( Pt 1)**: 231-237.

GENEBRIDGES (technical protocol 2007). Counter-Selection BAC Modificatiob Kit (Advanced BAC Modification Kit) - Version 3.0. R. E. Recombination.

GENEBRIDGES (technical protocol Feb 2005). Quick and Easy BAC Modification Kit, Version 2.4. R. E. Recombination.

Gleave, M. and H. Miyake (2005). "Use of antisense oligonucleotides targeting the cytoprotective gene, clusterin, to enhance androgen- and chemo-sensitivity in prostate cancer." World Journal of Urology **23**(1): 38-46.

Goldnersauve, A., C. Szpirer, et al. (1991). "CHROMOSOME ASSIGNMENTS OF THE GENES FOR GLUCOCORTICOID RECEPTOR, MYELIN BASIC-PROTEIN, LEUKOCYTE COMMON ANTIGEN, AND TRPM2 IN THE RAT." Biochemical Genetics **29**(5-6): 275-286.

Gong, S., L. Kus, et al. (2010). "Rapid bacterial artificial chromosome modification for large-scale mouse transgenesis." Nature Protocols **5**(10): 1678-1696.

Gutacker, C., G. Klock, et al. (1999). "Nerve growth factor and epidermal growth factor stimulate clusterin gene expression in PC12 cells." Biochemical Journal **339**: 759-766.

Guzman, L. M., D. Belin, et al. (1995). "TIGHT REGULATION, MODULATION, AND HIGH-LEVEL EXPRESSION BY VECTORS CONTAINING THE ARABINOSE P-BAD PROMOTER." Journal of Bacteriology **177**(14): 4121-4130.

Haddon, C. and J. Lewis (1996). "Early ear development in the embryo of the zebrafish, Danio rerio." Journal of Comparative Neurology **365**(1): 113-128.

Hammad, S. M., S. Ranganathan, et al. (1997). "Interaction of apolipoprotein J-amyloid beta-peptide complex with low density lipoprotein receptor-related protein-2 megalin - A mechanism to prevent pathological accumulation of amyloid beta-peptide." Journal of Biological Chemistry **272**(30): 18644-18649.

Harold, D., R. Abraham, et al. (2009). "Genome-wide association study identifies variants at CLU and PICALM associated with Alzheimer's disease." Nature Genetics **41**(10): 1088-U1061.

Hayashi, T., D. Cunningham, et al. (2007). "Loss of FGFR3 leads to excess hair cell development in the mouse organ of Corti." Developmental Dynamics **236**(2): 525-533.

Hertzano, R., M. Montcouquiol, et al. (2004). "Transcription profiling of inner ears from Pou4f3(ddl/ddl) identifies Gfi1 as a target of the Pou4f3 deafness gene." Human Molecular Genetics **13**(18): 2143-2153.

Hochgrebe, T. T., D. Humphreys, et al. (1999). "A reexamination of the role of clusterin as a complement regulator." Exp Cell Res **249**(1): 13-21.

Horton, P., K.-J. Park, et al. (2007). "WoLF PSORT: protein localization predictor." Nucleic Acids Research **35**: W585-W587.

Hudspeth, A. J. (1989). "HOW THE EARS WORKS WORK." Nature **341**(6241): 397-404.

Hume, C. R., D. L. Bratt, et al. (2007). "Expression of LHX3 and SOX2 during mouse inner ear development." Gene Expression Patterns **7**(7): 798-807.

Humphreys, D., T. T. Hochgrebe, et al. (1997). "Effects of clusterin overexpression on TNFalpha- and TGFbeta-mediated death of L929 cells." Biochemistry **36**(49): 15233-15243.

Humphreys, D. T., J. A. Carver, et al. (1999). "Clusterin has chaperone-like activity similar to that of small heat shock proteins." Journal of Biological Chemistry **274**(11): 6875-6881.

Hyman Lab Counter Selection BAC modification.

Inoue, T., Y. U. Inoue, et al. (2008). "Analysis of mouse Cdh6 gene regulation by transgenesis of modified bacterial artificial chromosomes." Developmental Biology **315**(2): 506-520.

Itahana, Y., M. Piens, et al. (2007). "Regulation of clusterin expression in mammary epithelial cells." Experimental Cell Research **313**(5): 943-951.

J. Chuck Harrell, C. A. S., Wendy W. Dye, Britta M. Jacobsen, and Kathryn B. Horwitz (2007) "ZsGreen Labeling of Breast Cancer Cells to Visualize Metastasis."

Jacques, B. E., M. E. Montcouquiol, et al. (2007). "Fgf8 induces pillar cell fate and regulates cellular patterning in the mammalian cochlea." Development **134**(16): 3021-3029.

James, R. W., A. C. Hochstrasser, et al. (1991). "CHARACTERIZATION OF A HUMAN HIGH-DENSITY LIPOPROTEIN-ASSOCIATED PROTEIN, NA1/NA2 - IDENTITY WITH SP-40,40, AN INHIBITOR OF COMPLEMENT-MEDIATED CYTOLYSIS." Arteriosclerosis and Thrombosis **11**(3): 645-652.

Jenne, D. E. and J. Tschopp (1989). "MOLECULAR-STRUCTURE AND FUNCTIONAL-CHARACTERIZATION OF A HUMAN-COMPLEMENT CYTOLYSIS INHIBITOR FOUND IN BLOOD AND SEMINAL PLASMA - IDENTITY TO SULFATED GLYCOPROTEIN-2, A CONSTITUENT OF RAT TESTIS FLUID." Proceedings of the National Academy of Sciences of the United States of America **86**(18): 7123-7127.

Jenne, D. E. and J. Tschopp (1992). "CLUSTERIN - THE INTRIGUING GUISES OF A WIDELY EXPRESSED GLYCOPROTEIN." Trends in Biochemical Sciences **17**(4): 154-159.

Jeong, Y. S., K. El-Jaick, et al. (2006). "A functional screen for sonic hedgehog regulatory elements across a 1 Mb interval identifies long-range ventral forebrain enhancers." Development **133**(4): 761-772.

Jin, G. and P. H. Howe (1997). "Regulation of clusterin gene expression by transforming growth factor beta." Journal of Biological Chemistry **272**(42): 26620-26626.

Jin, G. and P. H. Howe (1999). "Transforming growth factor beta regulates clusterin gene expression via modulation of transcription factor c-Fos." European Journal of Biochemistry **263**(2): 534-542.

Jomary, C., G. Chatelain, et al. (1999). "Effect of targeted expression of clusterin in photoreceptor cells on retinal development and differentiation." Journal of Cell Science **112**(10): 1455-1464.

Jones, S. E., J. M. A. Meerabux, et al. (1992). "ANALYSIS OF DIFFERENTIALLY EXPRESSED GENES IN RETINITIS-PIGMENTOSA RETINAS - ALTERED EXPRESSION OF CLUSTERING MESSENGER-RNA." Febs Letters **300**(3): 279-282.

Jordan-Starck, T. C., Witte, D., Aronow, B., and Harmony, J. A. K. (1992). "Apolipoprotein J: a memnrane policeman?" Current opinion in lipidology **3**: 75-85.

Jordanstarck, T. C., S. D. Lund, et al. (1994). "MOUSE APOLIPOPROTEIN-J - CHARACTERIZATION OF A GENE IMPLICATED IN ATHEROSCLEROSIS." Journal of Lipid Research **35**(2): 194-210.

Junping Wang, M. S., Jeanette Rientjes, Jun Fu, Heike Hollak, Wei Xie, A. Francis Stewart, and Youming, Zhang (2006). "An improved recombineering approach by adding RecA to λ Red recombination." Molecular Biotechnology3 **Vol.32 (1)**: pp.43-45.

Kang, S. W., Y. J. Shin, et al. (2005). "Clusterin interacts with SCLIP (SCG10-like protein) and promotes neurite outgrowth of PC12 cells." Experimental Cell Research **309**(2): 305-315.

Kaufman, M. H. B., J.B.L. (1999). The Anatomical Basis of Mouse Development. San Diego, Academic press.

Kelley, M. W. (2006). "Regulation of cell fate in the sensory epithelia of the inner ear." Nat Rev Neurosci **7**(11): 837-849.

Kelley, M. W. (2007). "Cellular commitment and differentiation in the organ of Corti." International Journal of Developmental Biology **51**(6-7): 571-583.

Kiernan, A. E., N. Ahituv, et al. (2001). "The Notch ligand Jagged1 is required for inner ear sensory development." Proceedings of the National Academy of Sciences of the United States of America **98**(7): 3873-3878.

Kiernan, A. E., A. L. Pelling, et al. (2005). "Sox2 is required for sensory organ development in the mammalian inner ear." Nature **434**(7036): 1031-1035.

Kiernan, A. E., J. Xu, et al. (2006). "The Notch ligand JAG1 is required for sensory progenitor development in the mammalian inner ear." Plos Genetics **2**(1): 27-38.

Kim, B. M., Y. M. Han, et al. (2001). "Clusterin expression during regeneration of pancreatic islet cells in streptozotocin-induced diabetic rats." DIABETOLOGIA **44**(12): 2192-2202.

Kim, B. M., S. Y. Kim, et al. (2006). "Clusterin induces differentiation of pancreatic duct cells into insulin-secreting cells." DIABETOLOGIA **49**(2): 311-320.

Kim, H.-M. and P. Wangemann (2010). "Failure of Fluid Absorption in the Endolymphatic Sac Initiates Cochlear Enlargement that Leads to Deafness in Mice Lacking Pendrin Expression." PLoS One **5**(11).

Kim, Y., E. Song, et al. (2007). "Engineering lacZ reporter gene into an ephA8 bacterial artificial chromosome using a highly efficient bacterial recombination system." Journal of Biochemistry and Molecular Biology **40**(5): 656-661.

Kirjavainen, A., M. Sulg, et al. (2008). "Prox1 interacts with Atoh1 and Gfi1, and regulates cellular differentiation in the inner ear sensory epithelia." Developmental Biology **322**(1): 33-45.

Kirszbaum, L., S. E. Bozas, et al. (1992). "SP-40,40, A PROTEIN INVOLVED IN THE CONTROL OF THE COMPLEMENT PATHWAY, POSSESSES A UNIQUE ARRAY OF DISULFIDE BRIDGES." Febs Letters **297**(1-2): 70-76.

Kirszbaum, L., J. A. Sharpe, et al. (1989). "MOLECULAR-CLONING AND CHARACTERIZATION OF THE NOVEL, HUMAN COMPLEMENT-ASSOCIATED PROTEIN, SP-40,40 - A LINK BETWEEN THE COMPLEMENT AND REPRODUCTIVE SYSTEMS." Embo Journal **8**(3): 711-718.

Klock, G., M. Baiersdorfer, et al. (2009). Cell Protective Functions of Secretory Clusterin (sCLU). Advances in Cancer Research, Vol 104. S. P. S. Bettuzzi. **104:** 115-+.

Kounnas, M. Z., Loukinova, E. B., Steffansson, S., Harmony, J. A. K., Brewer, B. H., Strickland, D. K., and Argraves, W. S. (1995). "Identification of glycoprotein 330 as an endocytic receptor for appolipoprotein J/Clusterin." Biochemistry **270**: 13070-13075.

Kunihiro Mizuta, A. S., Takahiro Watanabe, Mitsuyoshi Nagura, Masaaki Arakawa, Fujio Shimizu, Tomoyuki Hoshino (1999). "Ultrastructural localization of megalin in the rat cochlear duct." Hearing Research **129** 83-91.

Ladher, R. K., T. J. Wright, et al. (2005). "FGF8 initiates inner ear induction in chick and mouse." Genes & Development **19**(5): 603-613.

Lambert, J.-C., S. Heath, et al. (2009). "Genome-wide association study identifies variants at CLU and CR1 associated with Alzheimer's disease." Nature Genetics **41**(10): 1094-U1068.

Lanford, P. J., Y. Lan, et al. (1999). "Notch signalling pathway mediates hair cell development in mammalian cochlea." Nature Genetics **21**(3): 289-292.

Lanford, P. J., R. Shailam, et al. (2000). "Expression of Math1 and HES5 in the cochleae of wildtype and Jag2 mutant mice." JARO Journal of the Association for Research in Otolaryngology **1**(2): 161-171.

Lang, H. N., M. M. Bever, et al. (2000). "Cell proliferation and cell death in the developing chick inner ear: Spatial and temporal patterns." Journal of Comparative Neurology **417**(2): 205-220.

Lee, C., L. Atanelov, et al. (2003). "ASAP: the Alternative Splicing Annotation Project." Nucleic Acids Research **31**(1): 101-105.

Lee, Y.-S., F. Liu, et al. (2006). "A morphogenetic wave of p27(Kip1) transcription directs cell cycle exit during organ of Corti development." Development **133**(15): 2817-2826.

Legan, P. K., A. Rau, et al. (1997). "The mouse tectorins - Modular matrix proteins of the inner ear homologous to components of the sperm-egg adhesion system." Journal of Biological Chemistry **272**(13): 8791-8801.

Leger, J. G., M. L. Montpetit, et al. (1987). "CHARACTERIZATION AND CLONING OF ANDROGEN-REPRESSED MESSENGER-RNAS FROM RAT VENTRAL PROSTATE." Biochemical and Biophysical Research Communications **147**(1): 196-203.

Leon, Y., S. Sanchez-Galiano, et al. (2004). "Programmed cell death in the development of the vertebrate inner ear." Apoptosis **9**(3): 255-264.

Leskov, K. S., D. Y. Klokov, et al. (2003). "Synthesis and functional analyses of nuclear clusterin, a cell death protein." Journal of Biological Chemistry **278**(13): 11590-11600.

Li, C. W. and J. McPhee (1979). "INFLUENCES ON THE COILING OF THE COCHLEA." Annals of Otology Rhinology and Laryngology **88**(2): 280-287.

Li, C. W., T. R. Vandewater, et al. (1978). "FATE MAPPING OF 11TH AND 12TH DAY MOUSE OTOCYST - INVITRO STUDY OF SITES OF ORIGIN OF EMBRYONIC INNER-EAR SENSORY STRUCTURES." Journal of Morphology **157**(3): 249-267.

Li, S. G., S. M. Price, et al. (2002). "Hearing loss caused by progressive degeneration of cochlear hair cells in mice deficient for the Barhl1 homeobox gene." Development **129**(14): 3523-3532.

Lim, D. J. and M. Anniko (1985). "Developmental morphology of the mouse inner ear. A scanning electron microscopic observation." Acta oto-laryngologica. Supplementum **422**: 1-69.

Ling, I. F., J. Bhongsatiern, et al. (2012). "Genetics of clusterin isoform expression and Alzheimer's disease risk." PLoS One **7**(4): e33923.

Lipsick, J. S., J. Manak, et al. (2001). "Functional evolution of the Myb oncogene family." Blood Cells Molecules and Diseases **27**(2): 456-458.

Lundgren, S., Carling, T., Hja¨lm, G., Juhlin, C., Rastad, J., Pihlgren, U., Rask, L.,°kerstro¨m, G., and Hellman, G. (1997). "Tissue distribution of human gp330/megalin, a putative Ca 2+ sensing protein. J." J. Histochem. Cytochem. **45**: 383–392.

Lymar, E. S., A. M. Clark, et al. (2000). "Clusterin gene in rat Sertoli cells is regulated by a core-enhancer element." Biology of Reproduction **63**(5): 1341-1351.

Mansour, S. L. and G. C. Schoenwolf (2005). Morphogenesis of the inner ear.

Margaret L. Van Keuren, G. B. G., Wanda E. Filipiak, Michael G. Zeidler, and and T. L. Saunders (2009). "Generating Transgenic Mice from Bacterial Artificial Chromosomes: Transgenesis Efficiency, Integration and Expression Outcomes." Transgenic Res **18(5): 769–785. doi:10.1007/s11248-009-9271-2**.

Marovitz, W. F., J. M. A. Shugar, et al. (1976). "ROLE OF CELLULAR DEGENERATION IN NORMAL DEVELOPMENT OF (RAT) OTOCYST)." Laryngoscope **86**(9): 1413-1425.

Martin, P. and G. J. Swanson (1993). "DESCRIPTIVE AND EXPERIMENTAL-ANALYSIS OF THE EPITHELIAL REMODELLINGS THAT CONTROL SEMICIRCULAR CANAL FORMATION IN THE DEVELOPING MOUSE INNER-EAR." Developmental Biology **159**(2): 549-558.

McLaughlin, L., G. Zhu, et al. (2000). "Apolipoprotein J/clusterin limits the severity of murine autoimmune myocarditis." Journal of Clinical Investigation **106**(9): 1105-1113.

Michel, D., G. Chatelain, et al. (1995). "THE EXPRESSION OF THE AVIAN CLUSTERIN GENE CAN BE DRIVEN BY 2 ALTERNATIVE PROMOTERS WITH DISTINCT REGULATORY ELEMENTS." European Journal of Biochemistry **229**(1): 215-223.

Michel, D., G. Chatelain, et al. (1997). "Stress-induced transcription of the clusterin/apoJ gene." Biochemical Journal **328**: 45-50.

Michel, D., G. Chatelain, et al. (1997). "Stress-induced transcription of the clusterin/apoJ gene." Biochem J **328 ( Pt 1)**: 45-50.

Michel, D., G. Gillet, et al. (1989). "EXPRESSION OF A NOVEL GENE ENCODING A 51.5 KD PRECURSOR PROTEIN IS INDUCED BY DIFFERENT RETROVIRAL ONCOGENES IN QUAIL NEURORETINAL CELLS." Oncogene Research **4**(2): 127-136.

Michel, D., E. Moyse, et al. (1997). "Clusterin/ApoJ expression is associated with neuronal apoptosis in the olfactory mucosa of the adult mouse." Journal of Cell Science **110**: 1635-1645.

Miller, C. A., H. Ingmer, et al. (1995). "Boundaries of the pSC101 minimal replicon are conditional." Journal of Bacteriology **177**(17): 4865-4871.

Min, B. H., S. Y. Jeong, et al. (1998). "Transient expression of clusterin (sulfated glycoprotein-2) during development of rat pancreas." Journal of Endocrinology **158**(1): 43-52.

Min, B. H., B. M. Kim, et al. (2003). "Clusterin expression in the early process of pancreas regeneration in the pancreatectomized rat." Journal of Histochemistry & Cytochemistry **51**(10): 1355-1365.

Miyake, H., K. N. Chi, et al. (2000). "Antisense TRPM-2 oligodeoxynucleotides chemosensitize human androgen-independent PC-3 prostate cancer cells both in vitro and in vivo." Clinical Cancer Research **6**(5): 1655-1663.

Miyake, H., C. Nelson, et al. (2000). "Acquisition of chemoresistant phenotype by overexpression of the antiapoptotic gene testosterone-repressed prostate message-2 in prostate cancer xenograft models." Cancer Research **60**(9): 2547-2554.

Monks, D. C. and B. E. Morrow (2012). "Identification of putative retinoic acid target genes downstream of mesenchymal Tbx1 during inner ear development." Developmental Dynamics **241**(3): 563-573.

Morsli, H., D. Choo, et al. (1998). "Development of the mouse inner ear and origin of its sensory organs." Journal of Neuroscience **18**(9): 3327-3335.

Murphy, B. F., L. Kirszbaum, et al. (1988). "SP-40,40, A NEWLY IDENTIFIED NORMAL HUMAN-SERUM PROTEIN FOUND IN THE SC5B-9 COMPLEX OF COMPLEMENT AND IN THE IMMUNE DEPOSITS IN GLOMERULONEPHRITIS." Journal of Clinical Investigation **81**(6): 1858-1864.

Muyrers, J. P. P., Zhang, Y., Stewart, A.F. (2001). "Techniques: Recombinogenic engineering-new options for cloning and manipulating DNA." TRENDS in Biochemical Sciences **Vol.26 (5)**: pp.325-331.

Nakamura, S., Saito, D., Tanaka, M. (2008). "Generation of transgenic medaka using modified bacterial artificial chromosome." Development, Growth and Differentiation **Vol.50 (6)**: pp.415-419.

Navab, M., G. M. Anantharamaiah, et al. (2007). "Peptide mimetics of apolipoproteins improve HDL function." Journal of Clinical Lipidology **1**(2): 142-147.

Navab, M., G. M. Anantharamaiah, et al. (2005). "An oral ApoJ peptide renders HDL antiinflammatory in mice and monkeys and dramatically reduces atherosclerosis in apolipoprotein E-null mice." Arteriosclerosis Thrombosis and Vascular Biology **25**(9): 1932-1937.

Navab, M., S. HamaLevy, et al. (1997). "Mildly oxidized LDL induces an increased apolipoprotein J paraoxonase ratio." Journal of Clinical Investigation **99**(8): 2005-2019.

Nikolic, P., L. E. Jarlebark, et al. (2000). "Apoptosis in the developing rat cochlea and its related structures." Developmental Brain Research **119**(1): 75-83.

Nishikori, T., T. Hatta, et al. (1999). "Apoptosis during inner ear development in human and mouse embryos: an analysis by computer-assisted three-dimensional reconstruction." Anatomy and Embryology **200**(1): 19-26.

Nishizaki, K., M. Anniko, et al. (1998). "Programmed cell death in the developing epithelium of the mouse inner ear." Acta Oto-Laryngologica **118**(1): 96-100.

Nishizaki, K., M. Anniko, et al. (1998). "Programmed cell death in the mouse cochleovestibular ganglion during development." Orl-Journal for Oto-Rhino-Laryngology and Its Related Specialties **60**(5): 267-271.

Nizard, P., S. Tetley, et al. (2007). "Stress-induced retrotranslocation of clusterin/ApoJ into the cytosol." Traffic **8**(5): 554-565.

O'Sullivan, J., L. Whyte, et al. (2003). "Alterations in the post-translational modification and intracellular trafficking of clusterin in MCF-7 cells during apoptosis." Cell Death and Differentiation **10**(8): 914-927.

Obryan, M. K., S. S. Cheema, et al. (1993). "CLUSTERIN LEVELS INCREASE DURING NEURONAL DEVELOPMENT." Journal of Neurobiology **24**(4): 421-432.

Ovcharenko, I., M. A. Nobrega, et al. (2004). "ECR Browser: a tool for visualizing and accessing data from comparisons of multiple vertebrate genomes." Nucleic Acids Research **32**: W280-W286.

Ovidiu Ko¨nig, L. R. t., Marcus Mu¨ller, Ulrike Zimmermann, Bettina Erdmann, Hubert Kalbacher, Manfred Gross, and Marlies Knipper (2008). "Estrogen and the inner ear: megalin knockout mice suffer progressive hearing loss." FASEB J.

**22**: v410–417

Park, D. C., S. G. Yeo, et al. (2008). "Clusterin interacts with paclitaxel and confer paclitaxel resistance in ovarian cancer." Neoplasia **10**(9): 964-U943.

Pasinetti, G. M. and C. E. Finch (1991). "SULFATED GLYCOPROTEIN-2 (SGP-2) MESSENGER-RNA IS EXPRESSED IN RAT STRIATAL ASTROCYTES FOLLOWING IBOTENIC ACID LESIONS." Neuroscience Letters **130**(1): 1-4.

Poon, S., S. B. Easterbrook-Smith, et al. (2000). "Clusterin is an ATP-independent chaperone with very broad substrate specificity that stabilizes stressed proteins in a folding-competent state." Biochemistry **39**(51): 15953-15960.

Poon, S., M. S. Rybchyn, et al. (2002). "Mildly acidic pH activates the extracellular molecular chaperone clusterin." J Biol Chem **277**(42): 39532-39540.

Powles, N., C. Babbs, et al. (2004). "Identification and analysis of genes from the mouse otic vesicle and their association with developmental subprocesses through in situ hybridization." Developmental Biology **268**(1): 24-38.

Powles, N., H. Marshall, et al. (2004). "Regulatory analysis of the mouse Fgf3 gene: Control of embryonic expression patterns and dependence upon sonic hedgehog (Shh) signalling." Developmental Dynamics **230**(1): 44-56.

Pucci, S., E. Bonanno, et al. (2004). "Modulation of different clusterin isoforms in human colon tumorigenesis." Oncogene **23**(13): 2298-2304.

Puligilla, C., F. Feng, et al. (2007). "Disruption of Fibroblast growth factor receptor 3 signaling results in defects in cellular differentiation, neuronal patterning, and hearing impairment." Developmental Dynamics **236**(7): 1905-1917.

Puligilla, C. and M. W. Kelley (2009). "Building the world's best hearing aid; regulation of cell fate in the cochlea." Current Opinion in Genetics & Development **19**(4): 368-373.

Rau, A., P. K. Legan, et al. (1999). "Tectorin mRNA expression is spatially and temporally restricted during mouse inner ear development." Journal of Comparative Neurology **405**(2): 271-280.

Rau, A., P. K. Legan, et al. (1999). "Tectorin mRNA Expression Is Spatially and Temporally Restricted During Mouse Inner Ear Development." THE JOURNAL OF COMPARATIVE NEUROLOGY **405** 271–280.

Reddy, K. B., G. Jin, et al. (1996). "Transforming growth factor beta (TGF beta)-induced localization of apolipoprotein J/clusterin in epithelial cells." Biochemistry **35**(19): 6157-6163.

Redondo, M., E. Villar, et al. (2000). "Overexpression of clusterin in human breast carcinoma." American Journal of Pathology **157**(2): 393-399.

Represa, J. J., J. A. Moro, et al. (1990). "PATTERNS OF EPITHELIAL-CELL DEATH DURING EARLY DEVELOPMENT OF THE HUMAN INNER-EAR." Annals of Otology Rhinology and Laryngology **99**(6): 482-488.

Rizzi, F. and S. Bettuzzi (2010). "The clusterin paradigm in prostate and breast carcinogenesis." Endocr Relat Cancer **17**(1): R1-17.

Rizzi, F., M. Coletta, et al. (2009). "Chapter 2: Clusterin (CLU): From one gene and two transcripts to many proteins." Adv Cancer Res **104**: 9-23.

Robertson, G., M. Hirst, et al. (2007). "Genome-wide profiles of STAT1 DNA association using chromatin immunoprecipitation and massively parallel sequencing." Nature Methods **4**(8): 651-657.

Rosenberg, M. E., R. Girton, et al. (2002). "Apolipoprotein J/clusterin prevents a progressive glomerulopathy of aging." Molecular and Cellular Biology **22**(6): 1893-1902.

Rosenberg, M. E. and J. Silkensen (1995). "CLUSTERIN - PHYSIOLOGICAL AND PATHOPHYSIOLOGIC CONSIDERATIONS." International Journal of Biochemistry & Cell Biology **27**(7): 633-645.

Ruben, R. J. (1967). "Development of the inner ear of the mouse: a radioautographic study of terminal mitoses." Acta Oto-Laryngologica: 44.

Ryan, A. F. (1997). "Transcription factors and the control of inner ear development." Seminars in Cell & Developmental Biology **8**(3): 249-256.

Sanz, C., Y. Leon, et al. (1999). "Pattern of expression of the Jun family of transcription factors during the early development of the inner ear: implications in apoptosis." Journal of Cell Science **112**(22): 3967-3974.

Scaltriti, M., A. Santamaria, et al. (2004). "Intracellular clusterin induces G2-M phase arrest and cell death in PC-3 prostate cancer cells1." Cancer Res **64**(17): 6174-6182.

Schepeler, T., F. Mansilla, et al. (2007). "Clusterin expression can be modulated by changes in TCF1-mediated Wnt signaling." Journal of molecular signaling **2**: 6.

Schleif, R. (1992). "DNA LOOPING." Annual Review of Biochemistry **61**: 199-223.

Seiberg, M. and J. Marthinuss (1995). "CLUSTERIN EXPRESSION WITHIN SKIN CORRELATES WITH HAIR-GROWTH." Journal of Investigative Dermatology **104**(4): 638-638.

Sensibar, J. A., D. M. Sutkowski, et al. (1995). "PREVENTION OF CELL-DEATH INDUCED BY TUMOR-NECROSIS-FACTOR-ALPHA IN LNCAP CELLS BY OVEREXPRESSION OF SULFATED GLYCOPROTEIN-2 (CLUSTERIN)." Cancer Research **55**(11): 2431-2437.

Shannan, B., M. Seifert, et al. (2006). "Challenge and promise: roles for clusterin in pathogenesis, progression and therapy of cancer." Cell Death and Differentiation **13**(1): 12-19.

Sher, A. E. (1971). "The embryonic and postnatal development of the inner ear of the mouse." Acta oto-laryngologica. Supplementum **285**: 1-77.

Shyam K. Sharan, L. C. T., Sergey G. Kuznetsov, and Donald L. Court (2009). "Recombineering: A homologous recombination-based method of genetic engineering." Nature Protocols **Vol.4 (2)**: pp.206-223.

Silkensen, J. R., K. M. Skubitz, et al. (1995). "Clusterin promotes the aggregation and adhesion of renal porcine epithelial cells." Journal of Clinical Investigation **96**(6): 2646-2653.

Sparwasser, T., S. C. Gong, et al. (2004). "General method, for the modification of different BAC types and the rapid generation of BAC transgenic mice." Genesis **38**(1): 39-50.

Strange, R., F. Li, et al. (1992). "APOPTOTIC CELL-DEATH AND TISSUE REMODELING DURING MOUSE MAMMARY-GLAND INVOLUTION." Development **115**(1): 49-58.

Sun, B., S. Zhang, et al. (2007). "Clusterin is associated with spontaneous breast cancer in TA2 mice." Febs Letters **581**(17): 3277-3282.

Sylvester, S. R., C. Morales, et al. (1991). "LOCALIZATION OF SULFATED GLYCOPROTEIN-2 (CLUSTERIN) ON SPERMATOZOA AND IN THE REPRODUCTIVE-TRACT OF THE MALE-RAT." Biology of Reproduction **45**(1): 195-207.

Tenniswood, M. P., R. S. Guenette, et al. (1992). "ACTIVE CELL-DEATH IN HORMONE-DEPENDENT TISSUES." Cancer and Metastasis Reviews **11**(2): 197-220.

Teubner, B., V. Michel, et al. (2003). "Connexin30 (Gjb6)-deficiency causes severe hearing impairment and lack of endocochlear potential." Human Molecular Genetics **12**(1): 13-21.

Thomas-Tikhonenko, A., I. Viard-Leveugle, et al. (2004). "Myc-transformed epithelial cells down-regulate clusterin, which inhibits their growth in vitro and carcinogenesis in vivo." Cancer Research **64**(9): 3126-3136.

Thomas, D. J., K. R. Rosenbloom, et al. (2007). "The ENCODE project at UC Santa Cruz." Nucleic Acids Research **35**: D663-D667.

Tian, Y., S. James, et al. (2006). "Conditional and inducible gene recombineering in the mouse inner ear." Brain Research **1091**: 243-254.

Torres-Munoz, J. E., M. Redondo, et al. (2001). "Upregulation of glial clusterin in brains of patients with AIDs." Brain Research **888**(2): +297-301.

Trougakos, I. P., J. Y. Djeu, et al. (2009). "Advances and Challenges in Basic and Translational Research on Clusterin." Cancer Research **69**(2): 403-406.

Trougakos, I. P. and E. S. Gonos (2002). "Clusterin/Apolipoprotein J in human aging and cancer." International Journal of Biochemistry & Cell Biology **34**(11): 1430-1448.

Trougakos, I. P., A. So, et al. (2004). "Silencing expression of the clusterin/apolipoprotein J gene in human cancer cells using small interfering RNA induces spontaneous apoptosis, reduced growth ability, and cell sensitization to genotoxic and oxidative stress." Cancer Research **64**(5): 1834-1842.

Tsai, H., R. E. Hardisty, et al. (2001). "The mouse slalom mutant demonstrates a role for Jagged1 in neuroepithelial patterning in the organ of Corti." Human Molecular Genetics **10**(5): 507-512.

Vakeva, A., P. Laurila, et al. (1993). "CODEPOSITION OF CLUSTERIN WITH THE COMPLEMENT MEMBRANE ATTACK COMPLEX IN MYOCARDIAL-INFARCTION." Immunology **80**(2): 177-182.

Vakeva, A., S. Meri, et al. (1995). "ACTIVATION OF THE TERMINAL COMPLEMENT CASCADE IN RENAL INFARCTION." Kidney International **47**(3): 918-926.

Viard, I., P. Wehrli, et al. (1999). "Clusterin gene expression mediates resistance to apoptotic cell death induced by heat shock and oxidative stress." Journal of Investigative Dermatology **112**(3): 290-296.

Vuk Savkovic´ a, b., Helen Gantzer a, Ulrich Reiser a, Lena Selig a, Sebastian Gaiser a,, G. n. K. p. c. Ulrich Sack b, Joachim Mo¨ssner a, Volker Keim a, Friedemann Horn b,, et al. (2007). "Clusterin is protective in pancreatitis through anti-apoptotic and anti-inflammatory properties." Biochemical and Biophysical Research Communications 356 (2007) 431–437.

Wallis, D., M. Hamblen, et al. (2003). "The zinc finger transcription factor Gfi1, implicated in lymphomagenesis, is required for inner ear hair cell differentiation and survival." Development **130**(1): 221-232.

Water, V. D., Ed. (1983). Embryogenesis of the inner ear: "in vitro studuies". Development of Auditory and Vestibular Systems. New York, Academic Press.

Wilson, M. R. and S. B. Easterbrook-Smith (2000). "Clusterin is a secreted mammalian chaperone." Trends Biochem Sci **25**(3): 95-98.

Wilson, M. R. and S. B. Easterbrook-Smith (2000). "Clusterin is a secreted mammalian chaperone." Trends in Biochemical Sciences **25**(3): 95-98.

Wilson, M. R., J. J. Yerbury, et al. (2008). "Potential roles of abundant extracellular chaperones in the control of amyloid formation and toxicity." Molecular Biosystems **4**(1): 42-52.

Witte, D. P., B. J. Aronow, et al. (1994). "TEMPORALLY AND SPATIALLY RESTRICTED EXPRESSION OF APOLIPOPROTEIN-J IN THE DEVELOPING HEART DEFINES DISCRETE STAGES OF VALVE MORPHOGENESIS." Developmental Dynamics **201**(3): 290-296.

Wong, P., D. Taillefer, et al. (1994). "MOLECULAR CHARACTERIZATION OF HUMAN TRPM-2/CLUSTERIN, A GENE ASSOCIATED WITH SPERM MATURATION, APOPTOSIS AND NEURODEGENERATION." European Journal of Biochemistry **221**(3): 917-925.

Wyatt, A., J. Yerbury, et al. (2009). "The Chaperone Action of Clusterin and Its Putative Role in Quality Control of Extracellular Protein Folding." Advances in Cancer Research, Vol 104 **104**: 89-+.

Wyatt A, Y. J., Poon S, Dabbs R, Wilson M. (2009). "Chapter 6: The chaperone action of Clusterin and its putative role in quality control of extracellular protein folding.
." Adv Cancer Res. 2009;104:89-114.

Wyatt, A. R. and M. R. Wilson (2010). "Identification of human plasma proteins as major clients for the extracellular chaperone clusterin." J Biol Chem **285**(6): 3532-3539.

Wyatt, A. R., J. J. Yerbury, et al. (2011). "Clusterin facilitates in vivo clearance of extracellular misfolded proteins." Cell Mol Life Sci.

Wyatt, A. R., J. J. Yerbury, et al. (2009). "Therapeutic Targets in Extracellular Protein Deposition Diseases." Current Medicinal Chemistry **16**(22): 2855-2866.

Xiang, M. Q., W. Q. Gao, et al. (1998). "Requirement for Brn-3c in maturation and survival, but not in fate determination of inner ear hair cells." Development **125**(20): 3935-3946.

Yang, C. R., K. Leskov, et al. (2000). "Nuclear clusterin/XIP8, an x-ray-induced Ku70-binding protein that signals cell death." Proceedings of the National Academy of Sciences of the United States of America **97**(11): 5907-5912.

Yang, X. D. W., P. Model, et al. (1997). "Homologous recombination based modification in Escherichia coli and germline transmission in transgenic mice of a bacterial artificial chromosome." Nature Biotechnology **15**(9): 859-865.

Yerbury, J. J., E. M. Stewart, et al. (2005). "Quality control of protein folding in extracellular space." Embo Reports **6**(12): 1131-1136.

Yoko Itahana, M. P., Tomoki Sumida, Sylvia Fong, John Muschler, and Pierre-Yves, Desprez, et al. (2007). "Regulation of Clusterin Expression in Mammary Epithelial Cells."
Exp Cell Res. 2007 March 10; 313(5): 943–951.

Zellweger, T., K. Chi, et al. (2002). "Enhanced radiation sensitivity in prostate cancer by inhibition of the cell survival protein clusterin." Clinical Cancer Research **8**(10): 3276-3284.

Zhang, N., G. V. Martin, et al. (2000). "A mutation in the Lunatic fringe gene suppresses the effects of a Jagged2 mutation on inner hair cell development in the cochlea." Current Biology **10**(11): 659-662.

Zheng, J. L. and W. Q. Gao (1997). "Analysis of rat vestibular hair cell development and regeneration using calretinin as an early marker." Journal of Neuroscience **17**(21): 8270-8282.

Zheng, J. L. and W. Q. Gao (2000). "Overexpression of Math1 induces robust production of extra hair cells in postnatal rat inner ears." Nature Neuroscience **3**(6): 580-586.

Zheng, J. L., J. Y. Shou, et al. (2000). "Hes1 is a negative regulator of inner ear hair cell differentiation." Development **127**(21): 4551-4560.

Zhou, W., L. Janulis, et al. (2002). "A novel anti-proliferative property of clusterin in prostate cancer cells." Life Sciences **72**(1): 11-21.

Zou, D., C. Erickson, et al. (2008). "Eya1 gene dosage critically affects the development of sensory epithelia in the mammalian inner ear." Human Molecular Genetics **17**(21): 3340-3356.

Zuo, J., J. Treadaway, et al. (1999). "Visualization of alpha 9 acetylcholine receptor expression in hair cells of transgenic mice containing a modified bacterial artificial chromosome."

Proceedings of the National Academy of Sciences of the United States of America **96**(24): 14100-14105.

Zwain, I. and P. Amato (2000). "Clusterin protects granulosa cells from apoptotic cell death during follicular atresia." Experimental Cell Research **257**(1): 101-110.